DETOXIFICATION OF JATROPHA BIOMASS MEDIATED BY APPLICATION OF MICROBUBBLE AND PLASMA MICROREACTOR TECHNOLOGY

A Thesis submitted for the degree of Doctor of Philosophy (PhD) in the Department of Chemical and Biological Engineering at the University of Sheffield, United Kingdom

Candidate: Anggun Puspitarini Siswanto

Supervisors: Professor William BJ Zimmerman

Dr Jagroop Pandhal

DEPARTMENT OF CHEMICAL AND BIOLOGICAL ENGINEERING

UNIVERSITY OF SHEFFIELD

2016

ABSTRACT

Food security and alternative fuel production are a poignant concern for sustainable development. Oil rich crops with high nutritional content as a food source, are widely cultivated. It is desirable to attain high nutritional value without comprising on the supply of raw materials for biofuel production. The residual biomass in biofuel processing of *Jatropha curcas Linn* is called Jatropha meal. It is produced after mechanical pressing for oil extraction and has low economic value. Moreover, its utilisation is limited due to a constituent, a natural carcinogen: phorbol ester, although it also contains a high level of nutrients, potentially useful as feed stock or fertiliser.

This research aims to develop technology for detoxifying phorbol esters in jatropha meal while maintaining the protein content. Detoxification using combination of ozone application and microbubble technology could eliminate phorbol ester content. Ozone is expected to attack the carbon double bond in molecular structure of phorbol ester while microbubbles act as an auto catalyst in cell lysis. Furthermore, the protein content is expected to remain stable as detoxification occurs in room temperature and atmospheric pressure without any additional chemicals involve.

The experimental reactor was characterised by measuring the microbubble size distribution generated from a ceramic diffuser and ozone concentration produced from a plasma microreactor. The bubble sizes generated were an average diameter of 670 μm in steady flow at air flow rate of 2 L/min. Moreover, 1.4 ppm of ozone concentration in the gas phase and 1.2 ppm in the liquid phase (dissolved ozone) were reported during reactor characterisation experiments. Also, 35 °C of plasma microreactor maximum temperature was observed after 60 minutes of ozonolysis.

It was observed that only 40% reduction of synthetic phorbol ester was achieved after 30 minutes of aeration (without ozone activation) while 64% of degradation was detected after 5 minutes of ozonolysis (with ozone activation). Furthermore, a two staged extraction was performed in order to obtain natural phorbol ester extract from jatropha meal samples. Some major fatty acids were found in the hexane extract of jatropha meal: linolenic acid, linoleic acid, oleic acid, palmitic acid and stearic acid. A 65% total oil reduction was observed in the

hexane extract after 5 hours of ozonolysis. Moreover, phorbol ester concentration in the hexane extract after 1 hour of ozonolysis was 7 fold higher than in untreated sample. After 2 hours of ozonolysis, phorbol ester content decreased by 47% and it remained stable until 5 hours of ozonolysis. Furthermore, phorbol ester concentration in methanol extract was significantly decreased after 3 hours of ozonolysis with 92% of reduction was observed. A 97% reduction of phorbol ester content after 5 hours of ozonolysis resulted in a final phorbol ester concentration of 0.11 mg/g in jatropha meal sample. This value is also phorbol ester concentration found in the non-toxic Mexican variety which has become the limiting level for of jatropha edibility. Hydroxyl radicals (•OH) are reported to play a substantial role in phorbol ester detoxification that is also expected to influenced Protein Kinase C (PKC), in which stimulated neurotransmission of phorbol ester, is susceptible with •OH.

This research also explored the ozonolysis effect on lignocellulosic materials. Protein content of jatropha meal after detoxification was studied. It is observed that the protein content remains stable after 5 hours of ozonolysis. It was reported that total protein concentration ranged from 18-32% which meets the requirements for sufficient nutritional content. The protein molecular weight of jatropha meal was distributed from 5 to 60 kDa. Also, it was observed that protein sequence of Indonesian jatropha meal used in this research matched two other species which are *Ricinus communi* and *Eucalyptus grandis*. The second study is the ozonolysis effect on synthetic lignin experiments. It showed that 56% lignin reduction occurred after 15 minutes of ozonolysis and 76% lignin reduction after 3 hours duration.

These experimental results provide an integrated study of phorbol ester detoxification in which demonstrates both an ozonolysis effect on toxicity level and protein content of jatropha meal. Overall, there are two time scales and two mechanisms influencing the kinetics of ozonolysis in JM -- (i) cell lysis from cell wall breakdown which releases proteins, and (ii) degradation of proteins by ozonolysis. Furthermore, various benefits offered by developed technology in this research promise to overcome the conflict between oil and food supply. A higher economic value of jatropha meal as biofuel processing residual can be achieved.

DEDICATION

This thesis is dedicated to my parents, Mr Budi Siswanto and Mrs Zubaedah Monoarfa, also to my brother and sister, Mr Priyadyaksa Argya Mi'raj and Ms Ajeng Inggita Nitrawidya.

For their unconditional love, support and encouragement

"without effort, we will not pull a fish out of a pond" (traditional proverb)

ACKNOWLEDGMENT

I would like to express my sincere gratitude to my supervisors: Professor William Zimmerman and Dr Jagroop Pandhal for their constant support, guidance and inspiration for both professional and personal development.

To Dr Dmitriy Kuvshinov and Dr Elena Kuvshinova. Thank you very much for everything. Words will never been enough to express my gratefulness for having them since the first time I started my study in The University of Sheffield.

To Mr Teguh Wijayanto, Mrs Rully Damayanti and Master Narasatya Joy Wijayanto. The love, the care and the joy, they offer are precious. Thank you very much for unconditionally accepting me as a part of family. They have taught that family is not always biological.

To Dr Thomas Holmes, for the countless support. Thank you so much for the great teamwork. Dr James Hanotu, for both scientific and casual discussion for the past 3 years. Mr Richard Archer, for device training on Scanning Electron Microscope (SEM). Mr Pratik Desai, for the research collaboration. Biologist colleagues: Mr Benjamin Strutton, Mr Andrew Landels, Dr Joseph Longworth, Dr Narciso Couto, Dr Esther Karunakaran, Dr Joy Mukherjee. Many thanks for all the patience and help. Colleagues in Chemical and Biological Engineering (CBE) Department, Microfluidic Group 2012-2015, thank you so much for the cooperation.

Special thanks to CBE staffs. Departmental Technical Manager: Mr Richard Stacey. Electricians: Mr Mark McIntosh, Mr Usman Younis, Mr Oz McFarlane. Technicians: Mr Andy Patrick, Mr Stuart Richards, Mr Adrian Lumby, Mr Steven Blackbourn. Laboratory technicians: Mr Keith Penny, Mr James Grinham, Mr David Wengraf, Mr Mark Jones. Professional staffs: Ms Maria Soto, Ms Marine Percival, Ms Gillian Rhodes, Ms Rhian Park.

To dr. Edward Burton, thanks for being a doctor, a friend and a proof reader. Ms Linda Roth and Mr Stephen Talbert, for the writing advisory support.

To Ms Salma Dwikartika, Ms Dwenda Dexiana, Ms Afifah Eleksiani, Ms Yttria Ariwahjoedi, Mr Ranggi Ramadhan. Many thanks for the moral support. They have taught that best friends are like stars; I do not always see them, but I know they are always there.

To Kak Ita, Kak Faten, Nana, Kak Marin and Ain, for the sisterhood and great moments.

To Dr Rini Mulyani and Dr Meilinda Nurbanasari, for the patience and support. To Mr Silih Warni, Mrs Risky Nurtanti and Master Bagas Hamizan, for the genuine care and warmth.

I am profoundly grateful to Professor Fauzi Soelaiman, previously an Education Attaché of the Republic of Indonesia in London and currently an Ambassador/Alternate Permanent Delegate of UNESCO in Paris, Ms Dewi Mukti in Embassy of The Republic of Indonesia in London and Dr Ananto Kusuma Seta, Head of Bureau of Planning and International Cooperation, Indonesia. Also, to Directorate General of Higher Education and Ministry of Education and Culture, Indonesia for the postgraduate scholarship.

LIST OF ACHIEVEMENTS

Awards

1. Commendation Awards on Scientific Image Competition. December 2013. Kroto Research Institute. University of Sheffield. United Kingdom.
2. Poster Finalist in Royal Academy of Engineering Regional Poster Competition. 17 March 2014. University of Sheffield. United Kingdom.
   Authors: **Siswanto, A.**, Kuvshinov, D., Pandhal, J. and Zimmerman, W.
   Title: *Application of Advance Extraction by Modified Plasma Microreactor for Phorbol Ester Remediation*
3. Best paper presentation in International Conference on Chemical, Biological and Environmental Engineering. 15-16 September 2014, Paris, France.
   Authors: Kuvshinov, D., **Siswanto, A.**, Desai, P. and Zimmerman, W.
   Title: *Application of Microbubble Enhanced Microreactor Plasma Technology*
4. Poster Finalist in SET for Britain Poster Competition. 7 March 2016. House of Commons, Parliament, London. United Kingdom.
   Authors: **Siswanto, A.**, Kuvshinov, D., Pandhal, J. and Zimmerman, W.
   Title: *Plasma Microreactor and Microbubble Technology: An Advance Approach in The Treatment of Lignocellulosic Biomass*

Conference Proceedings

1. Kuvshinov, D., **Siswanto, A.**, and Zimmerman, W. 2014. *Microbubbles Enhanced Synthetic Phorbol Ester Degradation by Ozonolysis*. International Journal of Chemical, Materials Science and Engineering. Vol. 8 No.1. pp 78-81. International Conference on Chemical Engineering and Process Technology, 27-28 January 2014. Istanbul, Turkey.
2. Kuvshinov, D., **Siswanto, A.**, Lozano-Parada, J. and Zimmerman, W. 2014. *Efficient Compact Micro DBD Plasma Reactor for Ozone Generation for Industrial Application in Liquid and Gas Phase Systems*. International Journal of Chemical, Materials Science and Engineering. Vol. 8 No.1. pp 82-85. International Conference on Chemical Engineering and Process Technology, 27-28 January 2014. Istanbul, Turkey.
3. **Siswanto, A.**, Kuvshinov, D. and Zimmerman, W.B. 2014. *Investigation of Bubble Size Distributions in Oscillatory Flow at Various Flow Rates*. In: The University of Sheffield

Engineering Symposium Conference Proceedings Vol. 1. USES 2014 - The University of Sheffield Engineering Symposium, 24 June 2014, The Octagon Centre, University of Sheffield. DOI:10.15445/01012014.40.

4. Kuvshinov, D., **Siswanto, A.**, Desai, P. and Zimmerman, W. 2014. *Application of Microbubble Enhanced Microreactor Plasma Technology*. International Conference on Chemical, Biological and Environmental Engineering 15-16 September 2014, Paris, France. DOI: 10.1016/j.apcbee.2014.12.074.
5. Kuvshinov, D., **Siswanto, A.**, Desai, P. and Zimmerman, W. 2014. *Peculiarities of Energy Efficient Microbubble Generation Mediated by Oscillatory Flow*. International Conference on Chemical, Biological and Environmental Engineering 15-16 September 2014, Paris, France. DOI: 10.1016/j.apcbee.2014.12.087.

Journal Papers

1. Siswanto, A., Kuvshinov, D. and Zimmerman, W. 2015. *Phorbol ester detoxification of Indonesian Jatropha meal by Microbubble Enhanced Ozonolysis Technology*. Journal of Industrial Crops and Products, Elsevier. (In preparation)
2. Siswanto, A., Kuvshinov, D., Pandhal, J. and Zimmerman, W. 2015. *Investigation of Ozonolysis effect on Protein Content of Indonesian Jatropha Meal*. Journal of Bioresource Technology, Elsevier. (In preparation)
3. Kuvshinov, D., Siswanto, A., and Zimmerman, W. 2015. *Plasma technology application in food sector: A Review*. Journal of Food Science and Technology, Elsevier. (In preparation)
4. Kuvshinov, D., Desai, P., Siswanto, A., and Zimmerman, W. 2015. *Effect of membrane wettability on the bubble size distribution in a multi-porous capillary membrane*. Journal of Chemical Engineering, Elsevier. (In preparation)

Posters

1. **Siswanto, A.**, Kuvshinov, D., Pandhal, J. And Zimmerman, W. 2014. *Advance Ozonolysis Technology with Microbubbles Application for Synthetic Phorbol Ester Removal.* Poster presentation in Industrial Seminar. 6 February 2014. Chemical and Biological Engineering Department. University of Sheffield. United Kingdom.

2. **Siswanto, A.**, Kuvshinov, D., Pandhal, J. And Zimmerman, W. 2014. *Plasma Microreactor Modified By Microbubbles Technology for Biofuel Crop Detoxification.* Finalist for Royal Academy of Engineering Regional Poster Competition. University of Sheffield Delegation. 17 March 2014. Sheffield. United Kingdom.
3. **Siswanto, A.**, Kuvshinov, D., Pandhal, J. And Zimmerman, W. 2014. *Phorbol Ester Removal by Advance Ozonolysis Approach using Dielectric Barrier Discharge (DBD) Plasma Microreactor.* Poster presentation in Chemical Engineering Day UK. 7-8 April 2014. University of Manchester. United Kingdom.
4. **Siswanto, A.**, Kuvshinov, D., Pandhal, J. and Zimmerman, W. 2014. *Plasma Microreactor Modified By Microbubbles Technology for Biofuel Crop Detoxification*. Poster presentation in University of Sheffield Engineering Symposium (USES). 24 June 2014. Sheffield. United Kingdom.
5. **Siswanto, A.** 2014. *Detoxification of Carcinogenic Compound by Ozonolysis Enhanced Microbubbles.* Poster presentation on ICheme Biochemical Engineering Young Researcher's Meeting. 23-24 September 2014. University of Sheffield. United Kingdom.
6. **Siswanto, A.**, Kuvshinov, D., Pandhal, J. And Zimmerman, W. 2015. *Jatropha Biomass Treatment by Microbubble Enhanced Ozonolysis Technology for Food Industry.* Poster presentation for Chemical Engineering Day UK. 8-9 April 2015. University of Sheffield. United Kingdom.

TABLE OF CONTENTS

CHAPTER 1 1
INTRODUCTION 1
1.1 Background 1
1.2 Hypothesis and objectives of study 4
1.3 Scope of study 5
1.4 Significance of the study 6
1.5 Structure of study 6
CHAPTER 2 8
LITERATURE REVIEW 8
2.1. *Jatropha curcas Linn* 8
2.2. Phorbol ester 16
2.3. Existing technologies for phorbol ester detoxification 20
2.4. Proteomic study of *Jatropha curcas* meal investigation 23
2.5. Application of plasma reactor in ozone generation 25
2.6. Microbubble technology 36
2.7. Microbubble technology enhanced by plasma microreactor 44
CHAPTER 3 48
METHODOLOGY 48
3.1 Experimental set up 48
3.2 Reactor characterisation 53
3.2. 1 Characterisation of ceramic diffuser 53
3.2. 2 Characterisation of plasma microreactor 56
3.3 Detoxification of Phorbol Ester (PE) compound 59
3.3. 1 Detoxification of synthetic PE 60
3.3. 2 Detoxification of natural PE 61
3.4 Investigation of ozonolysis effect in lignocellulosic materials 63
3.4. 1 Ozonolysis of Jatropha biomass 64
3.4. 2 Ozonolysis of synthetic lignin 67
CHAPTER 4 68
REACTOR CHARACTERISATION 68
4.1. Characterisation of ceramic diffuser 69

4.2. Characterisation of plasma microreactor 84
4.3. Summary 93
CHAPTER 5 97
DETOXIFICATION OF PHORBOL ESTER COMPOUND 97
5.1 Detoxification of Synthetic Phorbol Ester 98
5.2 Detoxification of Natural Phorbol Ester 104
5.3 Summary 122
CHAPTER 6 126
OZONOLYSIS EFFECTSONLIGNOCELLULOSIC MATERIALS 126
6.1 Ozonolysis of Jatropha Biomass 127
6.2 Ozonolysis of synthetic lignin 140
6.3 Summary 144
CHAPTER 7 147
CONCLUSIONS AND RECOMMENDATIONS 147
7.1 Conclusions 147
7.2 Recommendations 154
REFERENCES 156
APPENDIX 165

LIST OF FIGURES

Figure 2.1 *Jatropha curcas* distribution in tropical and sub-tropical regions 10
Figure 2.2 Potency of *Jatropha curcas Linn* 11
Figure 2.3 Profile of *Jatropha curcas L* plant 12
Figure 2.4 Molecular structure of tigliane 16
Figure 2.5 Structures of Jatropha factors (C1 and C2) from *Jatropha curcas* 17
Figure 2.6 Structures of Jatropha factors (C3 to C6) from *Jatropha curcas* 18
Figure 2.7 Various states of matter 26
Figure 2.8 Configurations of non thermal plasma reactors 27
Figure 2.9 Plasma generation in Dielectric Barrier Discharge 28
Figure 2.10 Paschen curve of plasma breakdown voltage in various gases 29
Figure 2.11Ozone generation mechanisms through dielectric discharge 30
Figure 2.12Detail reactions of Criegee mechanism 34
Figure 2.13 Bubble growth mechanism 38
Figure 2.14 Model (a) and principle mechanism of fluidic oscillator 42
Figure 3.1 General view of reactor 49
Figure 3.2Setup diagram of experimental reactor 50
Figure 3.3 Cross sectional module drawing of plasma unit 51
Figure 3.4 Photograph and diagram of plasma microreactor 51
Figure 3.5 Schematic design of ceramic diffuser 53
Figure 3.6 Flow diagram of bubble size distribution experimental setup 54
Figure 3.7 Principal diagram of ozone concentration experimental setup 57
Figure 3.8 Flow diagram of synthetic PE treatment by ozonolysis 61
Figure 3.9 Principal diagram of jatropha ozonolysis treatment 62
Figure 3.10Principal diagram of biology investigation on jatropha sample 64
Figure 4.1 Bubble generation at flow rate 0.5 L/min 70
Figure 4.2 Bubble generation at flow rate 1.0 L/min 72
Figure 4.3 Bubble generation at flow rate 1.5 L/min 74
Figure 4.4 Bubble generation at flow rate 2.0 L/min 76
Figure 4.5 Bubble generation at flow rate 2.5 L/min 78
Figure 4.6 Bubble generation at flow rate 3.0 L/min 80
Figure 4.7 Breakdown voltage of plasma ignition at different flow rates 85
Figure 4.8 Oscilloscope readings of breakdown voltage at various flow rates 87
Figure 4.9Calibration curve of ozone concentration 89
Figure 4.10Ozone production in gas phase and liquid phase at 2 L/min air flow rate 90
Figure 5.1 Calibration curve of TPA equivalent prior to PE investigation 98
Figure 5.2 Chromatograms of HPLC detection after TPA aeration by air microbubble 99
Figure 5.3 Aeration effect of TPA treated by air microbubble without ozone activation 100
Figure 5.4 Chromatograms of HPLC detection after TPA ozonolysis 102
Figure 5.5Chromatograms of hexane extract before and after 1 hour of ozonolysis 106
Figure 5.6 Chromatograms of hexane extract at 2 and 3 hours of ozonolysis 108
Figure 5.7 Chromatograms of hexane extract at 4 and 5 hours of ozonolysis 109

Figure 5.8 Ozonolysis effect of phorbol ester concentration in hexane extract 110
Figure 5.9 Ozonolysis effect on oil content in jatropha meal during ozonolysis 112
Figure 5.10Chromatograms of methanol extract before and after 1 hour of ozonolysis 114
Figure 5.11 Chromatograms of methanol extract at 2 and 3 hours of ozonolysis 116
Figure 5.12 Chromatograms of methanol extract at 4 and 5 hours of ozonolysis 118
Figure 5.13 Ozonolysis effect of phorbol ester concentration in methanol extract 119
Figure 6.1 Replicate experimental result of ozonolysis effect in protein content 128
Figure 6.2 Profile of protein content during ozonolysis 132
Figure 6.3 SDS-PAGE gel analysis of the Jatropha Meal sample after ozonolysis 133
Figure 6.5 Ozonolysis effect on lignin content after 180 minutes duration 140
Figure 6.6 Cross sectional view of lignocellulosic structure 141
Figure 6.7 pH observation during ozonolysis of lignin alkali sample 144

LIST OF TABLES

Table 2.1 Fatty acid content (%) in various biofuels.....12
Table 2.2 Characterisation of Jatropha oil and diesel oil 13
Table 2.3 Composition (%) of Jatropha Nut, Shell and Meal 14
Table 2.4 Nutritious content (% in DM) of Jatropha meal from different varieties.....15
Table 2.5 Oxidising Potential of Various Oxidants.....31
Table 4.1 Statistical data of bubble size distribution.....83
Table 5.1 TPA concentration after ozonolysis 103
Table 6.1 Total protein in total samples (% wt), quantified by indirect method.....131
Table 7.1 List of research key findings.....154

NOMENCLATURE

A = cross sectional area (in dm^2)

AC = alternating current

cfg = centrifugal unit

CHNS Analyser = Carbon-Hydrogen-Nitrogen-Sulphur Analyser

cm = centimetre

CS = calibration solution

C_{cs} = concentration of calibration solution (in mol/L)

C_{ss} = concentration of stock solution (in mol/L)

C_{ws} = concentration of working solution (in mol/L)

DIW = distilled water

DM = dry matter

DBD = Dielectric Barrier Discharge

E = energy (in kWh)

eV = electron volt

FAO = Food and Agriculture Organisation

FO = fluidic oscillator

HPLC = High Performance Liquid Chromatography

JM = jatropha meal

PDA = Photo Diode Array

PKC = Protein Kinase C

ppm = part per million

K = Kelvin

kDa = kilo Dalton

kGy = kilogray

kHz = kilohertz

kV = kilo Volt

kWh = kilo watt hour

L/min = litre per minute (lpm)

mA = milliampere

mg = milligram

mg/g = milligram per gram

ml = millilitre

mm = millimetre

mM = millimolar

MS = Mass Spectrophotometer

ms = millisecond

m/s = meter per second

mV = millivolt

nm = nanometre

O_2 = oxygen molecules

O_3 = ozone molecules

P = power (in kW)

PE = phorbol ester

PEEK = polyetheretherketone

Q = volumetric flow rate (in $dm^3.min^{-1}$)

SDS-PAGE = Sodium Dodecyl Sulfate Polyacrylamide Gel Electrophoresis

SEM = Scanning Electron Microscopy

SIS = Stock Indigo Solution

TEAB = triethylammonium bicarbonate

TPA = phorbol-12-myristate-13-acetate

T_e = electron temperature

T_i = ion temperature

T_v = vibrational temperature

T_0 = gas temperature

UV light = ultraviolet light

V_T = total volume (in litre)

V_{ic} = volume of indigo calibration solution (in litre)

V_{iw} = volume of indigo working solution (in litre)

WS = working solution

w/w = weight/weight

µm = micrometre

γ-radiation = gamma radiation

% wt = percent weight

•OH = hydroxyl radical

CHAPTER 1

INTRODUCTION

This chapter introduces the research perspectives addressed in this thesis which is organised into several sections. The first section begins with a detailed explanation of the study background which then narrows down to the research problems and possible solutions. The hypothesis and objectives of the study are presented, followed by an outline of the scope of study. Next, the significance of this research for future applications is highlighted. In the final section, the structure of the study is described to provide a general perspective of the thesis organisation.

1.1 Background

Jatropha curcas Linn is well known as one of the raw materials in the biofuel industry. It is a member of the Euphorbiaceae family and has several advantages in terms of environmental conditions, such as robustness and resistance to low quality soil. The plant is cultivated in tropical and subtropical countries such as America, Africa and Asia (Waled Abdo Ahmed and Salimon., 2009). It has not only a high content of oil but also protein. The residual biomass from biofuel processing which uses jatropha plant as the source, is known as jatropha meal. It is produced after mechanical processing of the jatropha plant in oil extraction. The biofuel industries focus on processing oil from the jatropha plant and the meal which is left over, is less useful. However, some nutritional contents remain in the jatropha meal which may be used as food or fertilizer.

Some emerging factors such as food security and fuels consumption, have become worldwide issues which affect economic stability. Oil rich crops are widely cultivated as raw materials for the biofuel industry in developing countries. However, these crops are mainly also potential sources for food supply. Therefore, the crop supply for food and oil are competing, making a solution for this conflict highly desirable. Technological developments aimed to contribute to increasing supply of food and fuel in order to meet market demands are the next step in improving existing food and oil production. *Jatropha curcas Linn* is one such crop (Devappa et al., 2011) in the biofuel sector. The production of the Jatropha plant ranges from 0.6 to 4.1 tons of seed/ha and it is expected that, globally, 2 tons of jatropha oils/ha will be produced from 12.8 million hectares of jatropha plantation (Devappa et al., 2010b).

The primary reason why the use of jatropha meal is limited is the presence of a carcinogenic compound. The phorbol ester is a chemical component in Euphorbiaceae plants which is a tumour promoter (Gaur, 2009). It exists in jatropha meal even after industrial treatment in oil extraction for producing biofuel. This compound is harmful to humans as well as animals and therefore jatropha meal cannot be utilised as food or fertilizer without further detoxification. Principally, most jatropha plants contain phorbol ester which is also present in jatropha meal. However, the concentration of this compound varies from one cultivation region of jatropha plants to another, and therefore, it is unsuitable for consumption by humans and animals. To date, the species of jatropha plant grown in Mexico has the lowest content of phorbol ester (0.11 mg/g), and hence is edible (Gaur, 2009, Goel et al., 2007, Francis et al., 2013).

As the use of the jatropha plant in the biofuel industry increases, so too does the production of jatropha meal. The current use of jatropha meal as combustion material needs to be reconsidered on account of its high nutrition content which makes it a valuable food source.

This is seen as a promising solution which can address the conflict of oil and food supply. The Jatropha plant can be still used as a raw material for oil extraction for biofuel production while jatropha meal, as the left over, can be used for alternative food supply. This view can also increase the economic value of jatropha meal. However, a detoxification process is required for this purpose.

Several detoxification approaches have been proposed to detoxify phorbol ester content in jatropha meal (Makkar and Becker, 1999, Haas and Mittelbach, 2000, Gaur, 2009). The conventional procedure is an extraction process using methanol as the solvent. Methanol is a good solvent for remediating phorbol ester. However, this methodology is costly as methanol is expensive and it also requires additional treatment for solvent regeneration. Methanol use in a phorbol ester detoxification process will spoil its use for other applications. One less expensive solvent which commonly used is water. Nevertheless, water is a weak solvent for phorbol ester. It is insufficient to eliminate the phorbol ester content. This is because of the well known hydrophobic nature of phorbol esters (Devappa et al., 2010a).

The novelty of this research is to propose a detoxification process of phorbol ester in jatropha meal using a water based solution. Water is used as a solvent for dissolution of ozone produced by plasma microreactors with microbubble dispersion. Water molecules with dissolved ozone could be dissociated into OH radicals which are a highly reactive oxidant. They are expected to attack the carbon double bonds in the phorbol ester molecular structure. This process is similar to the Criegee mechanism that explains the breakdown of an ester compound in the presence of ozone (Criegee, 1975). The benefit of this novel technology is that no byproduct is left after ozonolysis treatment. Ozone which is not reacted will re-form oxygen molecules (Baber et al., 2005). This promises an economic and eco friendly process.

Ozone is a strong oxidant for potential use in the phorbol ester remediation process. It can be produced by air flow through a plasma microreactor. Utilization of water as a solvent will result in a solution that is rich in ozone. The plasma microreactor has promising advantages because of its low energy consumption, operation in atmospheric pressure and high conversion (Zimmerman et al., 2010). Treatment using a plasma microreactor is usually conducted at atmospheric pressure which contributes to economic effectiveness. No need for operation under vacuum. Therefore it is easier to handle the reaction process.

1.2 Hypothesis and objectives of study

This research aims to investigate and to develop an approach with new technology combinations in treatment of toxic biomass. Throughout this thesis, the term "microbubble" is defined as bubbles which have average diameter less than 1 mm. These bubbles are generated by the ceramic diffuser independently of fluidic oscillator application. In addition, "plasma microreactor" term is also used to refer to the main developed technology applied in this research. Furthermore, the term "ozonolysis" is referred to a chemical process which uses ozone as the main reactive driving force. In this research, ozone molecules are produced by the plasma microreactor. Interdisciplinary studies that are involved during these investigations include plasma chemistry, chemical analysis and proteomic characterisation. This thesis hypothesizes that ozone and its derivatives produced during ozonolysis can attack the carbon double bonds in the phorbol ester molecular structure while still maintaining the high protein content of jatropha biomass. Therefore, the objectives of this study are:

1. To develop a technology which can facilitate treatment of toxic samples and to characterise the technology irrespective of application.

2. Measure and quantify the reactor characterisation in relation to the bubble size distribution and ozone concentration in specific range of flow rates.
3. To detoxify phorbol ester content in jatropha meal using ozonolysis treatment by plasma microreactor and microbubble technology.
4. To compare phorbol ester degradation in absence of plasma activation during treatment using synthetic samples.
5. To quantitatively and qualitatively evaluate the protein content in jatropha meal as well as to study the ozonolysis effect on lignocellulosic materials.

1.3 Scope of study

The scope of this study is to develop technology for detoxification of carcinogenic compounds in jatropha biomass. The chemical and biological characteristics of samples presented in this research are limited to Jatropha meal from the Indonesian variety of the original plant *Jatropha curcas Linn.* This study focuses on the technology development, therefore, reactor characterisation data of the applied detoxification approach is presented in the chapters ahead. Moreover, the combination of ozonolysis and microbubble technology is considered as a novel technology in biomass treatment, hence the discussion of the ozonolysis effect in carcinogenic compounds and lignocellulosic materials are highlighted. Treated samples are expected to be highly nutritious products with edibility levels within threshold. Nevertheless, further investigation for food and fertiliser tests are beyond the research scope of this thesis.

1.4 Significance of the study

The results of this research are expected to be utilised for some outputs which are for human consumption, animal food or fertiliser. The detoxification approach with the developed technology could affect phorbol ester concentration in treated samples hence influence its edibility. Further investigations in food chemistry test and fertiliser analysis are required which are not covered in this research. However, these limitations do not affect the quality, notably, the significance of this study. The application of ozonolysis with microbubble technology offers high energy efficiency and low associated cost. In addition, moderate operating conditions (reactor operated at a room temperature and atmospheric pressure) during detoxification, are beneficial for maintaining nutritious content in the samples. Therefore, technology offered in this research can bring substantial influence in both concerns: chemical engineering and biological aspects. It can be widely applied in many industries such as food industry, oil recovery, biological treatment and composting manufacture.

1.5 Structure of study

This thesis is organised into seven chapters. The first chapter introduces the background of research problem and describes the research hypothesis, aims and objectives. The scope of study and significance of research are further explained. The second chapter discusses critical assessment of the literatures relevant to the detoxification study. Characterisation of Jatropha biomass, as the experimental sample, is first outlined both from chemical and biological viewpoints. Next, detailed characteristics of phorbol esters, as the toxic compound in Jatropha biomass, are described. A comprehensive literature review of established technologies for detoxification of phorbol ester is then presented. Afterwards, plasma reactors for ozone

generation and microbubble technology are discussed, followed by their advantages in relation to the purposes of detoxification. Chapter three provides details of the methodologies and materials used in this study. These include the description of the reactor assembly and experimental procedures employed in reactor characterisation. Further, methodologies of the detoxification study and biological investigation are also provided in detail.

The results and discussion part of this thesis are divided into three following chapters. Chapter four presents the reactor characterisation results. It includes discussions of bubble size distribution data in various flow rates and ozone concentration in two phases: gas and liquid. The aim is to assess performance of the experimental reactor leading to selection of specific operating conditions for application in detoxification experiments. The second set of results, application of microbubble and plasma microreactor technology in phorbol ester detoxification, is presented in chapter five. Study of synthetic and natural phorbol ester detoxification by the proposed technical approach in this research is reported. Detoxification results of treated samples under fixed operating conditions during various ozonolysis periods are analysed and discussed. The optimum ozonolysis period of phorbol ester detoxification is identified. The application of ozonolysis technology in treating lignocellulosic materials is given in chapter six. An integrated study of protein quantification in Jatropha biomass after detoxification is provided. Information about the effect of ozonolysis on total protein content and protein identification is presented. In addition, the ozonolysis effect on lignin content and pH conditions is also explained. Finally, the summary of the main findings, conclusions and recommendations for future work are presented in chapter seven.

CHAPTER 2

LITERATURE REVIEW

This chapter critically assesses related literature on the detoxification of lignocellulosic materials by the proposed technical approach. Detailed information concerning plant morphology of *Jatropha curcas Linn* is presented first, then later narrowed to Jatropha biomass identification. Secondly, the toxic compound, phorbol ester, which limits Jatropha utilisation, is explained with focus on chemical structure and its characterisation. Furthermore, established methods on phorbol ester detoxification are precisely assessed covering chemical, physical and biological treatments. The process efficacy in phorbol ester degradation and drawbacks of each method are discussed deliberately. Proteomic studies of *Jatropha curcas* meal is further described in the following section. Moreover, plasma reactor utilisation with emphasis for the purpose of ozone generation is introduced. The description of ozone reactions with chemical and biological materials is elaborated further. Microbubble technology is considered subsequently with some fundamental studies and highlights of its generation techniques. In summary, a discussion of microbubble enhancement by plasma microreactors as a novel technology proposed in this research is provided in the end of chapter. Application of integrated processes in detoxification approach is the research focus.

2.1. *Jatropha curcas Linn*

As an increase of alternative fuel is globally in demand, the utilisation of agricultural crops as the raw material in biofuel industries should be explored. Various crops have been used, for example corn, wheat, sugarcane, soybean, sunflower and *Jatropha curcas Linn*. In comparison to other crops, *Jatropha curcas Linn* usage has spread more widely due to its

cultivation in poor soils conditions (Mukherjee et al., 2011, Kandpal and Madan, 1995, Heller, 1996). It is a robust shrub or small tree belonging to the Euphorbiacea family. The jatropha genus has over 1000 species disseminated around the world (Heller, 1996, Gübitz et al., 1999, Devappa et al., 2011, Jongschaap et al., 2007). The plant is able to be grown in acid soil, very low soil fertility and also in areas which have high temperatures (Makkar and Becker, 2009). Therefore, this perennial plant is found in various regions around the world. It is widely cultivated in tropical and sub-tropical countries, from South and North America (Mukherjee et al., 2011), to Africa and South East Asia (Waled Abdo Ahmed and Salimon., 2009).

Figure 2.1 presents global distribution of *Jatropha curcas Linn* cultivation regions. It is stated that the approximate latitude for optimum growth of *Jatropha curcas Linn* is 30° N, 35° S where for palm trees (*Elaeis guineensis Jacq*), the growing zone is 4° N, 8° S (Jongschaap et al., 2007). Therefore, regions with extreme climate such as continuous frost are not applicable for *Jatropha curcas Linn* (Jongschaap et al., 2007, Heller, 1996). In addition, Heller (1996) reported that the Jatropha plant has been successfully grown in low altitude (0-500 m) regions with annual average precipitation and temperature, 300-1000 mm and 20-28°C, respectively. Nevertheless, reports on Jatropha growth in areas without rainfall as well as higher precipitation have also been recorded.

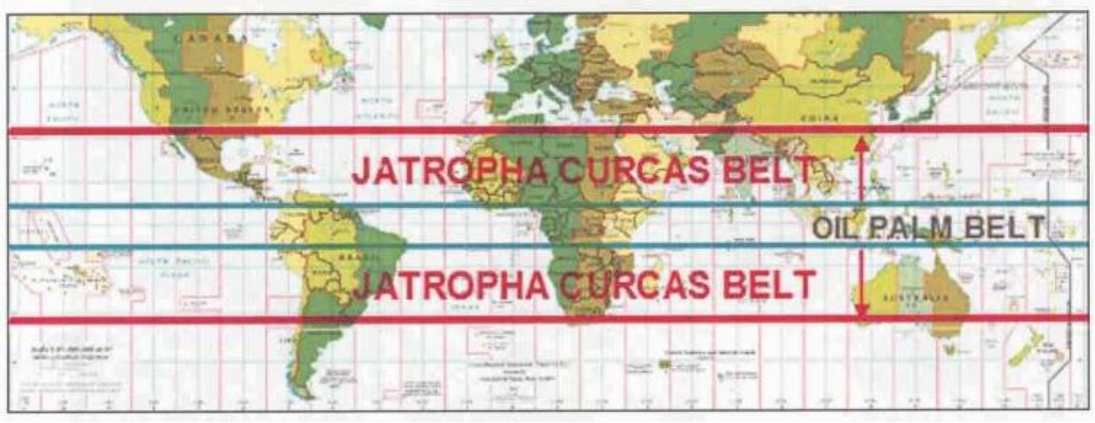

Figure 2.1 *Jatropha curcas* distribution in tropical and sub-tropical regions (Jongschaap et al., 2007)

There is much controversy concerning the native origin of Jatropha plants. It is speculated that the plant was naturally from Central America but no specific region has been identified yet. However, seafarers from Portugal were presumed to have held the key role for *Jatropha curcas Linn* distribution in Asia. It started from the Caribbean to Cape Verde Islands and Guinea Bissau then further distributed to Africa and Asia (Kumar and Sharma, 2008, Heller, 1996, Gübitz et al., 1999, Jongschaap et al., 2007).

Etymologically, the jatropha name is derived from the Greek word, jatrós (doctor) and trophé (food) which has some common medical therapeutic uses (Kumar and Sharma, 2008). The plant previously has been used for various healing treatments. Researchers have mentioned Jatropha use in medicine, for example the oil for skin disease, rheumatism and use of a leaf decoction for postnatal antiseptic (Heller, 1996, Nokkaew, 2008, Gübitz et al., 1999). Figure 2.2 shows the potency of the *Jatropha curcas Linn* components. It is shown that the majority of the plant components offer numerous advantages as a multipurpose crop.

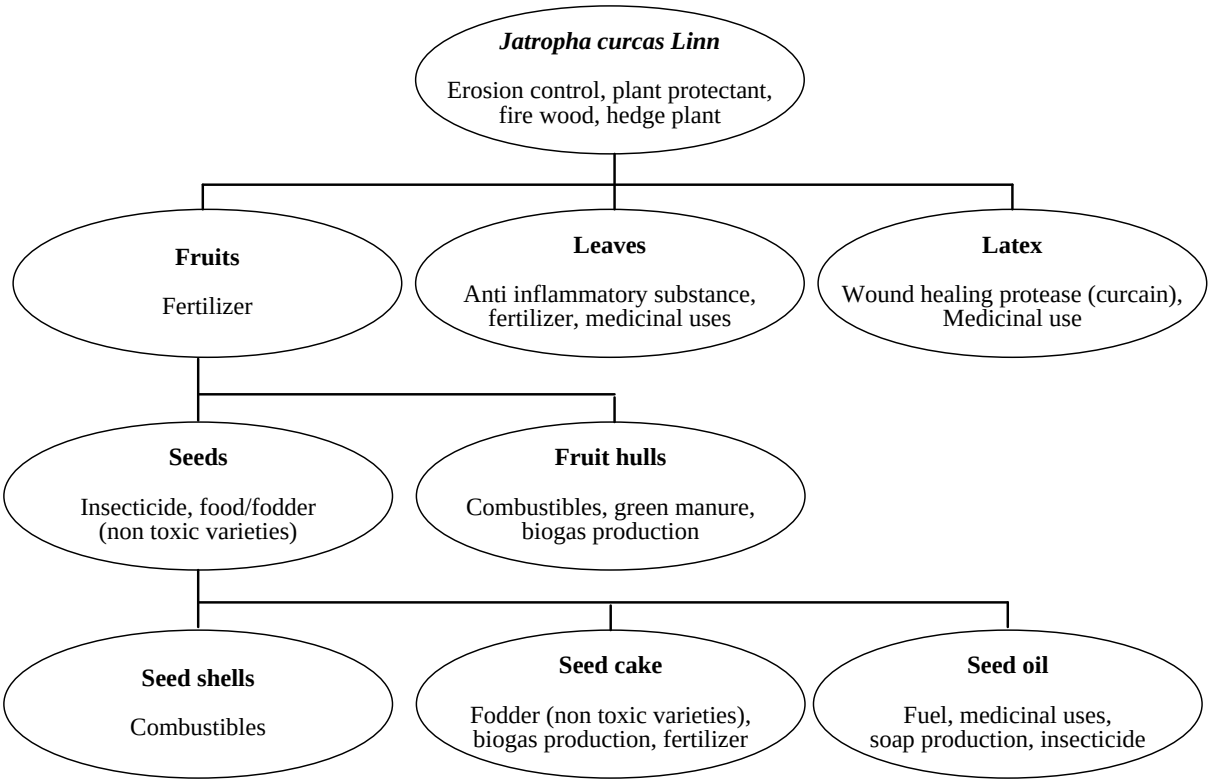

Figure 2.2 Potency of *Jatropha curcas Linn* (Gübitz et al., 1999, Jongschaap et al., 2007)

The jatropha plant is a shrub or small tree that grows with straight stalk to 2-8 meters high with a deep root system. It has a tap root and four lateral roots as the primary roots collated with many secondary roots. It was observed that this root configuration results in carbon storage, soil nutrition stability and water reservation. Latex is found in the branches of the Jatropha plant. The leaves are green with dimensions of length and width of 6-15 cm. Plant generation can be carried out by either generative or vegetative means. Flowers are unisexual where pollinations occur by insect assistance (Heller, 1996, He, 2011). It flourishes between November-December and occasionally in April-May. In addition, each fruit of *Jatropha curcas* consists of three seeds with approximate mass up to 700 mg whilst 60-70% is the seeds kernel (Kandpal and Madan, 1995, King, 2009, He, 2011). Figure 2.3 presents details of jatropha plants including young plant, flowers and seed.

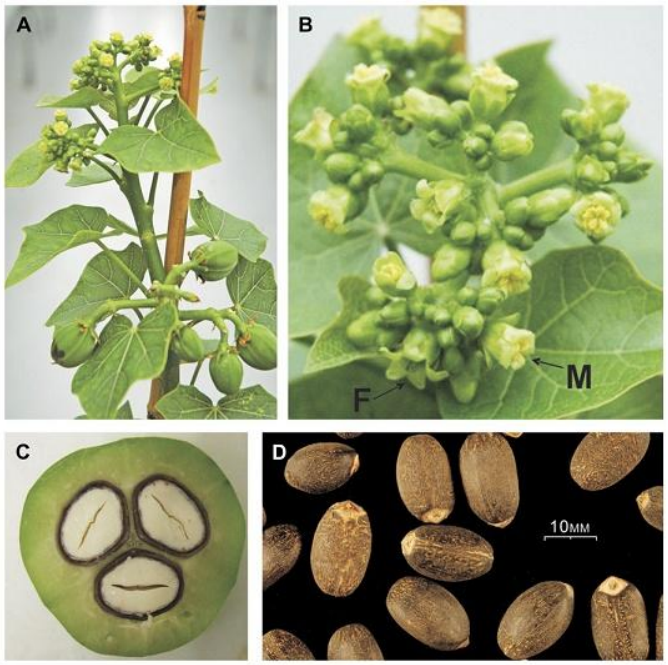

Figure 2.3 Profile of *Jatropha curcas L* plant (A) Young *Jatropha curcas* plant with flower and developing seed pods. (B) *Jatropha curcas* inflorescence contains male staminate flower (M) and female pistillate flowers (F). (C) *Jatropha curcas* seed seen from cross sectional side. (D) Mature seed of *J. Curcas* (King, 2009)

Furthermore, Heller (1996) reported that the four most important fatty acids are contained in *Jatropha curcas* seeds are palmitic acid (C16:0), stearic acid (C18:0), oleic acid (C18:1) and linoleic acid (C18:2). These contents indicate the major potential of *Jatropha* oil as an alternative fuel. Detailed percentages of fatty acid content in *Jatropha curcas* oil compared to other biofuels are provided in Table 2.1.

Table 2.1 Fatty acid content (%) in various biofuels (Gaur, 2009)

Fatty Acid	Jatropha curcas Oil	Palm Kernel Oil	Sunflower Oil	Soybean Oil	Palm Oil
Palmitic (16:0)	14.2	8.4	-	11.0	44.0
Stearic (18:0)	7.0	2.4	4.5	4.0	4.5
Oleic (18:1)	44.7	15.4	21.1	23.4	39.4
Linoleic (18:2)	32.8	2.4	66.2	53.2	10.2
Linolenic (18:3)	0.2	-	-	7.8	0.4

As characterisation of jatropha oil has been done with emphasis at chemical content of engine exhaust from different oils. It is found that the sulphur content in engine exhaust fuelled by Jatropha oil is less than with diesel. This fact is beneficial as sulphur content is a major source of air pollution (Kandpal and Madan, 1995). The potential of producing eco friendly fuel is offered by Jatropha oil. Table 2.2 provides characterisation of Jatropha oil and diesel oil.

Table 2.2 Characterisation of Jatropha oil and diesel oil (Kandpal and Madan, 1995)

Parameters	Jatropha oil	Diesel oil
Specific gravity	0.918	0.841
Sulphur (%)	0.13	1.2
Calorific value (kcal/kg)	9470	10,170
Flash point (°C)	240	50
Cetane value	51	50

Jatropha meal or commonly called jatropha cake is the byproduct after mechanical press of oil extraction from *Jatropha curcas Linn* raw material (He, 2011, Heller, 1996, Jongschaap et al., 2007). In the biofuel industry, the oil is further treated in order to comply with market specification. Jatropha oil is offered to the market to substitute petroleum oil. On the other hand, the byproduct biomass has received less attention relative to oil product. Whilst the oil price has significantly boosted the value of jatropha oil, the Jatropha meal has almost no economic worth. It is only utilised for combustion for internal use of industries.

Jatropha meal offers various potentials, for example its utilisation as cattle feed, fertiliser or human consumption (Wakandigara, 2013, Aderibigbe et al., 1997, Kumar et al., 2011, Makkar et al., 1997). It also can be also used for ruminant nutrition due to 50% higher glutelin fraction to protein. Consequently, low solubility is achieved which reduces rumen

degradability (Selje-Assmann et al., 2007). These potentialities create new market targets in order to increase the economic value of Jatropha meal.

Investigations on the chemical content in Jatropha meal have been performed by many researchers. It is confirmed that Jatropha meal contains high protein value and other essential amino acids (He, 2011, Xiao et al., 2011). Jatropha meal is the leftover biomass from oil extraction; the nutritious content remains. Percentage composition of the jatropha component is described in Table 2.3.High protein content in Jatropha meal gives promise for its further utilisation. Clearly the remaining protein content in Jatropha meal requires particular attention for exploitation. Furthermore, the high ability for gastric digestion makes Jatropha meal potentially favourable as a protein supply for monogastric animals (Selje-Assmann et al., 2007, Annongu et al., 2010).

Table 2.3 Composition (%) of Jatropha Nut, Shell and Meal (Lago, 2009)

Constituent	Nut	Shell	Meal
Protein	22-27	4.3-4.5	56.4-63.8
Oil	56.8-58.4	0.5-1.4	1.0-1.5
Ash	3.6-4.3	2.8-6.1	9.6-10.4
Neutral Detergent Fibre	3.5-3.8	83.9-89.4	8.1-9.1
Acid Detergent Fibre	2.4-3.0	74.6-78.3	5.7-7.0

As indicated, high protein content in Jatropha meal is the major additional benefit for further utilisation. It leads to a promising supply of a highly nutritious source. This distinctiveness enhances the economic value of Jatropha meal as a byproduct. Moreover, the nutrition content of Jatropha meal is above the suggested value by The Food and Agriculture Organization (FAO). It is equal to the intake for children (2-5 years old) of the essential amino acid content in soybean meal (Saetae and Suntornsuk, 2011, Makkar et al., 1998). Table 2.4 shows details of nutrition content in soybean meal and Jatropha meal from different varieties.

Table 2.4 Nutritious content (% in DM) of Jatropha meal from different varieties compared to soybean meal (Makkar et al., 1998)

Nutritious content	Jatropha Variety		Soybean
	Nicaragua	Non-toxic Mexico	
Crude protein	61.2	63.8	45.7
Ash	10.4	9.8	6.4
Lipid	1.2	1.0	1.8
Neutral detergent fibre	8.1	9.1	17.2
Acid detergent lignin	0.3	0.1	0.0

DM = dry matter

Along with the increasing *Jatropha curcas Linn* utilisation for producing biofuel, Jatropha meal production also rises. Makkar and Becker (2009) reported that 270 kg of Jatropha meal was produced from 1T of Jatropha seeds. The Jatropha meal contained approximately 60% of crude protein on a dry weight basis. The oil rich content and high nutritious value indicates that *Jatropha curcas Linn* is a prospective crop for fuel and food stuff. Consequently, exploitation of Jatropha meal along with Jatropha oil can address the demand of fuel and food without conflict. The production of oil will not be compromised because the food stuff will utilise the residuals subsequent to oil extraction. Unfortunately, it is reported that Jatropha meal is toxic for human and animal consumption due to the remaining phorbol ester content presented (Wink et al., 1997, Zucker, 1974, Aderibigbe et al., 1997). Therefore, although Jatropha meal contains various nutritious contents, its utilization is limited.

The phorbol ester compound is an original constituent to the Jatropha plant. The oil production treatments of *Jatropha curcas Linn,* result in no significant impact on this toxic compound. The phorbol ester remains in products, Jatropha oil and Jatropha meal. Genetically, there are two types of jatropha plants, toxic and non toxic varieties, which are

varying in phorbol ester content. The Mexican variety of the jatropha plant is non-toxic. The phorbol ester concentration detected in the Mexican variety is 0.27 mg/ml of oil (Goel et al., 2007, Martínez-Herrera et al., 2006). Genetic diversity results the complete absence of detectable phorbol ester in the Mexican variety, hence confirming its edibility. It is reported that *Jatropha curcas* seeds are consumed in some part of Mexico (He, 2011). Therefore, phorbol ester concentration in Mexican Jatropha derivatives is determined as the threshold for edible Jatropha. On the other hand, the majority of families of the jatropha plant widely cultivated around the world are toxic so non-edible.

2.2. Phorbol ester

Phorbol esters are natural compounds in plants from the Euphorbiacea family. The chemical compound has a polycyclic shape with two hydroxyl groups connected to carbon atoms with esterified fatty acid residuals. The major constituent of this compound is tigliane which is a tetracyclic diterpene and grouped as an alcoholic moiety (Gaur, 2009, Hecker, 1977, Hirota, 1988). It consists of 4 rings which are ring A, B, C and D. Figure 2.4 below shows molecular structure of tigliane. Moreover, some chemical reactions of this structure will result in various types of phorbol esters and affect its chemical behaviour.

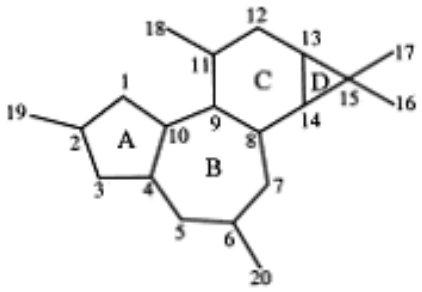

Figure 2.4 Molecular structure of tigliane (Gaur, 2009)

As mentioned above, the structure of the tigliane residue is changed when some chemical reactions occur. Different types of phorbol ester result from hydroxylation in different positions and application of ester bonding in various acid moieties on the tigliane skeleton (Devappa et al., 2010a). The variation of "–OH" group position in the molecular structure, result in two types of phorbol which are Phorbol (α) and Phorbol (β). Phorbol (β) is an active Phorbol which is able to stimulate Protein Kinase C (PKC) that in turns is involved in neurotransmission (Gaur, 2009, Caratsch, 1988), while Phorbol (α) is an inactive Phorbol. Haas et al (2002) isolated six different types of phorbol ester. Currently, there are various types of phorbol ester identified which are jatropha factors 1 to 6 (C1-C6). Figure 2.5 shows molecular structure of Jatropha C1 and C2.

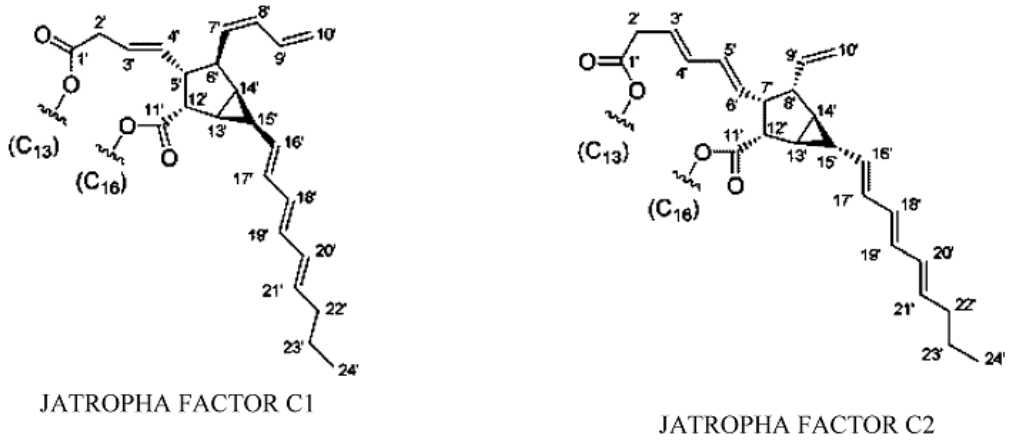

JATROPHA FACTOR C1 JATROPHA FACTOR C2

Figure 2.5 Structures of Jatropha factors (C1 and C2) from *Jatropha curcas* (Haas et al., 2002)

Jatropha factor C1 contains a single carbonyl ester chain at C-12', a bicyclohexane unit, a nonatrienyl residue and a vinyl group. Factor C2 is different to factor C1 in terms of carbon chain length (in factor C1 is C-6' and in factor C2 is C-8'), ester chain length which connects the bicyclohexane unit with C-13 (in factor C1 is C5' and in factor C2 is C7'), and configuration of C-6' in factor C1 and C-8' in factors C2.

Furthermore, jatropha factors C3 and C6 have a cyclobutane ring. Moreover, the difference between factor C6 and factor C3 is that the former has a trisubstituted cyclobutane unit rather than a tetrasubstituted unit of factor C3 and its ester chain length at C-13 of phorbol unit. Jatropha factor 4 and 5 could not be separated by chromatography because it is isolated as epimers. They are different to jatropha factor C1 in terms of carbon chains length and position as well as orientation between bicyclohexane unit and phorbol moiety. Detail of Jatropha factor C3-C6 are presented in Figure 2.6.

All intermolecular diesters result from two separated groups of monoesters and two dicarboxylic groups which are bonded to the phorbol skeleton in OH-13 and OH-16 (Goel et al., 2007). They are isolated from the same diterpene, 12-deoxy-16-hydroxyphorbol (Devappa et al., 2011).

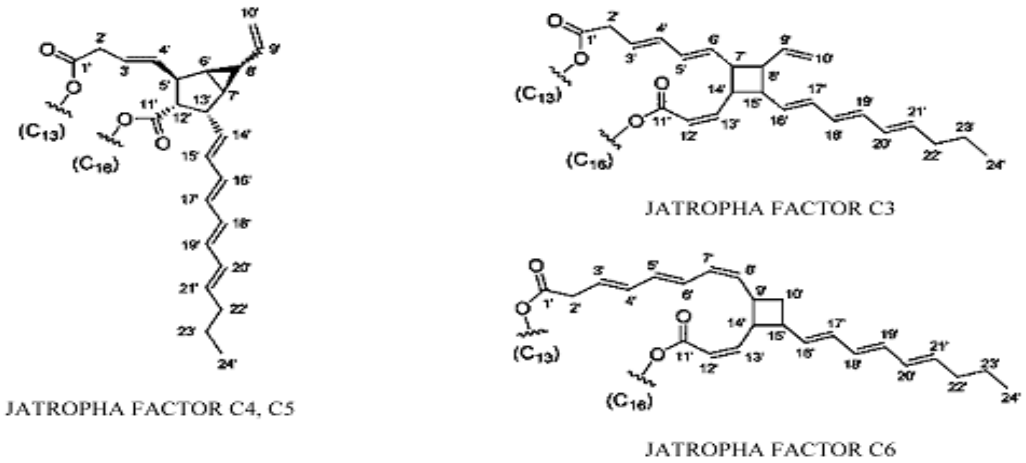

Figure 2.6 Structures of Jatropha factors (C3 to C6) from *Jatropha curcas* (Haas et al., 2002)

The toxicity of phorbol ester, with molecular formula $C_{44}H_{54}O_8Na$ (Mr = 733.37), is linked with cancer formation (Gaur, 2009, Hirota, 1988, Hecker, 1977). It does not cause tumours alone but acts as a tumour growth promoter in following the exposure to a subcarcinogenic dose (Hirota, 1988, Zucker, 1974, Goel et al., 2007). Jatropha meal is assumed to be toxic when the phorbol ester content is higher than the safety consent level for edibility (0.11

mg/g). Non toxic varieties of Mexican jatropha have negligible amounts of phorbol ester, e.g. 0.11 mg/g of kernel while phorbol ester content in toxic varieties ranged from 1-3.5 mg/g of seed kernels (Martínez-Herrera et al., 2006, Goel et al., 2007, Makkar et al., 1997, Nokkaew, 2008). Incidental consumption of Jatropha seeds was reported with effect of nausea, irritation of digestion system, diarrhoea, muscle pain and vomiting (Gübitz et al., 1999, Makkar et al., 1997, Wink et al., 1997). Fatality also occurs with excess presence of phorbol ester concentration in the blood system.

Many investigations have been performed in order to characterise stability of phorbol esters hence its detoxification is feasible. Phorbol ester is a stable compound which is not easily affected by treatment carried out to Jatropha raw material. It is found in the oil and in the defatted part of the plant. The concentration is diverse in different parts of *Jatropha curcas Linn*. Deachathai, et al (2010) investigated phorbol ester concentration in various part of *Jatropha curcas* plant which are leaf, stem and latex. It was reported that phorbol ester concentration were distinctively found in each part of the plant. Phorbol ester content in leaf and stem is 45-48 ppm and 18-19 ppm, respectively. However, no data on latex sample was reported due to incompatible experimentation methods.

Phorbol ester is soluble in polar organic solvent while unstable under acid and alkali conditions (Nokkaew, 2008, Jongschaap et al., 2007). In addition, it is sensitive to light and atmospheric oxygen (Dimitrijevic et al., 2007, Schmidt et al., 1975). Phorbol ester is not only presented as a natural compound, but also as a synthetic chemical. Phorbol-12-myristate-13-acetate (TPA) is used as a synthetic phorbol ester. Investigation was conducted with different temperature and illumination. TPA was diluted in acetone then was stored in normal room condition (25 ^{0}C, diffuse daylight) and controlled condition (4 ^{0}C and -20 ^{0}C, both in dark). It

was confirmed that after 3 months, significant autoxidation of TPA was detected to the sample stored at 25 ^{0}C, diffuse daylight. Furthermore, negligible degradation was found at 4 ^{0}C in dark. Whereas constant initial concentration was detected in sample stored at -20 ^{0}C in dark. In this research, TPA is used for experimental sampling to study the proposed effect of the technology on synthetic phorbol ester. The sample is treated with conditions recommended by Schmidt et al (1975).

2.3. Existing technologies for phorbol ester detoxification

Few approaches to phorbol ester detoxification have been studied, covering chemical, physical and biological treatment. The first approach was chemical extraction using 92% aqueous methanol or 80% ethanol (Makkar and Becker, 1999). Nevertheless, this methodology is not applicable for industrial scale. Methanol is an expensive solvent hence its utilisation in large amounts leads to increasing production cost. In addition, manufacturing cost is expected to rise as downstream treatment is required for the solvent regeneration process.

Furthermore, a combination of thermal treatment and chemical reaction for phorbol ester detoxification has been carried out (Aregheore et al., 2003). Unfortunately, it offered low feasibility as phorbol ester is stable at temperature 160°C for 30 minutes (Aregheore et al., 2003, Kumar and Sharma, 2008). The thermal treatment approach is also detrimental to nutrient content in Jatropha. The majority of protein and amino acids are easily affected by techniques applying high temperature conditions. High temperature treatment applied might cause protein denaturation. Obviously, nutrition content in detoxified jatropha needs to be considered when an edible food stuff product is targeted. Therefore, this method is less profitable in maintaining the protein content of a Jatropha sample.

Haas and Mittelbach (2000) have investigated a phorbol ester reduction method by application of traditional oil refining methods. Their investigation examined the degradation of phorbol ester in each step of the refining process. Phorbol ester concentration was analysed after degumming, neutralisation, bleaching and deodorisation. It was found that degumming and deodorisation resulted in negligible reduction of phorbol ester concentration. On the other hand, a substantial amount of phorbol ester was lost after neutralisation and bleaching process. In the overall analysis, only partial detoxification was achieved by this method. The phorbol ester content was reduced to 55% of its initial concentration. The sample after treatment remained toxic which is still inedible.

Gaur (2009) has studied phorbol ester detoxification by using various solvent extraction processes. It was stated that a sequence extraction procedure is the most efficient route for phorbol ester degradation. The combination of hexane extraction, as non polar solvent, followed by methanol extraction, as polar solvent, resulted in a highly effective process. Phorbol esters attach to lipids which are naturally bonded in the bulk of jatropha meal. It is difficult to extract lipids by polar solvent with phorbol ester attached. On the other hand, phorbol ester has higher polarity compared to triacyl glycerol, the major lipids in jatropha plant. Therefore, it is necessary to extract the non polar oil first to gain effective extraction of phorbol ester on the second stage of the process. However, this method is likely to be less economic since costly chemicals are used.

Other chemical treatments have been investigated to optimise the degradation of phorbol ester (Phasukarratchai et al., 2012, Nokkaew, 2008, Makkar et al., 2009). Makkar et al. (2009) advised additional silica treatment in the oil refining process. It is reported that the acid gums

and wash water after the degumming stage might be harmful for animal feedstock. In addition, wash water produced after the process is not environmental friendly. Nokkaew (2008) observed the utilisation of bentonite as an adsorbent for reducing phorbol ester content in Jatropha seed oil. The research also investigated soaking jatropha meal in a 95% ethanol solution. Moreover, Phasukarratchai et al (2012) used surfactants from the dehydol group or fatty alcohol and polyoxyethylene sorbitan group. Application of adsorbents and surfactants in phorbol ester detoxification approach requires post-treatment. A neutralisation treatment after using such chemicals is required. It is speculated that these chemicals affect the threshold requirement for edibility.

Recent attempts to solve the problem of phorbol ester detoxification include application of biological treatments (Phengnuam and Suntornsuk, 2013, de Barros et al., 2011, Joshi et al., 2011). De Barros et al (2011) used white-rot fungal strains mixed with jatropha cake to be treated as culture and control. Incubation of inoculated and non inoculated (control) samples was performed at a controlled temperature of 28°Cfor 30 days. Approximately 97% phorbol ester removal was achieved by this method. Phengnuam and Suntornsuk (2013) studied the effect of *Bacillus* strains on phorbol ester detoxification. Solid-state and submerged fermentation were carried out with different fermentation periods for each stage, 7 and 5 days, respectively. It was reported that 62% of phorbol ester was removed after fermentation processes with potential treated meal for animal feed. Furthermore, Joshi et al (2011) proposed utilisation of *Pseudomonas aeruginosa* (PseA) in fermentation of jatropha seed cake. Complete degradation of phorbol ester was reported after 9 days of fermentation. Biological treatments relatively require long durations. This is due to the nature of slow metabolic response for the proposed mechanism. It was mentioned that the enzymatic activity of microorganisms reacts to the phorbol ester structure which is hydrolysis-sensitive(de

Barros et al., 2011). The requirement of specific, well-controlled environmental conditions for microorganism growth is another drawback which makes biological treatment less favourable for industrial application.

2.4. Proteomic study of *Jatropha curcas* meal investigation

Currently, there are only a few studies reporting the effect of jatropha meal detoxification by proteomic study. Researchers have used proteomic study to gather more detailed information after protein isolation and separation. The quantitative study involves application of specific analytical devices such as mass spectrophotometer coupled by liquid chromatography and infrared spectroscopy (Ján A. Miernyk and Hajduch, 2011, Vaknin et al., 2011). Furthermore, application of Sodium Dodecyl Sulfate Polyacrylamide Gel Electrophoresis (SDS-PAGE) with electrophoresis is widely used for qualitative analysis (Lestari et al., 2010). In addition, proteomics study can also investigate the effect of detoxification to the protein profile (Liu et al., 2013). This purpose can be achieved through both quantitative and qualitative methods.

Makkar *et al*(2008) have studied the recovery process of protein concentrate from toxic variant *Jatropha curcas* pressed seed cake. Approximately 53% of total protein in seed cake was recovered under controlled solubilisation condition, pH 11 and 60 °C for 1 hour duration. Afterwards, the pH was decreased to 4 for the precipitation stage. Protein concentration was determined by multiplying nitrogen value with protein factor (N × 6.25). Nevertheless, significant traces of phorbol ester were found in the protein concentrate after treatment. It prevented utilisation of jatropha cake as a protein ingredient for cattle food. Further processing to reduce phorbol ester content was required to achieve the edibility requirement for livestock.

Investigation of protein recovery for non edible purpose has been performed with focus on process optimisation to improve protein concentration (Lestari et al., 2010). Experimentations were done by application of counter current multistage extraction. *Jatropha curcas* seed press cake was extracted with NaOH solvent in different ratios during counter current processing at room temperature. The recovery percentage value and protein functional properties were investigated. It was observed that higher ratio of solvent to solid led to higher protein recovery. The number of multistage extraction steps also affected the recovery value. Moreover, no effects on protein properties were detected during experimentation. SDS-PAGE with application of Electrophoresis with pre-cast gel was used to determine the protein molecular weight distribution. It showed that distribution of protein molecular weight remained within the initial range of 3-98 kDa.

Hydrolysis of protein from the non toxic variant of *Jatropha curcas Linn* has been observed by application of enzymatic activator (Marrufo-Estrada et al., 2013). Defatted Jatropha flours were hydrolysed with Alcalase enzyme and some pepsin. The protein hydrolysates were then further analysed by SDS-PAGE method. According to the resulted pattern, protein profile was characterised as low molecular weight with range 8-130 kDa. This indicated small peptides were produced during extensive hydrolysis of pepsin hydrolysates. The experimental results confirmed the nutritious contents of jatropha flour were enhanced by hydrolysis with enzymatic treatment. The utilisation of non toxic Jatropha derivates is possible for edibility.

Vaknin *et al* (2011) have used advance infrared spectroscopy for analysis of chemical and biological content of *Jatropha curcas* seed. Protein concentration was one of the parameters inferred by near infrared reflectance spectroscopy (NIRS). Moreover, the actual value was determined by Kjeldahl method with 5.75 conversion factor of nitrogen content. The

inference value of protein concentration from NIRS analysis gave a positive correlation to the actual value from conventional methods. It indicates that NIRS is feasible to be a potential analytical approach in proteomics.

As it has been explained, the majority of investigations focus on reduction of phorbol ester without simultaneously considering the protein content. Studies on proteomic concerns have been reported independently to the detoxification investigation. Therefore, an integrated study is required by developing a methodology which can detoxify phorbol ester but maintain the protein content in jatropha meal. A low energy mechanism is desirable to suppress production costs for competitive markets. Moreover, an eco-friendly and effective process would be favourable which is not time consuming to perform detoxification.

2.5. Application of plasma reactor in ozone generation

Plasma refers to an ionised gas which is electrically neutral, equal amounts of positively and negatively charged ions, and often defined as the fourth state of matter. The ionised gas results from oscillations considered as compressed electrical waves, similar to sound waves (Langmuir, 1928). It is also declared by Langmuir that: "Except near the electrodes, where there are *sheaths* containing very few electrons, the ionised gas contains ions and electrons in about equal numbers so that the resultant space charge is very small. We shall use the name *plasma* to describe this region containing balanced charges of ions and electrons". Plasma sheath is defined as the transitional region which separating plasma and its boundaries. Unlike the plasma and the boundaries, characteristics of plasma sheaths are distinctive which give an impetus to the movement of charged particles (Fridman, 2008). Figure 2.7 illustrates plasma existence compared to other state of matters.

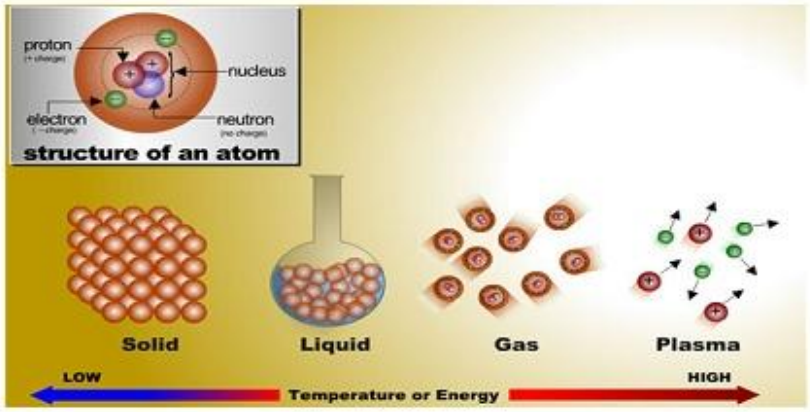

Figure 2.7 Various states of matter*

*adopted from NASA Live Solar Images in (Cheng et al., 2007)

In nature, plasma presents as lightning, solar corona, nebula, aurora borealis and in the ionosphere layer of the Earth. Furthermore, plasma generation for laboratory experimentations has been common over decades. In principal, plasma is classified into thermal and non thermal plasma of which natural examples are solar plasma and aurora borealis, respectively. Electron temperature (T_e), vibrational mode excitation temperature (T_v), ion temperature (T_i), rotational degrees of freedom of molecules (T_r) and gas temperature (T_0) are major parameters in plasma characterisation. It is determined in order as $T_e > T_v > T_r \approx T_i \approx T_0$. For research purposes, non thermal plasma is commonly applied. It is generated at low current and under high voltage discharge conditions. In addition, the gas temperature is found to be approximately the same as room temperature although the electron temperature is around 10,000K which is equivalent to a mean electron energy of about 1 eV (Fridman, 2008, Kogelschatz et al., 1988).

Nehra *et al* (2008) have summarised various types of non thermal plasma reactors. Corona discharge, atmospheric pressure plasma jet and dielectric barrier discharge were described. Corona discharge was the first type of plasma reactor. Typically, this reactor's discharge is produced from a pair of non symmetrical electrodes with dc voltage powering continuously or

by pulsing. The non homogenous configuration of electrode is surrounded by the electric field generated. An atmospheric pressure plasma jet creates radio frequency interference during discharge ignition. It speeds up the free electrons from the central electrodes hence energetic collisions within the feed gas occur quickly. Another class of plasma reactor, Dielectric barrier discharge (DBD) is also non thermal. DBD is called a silent discharge, since typical discharge is generated from AC power, and operates in atmospheric pressure and moderate gas temperature. Figure 2.8 shows the configurations of non thermal plasma reactors.

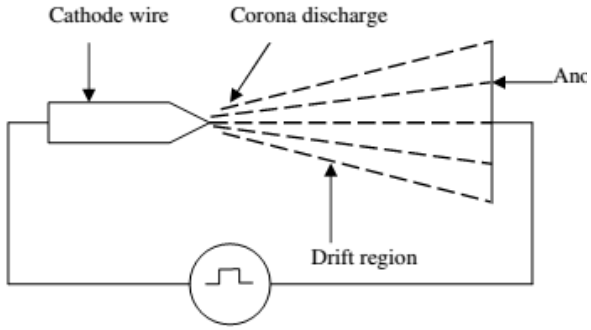

Corona discharge

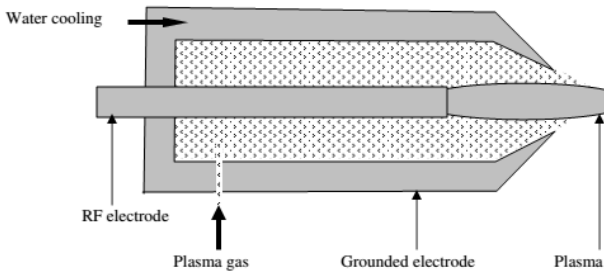

Atmospheric pressure plasma jet

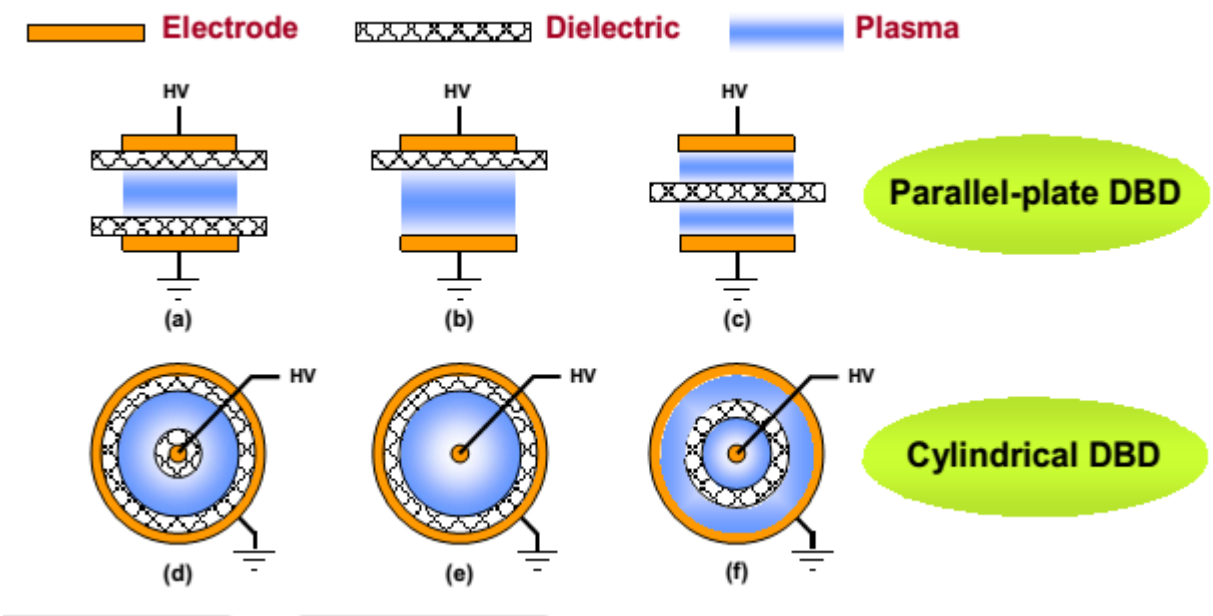

Dielectric barrier discharge

Figure 2.8 Configurations of non thermal plasma reactors (Nehra et al., 2008, Wu, 2012)

Typically a DBD reactor consists of two metal parallel electrodes which are separated by a small gap in between. To be termed a DBD reactor, at least one electrode is required to be

covered by a dielectric layer. The dielectric layers are exclusively made from insulators such as glass, ceramic and quartz. It aims to provide electrical pathway of micro-discharges distribution (Kogelschatz, 1997, Fridman, 2008, Wagner, 2003). In order to ignite plasma, gases are passed through the electrodes and induced by electrical current. Various gases can be used to generate plasma such as helium, neon, argon and air. The DBD plasma can consist of independent currents filaments, so called micro-discharges (Kogelschatz, 1997). The occurrence of micro-discharges in DBD configuration develops due to attaining a sufficiently strong electric field in the reactor gap to exceed the breakdown point. These micro-discharges are distributed homogenously on the dielectric surface with nanosecond duration (Wagner, 2003). Figure 2.9 shows plasma ignition in a DBD reactor where one electrode was covered by electric layer.

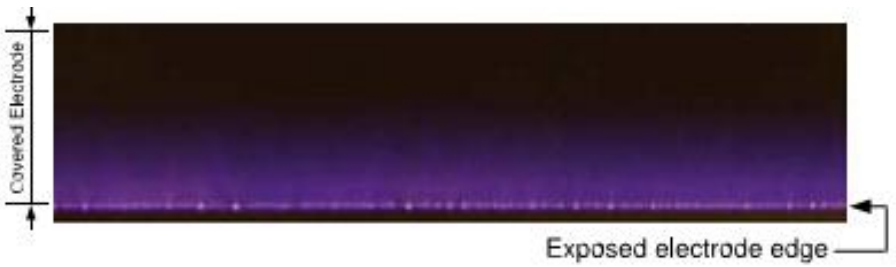

Figure 2.9 Plasma generation in Dielectric Barrier Discharge (Corke et al., 2009)

Fundamentally, the micro-discharge generation is determined by the breakdown voltage, the applied voltage for the onset of ionisation due to sufficient electric field. This breakdown voltage is dependent to two main parameters which are type of gas and gap distance between electrodes (Kogelschatz, 1997, Fridman, 2008, Wagner, 2003). This mechanism is commonly explained by the Paschen Curve, as presented in Figure 2.10. It presents possible breakdown voltage of various gases in related to the reactor configuration. Pd number is referred as correlation of pressure (p) and distance between electrodes (d). As mentioned before, a DBD reactor mainly operates under atmospheric pressure hence the gap between electrodes plays

the essential role. The closer distance between electrodes, the lower breakdown voltage required for most distances, certainly above minimum level of the breakdown voltage. This concept issued in plasma reactor design to gain optimum process efficacy.

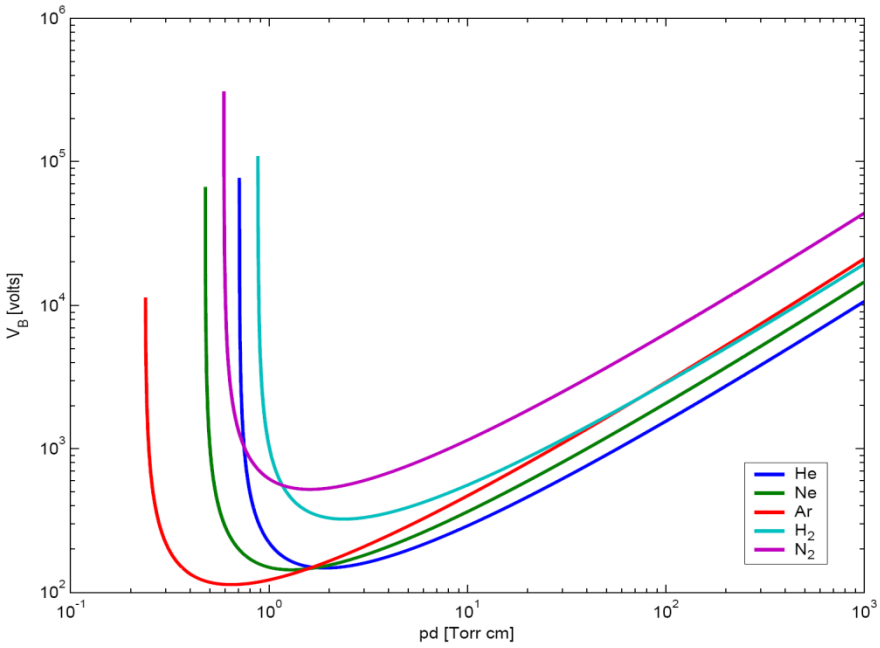

Figure 2.10 Paschen curve of plasma breakdown voltage in various gases

The capability of DBD reactor for operation under atmospheric pressure is the main advantage for its application in industrial sectors. It provides beneficial for low operating cost as no specific pressure controllers are required. In addition, the homogenous discharge generated by DBD reactors is significantly beneficial for chemical reactions. It has also been reported that DBD reactor offers low energy consumption and high conversion of yield (Lozano-Parada and Zimmerman, 2010).

One of the primary applications of plasma discharge is for ozone production which is widely used for water treatment. Ozone generally can be produced by several methods such as electrocatalysis, ultraviolet irradiation and electric discharge involvement. As described in Figure 2.11, ozone is produced by passing oxygen rich gas through high electric field. Due to the electrical induction, the oxygen molecules are split then further converted into ozone

molecules (Barlow, 1994, Pekárek, 2003, Chalmers, 1998). Utilisation of electric discharge, particularly plasma discharge, is favourable due to flexibility in controlling operation variables. The variables such as operating voltage, electrode geometry, type of gas and gas pressure can be adjusted. Consequently, desirable thermodynamic properties during processing can be obtained (Pekárek, 2003). Furthermore, ozone utilisation has been commercially applied in industries for various objectives such as water treatment (Agency, 1999), aquaculture, food processing and effluent treatment (Barlow, 1994).

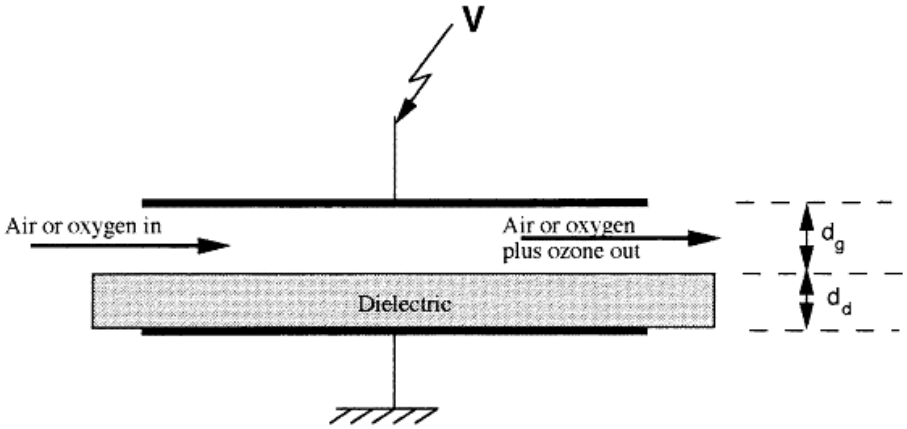

Figure 2.11 Ozone generation mechanisms through dielectric discharge (Chalmers, 1998)

Conventionally, corona discharges and DBD are the two most common non-thermal plasma reactors applied for ozone generation in industrial scale (Chalmers, 1998, Alemskaya, 2003). However, utilisation of corona discharge is limited due to the inhomogeneous electric field generated (Nehra et al., 2008). Corona reactors are not flexible in operation and produce excessive ozone that is expensive to be disposed. In addition, ozone production at industrial scale of corona reactors requires specialised high voltage power generators and dedicated physical infrastructure (Singh, 2007).Therefore, the DBD option is now well established as industrially reliable.

Ozone is an inorganic compound that consists of three oxygen atoms arranged in a linear structure. It is colourless, partially soluble in water and typically conductive in gaseous form. It occurs naturally in the earth's atmosphere when oxygen is activated by UV light and also produced in thunderstorms (Barlow, 1994, Franken, 2005). Moreover, artificially produced ozone can be found in photocopiers, electric motors, etc. Ozone is known to be a powerful oxidant with an oxidation potential of 2.07 V (Franken, 2005, Babikov, 2003). It has been successfully used in various applications, for example in killing bacteria, algae, spores and vanishing volatile organic compounds, odour treatment, enhancing fertilization and water treatment (Agency, 1999). Exclusively in water treatment, ozone has been recognised by its ability in oxidising materials over 100 times faster in comparison to other oxidant agents (Barlow, 1994). Table 2.5 presents the oxidation potential of various oxidant agents.

Table 2.5 Oxidising Potential of Various Oxidants (Barlow, 1994)

Oxidants	Oxidising Potential (V)
Fluorine	3.06
Hydroxyl free radicals	2.80
Atomic oxygen	2.42
Ozone	2.07
Permanganate	1.67
Chlorine dioxide	1.50
Chlorine	1.36
Oxygen	1.23
Bromine	1.09
Hypochlorite	0.94

In general, treatment using ozone technology has several advantages: (i) ozone can act as a neutralisation agent for removing organic odour; (ii) it is less corrosive compared to other common chemicals, (iii) its application requires little operator supervision (Franken, 2005). Chemical treatment using ozone is usually termed ozonolysis. This is a promising approach

for some experimental processes since it is inexpensive (Diwani et al., 2011). Ozonolysis is recognized as a clean technology as no byproduct is produced. The non reacted ozone molecules will dissociate back into oxygen. Consequently, there is no need to have additional processing for neutralisation which influences the process cost. Moreover, it is found that in one ozonolysis stage, spontaneous and exothermic decomposition occurs (Schiaffo and Dussault, 2008). This feature of chemical processing should be taken in to consideration when experimental work using ozonolysis is involved. Babikov et al (2003) suggested that as a metastable state, reaction involving ozone occurs quickly. It is beneficial for chemical reaction which requires fast process mechanism.

Ozonolysis has the advantage of ease of control in chemical processing (Banerjee and Wong, 2002). It efficiently acts as strong oxidative agent in cleavage of double bond carbons (Baber et al., 2005, Irfan et al., 2011). Several researchers have investigated ozonolysis treatment of unsaturated fatty acids to analyse its effect on the carbon double bond (Cvetkovic et al., 2008, Mittelbach and Poklukar, 1990, Neumeister et al., 1978). The difference in double bond location in fatty acid affects structural identification (Zhang et al., 2011). Furthermore, the existence of ozone molecule (O_3) and hydroxyl free radicals (•OH) are detected during ozonolysis. Their presence plays significant roles in chemical reactions within molecule structures of interest (Barlow, 1994, Kongmany et al., 2013). Ozone and hydroxyl radicals are expected to attack the carbon double bonds in fatty acids molecular structure.

Cvetkovic *et al* (2008) studied the effect of ozonolysis and chemical reduction in the molecular structure of some vegetable oils. The research was aimed to produce profitable monomers from soybean and castor oil. A commercial ozone generator was used in order to perform the ozonolysis. A chemical reduction pathway by sodium borohydride was carried

out subsequent to ozonolysis. It is found that oxidative cleavage occurred during ozonolysis. A well characterised product, 9-hydroxynonanoic acid methyl, was produced after ozonolysis was followed with the step reductive. This monomer is useful for polyester synthesis.

The investigation of ozonolysis for polyunsaturated fatty esters in solvent mixtures was reported by Mittlebach and Poklukar (1990). The study focused on ozonolysis of unsaturated fatty acids for structural analysis. A hydrogenchloride-methanol mixture was used during experimentation with no specification for the ozone production method used. Results of complete and partial ozonolysis on chemical product detection were compared. In complete ozonolysis, the expected methyl 3,3-dimethoxypropanoate was produced. There was no byproduct detected afterwards which confirmed that complete decomposition had occurred. However, regioselective pathways did not take place in partial ozonolysis as predicted. Regioselective was defined as a preference of specific direction in chemical bonds, in this case double bonds, in polyunsaturated fatty esters. This phenomenon indicates that ozone randomly attacked the molecular structure of fatty esters. All double bonds were equally labile.

Ozone cleavage for esters has been explored over decades (Neumeister et al., 1978). Ozonolysis was performed with olefins solvated by alcohols mixture with anhydrous hydrochloric acid. The double bond cleavage was observed in excessively low operating temperature -50 to -70 °C. Approximately 90% of expected esters were produced and only 62-85% of isolated esters were detected. The lower yield was believed to be due to incompatible process procedures.

Ozonolysis of carbon double bonds is well described by the Criegee mechanism, shown in Figure 2.12. The reactions occurs in three different stages which are (Reaction I) "primary ozonide" formation, (Reaction II) "primary ozonide" decomposition to be carbonyl compound and "carbonyl oxide", (Reaction III) "carbonyl oxide" insertion to carbonyl compound structure. It is reported that during the decomposition stage (Reaction II), selective cleavage of chemicals bonds takes place. The oxygen bond (O-O) and carbon bond (C=C) split whereas the stronger bond (C-O) remains intact (Criegee, 1975).

Reaction I Reaction II

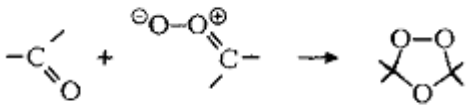

Reaction III

Figure 2.12 Detail reactions of Criegee mechanism (Criegee, 1975)

Ozone technology has been specifically applied to study its effect on carbon double bonds of biodiesel (Baber et al., 2005) and in phorbol ester detoxification field (Kongmany et al., 2013, Diwani et al., 2011). Ozone is expected to attack carbon double bonds (C=C) in the phorbol ester structure which might cause its molecular recombination. The double bond cleavage is predicted to modify the molecular strength of its configuration hence toxicity level is affected.

Investigation of the effect of ozonolysis in biodiesel, particularly on the carbon double bonds under extreme operation conditions, has been reported (Baber et al., 2005). Methanol and dichloromethane were used as solvent with triethylamine as catalyst where ozonolysis was

carried out at -75 ^{0}C. The study aimed to analyse the molecular structure of methyl soyate as biodiesel sample after ozonolysis. Fourier Transform Infrared Spectroscopy (FTIR), Gas Chromatography (GC) and Gas Chromatography-Mass Spectrometry (GC-MS) were used for structural analysis. A reduction of 90% of the number of double bonds in the mixtures resulted after 2 hours of ozonolysis. The theoretically predicted ester products of ozonolysis were found. This indicates that chemical based reaction in combination with ozone treatment influences the double bond configurations. Further experimentation into ambient temperature was recommended to meet industrial process requirements.

Kongmany et al (2013) have studied phorbol ester (PE) reduction by ozone in micro-litre scale with preliminary experimentation. The plasma plume was directly irradiated towards prepared pure PE solutions. Helium gas was passed through dielectric barrier discharge (DBD) reactor in order to generate plasma. Synthetic and natural PE samples prepared in aqueous and methanol solutions were used during the investigation. Natural PE was obtained from Jatropha PEs stock solution with no specification of the extraction method. Ozone was produced due to high energy contact of plasma with oxygen molecules (O_2) and water vapour (H_2O). The process led to ozone (O_3) and •OH formation which further diffused to the system through the air-liquid interface. Approximately 16% of synthetic PE and complete natural PE were degraded after 15 minutes of plasma irradiation in aqueous solution. Furthermore, complete degradations of both synthetic and natural PE in methanol solution were achieved after 15 minutes treatment. However, helium utilisation and direct contact of plasma irradiation into toxic samples have raised safety concerns. In addition, helium is an expensive gas hence its application for large scale processing is not economically feasible.

Ozone treatment combined with chemical catalysis has been performed to reduce phorbol ester (PE) content in Egyptian Jatropha seed cake (Diwani et al., 2011). In addition, γ-radiation treatment was conducted in order to study the process efficacy of the detoxification approach. Fifty milligrams per litre of ozone were dosed into samples subsequent to sodium bicarbonate ($NaHCO_3$) addition. It is observed that PE reduction through γ-radiation was close to that of ozone-chemical based. The γ-radiation was carried out from a cobalt source with dose 50 kGy. Over 75% of PE was reduced after ozone-chemical treatment while 71% reduction was detected after γ-radiation. Nevertheless, this method has not been seen as technically applicable for industrial application. It is rather difficult to control the process in particular for process stability, safety and reliability.

It looks promising to realise the ozonolysis performance via ozone injection to the bulk of liquid. The key factors for efficiency of gas-liquid processes are a surface of gas-liquid interface and gas-liquid diffusion coefficient. In order to maximize it, gas should be injected to the liquids in form of microbubbles (Zimmerman, 2008). The basic components of microbubble ozone injection techniques have been reported (Kuvshinov et al., 2014a).

2.6. Microbubble technology

Microbubble technology has been recognised over decades as a promising route for intensification of water treatment processes and chemical reactions. Some fields of applications are separation, de-emulsification, aeration, micro algal flotation and electro-flotation (Muroyama et al., 2013, Agarwal et al., 2011, Hanotu et al., 2013). This technology offers effective impact to some emerging issues because of its unique characteristics. There is no agreement yet between researchers about the size range for microbubbles but it is currently defined as bubbles for which size ranges from 1-1000 μm (Parmar and Majumder, 2013).

Bubble characterisation and visualisation has been previously carried out using several techniques including photonic, acoustic and optical micromanipulation as well as high speed camera (Vagle, 1998, Garbin, 2006).

The methods for microbubble generation including nozzles, membrane and gas sparger have been summarised by Li (2006a). According to the generation mechanism, there are three types of methods which are pressurisation, cavitation and rotating flow. The pressure difference is the main driving force in microbubble generation. Highly pressurised water is saturated with gas then injected to ambient pressure through a small nozzle. Therefore, microbubbles are generated due to instantaneous pressure reduction. Furthermore, microbubble generation by cavitation mainly occurs in Venturi tubes. Cavitation is defined as the formation of vapour cavities in the liquid due to quick pressure decreases. Stabilised vapour cavities become bubbles. Following the design of a Venturi tube, small bubbles are produced in a liquid flow by a downstream pump. Subsequent to rising velocity and a decrease of pressure, gas is sucked into the tube then collapses. This phenomenon results in small bubble generation. Moreover, rotating flow also generates bubbles in a conical chamber. The mechanism uses a water pump injected tangentially. It results in rotational fluid flow forming the vortex motion. Microbubbles are produced from high rotational velocity from low pressurised area in the centre of chamber.

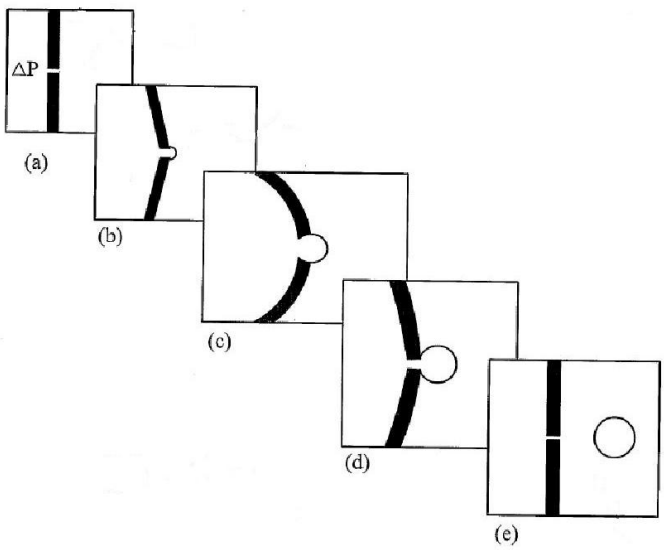

Figure 2.13 Bubble growth mechanism (Zimmerman and Tesar, 2008)

Figure 2.13 illustrates physical mechanism of bubble growth from a pore of a membrane. In a surface of the membrane, pressure difference exists in a pore (a) due to gas flow which expands the pore. In proportion to gas flow through the system, pressure increase therefore the pore is deformed along with bubble generation (b). Bubble generation is accelerated because of this phenomenon (c). Nevertheless, in (d), pressure drop is decreasing in which natural rebound because of membrane elasticity, is started. Further of this natural force facilitation, bubble is released and pore is closing off (e).

High specific interfacial area, slow rising velocity and high internal pressure are major advantages of microbubble technology (Li, 2006a, Parmar and Majumder, 2013). Specific interfacial area is defined as the ratio of interface surface area per unit volume of dispersions. This feature can be expressed by Equation (2.1) and (2.2) as explained in Hanotu (2013). Smaller bubbles lead to higher specific interfacial area as the surface area interface increases. Larger contact area, due to wider surface area, results in greater mass transfer across gas-liquid interfaces.

$$\frac{S}{V} = \frac{4\pi r^2}{\frac{4}{3}\pi r^3} \quad (2.1)$$

$$S = \frac{3}{r} V \quad (2.2)$$

Where S is the surface area of bubble and r is the radius of bubble. The calculation shows that the bubble diameter rises inversely proportional to bubble surface area to volume ratio. Moreover, longer residence time of bubble is a consequence of slow rising velocity hence the contact time between bubbles and chemicals of interest is also longer. It is useful because longer contact of bubbles affects the effectiveness of chemical reactions. Tesar, et al (2008) explained in their patent document, bubble breaks off due to buoyancy force exceeding wetting force. Buoyancy force is defined as a net upwards force of an object submerged in a liquid (Wilkes, 1999). Figure 2.14 illustrates various forces acting on a submerged object.

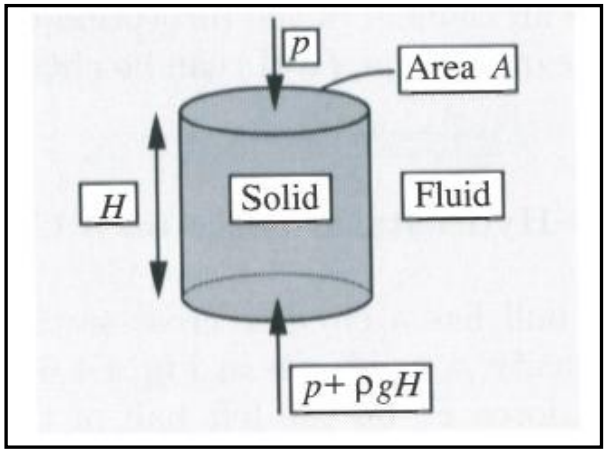

Figure 2.14 Existing pressure force of a submerged object in a liquid (Wilkes, 1999)

Forces on curved surface of vertical direction may be neglected because they act horizontally towards curved vertical surface. Therefore, the net upwards force because of pressure drop between bottom and top surfaces is explained by equation (2.3) as bellow:

$$F = (p + \rho gH - p)A = \rho gHA \quad (2.3)$$

F is the net upwards force where p is pressure, ρ is density of the liquid, g is gravity, H is the height of an object and A is the area of an object. The buoyancy force is equal to the weight of displaced liquid (Wilkes, 1999). It is shown that this force is proportional to area of a submerged object. A smaller bubble has smaller area, hence results in a smaller buoyancy force thus lower bubble rising velocity, according to Stokes Law (Wilkes, 1999).

Furthermore, high internal pressure inside bubble is enforced by surface tension. Surface tension is defined as a physical property of liquid which represents "the surface free energy per unit area at constant temperature" (Clift et al., 1978). Smaller size of bubble generates greater pressure inside bubbles which also positively influences mass transfer during reactions. This phenomenon is explained by the Young-Laplace equation (Eq. 2.4) as follow:

$$P_{internal} - P_{external} = \frac{4\sigma}{D_b} \quad (2.4)$$

P is defined as pressure in which represents as inside and outside bubble where σ is the surface tension of the liquid and D_b is the bubble diameter. It is shown that pressure difference between bubble and its surrounding is inversely proportional to bubble diameter. Higher pressure drop results in smaller size of bubbles generated. Moreover, the highest pressure drop is created at the stage of bubble collapsing. It further affects the quantity of dissolved gas surrounding collapsed bubbles. The amount of dissolved gas is rising when gas pressure increases (Parmar and Majumder, 2013, Agarwal et al., 2011). Therefore, microbubbles technology is beneficial to be applied with other chemical process, for example ozone treatment. The production of free radicals during ozone treatment is accelerated due to rising amount of ozone decomposition due to the dissolution of microbubbles (Takahashi et al., 2007).

Microbubble technology has been applied in combination with chemical processes, i.e ozone treatment and other liquid based processes (Agarwal et al., 2011, Kuvshinov et al., 2014b, Li, 2006b). Agarwal et al (2011) have discussed the application of microbubble in disinfection of waste water by ozonation approach. The formation of •OH in a bubble environment is believed to be the key factor which leads to the reaction. They investigated the effect of ozone microbubble for *Escherichia coli* treatment. The experiments were conducted at pressure of 304–1013 kPa. It was confirmed that ozone dissolved more quickly from microbubbles compared to conventional technology (Parmar and Majumder, 2013, Takahashi et al., 2007).

Furthermore, published work along with this research has been conducted by using microbubbles in combination with ozone treatment. This study focused on the molecular recombination of toxic chemicals by the ozone-microbubble delivery mechanism (Kuvshinov et al., 2014b, Siswanto et al., 2014). Microbubble technology is seen as an alternative mechanism to deliver ozone molecules into the bulk of liquid. Ozone dispersion into an aqueous system enhances mass transfer across the gas-liquid interface during processing. This is due to the reactivity of ozone in the liquid phase, which according to Le Chatelier's principle, results in greater mass transfer. It has been studied that ozone solubility in water-based system is relatively efficient for chemical reactions (Bińˌ 2004).

In addition, the specific features offered by microbubble technology are observed as favourable for gas diffusion. Microbubbles are regarded as an effective way to enhance the mass transfer in ozonolysis. The mass transfer efficiency between gas phase and liquid phase of ozone has been evaluated (Li, 2006b). Microbubbles were generated through high velocity of air rotating flow in water system while ozone molecules were produced by a purchased

ozone generator. It reported that high ozone transfer efficiency is achieved in low air flow rate; less than 5 L/min.

As described before, microbubbles provides high surface area to volume ratio, fast heat and mass transfer as well as longer residence time. This gives higher efficiency in staging a multiphase process (Zimmerman, 2008, Burns et al., 1997). Energy efficient microbubble generation is not widespread yet in industry. Nevertheless high demand for gas-liquid process intensification has driven development of new microbubble generation techniques. Zimmerman et al (2008) have proposed fluidic oscillator application as an profitable option in microbubble generation which can condition the bubble size. A fluidic oscillator device and its principle mechanism are shown in Figure 2.14 below.

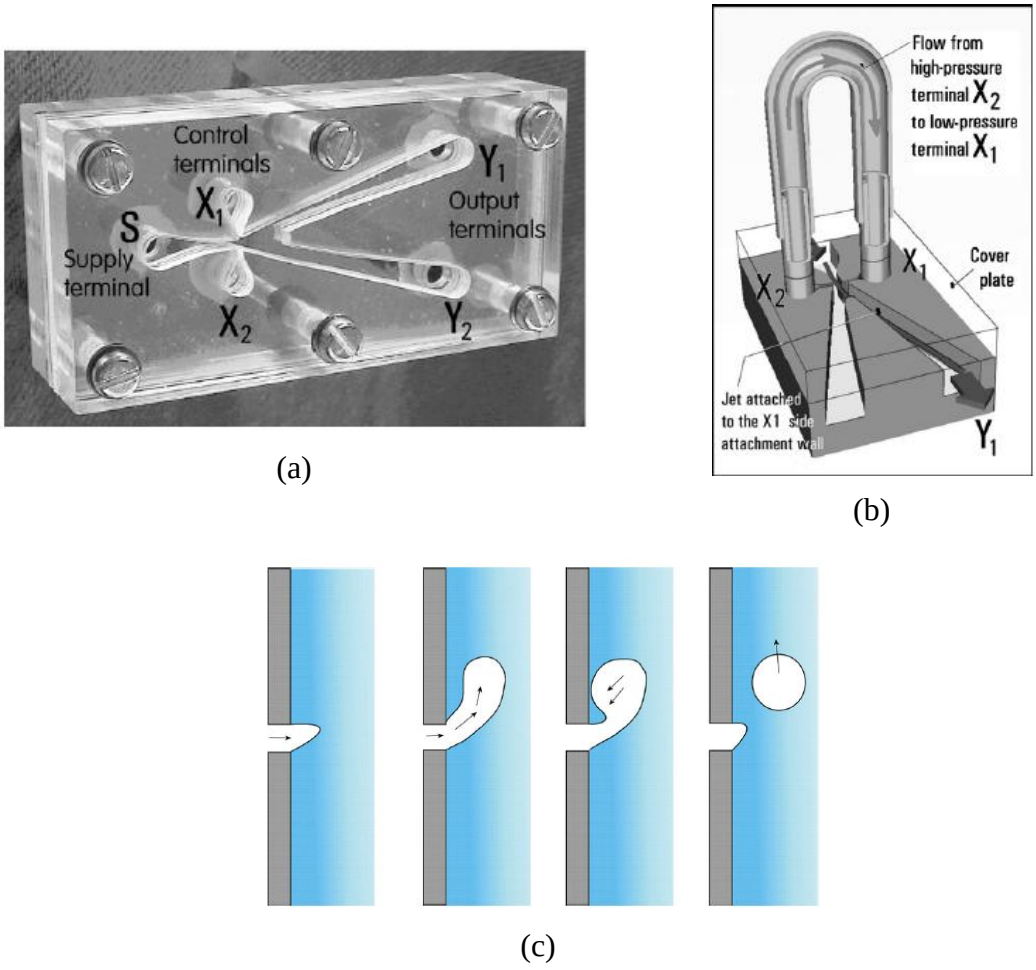

(a) (b)

(c)

Figure 2.14 Model (a) and principle mechanism of fluidic oscillator (Zimmerman, 2008)

Microbubble generation via fluidic oscillation has shown a remarkable improvement in bubble throughput and dramatic reduction in bubble size without the concomitant expenditure of high energy. This process therefore can be seen as a highly sustainable and economic way to generate microbubbles. A fluidic oscillator has been described by Tesař (2012) as a no moving part synthetic hybrid jet microfluidic device (Figure 2.14 a). Fluidic oscillator (FO) is one of the microbubble generators which offer low power consumption with bubble size as desired (Zimmerman, 2008). The basic principle of FO is the pulsation of air flow. Air passes from supply terminal then switches from one control terminal to the opposite one due to the Coanda effect (Brittel et al., 2015, Zimmerman, 2008). The FO consists of a fluidic valve for jet diversion, with a feedback loop attached to self actuate the switching of the jet periodically (Figure 2.14 b). There are no moving parts, hence no mechanical maintenance issues. The compact and robust design of FO makes it applicable for industry plants of different scale.

Zimmerman and Tesar (2008) explained the detailed mechanism of fluidic oscillation driven microbubbles generation (Figure 2.14 c). The upstroke of fluidic pulse results in hemispherical cap while the down stroke pinches off due to small backflow. There is an overall force imbalance since the inertial force of the gas pulse exceeds the wetting anchor force. There is a smaller wetting force due to small backflow creating a lubrication effect on the pore wall. Inertia is higher for the same exposure time for steady flow as the pulse has more than double the amplitude of the constant inertia of steady flow with the same headloss. Bubble detachment is controlled by frequency. The higher frequency, the smaller the bubble size produced, until the inertial of the pulse becomes insufficient to overcome the wetting force. Thereafter there is only a modest difference in average bubble size with frequency rise (Brittle et al., 2015).

2.7. Microbubble technology enhanced by plasma microreactor

An integrated approach is required by developing technology for the degradation of toxic materials which does not negatively affect the nutritious components. This research focuses on the development of technology to detoxify phorbol ester but maintain the protein content in Indonesian Jatropha Meal. The hypothesis that is tested is that partial ozonolysis can result in the chemical conversion of phorbol ester to harmless organic molecules while maintaining sufficient protein content for substantial nutritious value. This is based on the intuition that the unsaturated double bonds in the phorbol ester are more labile than the peptide bonds of the Jatropha meal proteins, hence kinetically phorbol ester degradation will outpace protein destruction. In addition, the study of the effect of ozonolysis on cell lysis has been conducted as the preliminary work on another type of lignocellulosic material. The aim is to test the parallel hypothesis that partial ozonolysis can act as a low power consumption approach to breaking down lignocellulosic materials into sugary materials suitable for bacterial digestion, since complete ozonolysis would result in the combustion products of CO_2 and water. Low energy operation is desirable for suppressing production costs for competitive markets. Moreover, eco-friendly, fast and effective processing is favourable to perform detoxification.

Ozonolysis with plasma reactors is proposed for detoxification of lignocellulosic biomass due to the fact that it is an energy efficient and inexpensive method. The capability of ozone to cleave carbon double bonds is the key factor in potential toxicity reduction. Furthermore, the study of ozonolysis on protein stability has been performed by many researchers (Uzun et al., 2012, Uppu and Pryor, 1994, Mudd et al., 1969). It is confirmed that ozonolysis creates little variation in protein content. Mudd *et al* (1969) studied ozone treatment effect in various solutions of amino acids and protein. They generated ozone by passing through oxygen gas into high voltage discharge. Ozone then further injected into amino acids solutions. It is

reported that some amino acids in protein were not damaged by the presence of ozone. In addition, protein functional properties could even been enhanced by ozone treatment (Uzun et al., 2012). Uzun *et al* (2012) investigated ozone effect in aqueous protein solution and in protein powder samples. They found that ozone solubility is distinctive in aqueous and gaseous system. Various investigations focus in proteomic studies by ozone utilisations have been conducted over decades. However, integrated study of phorbol ester reduction with maintained protein content in Jatropha Meal using ozone-microbubble treatment has never been investigated.

Electric plasma discharge approaches for ozone production is usually accompanied by formation of some intermediate species of oxygen - oxygen radicals and ions (Beltrán, 2004). These intermediate species have a life time similar to a short ozone recombination time. Therefore ozone based processes are considered as clean technology with high attention given for further development and application. Large scale unit operation at relatively high current and voltage results to high power consumption. This makes ozone production energy intensive. All these features lead to high capital investment and limit wide ozone application for industrial use.

Practically, there are a number of ozone applications which require ozone to be delivered to specific points along the production pipe network. However, due to constraints of modern chemical reactor construction, high reactivity and short ozone life time, the use of standard ozone generators with a single point of ozone injection to the reaction volume is limited. Besides, the nature of ozone in form of gas which cannot be stored obliges on-site production, consequently compact devices are necessary (Chalmers, 1998, Kogelschatz et al., 1988). This

demands development of micro scale ozone generation units that can be directly incorporated into a certain points of a pipeline or reaction volume.

Miniaturised dielectric barrier discharge plasma reactors are good alternatives to corona reactors. DBD plasma reactors can operate at atmospheric pressure, at room temperature, use air as a feed gas and ignite plasma at lower voltage in compare to corona reactors. This research is aiming to develop a low power consumption DBD plasma reactor with possibility to *in-situ* ozone generation to the liquids of interest.

In order to improve ozonolysis as a multiphase process, modern microbubble technology is introduced. Microbubbles stay longer in the bulk of liquid therefore the contact time between gas and a liquid is longer. Smaller bubble size enhances the transfer rate in interfacial surface area resulting in higher process effectiveness (Zimmerman, 2008). The properties of microbubbles discussed herein are uncoated and therefore have a water-air interface. It is important to note that air can be replaced by any gas or a mixture of gases resulting in a widening of application fields and change of bubble dynamics thereby changing the bubble formation characteristics and behaviour. However, air was used in experimentations of current research in order to study ozonolysis performance that can be scaled up for industrial applications.

The current research proposes plasma microreactor development in combination with microbubble generation as a novel technology in treatment of lignocellulosic materials. The major key findings in this research are the experimental design and detoxification approach particularly for Indonesian Jatropha Meal. The reactor configuration is specifically designed to allow *in-situ* processing of ozone by injection in form of microbubbles. A miniaturised

plasma reactor for ozone generation is proposed in order to ignite plasma at less than 5 kV. A bespoke power supply is used to enable plasma ignition at low energy consumption compare to conventional approaches which require voltage 7-70 kV (Nehra et al., 2008[Pekárek, 2003 #306, Warsito et al., 2011, Cheng et al., 2007). Detoxifications of phorbol ester compound and protein maintenance are the two major focuses highlighted during investigation. Furthermore, the experiment programme is also extended for the treatment of synthetic lignocellulosic materials by using proposed technology as a low power consumption substitute for hydrolysis. In general, the study involves interdisciplinary concerns which are chemical analysis, biotechnology and plasma chemistry.

CHAPTER 3

METHODOLOGY

This research aims to investigate the ozonolysis effect in relation to the detoxification of biomass samples. In this process, chemical and biological methods were used to analyse the samples. The experiments were conducted using a be-spoke reactor designed specifically for this *in situ* process, which involved ozone and microbubbles. This chapter is divided into four sections. The first section describes the experimental set up and gives details of the reactor assembly. In the second section, methods of reactor characterisation are described. In general, the experimental reactor is considered as a compact device equipped with a ceramic diffuser and plasma microreactor. In order to study bubble size distribution, air passes through the ceramic diffuser which thereby acts as a microbubble generator. Next, a plasma microreactor with low energy power supply was applied to produce ozone. The ozone concentration was monitored to identify the power supply performance. In the third section, details of the experiments procedures focus in chemical analysis are described. The ozonolysis effect of phorbol ester (PE) degradation was explored, using synthetic and natural PE. Then, section four describes experiments procedures focus in proteomic investigation. Study of ozonolysis effect in lignocellulosic materials is described. Both quantitative and qualitative biological methods were used in this process.

3.1 Experimental set up

An overview of the experimental setup is presented on Figure 3.1. The bespoke setup consists of an experimental reactor, a power supply and flow network. The reactor (Figure 3.2), 2L in volume, has a stainless steel cylindrical body with a plasma unit as the core of experimental

setup. The reactor has a flange at the top with connectors for an air exhaust, a temperature monitor and a sampling line. On the side lines of the reactor, valves were attached to enable liquid sampling during the experiments. The plasma unit (Figure 3.3) is incorporated at the bottom flange of the reactor and a standalone device attached to a plasma microreactor and a ceramic diffuser (Figure 3.4).

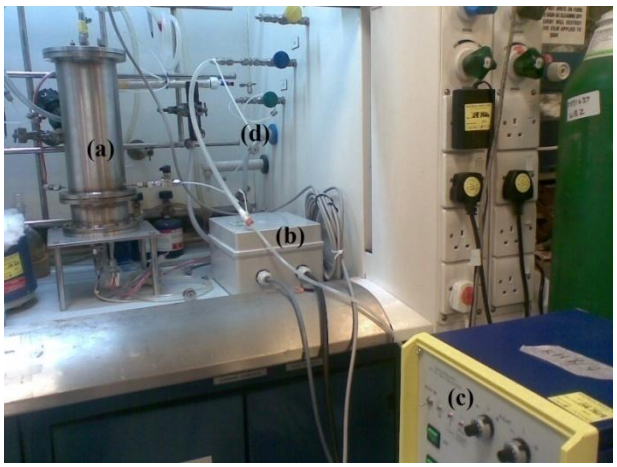

Figure 3.1 General view of reactor (a) with transformer (b), power supply (c) and flow network (d)

Figure 3.2 shows a diagram of the experimental reactor performing ozonolysis. The gas was injected through a gas inlet at the bottom of the plasma unit, while the gas outlet is at the top of the reactor. The gas flow was controlled by a rotameter and pressure gauge. Ozone concentration was monitored using the ozone detector at the top of the reactor. Sampling was done through sampling lines at the side and top of the reactor.

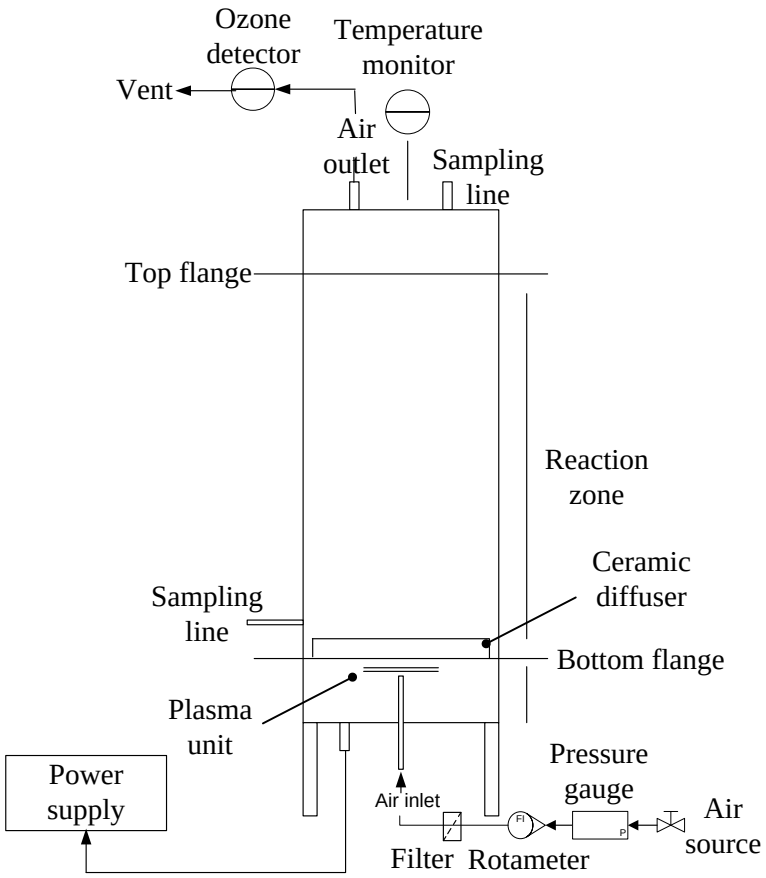

Figure 3.2 Setup diagram of experimental reactor

The design of the plasma microreactor for this investigation is shown in Figure 3.3. In this experiment, a Dielectric Barrier Discharge (DBD) type of plasma with an outer cover made of PEEK was used. The reactor consists of several parts; rod, top and bottom caps, and together with circular electrodes. Two coaxial parallel circular copper electrodes, with a 300 µm gap between them, were each covered with a glass wafer, which acted as a dielectric layer. The glass wafers (from Thermo Scientific, Menzo Glässer) were 28 mm in diameter with 140 µm thickness.

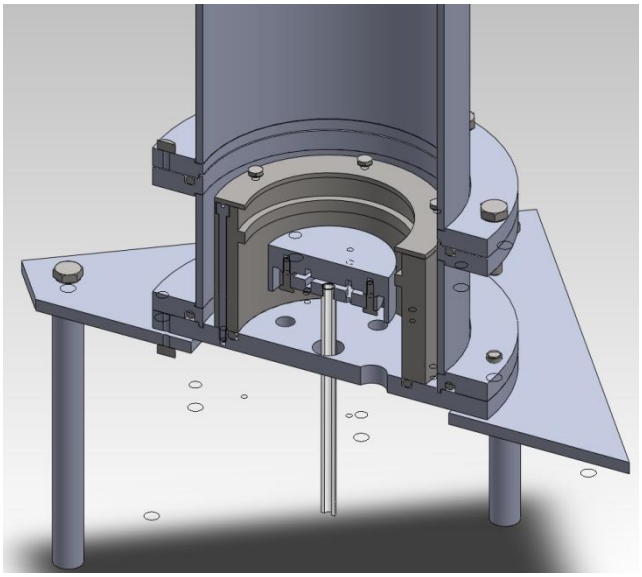

Figure 3.3 Cross sectional module drawing of plasma unit

The air was used as the gas phase during the experiments, where the oxygen molecules were converted to ozone. The air was supplied to the inter electrode gap through the rod. It passed the inlet to the drilled bottom cap, bottom electrode and dielectric layer. The presence of air in electric field causes plasma ignition leading to ozone formation. This ozone-air mixture entered the reactor, passing through the ceramic diffuser. The plasma microreactor is shown in detail in Figure 3.4.

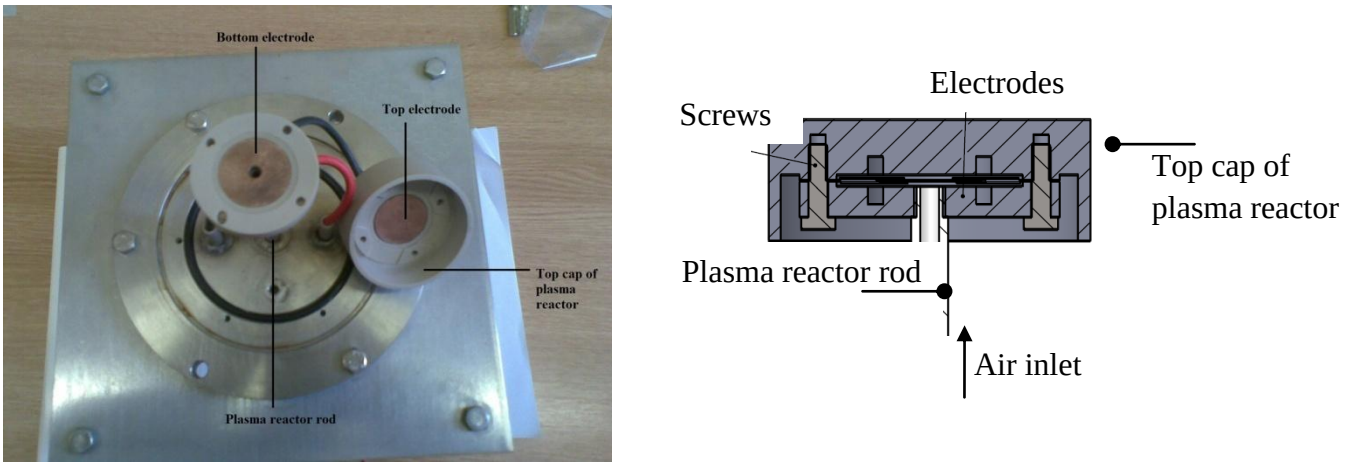

Figure 3.4 Photograph and diagram of plasma microreactor

Pollution on the surface of the electrodes during these experiments is inevitable, frequently leading to the formation of solid deposit. This would decrease the efficiency of plasma performance due to the local disturbance of plasma uniformity as a result of a narrowing of the gap between the electrodes. In addition, solid deposits lead to overheating which affects the kinetics of plasma. Pollution on the surface of electrodes and solid deposits mainly come from experimental samples. A top cap was designed to function as an air lock in order to protect the electrodes from the liquid in which the reactor was submerged. Protecting the electrodes from pollution is particularly important when starting up and shutting down the reactor.

In order to generate ozone, the plasma unit was connected to a 500W/50kHz/4kV plasma power supply made by Dipl.Ing.H.Bayerle, Germany. It was equipped with a second transformer with Trafo FE 48V/4kV. The plasma microreactor used in this research was designed to work at a voltage of up to 6 kV. However, the suggested working voltage level for this type of reactor is 4kV. As electrode arching may occur when a higher voltage is applied.

During the experiments, the power supply network was applied with a combination of an oscilloscope and a high voltage probe, TES TEC HVP-15 HF. The oscilloscope Picoscope ADC-212 was connected to the output of the high voltage probe which in turn was connected to the power supply. The signal from the high voltage probe was transmitted to the computer. Picoscope ADC-212 software was used for data processing during voltage reading.

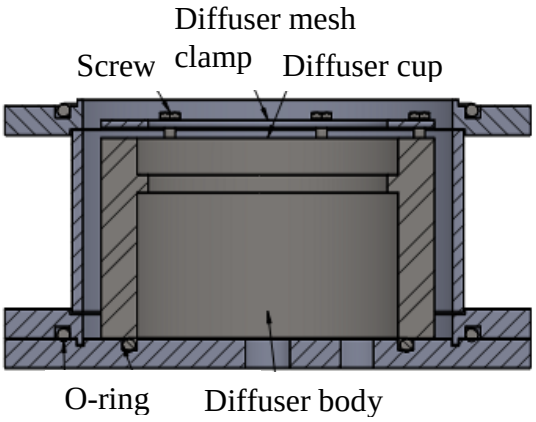

Figure 3.5 Schematic design of ceramic diffuser

The ozone-air mixture was introduced into the liquid through a ceramic diffuser in the form of microbubbles. The ceramic diffuser, Figure 3.5, which surrounds plasma unit, is a disc shape plate with diameter of 7.2 cm and thickness of 0.5 cm, made of sintered porous alumina and silica (80:20 w/w) with 20 µm pore size. The ceramic diffuser used in this research has a relatively hydrophobic nature due to its manufacture. The sintering process is a well developed technique for porous ceramic production (Küçük, 2009). High temperature, more than 1500 °C, applied during sintering is believed to affect properties of materials (Laskowski and Kitchener, 1969). They studied the transition from hydrophilic natural silica to be relatively hydrophobic by application of strong heat. Moreover, the ceramic diffuser, used in this thesis, was supplied by HP Technical Ceramic, Sheffield, United Kingdom (www.tech-ceramics.co.uk).

3.2 Reactor characterisation

3.2. 1 Characterisation of ceramic diffuser

The ceramic diffuser was characterised by the study of bubble size distribution. The investigation included two types of flow: oscillatory flow and steady flow. The ceramic diffuser was placed in a transparent glass tank, filled with water, to facilitate image capturing

during bubble production. For bubble production in oscillatory flow, a fluidic oscillator (FO) was applied to the setup. In the steady flow study, however, the FO was not used.

The gas flow through the system was controlled by flow controller (Key Instruments 0-5 lpm). The FO at a given flow rate oscillated at a known frequency. Flow down to the diffuser was controlled by bleeding lines installed with control valves. The inlet flow to the FO was controlled so that it could be compared with the steady flow. The experiments were conducted by bubbling air into the water which flowed through diffuser at a variable rate of 0.5 – 3 L/min. In the oscillatory flow study, however, an additional oscillation frequency of 284 Hz was applied. Figure 3.6 shows the experimental set up for ceramic diffuser characterisation.

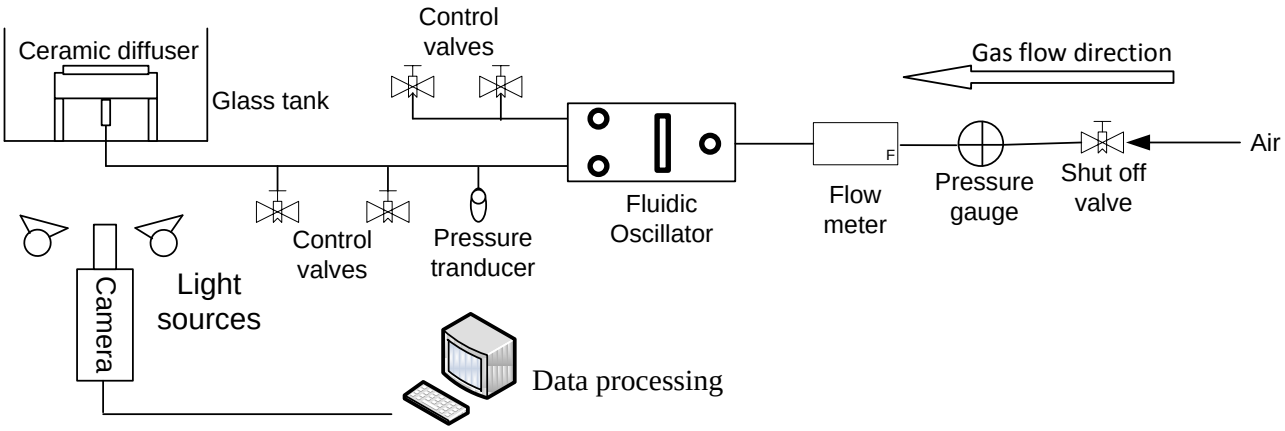

Figure 3.6 Flow diagram of bubble size distribution experimental setup

In order to characterise the bubble cloud dynamics, high speed photography has commonly used (Jian Xie et al., 2012, Dietrich et al., 2013, Bari and Robinson, 2012). In this experiment, the FastCam HS3 Photron camera, equipped with Nikon AF Lens was used to gather data about the bubble size distribution. The camera was computer controlled by PFV Photron Fastcam program and ImageJ, publicly available analysis software, was used for data processing. Thresholding, segmentation, and analysis were conducted by ImageJ to provide

bubble sizing estimates from images captured from the high speed camera. Analysis with ImageJ was performed by applying the threshold subcommand to the images. The threshold subcommand was used under command "image" and further "adjust". It limits measurement only for bubbles which are in focus. Also, the threshold intensity establishes segmentation on the analysed image in order to match every pixel of the image with the set threshold (Grau, 2006). Afterwards, the reference scale was set then a further "*Analyse tool*" commander was employed. Analysis distribution results were then generated by the program and presented as bubble diameter. Typical images of the ceramic diffuser and microbubbles cloud formed are provided in the result and discussion, Chapter 4. Images were taken at 2000 frame per second of a high speed camera with 1024 x 1024 resolution.

Often bubble size distributions are characterised by their mean and standard deviation, which is calculated through Equation 3.1. However, the latter is an impractical parameter to specify distribution of bubble size (Engelsen et al., 2002). As shown in Hanotu (2013), standard deviation value only represents the variability of bubble average size but not the range of bubble size distribution. One statistic which is commonly used to determine the width of bubble size distribution, is the span value. Others include the polydispersity index (PDI), and higher central moments (Pabst et al., 2002, Weiner, 2011, Hanotu, 2013, Engelsen et al., 2002, Agarwal et al., 2011). In this thesis, the span method was chosen due to its simplicity and relevancy to the main purpose -- investigating the relative narrowness of bubble distribution. Equation 3.2 is the formula for the relative span calculation for bubble distribution curve.

$$Standard\ deviation = \sqrt{\sum \frac{(x-\bar{x})^2}{(n-1)}} \quad (3.1)$$

$$Span = \frac{D_b^{90} - D_b^{10}}{D_b^{50}} \quad (3.2)$$

In Equation 3.1, x takes on each value in the set, $\bar{x}$ is an average (statistical mean) of the value set and n is a number of values. Standard deviation is automatically generated by the post processing program used. Moreover, in Equation 3.2, D_b^{90} corresponds to the bubble diameter of the 90th centile. D_b^{10} is defined as the 10th centile while D_b^{50} is the median bubble diameter. These values are obtained from the cumulative bubble population distribution. Span is a dimensionless unit where smaller value represents narrower range of distribution (Hancocks, 2011). In addition, kurtosis is another statistic that is commonly used to determine a shape of bubble size distribution (Sheikhi et al., 2013). It quantifies the "flatness" of the distribution, once benchmarked against the normal distribution. The kurtosis of a normal distribution is 3 while relatively flat distribution has kurtosis value less than 3. The formula for kurtosis is defined in Equation 3.3, below. x is the value of data set and $\bar{x}$ is a mean while n is a number of data and σ is a standard deviation.

$$Kurtosis = \frac{\sum_{i=1}^{n}(x_i - \bar{x})^4}{(n-1)\sigma^4} \qquad (3.3)$$

3.2. 2 Characterisation of plasma microreactor

The plasma microreactor performance was characterised by ozone concentration measurement using the Indigo Method (Bader and Hoigné, 1981). This is widely accepted as a very sensitive, precise and fast method for determining ozone concentration. Ozone decolorizes the indigo solution by cleavage of indigo bonds which leads to formation of a colourless product.

The calculation of ozone concentration using the indigo reagent is based on a ratio where 1 mol of decolourised indigo is equal to 1 mol of ozone detected, assuming that the applied potassium indigo trisulfonate was pure. The decolourisation value was measured using a

spectrophotometer, DR 2800 Hach-Lange, at wavelength 600 nm. The experiment flow diagram is presented in Figure 3.7.

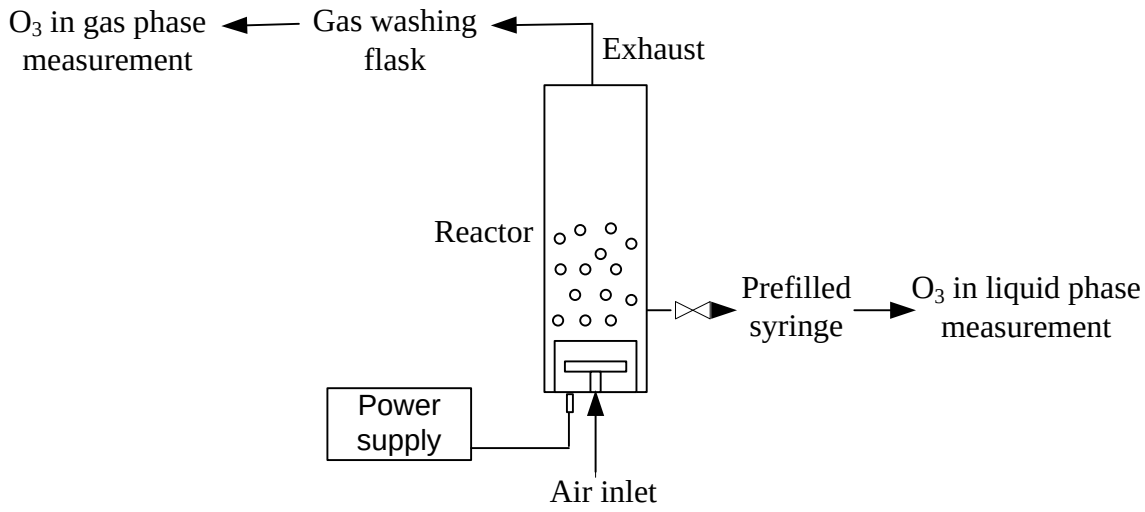

Figure 3.7 Principal diagram of ozone concentration experimental setup

The change in light absorbance at 600 nm indicates the amount of indigo that reacted, which is in proportion to the ozone concentration. Equation (3.4) presents the calculation of indigo concentration in the stock solution:

$$C_{ss} = \frac{m_{pi}}{mw_{pi}} \times \frac{1}{V_T} \qquad (3.4)$$

Where C_{ss} is the concentration of stock solution (mol/L), m_{pi} is the mass of potassium indigo (g), mw_{pi} is the molecular weight of potassium indigo (g/mol) and V_T is the total volume of the mixture (L). A stock indigo solution (SIS) was prepared by mixing 0.385 g of potassium indigo trisulfonate and 0.5 ml of concentrated phosphoric acid in 500 ml of distilled water (DIW). A working solution (WS) was prepared by diluting 20 ml of SIS in 1-L of distilled water to which 10 g of sodium dihydrogen phosphate and 7 ml of concentrated phosphoric acid were added. Equation (3.5) shows the calculation of the indigo concentration in the WS:

$$C_{ws} = \frac{C_{ss} \times V_{iw}}{V_T} \qquad (3.5)$$

Where C_{ws} is the concentration of the working solution (mol/L), V_{iw} is the volume of indigo in the working solution (L).Ozone concentrations were determined by using a calibration curve. For this purpose, calibration solutions (CS) were prepared by diluting 5 ml of WS into several volumes of DIW (5 ml, 10 ml, 15 ml, 20 ml and 25 ml). The indigo concentration in a CS (C_{cs}) was calculated using Equation (3.6) below. To perform the calibration, the absorbance of a set of CS's was plotted against indigo concentration:

$$C_{cs} = \frac{C_{ws} \times V_{ic}}{V_T} \qquad (3.6)$$

V_{ic} is the volume of indigo in the calibration solution (L). The SIS used in this experiment was a fresh solution used immediately after been prepared. The remaining stock solution was stored in dark room at 4 °C to prevent degradation. In principal, degradation can be characterized by a reduction in absorbance below 80% of the initial value, which typically occurs within 3-4 months of storage.

The reactor was filled with 1.5 L of DIW. Sampling was done every 2 minutes. Four kV voltage was applied for plasma ignition, while 3.8 kV was applied as a working voltage. An air flow rate of 2 L/min was chosen as the operating gas flow. During the experiment, the ozone concentration was measured both in the liquid and gas phase as a function of air flow rate at a fixed voltage level. Measurement of ozone content in the gas phase was conducted by sampling from the top flange of the reactor. Sampling was performed by flushing the mixture containing ozone emitted from the outlet of the reactor through the washing flask filled with indigo solution. This gas was then mixed with the indigo solution by bubbling it for 30 seconds. The change in absorbance of the indigo solution before and after bubbling of the mixture containing ozone gave the concentration of the ozone in the gas phase.

For ozone concentration measurement in the liquid phase, a technique developed by the researcher was applied. A 4 mL sample of water containing ozone was taken from the side sampling line of reactor and loaded into a syringe preloaded with 4 mL of indigo solution. This mixture was homogenised by vibrating it for 30 seconds, and was then analysed using a spectrophotometer. A dilution 1/1 factor was taken into account. The change in absorbance of the indigo solution before and after sampling gave the concentration of the ozone in the liquid phase.

3.3 Detoxification of Phorbol Ester (PE) compound

The study of the effect of ozonolysis on phorbol ester (PE) content is the main objective in this research from a chemical engineering point of view. The bespoke technology used aims to facilitate the detoxification of PE with low energy consumption. PE detoxification by ozonolysis was carried out using synthetic and natural PE. Phorbol-12-myristate-13-acetate (TPA) was used as the sample in synthetic PE detoxification. TPA was chosen due to the similarity of its chemical structure to PE compound in the plant, *Jatropha curcas Linn*, as mentioned in Chapter 2. In addition, natural sample of PE was obtained from Jatropha meal (JM), as explained in Chapter 2.

A High Performance Liquid Chromatography (HPLC) technique is commonly used for PE detection which mainly utilized normal phase and reverse phase chromatography (Dimitrijevic et al., 1996). HPLC Varian Pro Star reverse-phase C18-A Polaris 5 µm 150 x 4.6 mm column (Agilent) was applied in these experiments. This was equipped with a 100 µm stainless steel sampling loop. A mixture of 80% acetonitrile and 20% water were used as the mobile phase in an isocratic elution with flow rate 1 ml/min. The samples were filtered by a 2

µm PEEK filter capsule, Upchurch Scientific Rheodyne, prior to injection. All chemicals were HPLC grade purchased from Sigma Aldrich. The peaks were detected by a ProStar 330 PDA detector at 232 nm wavelength.

The calibration of HPLC was carried out based on the method presented by Deachathai et al (2010). Phorbol-12-myristate-13-acetate (TPA) was used as an external standard for calibration purposes. A stock solution was made to prepare the series of calibration standard solutions. TPA was dissolved with methanol to produce 500 ppm of stock solution. The stock solution was stored in the freezer at controlled temperature of -20 °C. The calibration solutions were prepared by diluting the stock solution with methanol in various concentrations (10, 20, 30, 40 and 50 ppm). Triplicate experiments were conducted in each concentration of calibration sample. The calibration peak appeared in HPLC chromatogram at 17 minutes. The PE concentration was determined by plotting the TPA concentration against the height of TPA peak.

3.3. 1 Detoxification of synthetic PE

The sample of TPA containing distilled water (DIW) mixture was made in two steps. Firstly, 1000 µg of granulated TPA were dissolved in 2 ml of methanol. This step was taken to avoid problems with low solubility of TPA in water. Secondly, 8 ml of methanol mixture was diluted with DIW to produce 400 ml of the TPA mixture, producing a TPA concentration of 12 ppm. The TPA was purchased from Acros Organics, New Jersey, USA while the DIW and methanol were HPLC grade purchased from Sigma Aldrich.

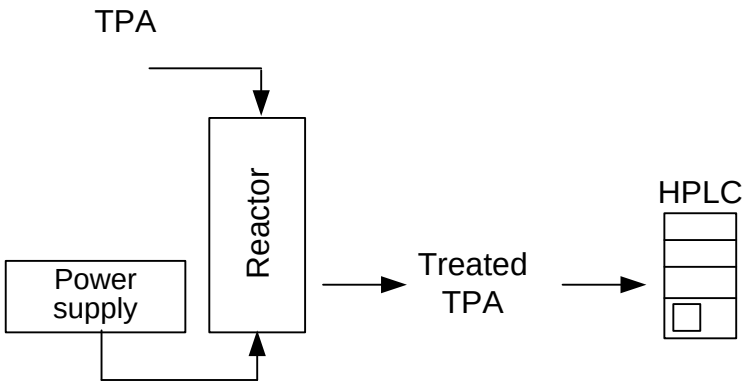

Figure 3.8 Flow diagram of synthetic PE treatment by ozonolysis

Figure 3.8 presents the flow diagram of synthetic PE treatment by ozonolysis. The TPA mixture was treated with ozone for 30 minutes. Samples were taken every 5 minutes. The air flow rate was set to 2 L/min. The experimental procedure was developed to taken into account the safety of the immersed high voltage plasma device. Before TPA mixture was loaded, the air flow was switched on to keep the plasma microreactor dry in the internal chamber of the diffuser. 400 ml of the TPA solution was loaded into the reactor. At the start of the experiments, the plasma reactor was powered up at 4 kV for 10 seconds in order to ignite the plasma for ozone production. Subsequently, the voltage was decreased to a working voltage of 3.8 kV during ozonolysis of TPA degradation.

At the start of sampling the DBD plasma unit was powered down and 1 ml of treated sample was flushed through the side sampling line to wash out previous samples. Afterwards, 1 ml of treated sample was collected in vials and taken for HPLC analysis.

3.3. 2 Detoxification of natural PE

For the research presented in this work a Jatropha meal (JM) was obtained from Indonesia. This variety was cultivated on a jatropha plantation in Gunungkidul Regency, Jogjakarta

Province, Indonesia. JM was produced by a company named PT Jatropha Green Energy, Kudus Regency, Central Java Province, Indonesia using a mechanical press of *Jatropha curcas* seeds. The jatropha seeds were pressed for 15 minutes at 50-70 ^{0}C to extract the oil. This defatting process resulted in 20% of oil and 70% of meal. The meal was collected straight after the defatting process and immediately air freighted in a dark airtight plastic bag.

After delivery, the sample was stored in a dark air conditioned room at 4 °C before further laboratory treatment. These conditions prevent autoxidation of Phorbol ester (Schmidt and Hecker, 1975).Before ozonolysis treatment, JM was manually ground to produce samples ranging in particle size from 0.63 to 1.88 mm. The grinding was done with a porcelain bowl and an aluminium foil covered-mortar in dark fume cupboard to avoid light induction and then was stored in amber bottles for further experimental purposes.

The sample for ozonolysis was a mixture of ground JM and distilled water at a ratio of 1:10 (w/w). The air flow rate was set to 2 L/min before the sample was loaded into the reactor. The ignition voltage of plasma was 4 kV while the working voltage was 3.8 kV. The mixture was treated with ozone for 1 to 5 hours. A fresh sample was used for each experiment. Figure 3.9 shows the principal diagram of jatropha ozonolysis treatment.

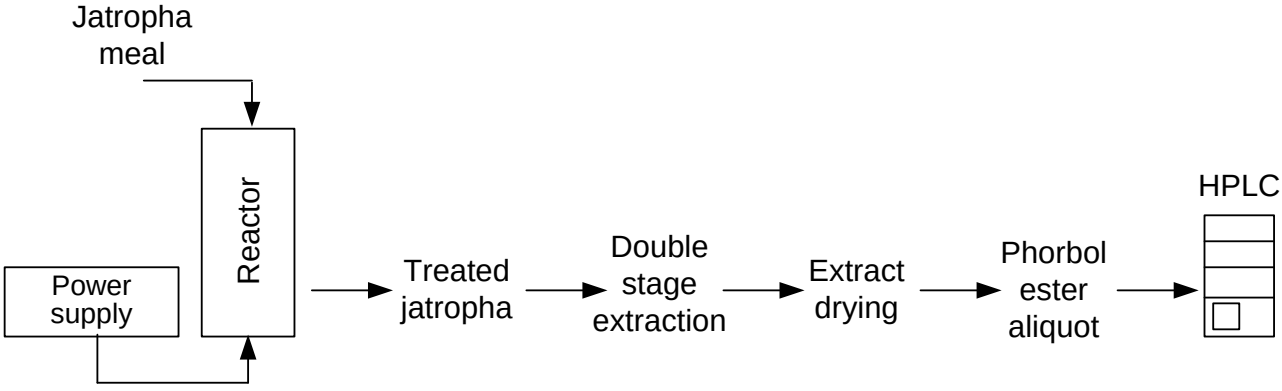

Figure 3.9 Principal diagram of jatropha ozonolysis treatment

The samples were further treated prior to HPLC analysis. PE aliquot for HPLC analysis was isolated from the process of double stages extraction which was based on the method used by Gaur (2009). The first extraction was conducted using hexane solvent for 24 hours, followed by extraction using methanol solvent for 72 hours. The extract from each stage was further treated separately. Extract of hexane and methanol was dried using a rotary evaporator, BÜCHI Rotavapor R-200, for 60 and 30 minutes, respectively. Temperature during drying was kept at 30 °C. Phobol ester aliquots from each extract was then analysed as an individual sample in HPLC. All solvents used were HPLC-grade purchased from Sigma Aldrich. PE peaks appeared in the HPLC chromatogram after 20-28 minutes.

3.4 Investigation of ozonolysis effect in lignocellulosic materials

Considering the benefits offered by ozone treatment, the other field of interest in this research is the study of the variation of the biological materials. Some different materials were treated in the experimental reactor for biological investigation purposes. The study focused on the ozonolysis effect of specific content in the sample by using natural and synthetic biological materials. In relation to the detoxification of PE in JM sample by ozonolysis, an investigation of protein content after JM detoxification was carried out. It aimed to provide an integrated study of the ozonolysis effect on both toxicity and protein content. In addition, ozonolysis of synthetic lignin was carried out in this research. The purpose of this investigation is to study the effect of ozonolysis in cell lysis as well as ozone utilisation in the molecular structure of lignin.

3.4. 1 Ozonolysis of Jatropha biomass

Ozonolysis of ground Indonesian JM was conducted for 1-5 hours with sampling performed every 30 minutes. The treated JM samples were dried and further used for protein quantification. Figure 3.10 illustrates the stage of biology investigation on the jatropha.

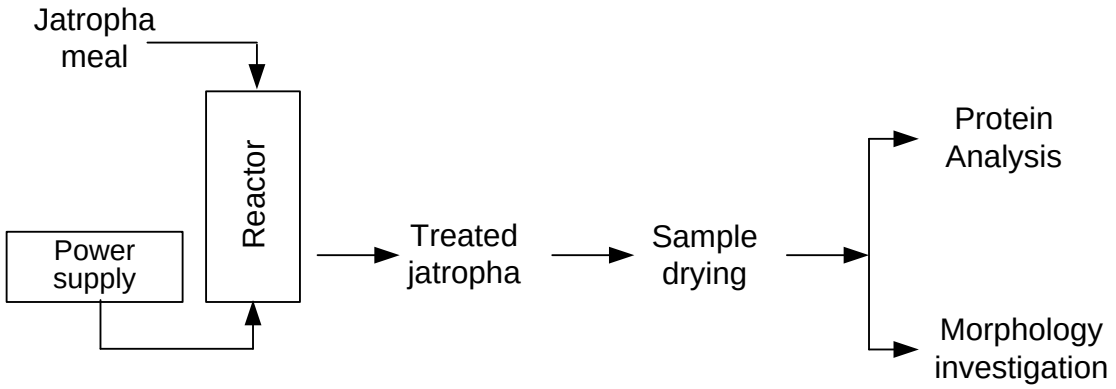

Figure 3.10 Principal diagram of biology investigation on jatropha sample

Analysis was performed on JM samples, both before and after ozonolysis by extracting protein using triethylammonium bicarbonate (TEAB) buffer. All chemicals used were of analytical grade purchased from Sigma Aldrich. In order to extract the protein, samples were mixed with TEAB followed by centrifugation using Eppendorf 5424 Centrifuge, for 20 minutes (2100 cfg). The resulting supernatants were stored at a temperature of -20 ^{0}C for further analysis.

Investigation of protein quantification was carried out by direct and indirect methods in order to obtain relative comparison results. Bradford Assay was used as the direct method for protein quantification. To this end, the protein extracts were mixed with Bradford Ultra Reagent. Absorbance was measured at 595 nm using a spectrophotometer, Ultrospec 2100 pro Amersham Biosciences. This experiment was performed three times.

The indirect method for protein quantification involved the use of a particle analyzer device. Flash 2000, Organic Elemental Analyser from Thermo Scientific was used for this purpose. The analytical device was supported by CHNS Eager Experience from CE Instrument Flash software for data processing. Protein concentration was determined by multiplying data by 6.25 as the protein factor for wheat or soybean (Tkachuk, 1969).

Next, the SDS-PAGE method was applied for protein qualification in support to the result of Bradford Assay. Laboratory-made gel, containing 15 wells with 15-20 µl of maximum loading volume per well, was used for this purpose. Samples were prepared by mixing 5 µl of the sample with 5 µl of Laemmli Buffer 2X, as the sample buffer. The homogeneous mixture then incubated in a heat block for 5 min at 95 °C. Afterwards, the samples were cooled down to a room temperature of 24 °C, and were then spun in order to mix them with the resulting water vapour. They were loaded into each well after which the two stages of electrophoresis were performed. In the first stage of this process, the sample was treated for 30 minutes using a voltage of 80 mV. Subsequently, the voltage was increased to 45 mV and the process continued for a further 45 minutes. The gel was disassembled from the electrophoresis setup, stain buffer was added, and the mixture was then stored at a temperature of 4 °C for 12 hours, to allow staining to occur. Following this stage, the gel was de-stained by replacing the stain buffer with distilled water.

In addition to the SDS-PAGE processing, the gel was further investigated using a Mass Spectrophotometer (MS). Prior to the MS Analysis, a gel digestion procedure was applied. Each band of interest from the gel was cut and washed with several solvents. First of all, they were washed with 500 µl of 100 mM ammonium bicarbonate solution in water (Ambic A). The mixture was put in a shaker rack for 10 minutes. Next, the washing solution was replaced

with 500 µl of 100 mM ammonium bicarbonate solution in acetonitrile (Ambic B), and samples were put on the shaker rack for another 10 minutes.

The band washing stages were repeated until the mixture was clear. Once decolourised, the bands were dehydrated using a third solvent, which was 100% acetonitrile (ACN). The ACN solution was then removed and replaced using a fourth solvent, dTT solution. A 200 µl of dTT solution was prepared by adding 10 mM Dithiothreitol to 100 mM Ambic A. The mixture of band and solution was incubated in a heat block for 45 minutes at 60 °C. Subsequent to incubation, the dTT solution was removed and the gel was re-dehydrated using 500 µl of ACN (2x). 55 mM Iodo-acetamide, diluted in 100 mM Ambic A, was used for further the washing solution. 200 µl of 55 mM Iodo-acetamide was added to the re-hydrated gel for further 1 hour incubation period in the dark at room temperature. The final step in gel washing was the removal of Iodo-acetamide solvent, followed by gel re-dehydration using 500 µl of ACN (2x).

The washed bands were mixed with 30 µl of trypsin, prepared by dissolving 10 µg in 1000 µl of 100 mM ammonium bicarbonate, which were held at a temperature of 4 °C for 10 minutes. Once the gels and trypsin had solidified, 50 µl of 100 mM Ambic A, were added. The mixture was put in an incubator at a temperature of 37 °C for 16 hours. After this stage, the peptide from each bands of gel was extracted, to be used as the sample for MS analysis. The peptide extraction was conducted by adding 70 µl of 5% ACN with 0.1% of formic acid to the mixture, which was then incubated at a temperature of 37 ^{0}C for 10 minutes. Afterwards, the solution from each sample vial (Vial A) was transferred to another vial (Vial B). Next, 150 µl of 50% ACN with 0.1% formic acid was added to the remaining mixture of gel and trypsin. The mixture was re-incubated at a temperature of 37 °C for 10 minutes. This solution was

added to Vial B. The solutions containing the peptides were evaporated for 6 hours and the resulting dried samples were stored at a temperature of -20 °C before further MS analysis.

The aim of MS analysis was to investigate the effect of ozonolysis in relation to a particular type of protein. For this purpose, a combination of an Ultimate 3000 capillary LC system (Dionex, Surrey, UK) with an Amazon ion trap instrument (Bruker, Bremen, Germany) was used. A 75 μm x 15 cm C18 analytical reverse phase column (LC Packings, CA, USA) was applied to the system. A mixture of 3% Acetonitrile and 0.1 % TFA was used as a loading buffer with a flow rate of 300 nL/min. Dried samples after gel digestion stage were re-suspended in 20 μl of loading buffer. The mixture was then sonicated using an Elmasonic S30H-Fischer Scientific, for 5 minutes which was then spun using an AccuSpin Micro 17 Centrifuge-Fischer Scientific, for 5 minutes at 13000rpm. 20 μl of the mixture was then loaded into the MS.

The morphology of the JC was investigated using a Scanning Electron Microscopy (SEM) together with a JSM-6010LA Analytical SEM JEOL microscope. Image capturing was performed in a magnification factor of 2000 which secondary electron imaging (SEI) was set as a standard detection mode.

3.4. 2 Ozonolysis of synthetic lignin

The samples were prepared by mixing lignin alkali, purchased from Sigma Aldrich, with distilled water at a ratio 1:1 (w:w). Ozonolysis was performed for 3 hours with a sample taken every 15 minutes. The air flow rate in the reactor was fixed at 2 L/min. Triplicate experiments were carried out. The absorbance was measured at 340 nm using a spectrophotometer; Ultrospec 2100 pro Amersham Biosciences.

CHAPTER 4

REACTOR CHARACTERISATION

This chapter presents the experimental results of reactor characterisation prior to the investigation of sample treatments. The reactor was characterised by observing the performance of both the ceramic diffuser and plasma microreactor. The ceramic diffuser performance was independently characterised by the bubble size distribution during microbubble generation. Its characterisation was performed in both steady and oscillatory flows. Study of bubble generation in steady flow was conducted without applying the fluidic oscillator (FO). The FO was then applied for oscillatory flow investigations. The differences of bubble size distributions with and without FO application are reported. The experimental procedures used for this chapter have been described in detail in Chapter 3. A high speed photography method was used for the bubble size distribution study. Numerical data of bubble size distribution and captured images during microbubble generation are presented in the first section. Next, experimental data of plasma microreactor performance is discussed in the second section of this chapter. Ozone concentration measurement was done in order to characterise the plasma microreactor performance. Indigo Method was used for ozone concentration determination. Ozone concentration was measured in liquid and gas phase for a range of flow rates between 0.5-3.0 L/min. Finally, oscilloscope images of plasma ignition during ozone production and temperature monitoring of Dielectric Barrier Discharge (DBD) caps are provided to give information about reactor performance.

4.1. Characterisation of ceramic diffuser

Six flow rates, ranging from 0.5 to 3.0 L/min, were selected in order to characterise the ceramic diffuser. The range of flow rates was chosen after technical consideration of the available flow meter. The upper flow rate limit was set at the level where single bubbles in the cloud can still be distinguished from the cloud itself. Above this flow rate, denser bubble clouds were generated, therefore, bubble size quantification was not possible. This was due to shadowing effects of the bubbles upon one another, visual obscuration and overlapping as well as optical refraction effects. Consequently, individual diameters of the bubbles could not possibly be made out. The lower flow rate limit was chosen due to the limitations of instrument accuracy. Application of electronic flow measurement technique was impracticable due to plasma EMI (Electron Magnetic Interference). Bubbles size distributions were determined with steady flow and oscillated flow for each flow rate. The individual diameters of the generated bubbles were recorded to compile the bubble size distribution data for each experiment.

Span and kurtosis values were calculated in order to determine narrowness and flatness of bubble size distribution, respectively (Hancocks, 2011, Sheikhi et al., 2013). Narrow distributions were indicated by a span value less than 1 (Bitra et al., 2008) while a kurtosis value less than 3 represents relatively flat distributions. The following figures (Fig. 4.1 – Fig. 4.6) present analysis of images and statistical data of bubble size distribution from six chosen flow rates (0.5 – 3.0 L/min).

(a)

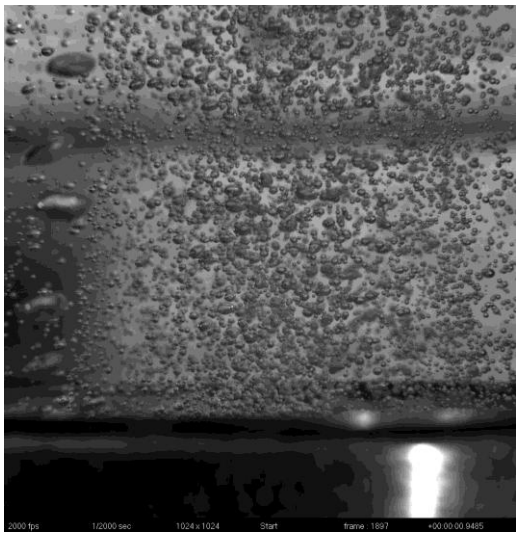

(b)

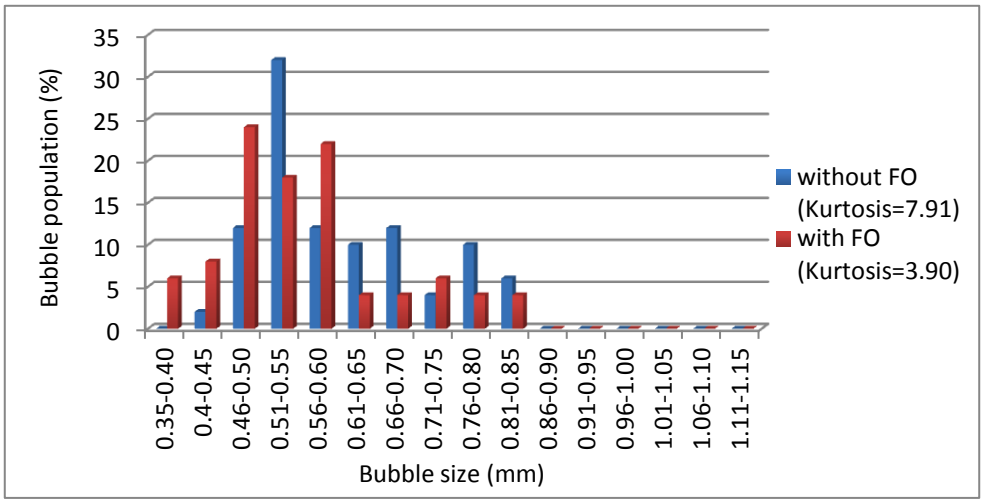

(c)

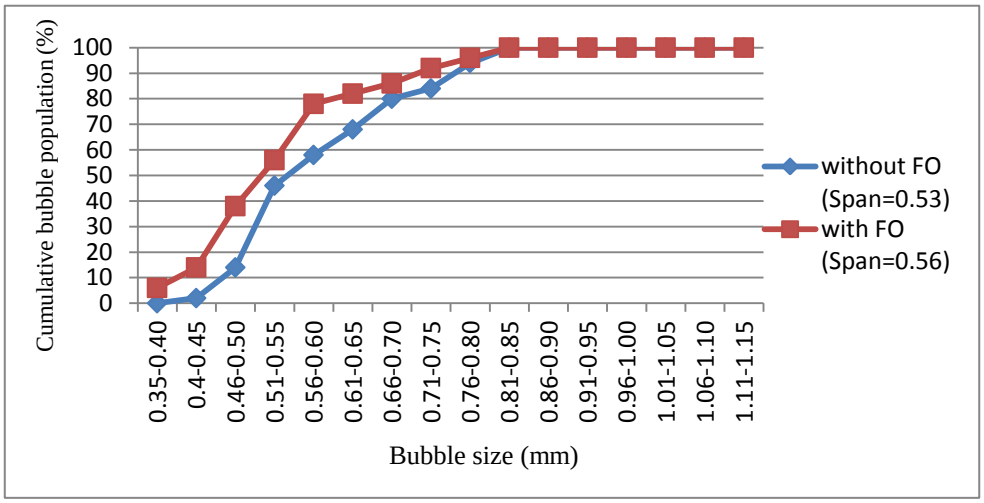

(d)

Figure 4.1 Bubble generation at flow rate 0.5 L/min; (a) without FO application, (b) with FO application, (c) comparison of bubble size distribution, (d) cumulative distribution curve

Figure 4.1shows bubble size distribution at the lowest chosen flow rate, 0.5 L/min. Figure 4.1 (a-b) show images of bubbles generation in steady flow and oscillatory flow, taken by high speed camera technique. It can be seen that narrow bubble distribution occurred in bubbles generation without presence of FO compared to with FO application. Peaked distributions exhibited high kurtosis values: 7.91 for a steady flow and 3.90 for an oscillated flow, respectively (Fig 4.1 c). It is also supported by small span values of 0.53 and 0.56 for condition without FO and with FO application, respectively (Fig 4.1 d). In steady flow, without FO application, bubbles sizes ranging from 0.40 to 0.85 mm were generated wherein the majority of bubbles produced had a size range approximately 0.51-0.55 mm. On the other hand, smaller bubbles were counted in oscillatory flow where FO was present. This resulted in a wider bubble size distribution which ranged from 0.35 to 0.85 mm in which the majority of bubbles generated are finer bubbles, 0.46-0.50 mm.

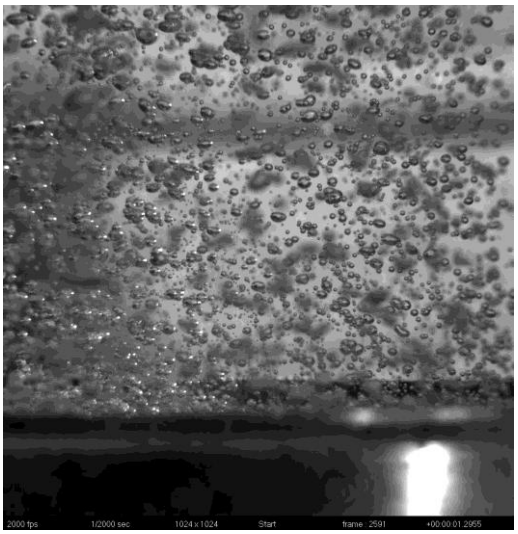

(a)

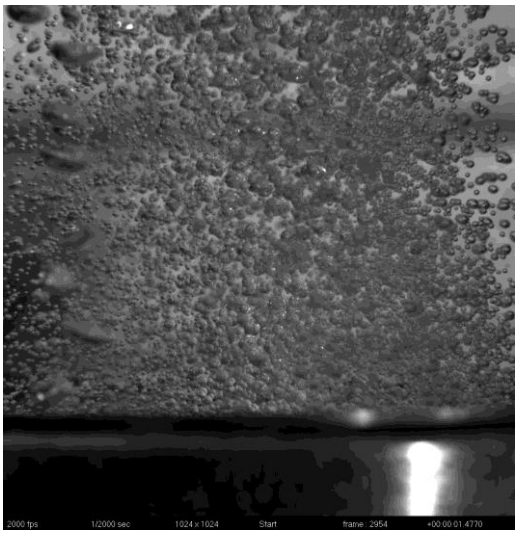

(b)

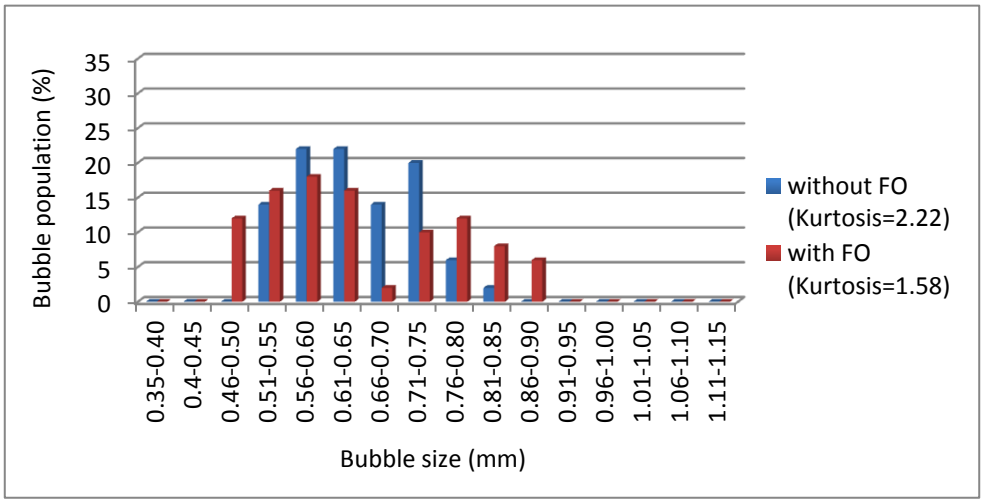

(c)

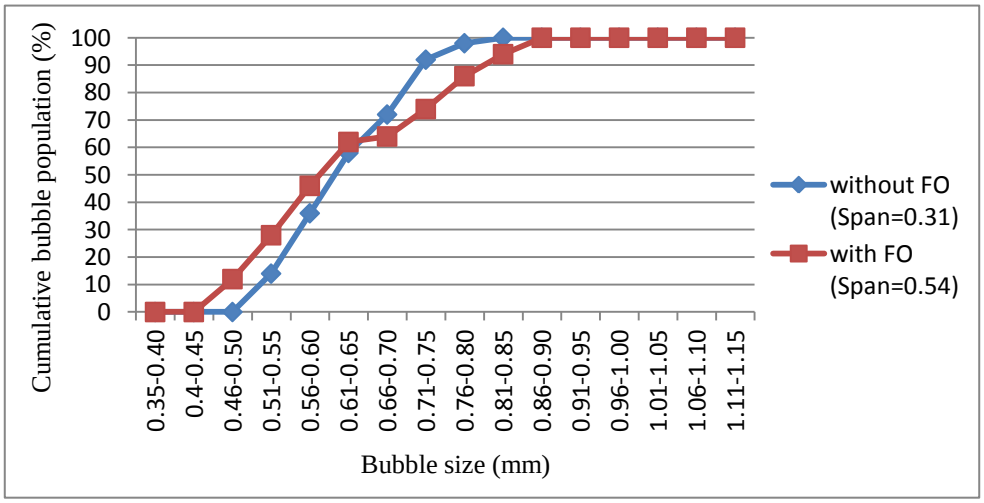

(d)

Figure 4.2 Bubble generation at flow rate 1.0 L/min; (a) without FO application, (b) with FO application, (c) comparison of bubble size distribution, (d) cumulative distribution curve

Figure 4.2 presents bubble distribution at a higher flow rate of 1 L/min. The captured image of bubble generation at steady flow (Fig 4.2a) showed that bigger bubbles were generated in comparison to oscillatory flow (Fig 4.2b). A less significant amount of bubble were produced at average bubble size of 0.66-0.70 mm at both flow conditions (Fig 4.2c). This anomaly might be a result of pore size divergence in which specific characteristic of the ceramic diffuser. Due to the nature of ceramic diffuser production, pore sizes are vary (Reif and Dittmeyer, 2003) therefore, fewer number of bubbles in a specific size may be produced. Furthermore, in cumulative distribution curve (Fig 4.2d) suggests narrower bubble distributions occurred in steady flow, with span value of 0.31 and kurtosis of 2.22, than in oscillatory flow, which span value of 0.54 and kurtosis of 1.58. Bubble size distributed from 0.51 to 0.85 mm was measured in steady flow while 0.46-0.90 mm of bubbles were generated in oscillatory flow. The maximum diameters 0.56-0.60 mm of bubbles were mainly produced at both steady as well as oscillatory flow.

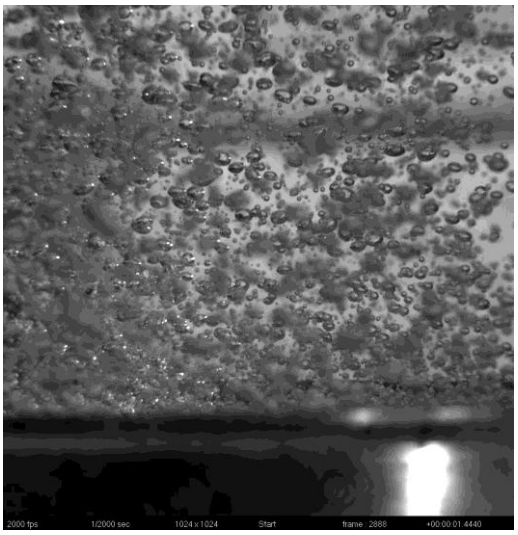

(a)

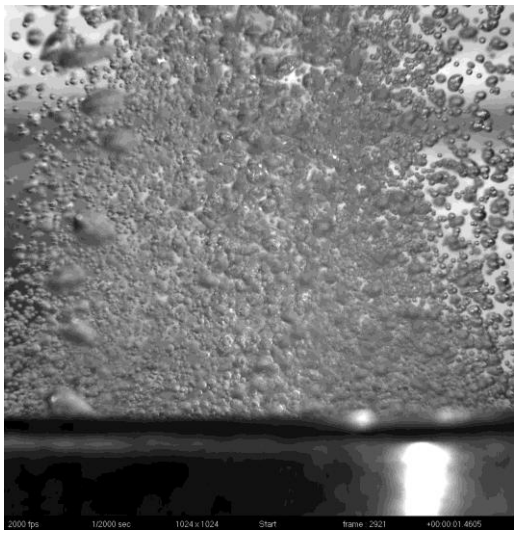

(b)

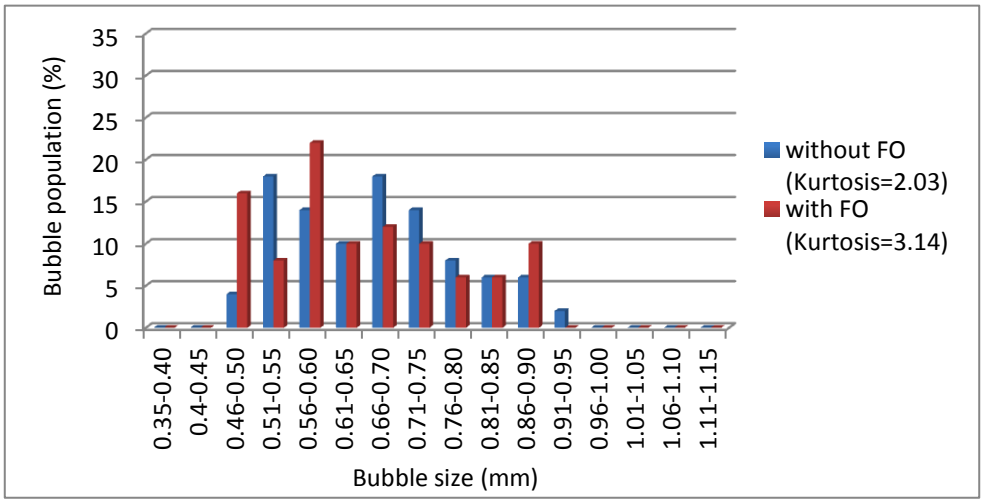

(c)

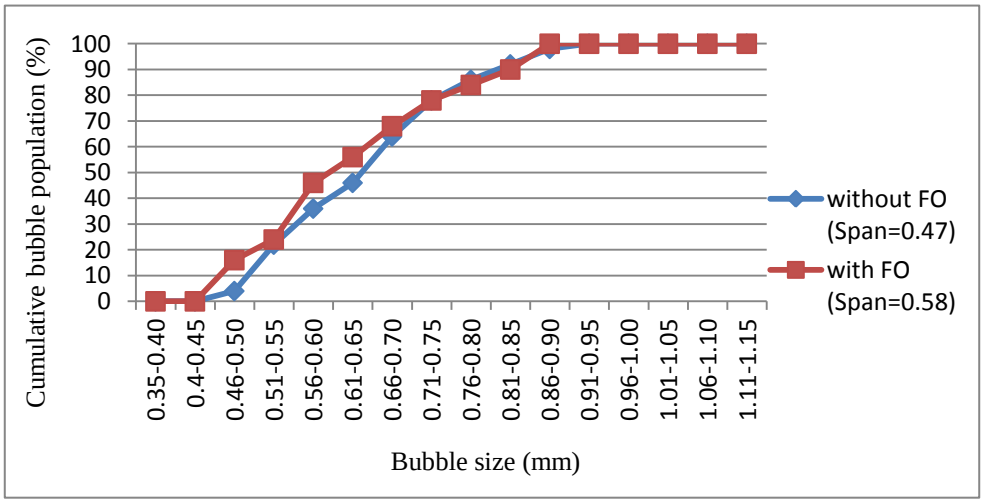

(d)

Figure 4.3 Bubble generation at flow rate 1.5 L/min; (a) without FO application, (b) with FO application, (c) comparison of bubble size distribution, (d) cumulative distribution curve

Figure 4.3 indicates bubbles generation at 1.5 L/min without presence of FO (a) and with presence of FO (b). It is showed that a larger number of bubbles were present in the population and larger average bubble sizes were obtained with higher flow rates with FO application. According to the bubble size distribution data (c), relatively flat distributions have continued independently of FO presence. It is shown by the kurtosis value of 2.03 as well as the span value of 0.47 as presented in cumulative distribution curve (d). In absence of FO, bubbles generated were ranged 0.46-0.95 mm in size with majority of bubbles had 0.51-0.55 mm and 0.66-0.70 mm of diameter.

However, a wider distribution occurred in bubble generation with the presence of the FO, which has a span value of 0.58. This resulted in a finer bubble distribution with range 0.46-0.90 mm while 0.56-0.60 mm was determined as the majority bubble diameter range. As stated in Brittle et al, (2015) a wider bubble distribution is not economically preferable for industrial application. Some additional processes are required to meet specific needs of bubble size, for example centrifugation to select desirable bubble size for application in medical field (Feshitan et al., 2009).

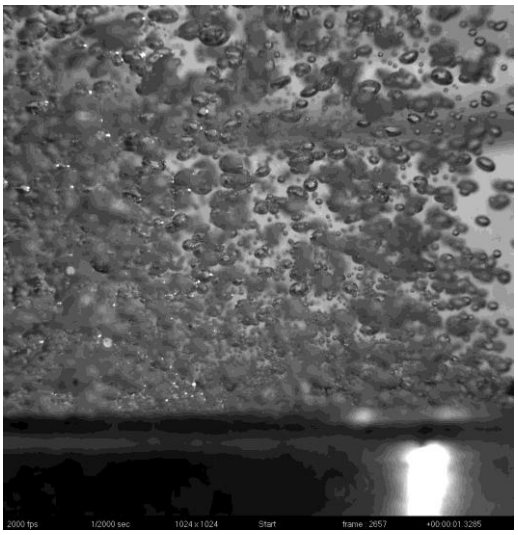

(a)

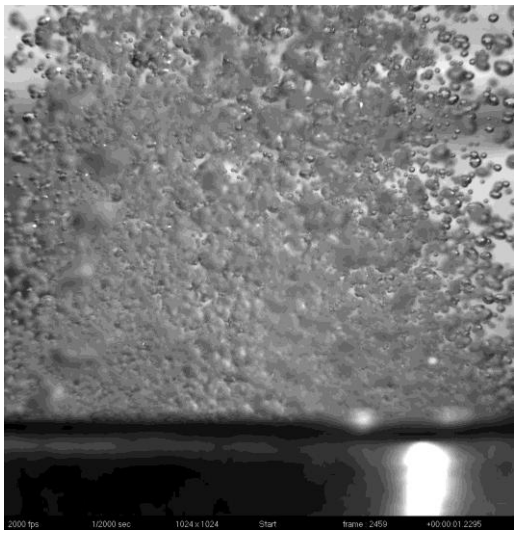

(b)

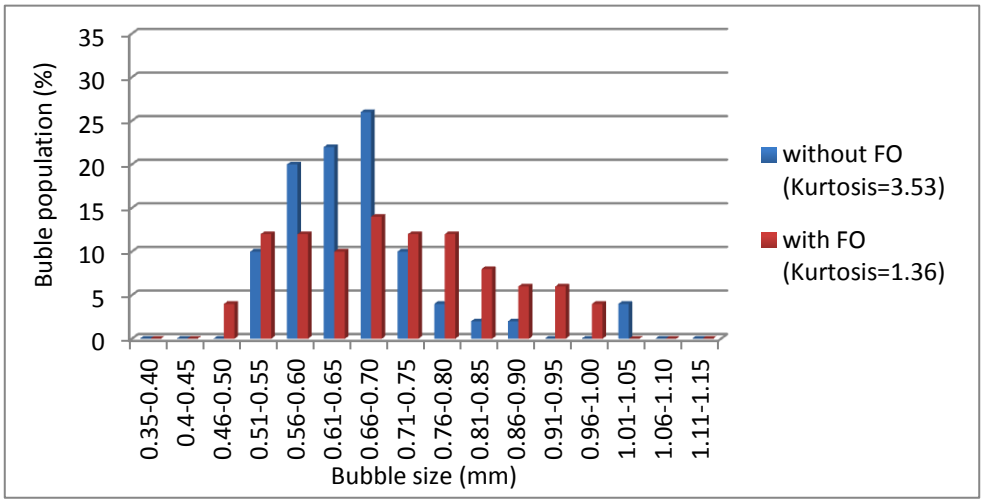

(c)

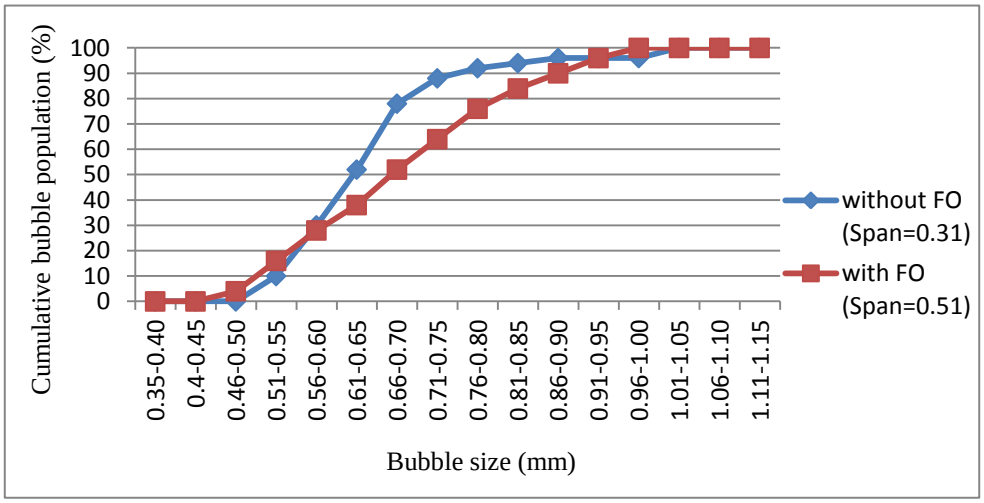

(d)

Figure 4.4 Bubble generation at flow rate 2.0 L/min; (a) without FO application, (b) with FO application, (c) comparison of bubble size distribution, (d) cumulative distribution curve

Figure 4.4 illustrates bubble generation at 2 L/min in steady (a) and oscillatory (b) flow. Noticeable different of bubbles size and bubbles population were found in captured images which supported by bubble size distribution data (c). Narrow distribution was observed at steady flow, with a kurtosis value of 3.53, while relatively flat distribution was obtained in oscillatory flow, with a kurtosis value of 1.36. Furthermore, according to cumulative distribution curve (d), the span value is 0.31 for steady flow and 0.51 for oscillatory flow. The bubble distribution was ranged from 0.51 to 1.05 mm in absence of FO with significant amount of bubbles were generated in size 0.66-0.70 mm. However, in the presence of FO, bubble distribution indicated relatively wider shape with ranges of bubbles was 0.46-1.00 mm. Majority of bubbles were generated at size of 0.66-0.70 mm with well distributed bubble population.

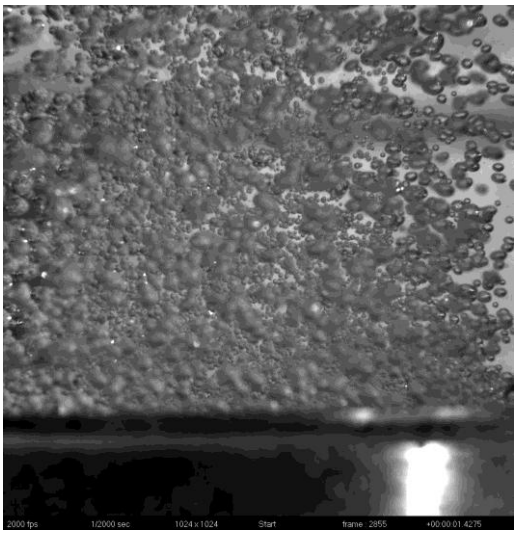

(a)

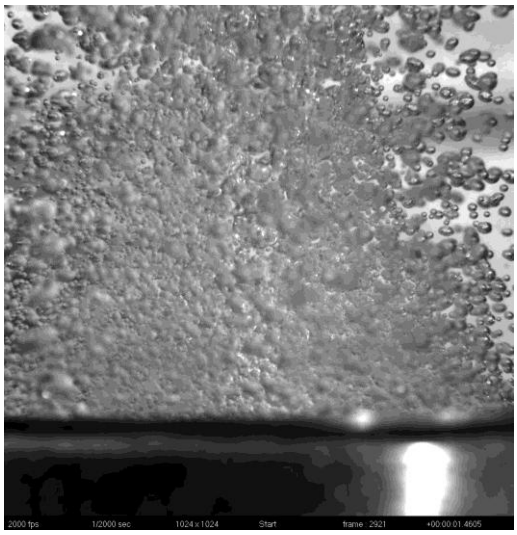

(b)

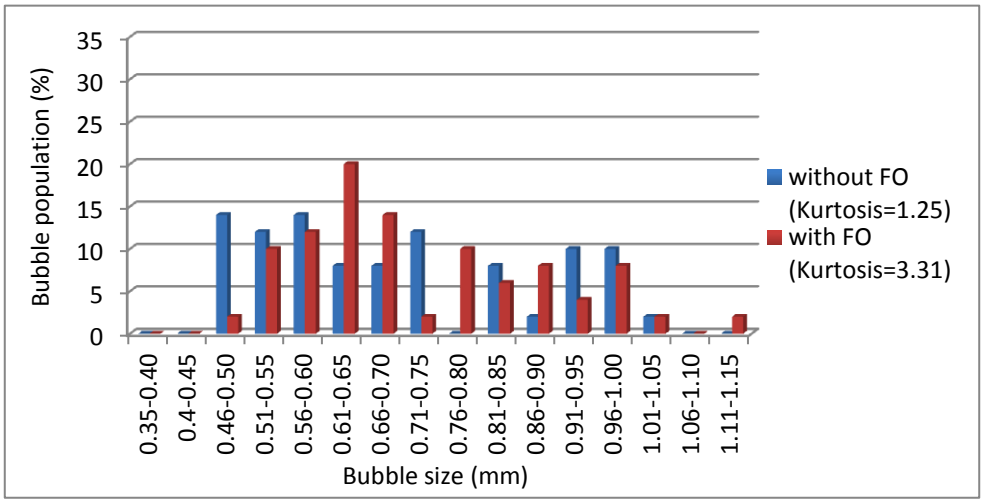

(c)

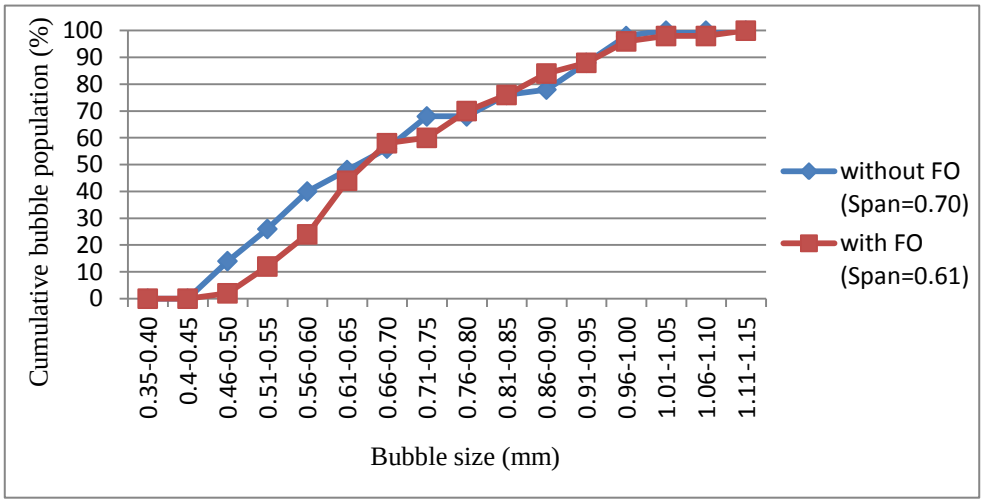

(d)

Figure 4.5 Bubble generation at flow rate 2.5 L/min; (a) without FO application, (b) with FO application, (c) comparison of bubble size distribution, (d) cumulative distribution curve

Figure 4.5 describes the bubble generation at 2.5 L/min without FO application (a) and with FO application (b). Both flow conditions; with and without FO application, indicated wide distributions of bubble generation (c). However, wider distribution observed in steady flow compare to in oscillatory flow. It is supported by higher span value in the absence of FO, 0.70 while only 0.61 of span value found in presence of FO (d). Uniformly distributed of bubbles, from 0.46-1.05 mm, were shown in distribution data of FO absence while majority of bubbles produced in oscillatory flow ranged 0.61-0.65 mm in size. Bubbles generated in oscillatory flow were ranged from 0.46-1.15 mm of bubble size. Near to normal distributions were achieved at higher flow rates tested.

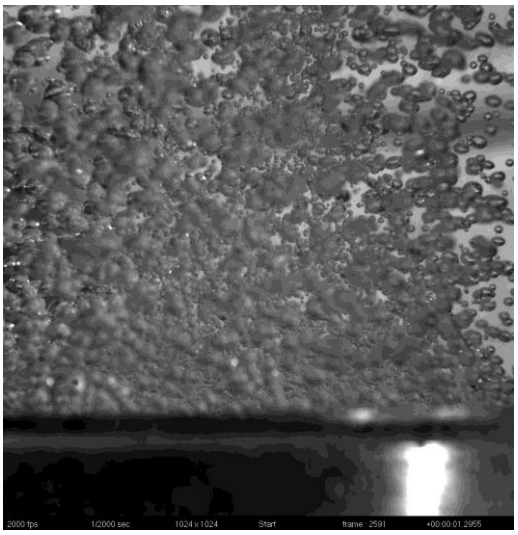

(a)

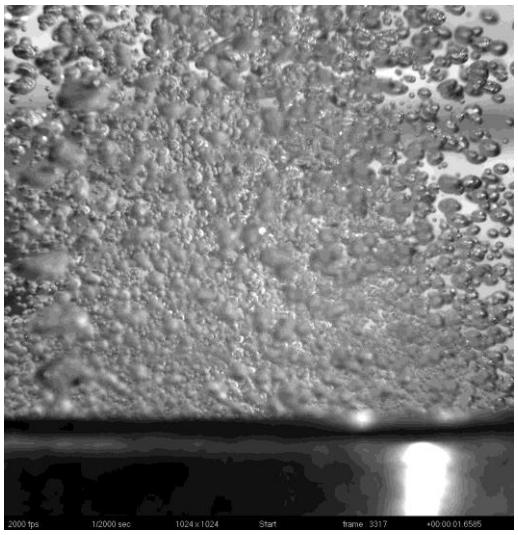

(b)

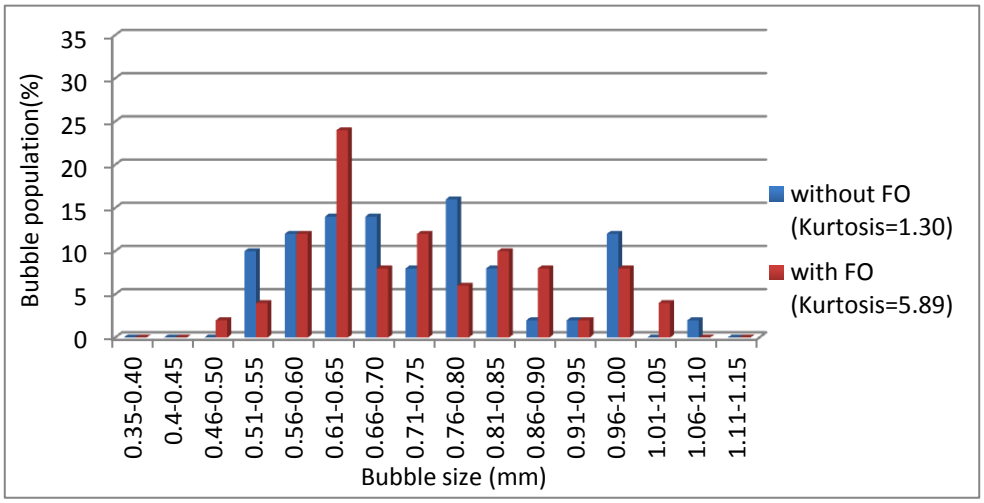

(c)

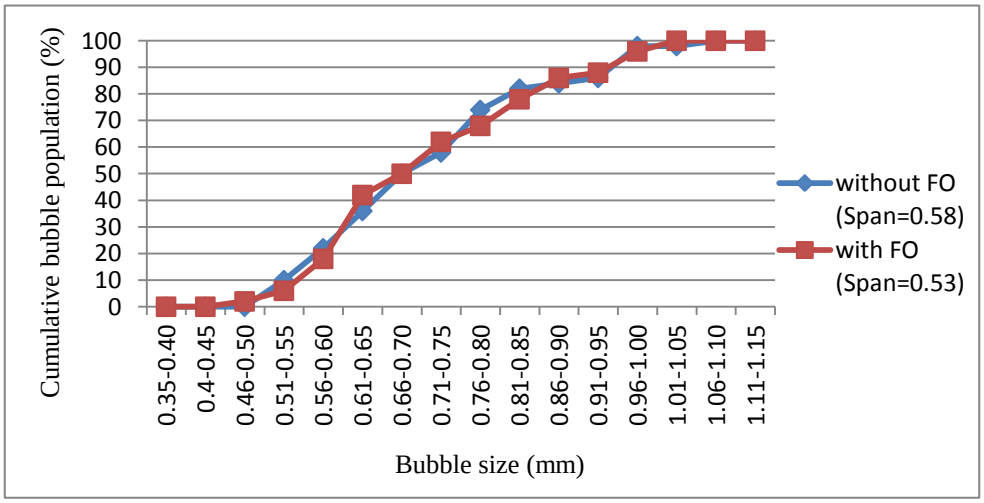

(d)

Figure 4.6 Bubble generation at flow rate 3.0 L/min; (a) without FO application, (b) with FO application, (c) comparison of bubble size distribution, (d) cumulative distribution curve

Figure 4.6 expresses bubble generation at the highest set of flow rate, 3 L/min at steady flow (a) and at oscillatory flow (b). Bigger size of bubble and more dense bubble population was noticed in the bubble size distribution histogram (c). Flat distribution of bubble generation, ranged from 0.51 mm to 1.10 mm, was generated at steady flow with majority of bubbles sized 0.76-0.80 mm. It was indicated by low kurtosis value which was 1.30. Near to a normal distribution was observed at bubble generation with presence of FO, in oscillatory flow. Finer bubbles were produced at 0.46-0.50 mm in size whilst 0.61-0.65 mm was defined as diameter where the pluralities of bubbles were generated. Cumulative distribution curve (d) shows relatively similar width of bubble distributions were observed with span value of 0.58 and 0.53 for steady and oscillatory flow, respectively.

The material properties of diffuser are major factors influencing bubble distribution. In this research, a bespoke sintered alumina-silica ceramic diffuser with some special features was used. Due to its manufacture, it has relatively hydrophobic properties with asymmetrical pore arrangement. Asymmetrical property of pore sizes in ceramic membranes is believed to influence bubble size during bubble generation (Reif and Dittmeyer, 2003). In addition, constant gas flow also played role in generating flat bubble size distribution at tested ranges of flow rate. The bubble formation process is governed mainly by wetting properties of bubble forming surface and pressure drop across diffuser (Rosso et al., 2008). It is important to note that once engaged to the bubble formation, the bubbles formed through the pores. As result a limited fixed number of pores with the smallest pressure drop were involved in bubble formation at the low flow rate. Therefore, narrow bubble size distributions were achieved during experimentations.

Along with rising flow rate, increased bubble size was observed, which may have been due to the rapid break off mechanism where coalescence with neighbouring bubbles occurs. In addition, flow and pressure conditions have become essential factors in the utilisation of ceramic diffusers (Reif and Dittmeyer, 2003). The phenomena took place at higher flow rate where pressure builds up under the diffuser plate (Clift et al, 1978). Furthermore, at the same pressure drop across the diffuser, it is possible more pores of different diameters became involved in the bubble formation (Burns et al., 1997). This effect is reflected in the deformation of the bubble size distribution from the normal to the flat shape observed from the 2.5 L/min of flow rate.

Study of microbubble generation related to flow oscillation has been previously investigated by other researchers (Tesar, 2014, Zimmerman et al., 2009, Rehman et al., 2015). FO does not change averaged flow rate but alters a pressure field within a flow during process. A steady pressure transforms to a sequence of pressure waves approaching a diffuser (Al-Mashhadani, 2013). Rising pressure initiates bubble formation from wide range of pores. Bubbles to be formed have very large surface curvature and require small pressure of air to continue growing (Zimmerman and Tesar, 2008). Nevertheless a gas-liquid interface surface curvature decreases rapidly and pressure of air has to be higher to continue bubble growth, as it follows from the Young-Laplace law (Hancocks, 2011). At this moment a pressure wave experiences a negative phase.

Tesař and Zimmerman (2008), in their patent document, explained that there are two main complex competing processes to take into account for a bubble formation mechanism. First is gas diffusion from the half way formed bubble back to the feeding pore. This results due to higher pressure in the volume of attached bubble in comparison to other side of the diffuser

which is experiencing a negative phase of a pressure wave as the jet in the oscillator switches to the other outlet leg. As gas from the big pores with a low pressure drop withdraws, the bubble formation process terminates. Bubbles initiated on the pore with higher pressure drop cannot get bigger due to pressure reduction in the pore. Second is a strong adverse effect of surface tension at this higher curvature to complete and detach bubble. For a given surface properties and a wide set of feeding pores this results in a narrow set pores which will be able to form bubbles. This situation repeats for every pressure wave arriving to a membrane. This is one of the reasons for the diverse bubble distribution obtained in oscillatory flow by comparison to steady flow.

Table 4.1 Statistical data of bubble size distribution

Flow rate (L/min)	Average bubble diameter (mm)		Span		Kurtosis	
	Without FO	With FO	Without FO	With FO	Without FO	With FO
0.5	0.61±0.11	0.56±0.11	0.53	0.56	7.91	3.9
1	0.65±0.08	0.65±0.12	0.31	0.54	2.22	1.58
1.5	0.67±0.11	0.65±0.13	0.47	0.58	2.03	3.14
2	0.67±0.11	0.70±0.13	0.31	0.51	3.53	1.36
2.5	0.70±0.18	0.72±0.16	0.70	0.61	1.25	3.31
3	0.73±0.15	0.74±0.14	0.58	0.53	1.3	5.89

It has been observed that rising of flow rate at steady and oscillatory flow conditions resulted in complex behaviour of the bubble formation mechanism. Table 4.1 shows statistical data of bubble size distribution in both flow conditions. It is shown that there is no significant increase of average bubble size in absence of FO and presence of FO application. This may be due to small variance between tested flow rates, 0.5 L/min, hence pressure drop in the system is not significantly differed. As discussed in section 2.6, Chapter 2, pressure drop is one of the essential parameters in bubble generation (Clift et al., 1978, Agarwal et al., 2011, Hanotu,

2013). Small pressure difference between bubble and its surrounding results bigger size of bubbles. This peculiarity could also be explained by non uniformity of ceramic diffuser pore size (Colt et al., 2010, Reif and Dittmeyer, 2003). It is thought that the sintering process during ceramic diffuser production had resulted in a diversity of product pore sizes. Therefore, when pressurised gas flow by FO is applied through the ceramic diffuser, uncontrollable larger bubbles were produced. Relatively narrow distributions were observed at a flow rate of 2 L/min, in both flow conditions. The span value of 0.31 and 0.51 were calculated under conditions of without and with FO application, respectively. In addition, a peaked distribution with the kurtosis value of 3.53 was reported without FO application. Sheikhi et al (2013) reported that a large kurtosis value reflects equilibrium between bubble coalescence and breakage mechanism. This means there are relatively greater fractions of bubbles near the average size compared with the fraction of bubbles with either small and large sizes. The air flow rate of 2 L/min was found to be the point where the balance between bubble density and bubble uniformity was most suitable for the ozonolysis. At higher flow rates, faster bubble detachment from ceramic surface was occurred. This caused shorter contact time between ozone-rich bubbles and samples. Therefore, detoxification may not perform effectively because chemical reaction of ozone and phorbol ester content in jatropha samples was not completed. On the other hand, at lower flow rates, relatively wider ranges of bubble distributions, shown by bigger values of spans, were produced which influenced the uniformity of bubble size. This affects mass transfer during ozonolysis as ozone cannot diffuse completely to the shell wall of jatropha meal molecular structure.

4.2. Characterisation of plasma microreactor

Experiments were begun by investigating the breakdown voltage for whole range of air flow rates, 0.5-3.0 L/min. The voltage signal for each flow rate was recorded in order to find the

voltage required for ozone generation at each specific flow rate. The study was further conducted for performance characterisation of the plasma microreactor by monitoring its ozone production. Gas and liquid phase measurement of ozone concentration was done using the Indigo Method (Bader and Hoigné, 1981). Measurement was performed at air flow rate of 2 L/min because it is the margin point of bubbles uniformity and density observed in this experiment. In addition, temperature of Dielectric Barrier Discharge (DBD) plasma caps, Figure 3.4 in Chapter 3 page 52, was monitored for 2 L/min of flow rate. In principle, FO application was aimed at controlling the bubble size during microbubble generation, as described in Chapter 2. The FO is assumed to have negligible influence on the ozone production of the reactor because the oscillation frequency is too high.

Because the effect of FO application for the target of ozone generation with this system resulted in a large disparity in bubble size distribution, this was counter productive for the objective of regularity of bubble contact time. Therefore, experiments assessing Jatropha remediation are only performed in steady flow.

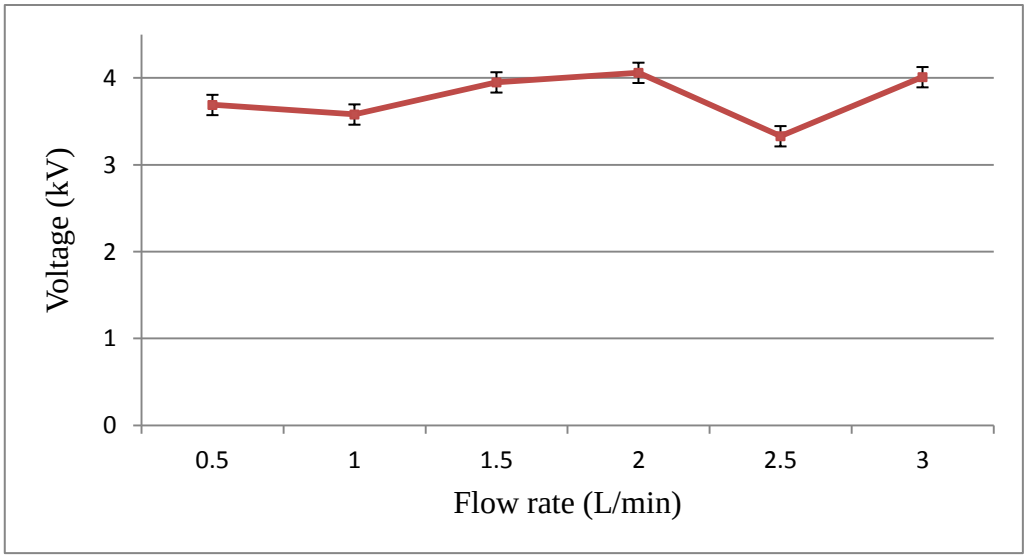

Figure 4.7 Breakdown voltage of plasma ignition at different flow rates

Figure 4.7 presents the breakdown voltage over the full range of air flow rates (0.5-3 L/min). As discussed in Chapter 2, the breakdown voltage, also known as ignition voltage, is defined as an initial voltage where plasma is ignited (Kogelschatz, 1997, Fridman, 2008, Wagner, 2003). Once breakdown voltage been achieved, this voltage then decreased to the working voltage to maintain plasma discharge. Voltage reduction is advisable in order to avoid plasma arcing on the surface of dielectric layers. The working voltage was determined by observing the minimum level of voltage where plasma discharge is still maintained.

In general, there is a modestly positive trend relating flow rate and breakdown voltage during experimentation. There is no significant difference in breakdown voltage along with increasing of flow rate. However, an anomaly was also observed at a flow rate of 2.5 L/min that the breakdown voltage dropped. The absence of significant variation of voltage difference is expected due to moderate pressure divergence inside DBD configuration. Theoretically, an increase in applied gas flow rate results in higher average pressure drop in plasma gap, therefore higher breakdown voltage is required (Alemskaya, 2003, Pekárek, 2003). Referring to the Paschen Curve, breakdown voltage determination is influenced by the operating conditions, gas composition and reactor configuration (Opalinska, 2002, Nehra et al., 2008, Fridman, 2008). Operating conditions are determined as gauge pressure, gas composition, temperature and flow rates while reactor configuration refers to geometry (especially gap distance between electrodes) and materials of the reactor. In these experiments, gap distance and the materials (for detail specification, see Chapter 3) was kept constant while pressure was relatively stable as minor variations in air flow rates were applied. Therefore, a narrow range of breakdown voltage, 3-4 kV, was observed during experiments.

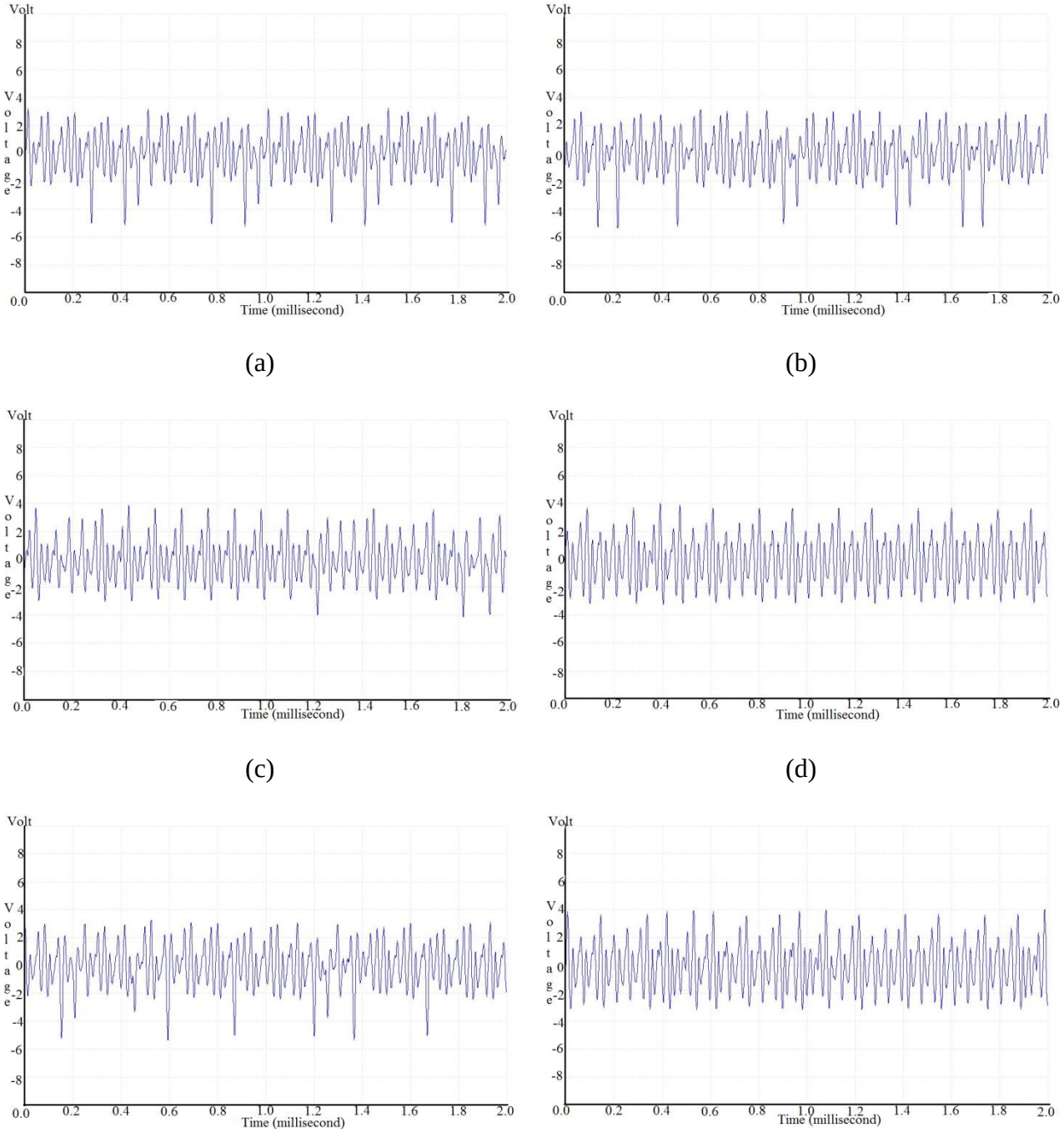

Figure 4.8 Oscilloscope readings of breakdown voltage at various flow rates, (a) at 0.5 L/min, (b) at 1.0 L/min, (c) at 1.5 L/min, (d) at 2.0 L/min, (e) at 2.5 L/min, (f) at 3.0 L/min. The axis label is shown as volt, however, actual value shows kilovolts due to a scale factor of 1000.

Figure 4.8 shows the voltage signal within the first 20 ms of plasma ignition at the various flow rates. The horizontal axis represents the time duration for which the signal was captured, in milliseconds. This is consistent with previous observation where plasma breakdown

occurred in less than a second (Wagner, 2003, Lozano-Parada, 2010, Beltrán, 2004). Ozone is generated instantaneously from the presence of oxygen in the plasma, which is also occurs in less than a second of residence time (Wagner, 2003, Lozano-Parada, 2010). The axis label of breakdown voltage is shown as volt, however, the actual value shows kilovolts due to a scale factor of 1000.

The plasma unit investigated here, fabricated from peek material, was designed to work at voltages of up to 6 kV. According to the experimental experience an optimal "safe" voltage level for this type of unit is approximately 4kV. Therefore, 4 kV was further determined as the ignition voltage while 3.8 kV was applied as the working voltage. Moreover, the current was observed to be relatively constant, approximately 25 mA, which was selected by the auto-tuning system of the bespoke power supply. Higher voltage causes higher power consumption by the reactor. However, the working voltage should be minimal in order to preserve the lifetime of plasma reactor. The working voltage was set to be 3.8 kV because below this level, the plasma discharge becomes unstable.

In accordance with the bubble size distribution results, the air flow rate of 2 L/min was chosen to be the working flow rate within these experiments. Lower flow rates resulted in a less dense cloud of bubbles, affecting adversely the mass transfer rates during ozonolysis. Ozone molecules could not diffuse effectively into jatropha molecular shell. On the other hand, at higher flow rates, bubbles detached faster, therefore resulting in lower contact time between ozone-rich bubbles and phorbol ester molecules. Moreover, the ignition voltage of 4.06 kV was considered as within the recommended safe range for applied voltage: 4 kV ± 10%. Ozone concentration measurement was only conducted at the flow rate of 2 L/min, where prior experimental calibration was done.

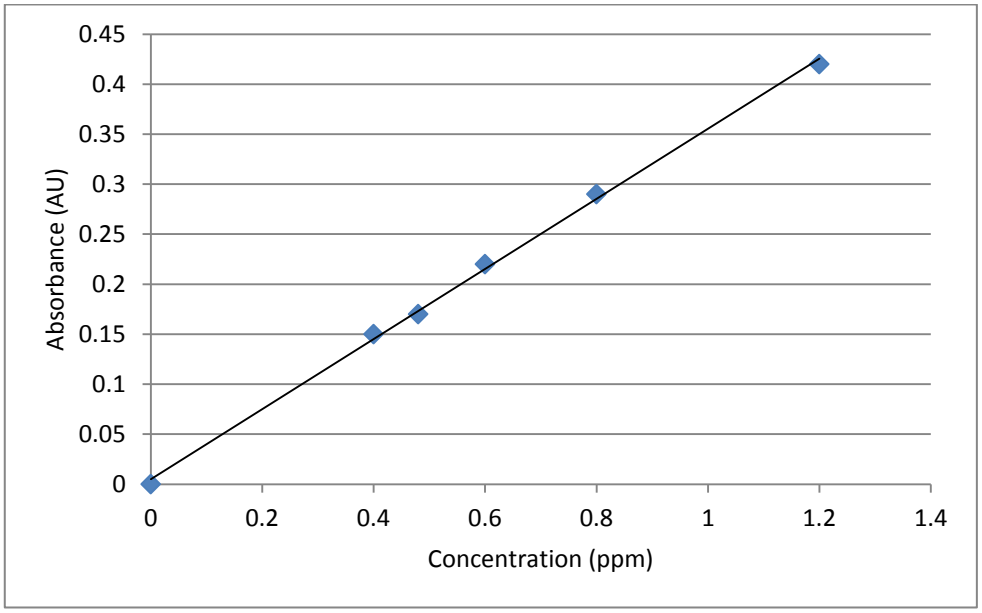

Figure 4.9 Calibration curve of ozone concentration

Figure 4.9 shows the calibration curve for the indigo experiments for ozone concentration determination. The calibration was performed at the range of ozone concentrations (0-2 ppm) that designed plasma microreactor produced. Calibration curve was determined by plotting indigo concentration against detected absorbance. Based on Indigo Method (Bader and Hoigné, 1981), 1 mol of decolorised indigo solution equals to 1 mol of produced ozone. Double bonds in Indigo molecules were broken by reaction with ozone, therefore, the amount of degraded indigo molecules corresponds to ozone molecules reacted. The gradient of calibration curve was then used to determine the ozone concentration measurement, in Fig 4.10.

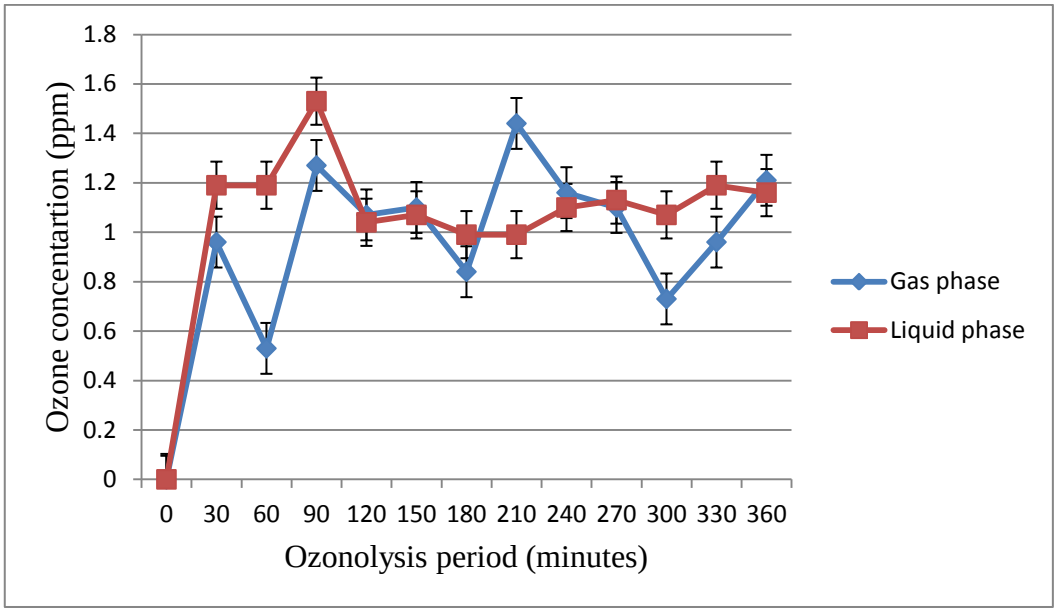

Figure 4.10 Ozone production in gas phase and liquid phase at 2 L/min air flow rate

Figure 4.10 shows ozone concentration in gas and liquid phase at flow rate of 2 L/min. The overall ozone production ranged from 0.6 to 1.6 ppm. This phenomenon results from a particular feature of the plasma microreactor design. The configuration and dimension of a DBD reactor as well as power supply used play some key roles. The ozone concentration in gas phase fluctuated between 0.6-1.6 ppm during experiments. Furthermore, ozone concentration in the liquid phase (dissolved ozone) was relatively constant over the time scale 6 hours with approximately 1.2 ppm of ozone was detected. The highest concentration of dissolved ozone was observed as 1.6 ppm after 90 minutes which was higher than ozone concentration in the gas phase at this point. This is in agreement with the investigation by Burgassi, et al (2009) who found that the concentration of dissolved ozone tends to be higher than the ozone concentration in the gas phase at equilibrium. It was assumed that the ozone reaction has equilibrated because the bubble residence time was long enough. Therefore, longer bubble stays in liquid, higher probability of equilibrium reached. In addition,

approximately of 10-fold higher ozone solubility compare with oxygen is reported in pure water study (Burgassi et al., 2009).

Ozone concentration measurement was performed at 30 minute intervals throughout 6 hours continuous duration of ozone production. Six hours treatment was determined as the maximum duration of continuous ozonolysis with designed reactor in this research in order to avoid plasma arcing. A plasma arcing is defined as an electrical breakdown of a gas in which be avoided because it permits current through electrodes. If this phenomenon occurs, plasma discharge cannot be produced uniformly hence it affects the density of plasma. Plasma arcing was observed after 6 hours continuous ozonolysis. Figure 4.11 shows DBD plasma microreactor after plasma arcing occurred.

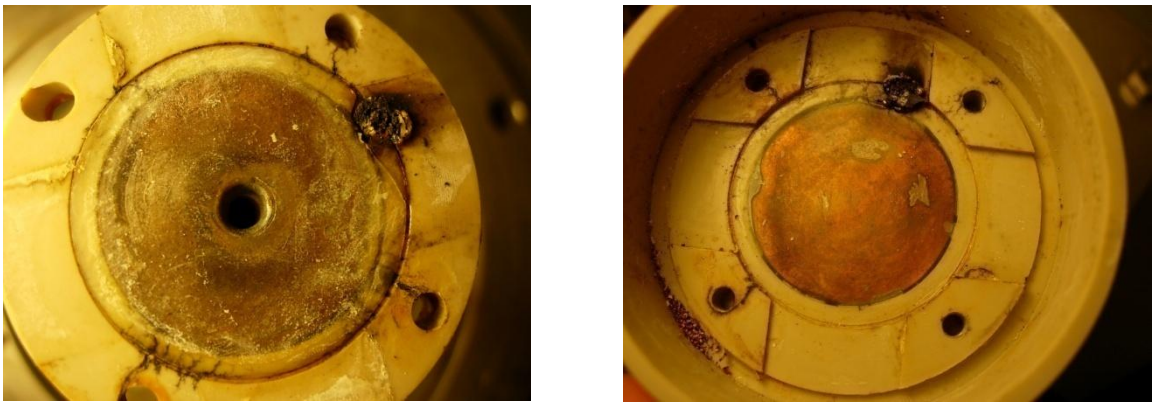

(a) (b)

Figure 4.11 Plasma microreactor after plasma arcing (indicated by burning part in the edge of electrodes); (a) is the bottom electrode and (b) is the top electrode

Further sets of experiments in this research were conducted within this range of ozonolysis duration. Subsequently, a further experiment was done which aimed to directly measure the temperature of plasma caps on DBD microreactor, Figure 3.4 in Chapter 3, Temperature measurement aimed to monitor the temperature of plasma caps during ozonolysis. This research aimed to develop technology which can detoxify phorbol ester content but maintain the protein content in jatropha meal. Therefore, it is essential to study the temperature

distribution in relation to its effect in biological content of jatropha sample during detoxification. Table 4.2 shows temperature data monitored during experiments.

Table 4.2 Temperature monitoring of DBD plasma microreactor

Duration (minutes)	Caps Temperature (^{0}C)	
	Top Cap	Bottom Cap
0	27.2	28.4
10	35	35
40	30.6	34.2
60	32.6	34.2

These experiments were performed for only 60 minutes due to laboratory safety requirements, detailed experimental procedures were presented in Chapter 3. Temperature of DBD caps was measured by directing the infrared thermometer to the cover surfaces. Top cap was defined in Chapter 3, Figure 3.4 as cover of the top electrode while bottom cap is covering the bottom electrode. In addition, the metal part of the reactor body had to be disassembled hence the DBD caps were exposed. The plasma discharge was ignited at the given times while temperature measurements were taken straight after electrical cut off. The temperature data indicates that temperature before and after plasma ignition was 6-7 °C higher. This is due to heat generated by the plasma. It is likely that the temperature within the plasma chamber (i.e. the surface of dielectrics) would be higher. In addition, the air stream was from bottom side hence top cap of DBD reactor was cooler. Approximately a 20% increase in temperature was observed after 60 minutes of plasma operation. After 60 minutes of operation, the plasma reactor will not reach temperature in excess of 35 °C (slightly above room temperature). Therefore, a cooling system is not required to prevent overheating that could damage the reactor. Furthermore, temperature of 35 °C is optimal for many biological processes especially in to avoid protein denaturation.

4.3. Summary

The air flow rate at 2 L/min in steady flow was chosen to be the operating condition for further experiments. The bubble sizes generated were 0.67 mm and 0.7 mm, in steady and oscillatory flow, respectively. It showed that there was no significant difference on bubble size distribution between steady flow and oscillatory flow. It was also observed that relatively narrow distribution occurred at a flow rate of 2 L/min with span value of 0.31 and 0.51 at steady and oscillatory flow, respectively. In addition, kurtosis value of 3.53 was reported for steady flow and 1.36 for oscillatory flow. Moreover, the ceramic diffuser characterisation showed that the fluidic oscillator (FO) application at a low flow rate produced finer bubbles by representing of 10% reduction in their average diameter. In addition, greater bubble population was achieved by using a fluidic oscillator (FO).

This phenomenon can be explained by material features of that ceramic diffuser which are emergent from the sintering process (Colt et al., 2010, Khirani et al., 2011, Reif and Dittmeyer, 2003). Specifically, it has been explained how the hydrophobicity opposes lubrication, but also leads to creation of least resistant-path pores from which fairly regularly sized bubbles are generated from steady flow. Pulsating flow results in much more evenly distributed flow through the porous media, and hence a wider range of bubble sizes.

The aim of this research was to study the effect of microbubble application and ozone treatment in chemical reactions of carbon double bonds (C=C). Ozone is expected to be delivered to the bulk of the liquid in the form of microbubbles generated from a ceramic diffuser. The compact design of the modified reactor used in this experiments, facilitated this mechanism. In order to investigate microbubble performance during ozonolysis, bubble

resident time was calculated based on average bubble velocity in the volumetric flow rate equation (4.1), as below.

$$Q = A\bar{v} \qquad (4.1)$$

Q is defined as volumetric flow rate ($dm^3.min^{-1}$) where A is the cross sectional area (dm^2) and $\bar{v}$ is the average velocity ($dm.min^{-1}$). In this research, volumetric flow rate is the chosen air flow rate, of 2 L/min. Furthermore, A refers to the cross sectional diameter of DBD microreactor of 28 mm chip diameter. The average velocity of bubble was further determined using a converted unit of Equation (1) which is equal to 0.054 m/s. Furthermore, the bubble resident time was calculated by using the radius of the DBD chip, with a result of 0.259 seconds. It was found that ozone-rich bubbles remained for 0.259 seconds in the DBD chip of plasma microreactor configuration. This is beneficial as some of ozone applications require short contact time for chemical reaction efficiency (Avery et al., 2013, EPA, 1999).

Plasma microreactor characterisation was started by investigating breakdown voltage in various tested flow rates (0.5-3.0 L/min). Study was then continued with ozone concentration measurement and temperature monitoring of DBD caps. Moreover, 1.4 ppm of ozone was observed in the gas phase while 1.2 ppm of dissolved ozone was detected during the plasma microreactor characterisation. Furthermore, in order to estimate the energy consumption of the plasma microreactor, the basic equation of power (4.2) and energy (4.3) was applied, which is

$$P = VI \qquad (4.2)$$

where power is defined as P (measured in Watt), V is voltage level (measured in Volts) and I is current (measured in Ampere). The power was calculated considering an applied voltage

(V) of 3.8 kV and a measured current (I) of 25 mA. The applied voltage was determined as working voltage used during experimentation of ozonolysis. From Equation (4.2), power was calculated as equal to 95 W. From the power, the energy consumed by the reactor over a given time (t), can be calculated using the following equation:

$$E = P\mathrm{t} \qquad (4.3)$$

Where E is energy (measured in kWh), P is power (measured in kW) and t is time that determined as period of plasma treatment during ozone generation (measured in hour). It is shown that consumed energy is proportional to the magnitude of required power and treatment period. The unit of energy consumption was presented in kWh, instead of Wh, because kWh is mainly used in industries at this field. The energy consumption measured over the maximum period (5 hours of ozonolysis) was that equal to $4.75\text{x}10^{-1}$ kWh.

According to the reactor characterisation results above, it can be reported that ozonolysis was able to be performed in aqueous conditions. The modified plasma microreactor permits ozone delivery to the bulk liquid in the form of microbubbles in which a new design of the plasma unit with compact configuration of ceramic diffuser, has provided possible gas-liquid-solid contact simultaneously. Conventional methods were limited for application of submerged plasma reactors. Furthermore, proposed technology in this research has been introduced to overcome this limitation. Covered plasma chips under a metal housing of the ceramic diffuser, offers secure ozone production during experiments. Also, microbubbles remaining longer in the liquid provide large gas-liquid contact areas which significantly enhance ozone dissolving rates. In addition, temperature monitoring on the DBD caps showed only small temperature increase after plasma treatment (in Table 4.2). This characteristic is beneficial for many fields

of application especially in biological treatments such as food processes which restrict heat treatment in order to prevent protein denaturation.

Reactor characterisation (the ceramic diffuser and plasma microreactor studies) has been explored in this chapter to be used prior to proposed experiments in the next chapters. Bubble size distribution, ozone concentration and DBD caps temperature have been reported. Bubble size distribution showed that an air flow rate of 2 L/min is favourable to be used in further treatments of jatropha ozonolysis. This is because more uniform bubbles were produced in this flow rate. Also, at 2 L/min of the flow rate, bubbles density is most suitable for ozonolysis. Higher flow rates caused faster bubble detachment, therefore, shorter contact time of bubbles and samples occurred. It affected ozone molecules could not effectively react with carbon double bonds in the phorbol ester molecular structures. Consequently, phorbol ester detoxification may not be achieved during ozonolysis as expected. However, lower flow rates result in wider bubble distribution which affects the uniformity of bubbles produced. It influences mass transfer of ozonolysis since ozone-rich bubbles cannot diffuse effectively through the jatropha kernel wall. Furthermore, it is reported that ozone concentration at a flow rate of 2 L/min was 1.4 ppm in the gas phase and 1.2 ppm in the liquid phase (dissolved ozone). In addition, the maximum temperature of the DBD caps after 60 minutes of ozonolysis was 35 °C which is actually favourable for many biological processes in relation to maintain the nutrient content in the samples. These parameters can now be used as a reference of operating conditions in further experiments. Investigations continued, reported in two following chapters, by processing samples of interest in an experimental reactor for ozonolysis treatment. Chapter 5 and 6 present the effect of ozonolysis on samples with chemical and biological studies.

CHAPTER 5

DETOXIFICATION OF PHORBOL ESTER COMPOUND

This chapter presents the application of the microbubble intensified ozonolysis method for detoxification of phorbol ester (PE) compounds. Ozonolysis was performed by application of plasma microreactor technology. Two studies of the effect of ozonolysis on synthetic and natural PEs are reported in different sections of this chapter. The first section describes the investigation of the ozonolysis effects on synthetic PEs. This section is a fundamental study of ozone reactions with manufactured PE chemicals. The second section discusses the study of ozonolysis effects on natural PEs. A natural PE is defined as a PE chemical which was obtained from natural sources. The study in the second section explores chemical reactions during ozonolysis of Jatropha biomass samples. The mechanisms for ozone reaction with PE compounds within the Jatropha intracellular structure are discussed. Details of experimental materials and methods employed in this research are described in Chapter 3, Section 3.3.1 for ozonolysis effects on synthetic PEs and Section 3.3.2 for ozonolysis effects on natural PEs. The experimental reactor, characterised prior to these investigations with detailed results reported in Chapter 4, was used to perform the ozonolysis experiments in this Chapter. Experiments were performed at atmospheric pressure and room temperature under steady flow conditions without use of a fluidic oscillator. Specific experimental parameters were chosen, as suggested in the summary section of Chapter 4. A High Performance Liquid Chromatograph (HPLC) was used as an analytical technique for PE detection. Chromatograms of PE detection after treatments are presented later in the chapter.

5.1 Detoxification of Synthetic Phorbol Ester

The detoxification study for synthetic PEs was conducted via two different treatments--aeration and ozonolysis. It aimed to compare the effect on PE concentration with and without ozone dosing. Aeration experiments were performed by bubbling the air through samples in the reactor. The microbubble influence on PE concentration is then isolated without ozone generation. Thereafter, ozonolysis was implemented in the treatment of synthetic PEs. HPLC with reverse phase mode was applied for PE analysis purposes (Dimitrijevic et al., 1996). The HPLC was calibrated prior to the investigations with a method adopted from Deachathai *et al* (2010). Triplicate experiments were performed for which the calibration curve is presented in Figure 5.1.

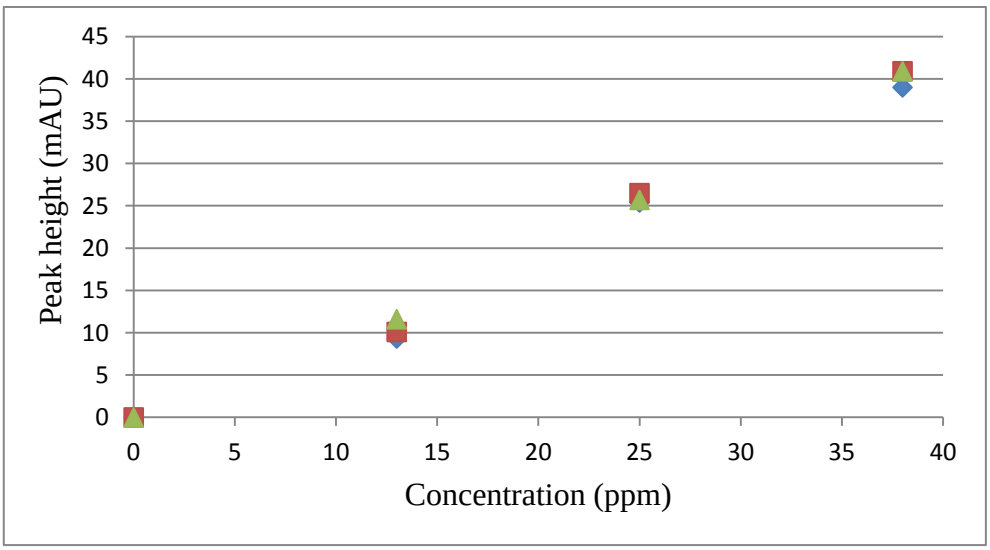

Figure 5.1 Calibration curve of TPA equivalent prior to PE investigation

Figure 5.1 shows calibration results of HPLC prior to the PE investigations. Calibration was conducted using a Phorbol-12-myristate-13-acetate (TPA) chemical as an external standard. TPA was also used as an experimental sample for ozonolysis on synthetic PEs. Absorbance of TPA at 232 nm wavelength was used during calibration. The calibration curve was determined by plotting TPA concentration against peak height. Peak height was chosen due to

higher precision in the measurement compared to peak area for the case of small peaks. It is also less influenced by error in establishing chromatograms during peak detection. An equation fitting the calibration curve was then used to determine TPA concentrations. Experiments were initiated with study of the effect of aeration on TPA concentration. Each sample of TPA after treatment by aeration was analysed using HPLC to determine the remaining PE concentration. Chromatograms of detected PE peak are provided in Figure 5.2.

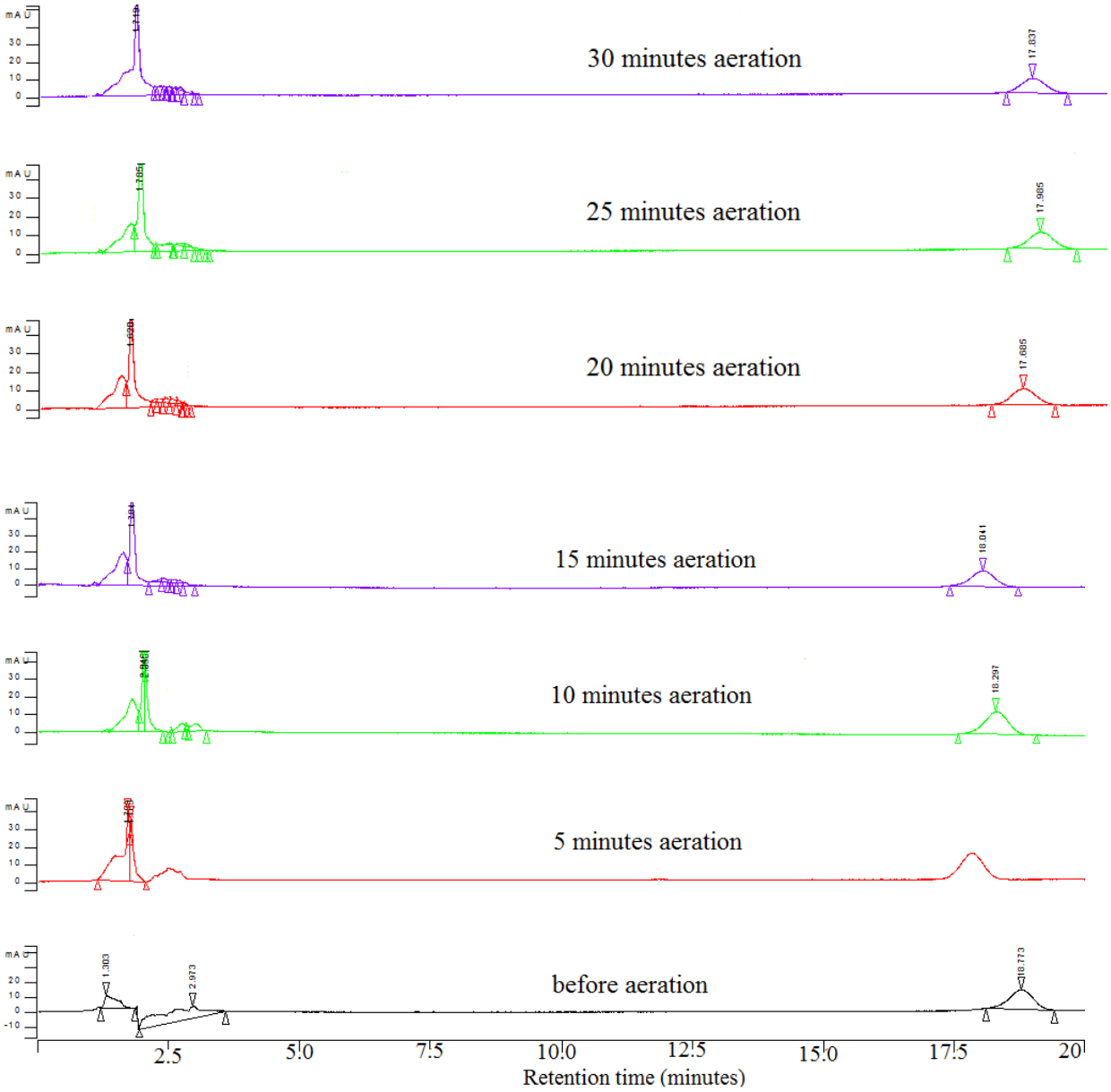

Figure 5.2 Chromatograms of HPLC detection after TPA aeration by air microbubble; x-axis represents the retention time in minutes, y-axis is the peak absorbance

Figure 5.2 presents chromatograms of TPA detection during aeration without ozone involvement. TPA peak appeared at a retention time of 16-18 minutes while peaks appearing in a region around 2.5 minutes are solvent peaks. A well defined peak of interest was observed in each chromatogram as the pure chemical of TPA was used during experiments. It was shown that PE peak was constantly detected until experimentation completed. Peak height was relatively stable in every sampling period which indicated no significant reduction of PE concentration. TPA concentration was further calculated, and this is shown in Figure 5.3.

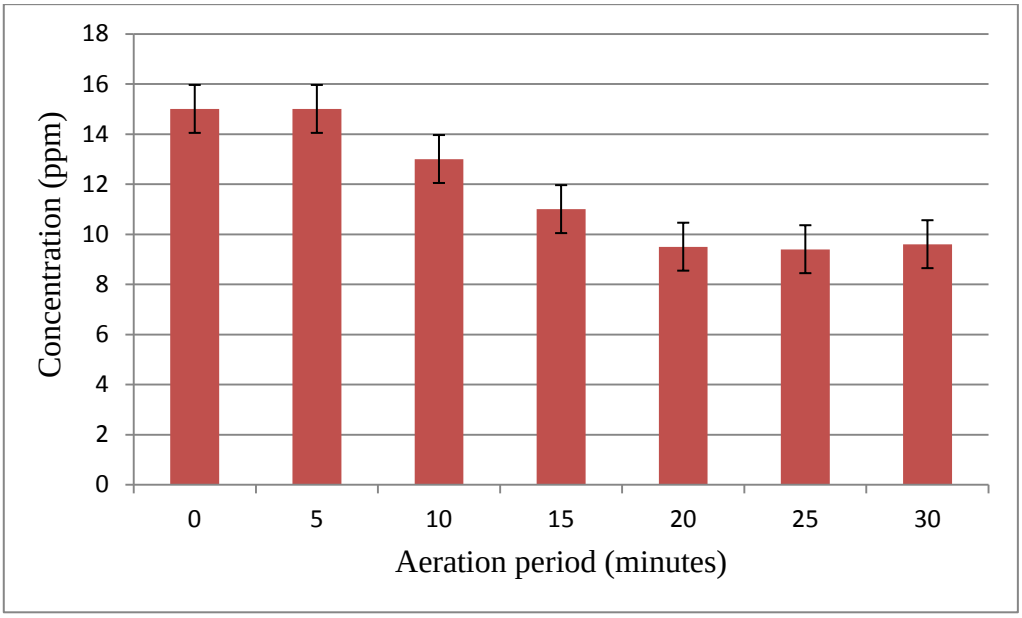

Figure 5.3 Aeration effect of TPA treated by air microbubble without ozone activation

Figure 5.3 indicates aeration effect of TPA for 30 minutes duration of treatment. Experiments were conducted by passing the air through experimental reactor without plasma ignition. As a consequence, ozone production was absent during experiments whilst microbubble and other components of air showing the gas supply influence were isolated. A significant reduction of TPA, 40%, was noted after 30 minutes of aeration. Nearly all the TPA concentration reduction occurred in the first 15 minutes.

Aeration via microbubbles enriches the oxygen supply to the reaction system. Microbubbles intensify mass transfer across gas-liquid interface which improves oxygen dispersion (Kawahara et al., 2009, Muroyama et al., 2013, Parmar and Majumder, 2013). A previous study by Li, Pan (2006a) mentions that reduction of bubble size influences oxygen concentration produced. Oxygen, with an oxidising potential of 1.23 V, is a common oxidant for some chemical reactions (Barlow, 1994). Oxygen molecules reacted with phorbol ester, as the chemical of interest in this experimentation. However, oxidising potential of oxygen provided insufficient energy to break carbon double bonds in TPA molecular structure. Therefore, no significant detoxification of TPA was achieved after treatment by aeration.

The study continued by applying ozonolysis with the air passing through electrical discharge of plasma ignition. A fresh sample of TPA solution as the synthetic PE was prepared for ozonolysis treatment. The process was conducted in triplicate and samples collected for analysis. Chromatograms of TPA degradation by ozonolysis are presented in Figure 5.4.

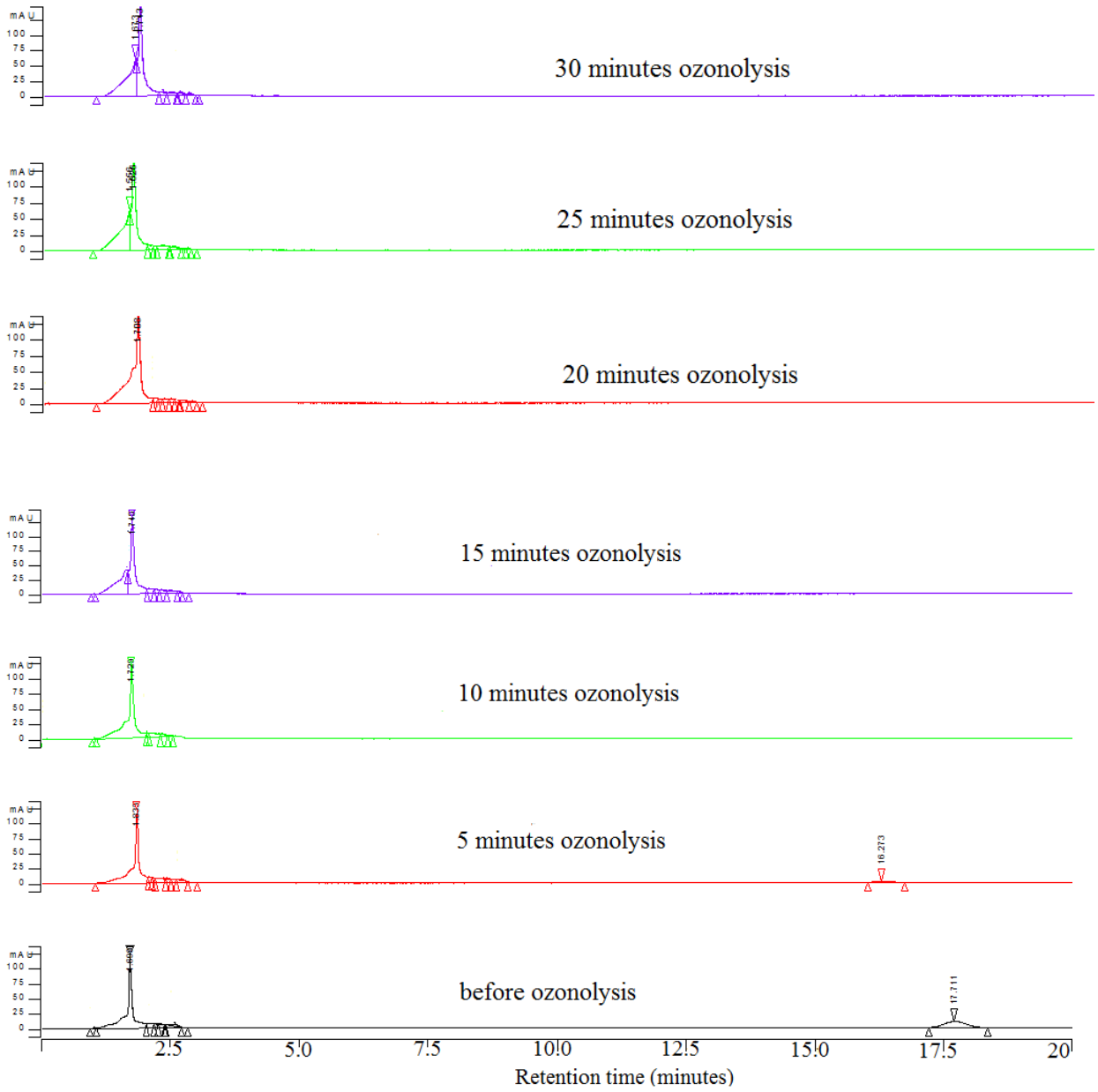

Figure 5.4 Chromatograms of HPLC detection after TPA ozonolysis; x-axis represents the retention time, y-axis is the peak absorbance

Figure 5.4 describes chromatograms of TPA with peak detection after ozonolysis. The initial TPA peak before treatment appeared at 17.5 minutes of retention time. A relatively detectable peak was observed after 5 minutes of ozonolysis. Significant reduction of peak height corresponds to substantial decrease of TPA concentration in treated sample. Furthermore, from 10 minutes of treatment until completion, there was no peak detected in the region of

interest. It indicated that TPA concentration in samples was below the limit of HPLC detection. In addition, calculation results are presented in Table 5.1.

Table 5.1 TPA concentration after ozonolysis

Ozonolysis period (minutes)	Concentration (ppm)
0	11
5	4
10	ND
15	ND
20	ND
25	ND
30	ND

*ND= not detected

Table 5.1 describes TPA concentration data detected by HPLC after ozonolysis was performed. It showed a striking reduction of TPA concentration after 5 minutes ozonolysis. The initial TPA concentration was 11 ppm and after 5 minutes of ozonolysis decreased to be 4 ppm. It indicated that 64% of reduction was successfully achieved. Experiments continued, however, TPA peaks after 10 minutes of treatment could not be detected as it was below the HPLC detection limit. This condition remained until 30 minutes of treatment completion. It suggested that lower limit of HPLC detection for current set up in this research is below 4 ppm of PE concentration.

Phorbol ester degradation during ozonolysis results from reaction of ozone and its derivatives with the chemical structure of PE. Principally, direct and indirect reaction mechanisms occur during ozonolysis which produce free radicals due to ozone decomposition. Direct reaction is defined as an actual ozone reaction which ozone molecules mostly play important roles. Moreover, indirect reaction occurs when free radical species are formed from the breakdown

of ozone. Direct reaction is considered as an initiation step which lead to indirect reaction (Beltrán, 2004). Existence of both mechanisms is mainly influenced by pH condition of reaction zone (Eriksson, 2005, Kuntia et al., 2013, Hoigné and Bader, 1978, Beltrán, 2004). At pH <9, the direct reaction mechanism predominates in ozone decomposition.

5.2 Detoxification of Natural Phorbol Ester

An investigation of natural phorbol ester detoxification was carried out by performing ozonolysis of Indonesian jatropha meal samples. The phorbol ester (PE) compound was obtained by extracting jatropha meal (JM) using two types of solvents, hexane and methanol. First of all, hexane extraction was performed while the resulting extract was further analysed by a High Performance Liquid Chromatography (HPLC). Next, extraction was continued using methanol solvent and resulting extract was also analysed using the HPLC Method. The double stages of extraction and chromatography analysis were conducted following to investigation done by Gaur (2009). He mentioned that a double stage extraction was performed due to natural characteristics of PE. As described in Section 2.2 of Chapter 2, PE is naturally esterified in a matrix of fatty acids, therefore, prior extraction of lipid compounds is required, in order to obtain the PE extracts efficiently. Forson, *et al* (2004) suggested hexane as a solvent for lipid extraction because 98% of lipid extract in jatropha oil was achieved. Moreover, PE is also reported more polar than the major lipids that compose jatropha meal (JM), triacyl glycerols, hence a polar solvent such as methanol was further used for extraction. Methanol is also known as a favourable solvent to extract biological compounds from plants (Saetae and Suntornsuk, 2010).

The HPLC chromatograms of both hexane and methanol extracts are presented in this section. Chromatograms of hexane extract showed peaks of PEs as well as the presence of fatty acid

fractions. The main free fatty acids detected in jatropha oil are linolenic acid (18:3), linoleic acid (18:2), oleic acid (18:1), palmitic acid (16:0) and stearic acid (18:0) (Kaushik and Bhardwaj, 2013, Gübitz et al., 1999, Gaur, 2009, Rodríguez et al., 2011, Wink et al., 1997). In this experiment, fatty acids peaks appeared before 15 minutes of retention time while PEs peaks appeared from 16 to 28 minutes. In addition, the PE peak during calibration appeared at 17 minutes of retention time.

Diwani, *et al* (2011) observed that PE peaks could appear in a range of 10 minutes after the calibration peak appeared. Therefore, peaks appearing beyond that range were considered as non-PE peaks which might result from chemical reactions such as interference of the fatty acids matrix and cleavage of PE molecular cells (Devappa et al., 2013). Figure 5.5 shows the HPLC chromatogram of fresh JM and 1 hour treated JM in hexane extract. Before ozonolysis was performed, fresh JM was extracted in order to analyse the original concentration of PE content.PE peaks detected in hexane extract were considered as PE compound which were bonded in lipid fractions.

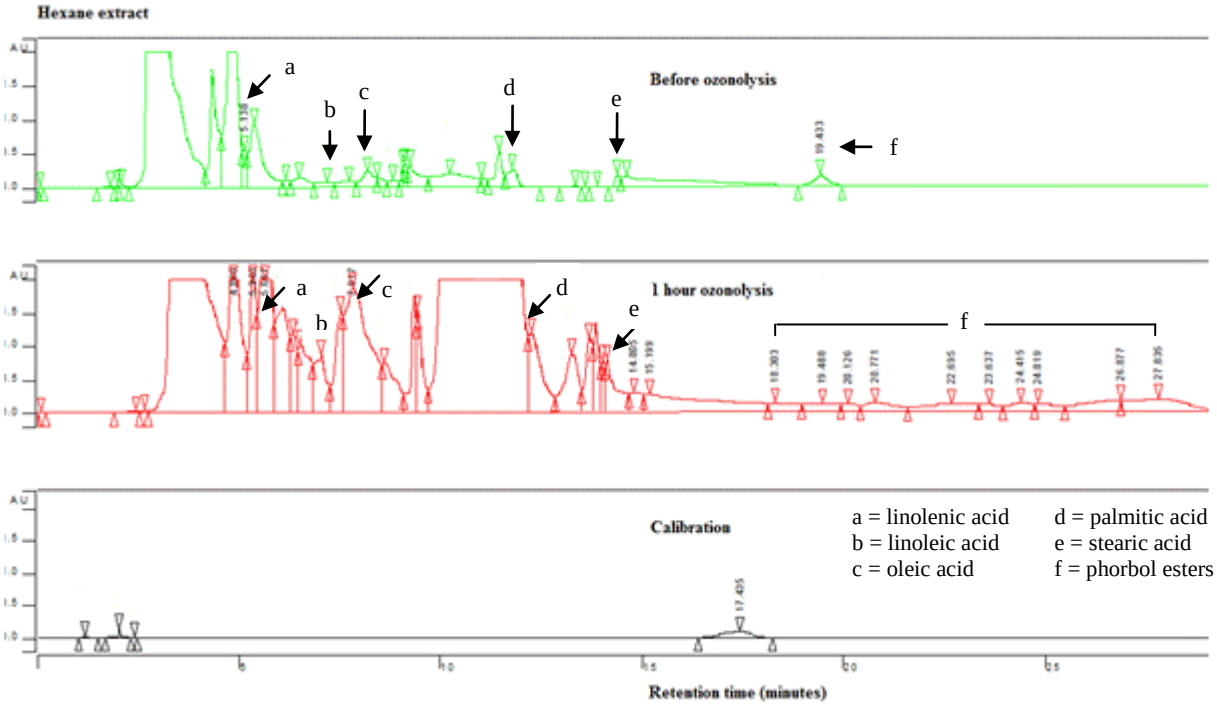

Figure 5.5 Chromatograms of hexane extract before and after 1 hour of ozonolysis

Figure 5.5 illustrates chromatograms of PE calibration and hexane extracts of JM samples before and after 1 hour of ozonolysis. In calibration chromatograms, a group of peaks appeared between 1 to 3 minutes which representing solvent peaks from mobile phase used during HPLC analysis. The mobile phase used for solute elution in HPLC was a mixture of acetonitrile and water. The water peak appeared at 1 minutes and the acetonitrile peak appeared at 2 minutes while the other peak indicates the resulting component of the mixture. Moreover, a single peak appeared at 17 minutes of retention time which was further considered as a PE peak. No other peaks were detected afterwards. Fatty acids peaks also appeared in the chromatograms of PE extraction from JM samples. Peaks of linolenic, linoleic, oleic, palmitic and stearic acids appeared at 5, 7, 8, 12 and 14 minutes of retention time, respectively.

Based on the chromatograms, the shape of fatty acids peaks before and after 1 hour of ozonolysis were different. Quantitative analysis of fatty acids concentration was not performed because it is beyond the scope of this research. However, the overall oil content was analysed and the result is presented in this section. A significant height of fatty acids peaks were observed after 1 hour of ozonolysis. This indicates that cell wall breakdown of JM molecular structure occurred due to ozone presence. Consequently, more fatty acids were released therefore detected during chromatography analysis. Uppu and Pryor (1994) reported ozone reactions that occurred in a biological material which involved ozone exposure into fatty acids compounds. Furthermore, a single peak of PE was detected at 19 minutes in the chromatogram of untreated JM sample, before ozonolysis was performed. Next, group of phorbol ester peaks were detected after 1 hour of ozonolysis. The PEs peaks appeared at retention time ranging from 18 to 28 minutes. Formation of a PEs group of peaks was assumed as a result of ozone reaction with phorbol ester in a medium including fatty acids.

Figure 5.6 presents the chromatogram of JM samples in hexane extract after 2 and 3 hours of ozonolysis was performed. The peaks positions show features that are significantly distinct compared to peaks appearing in the chromatogram after 1 hour of ozonolysis.

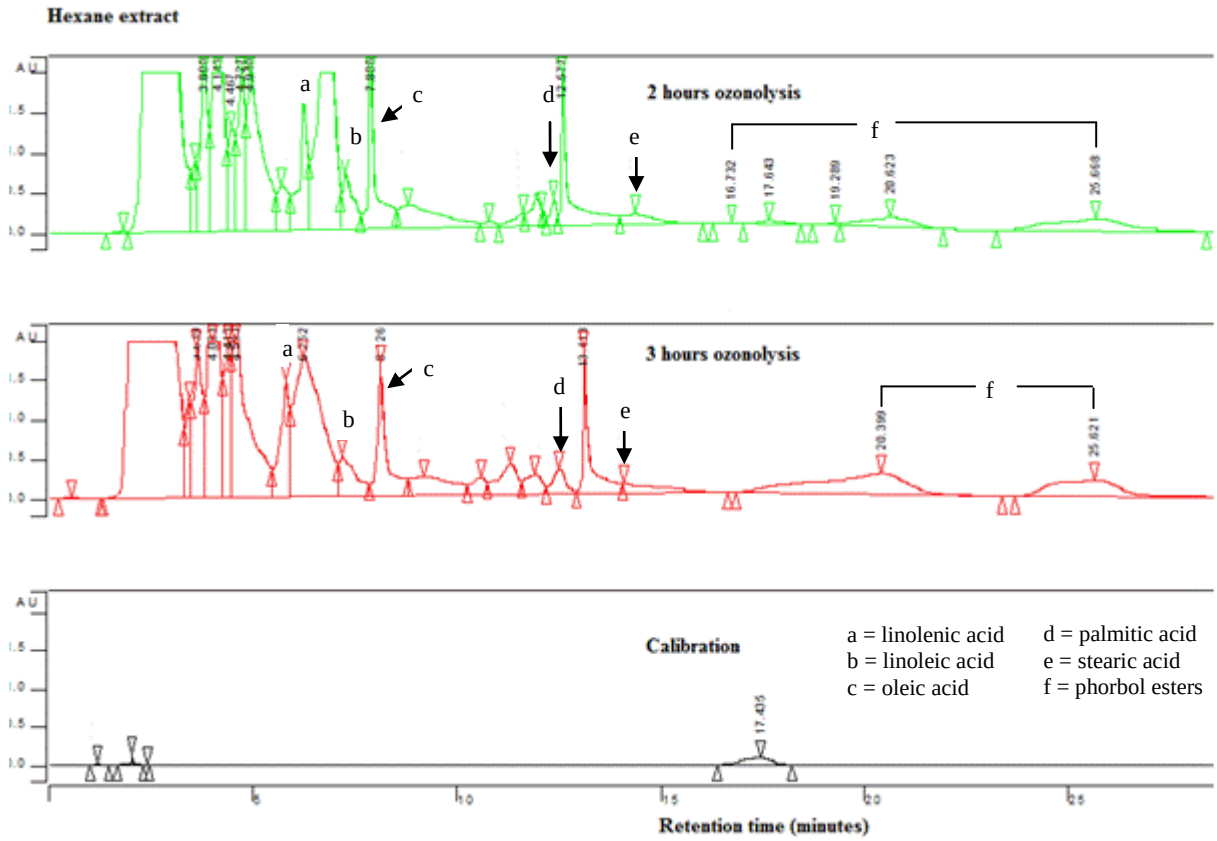

Figure 5.6 Chromatograms of hexane extract at 2 and 3 hours of ozonolysis

Peaks of fatty acids and PEs were observed in the chromatogram of hexane extract after 2 and 3 hours ozonolysis, as shown in Figure 5.6. Compared to chromatogram after 1 hour of ozonolysis, Figure 5.5, the linolenic acid peak (a) showed stability of its height while peaks of other fatty acids (b-e) were changed in height. Peak heights of linoleic acid (b), palmitic acid (d) as well as stearic acid (e) were reduced after 2 hours of ozonolysis and remained constant after 3 hours of ozonolysis. On the other hand, peak height of oleic acid (c) increased after 2 hours of ozonolysis and remained stable at 3 hours ozonolysis. In addition, five peaks of phorbol esters (f) were detected after 2 hours of ozonolysis while after 3 hours of ozonolysis only 2 peaks were detected. PE peaks after 2 hours of ozonolysis appeared at a range of retention time from 16 minutes to 26 minutes. Moreover, after 3 hours of ozonolysis, PE peaks appeared at 20 minutes and 25 minutes of retention time.

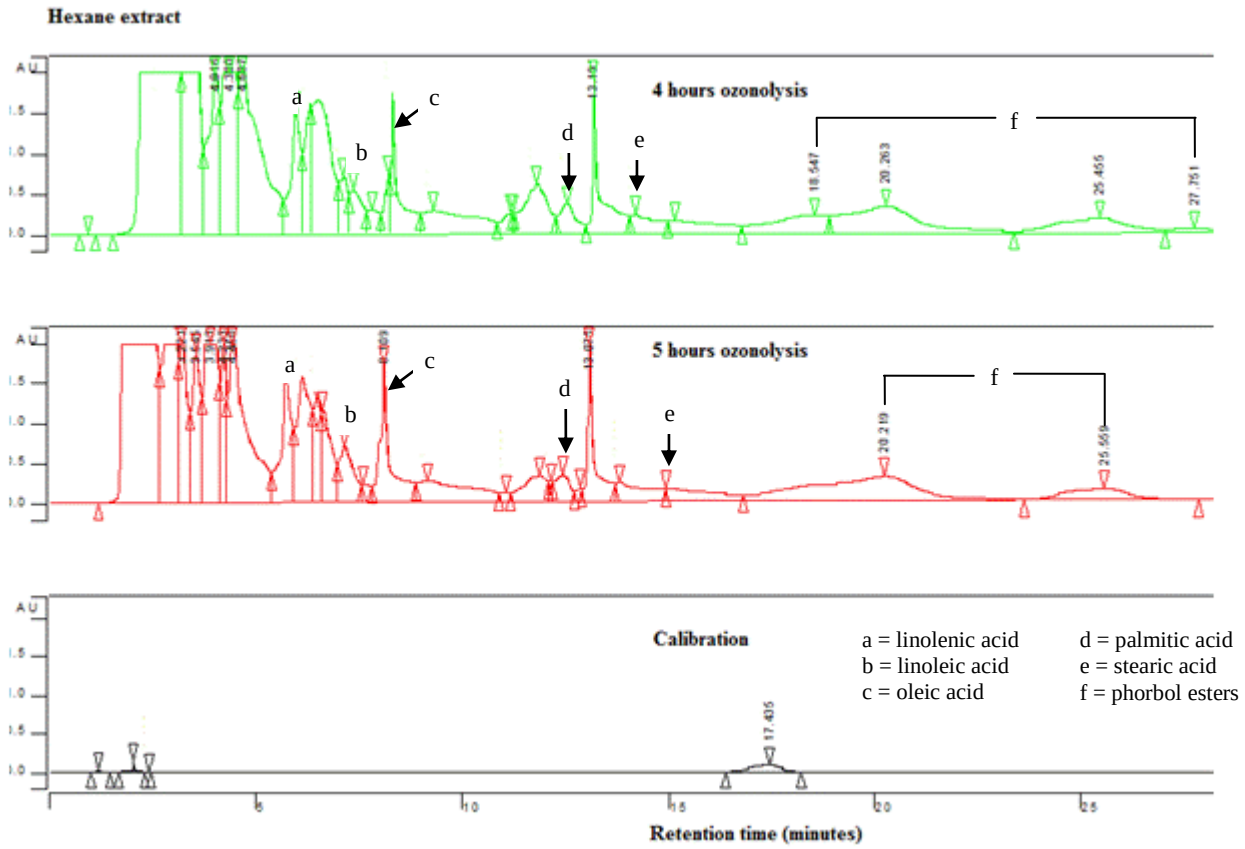

Figure 5.7 Chromatograms of hexane extract at 4 and 5 hours of ozonolysis

Figure 5.7 shows HPLC chromatograms resulting from a JM sample in hexane extract after 4 hours and 5 hours of ozonolysis. There was no signification difference observed in fatty acids peaks compared to previous chromatogram, Figure 5.6. Peaks heights of linolenic acid (a), linoleic acid (b), palmitic acid (d) and stearic acid (e) remained constant than chromatograms of hexane extract at 3 hours, 4 hours and 5 hours of ozonolysis. However, peak height of oleic acid (c) at 4 hours of ozonolysis was lower compared to chromatograms at 3 hours and 5 hours of ozonolysis. Furthermore, four peaks of PE appeared at 18-27 minutes of retention time after 4 hours of ozonolysis and two peaks of PE, where retention time is 20 and 25 minutes, were observed at chromatogram after 5 hours of ozonolysis.

Phorbol ester concentration was examined individually in hexane and methanol extract. Figure 5.8 shows the PE concentration in hexane extract before and after ozonolysis. PE concentration was determined by summing the height of the PE peaks and converting to TPA equivalent. This approach was used in following to previous researchers (Haas and Mittelbach, 2000, Makkar et al., 2009, Kuvshinov et al., 2014b).

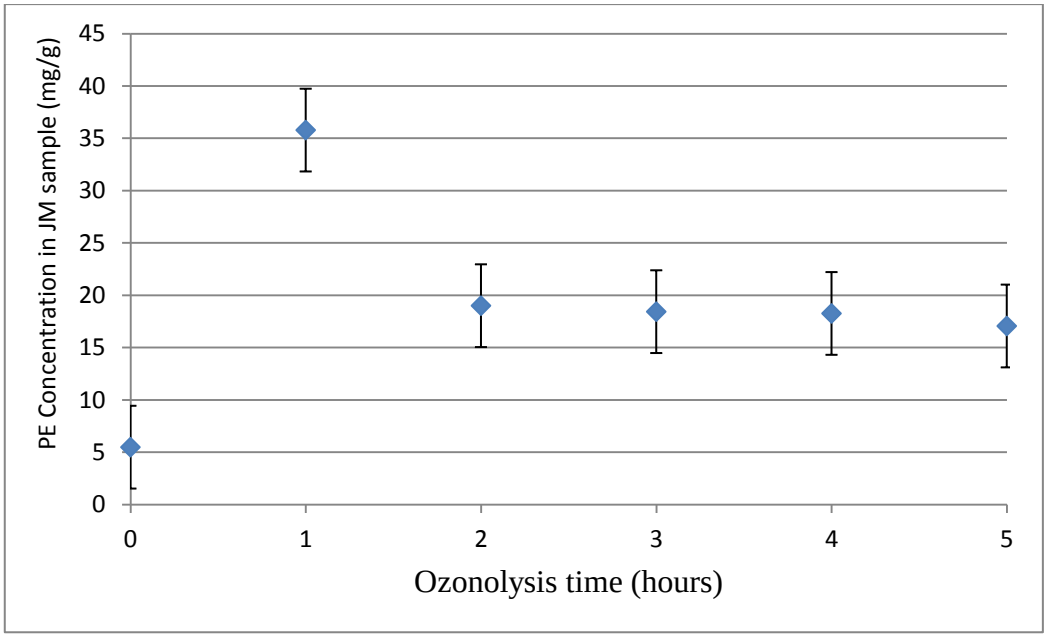

Figure 5.8 Ozonolysis effect of phorbol ester concentration in hexane extract

Figure 5.8 shows PE concentration in hexane extract of JM sample during ozonolysis was performed. PE content in JM original sample, before ozonolysis, was 5.49 mg/g, however, 7 fold higher PE concentration was observed in the sample after 1 hour of ozonolysis. It was assumed that greater fatty acids content in JM sample was released due to ozone reaction. Ozone molecules and its derivates damaged the molecular cell of JM resulting in their exposure to PE compounds. This cell lysis affected more PE bonded in lipid was released, which was then detected in chromatograms. This result is supported by significant fatty acids peaks appearing in the chromatogram after 1 hour of ozonolysis, as presented in Figure 5.5.

At 2 hours of ozonolysis, PE concentration decreased by 47% while its content was relatively stable until 5 hours of ozonolysis.

The chromatograms of hexane extract showed that ozone molecules influenced the PE concentration in oil extraction from the jatropha shell. This diffusion phenomenon occurred due to the lipophilic property of ozone treatment (Pryor et al., 1991). Furthermore, PE has well known natural characteristics which are hydrophobity and solubility in oil (Devappa et al., 2010a). High solubility of PE in an oil fraction can be facilitated by introducing ozone through the molecular cell of JM samples. This process led to cell lysis in which JM shell was broken down. In addition, during ozonolysis, hydroxyl radicals (•OH) were produced along with ozone molecules in which acted as an auto catalyst during the cell lysis. Microbubble application supported the auto catalysis of JM cell wall by enhancing its mass transfer. Therefore, ozone and hydroxyl radicals could infiltrate through a JM cell although a water based solution was used during ozonolysis. Subsequent to the cell lysis, ozone and its derivatives then attacked carbon double bonds in fatty acids compounds. Subsequently, it affected the oil mass in JM samples. The mass of oil recovered from hexane extraction was evaluated by calculating its mass relative to the mass of JM sample used in extraction. The profile of this quantity varying with the time of ozonolysis exposure is shown in Figure 5.9.

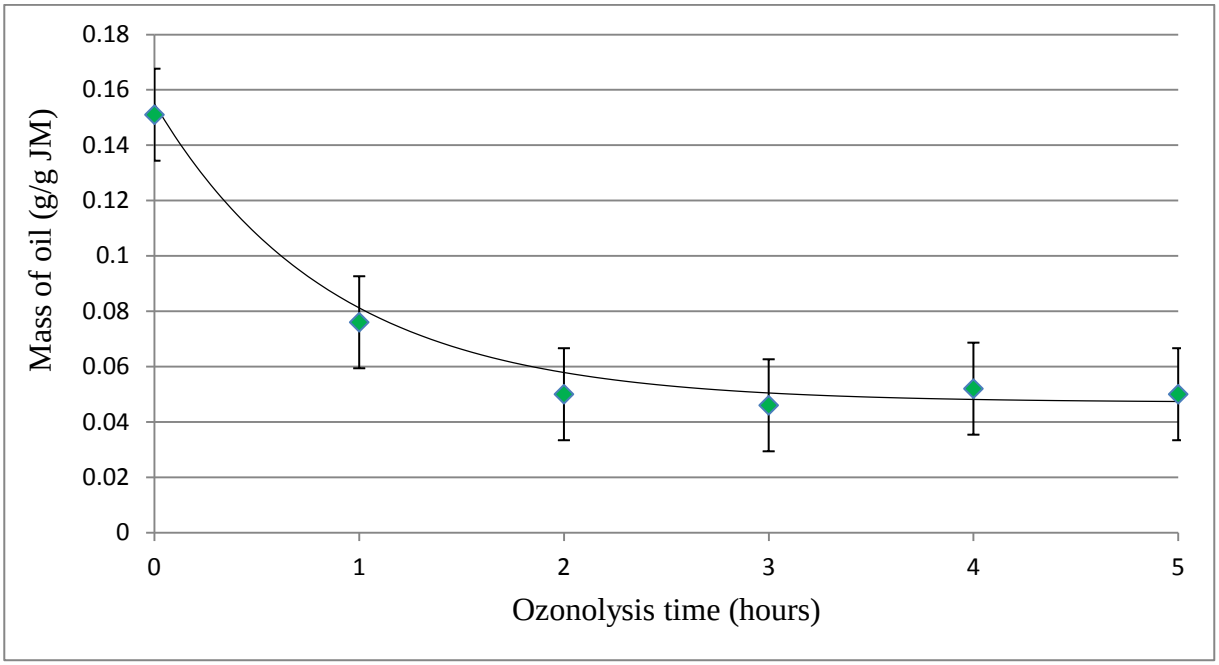

Figure 5.9 Ozonolysis effect on oil content in jatropha meal during ozonolysis

Figure 5.9 illustrates the oil content in JM sample before, during and after ozonolysis. The equation is stated as below (Eq. 5.1) while the R^2 value is 0.71. The R^2 value shows how close the data which fit to a linear model. Moreover, y is defined as a mass of oil per gram of sample (g/g JM) and x is defined as an ozonolysis period (hours).

$$y = 0.108e^{-1.15x} + 0.047 \qquad (5.1)$$

As explained previously, the oil content of the JM sample was considered as the resulting oil after hexane extraction. This is because the majority of fatty acids components were effectively extracted by hexane solvation (Gaur, 2009, Forson et al., 2004). A significant and rapid reduction was observed during the first 2 hours of ozonolysis for which an exponential decay fits the curve. This is consistent with first order kinetics as an expected outcome due to sufficient excess of one reagent. The rate law of this phenomenon is expressed by Fogler (2006) in Equation 5.2 as below.

$$\frac{d[y]}{dt} = -\alpha\,[y] \qquad (5.2)$$

The oil content was reduced by 69% while a slight increase was observed at 4 hours of ozonolysis. A 66% total reduction in oil content was achieved after 5 hours of ozonolysis. In contrast, the chromatograms of fatty acids peaks that showed greater lipid content were detected during chromatography analysis (Figure 5.5 – Figure 5.7). This phenomenon was expected because of ozone selective reaction to specific types of fatty acids. The mass of oil content in JM sample might be independently related to concentration of fatty acids.

Furthermore, the effect of ozone treatment on specific fatty acids was studied by some researchers. Pryor *et al* (1991) reported that stearic acid does not react with ozone. On the other hand, other forms of fatty acids found in jatropha oil such as oleic, linoleic and linolenic acids are reactive to ozone, producing mixtures with lower molecular weight constituents (Baber et al., 2005). This is in agreement to chromatograms after hexane extraction (Figure 5.5 – Figure 5.7). The stearic acid peak remained stable (peak e) during 5 hours ozonolysis while significant changes were observed in oleic, linoleic and linolenic acids peaks.

Following the hexane extraction of JM samples before and after ozonolysis, methanol extraction was performed. Resulting extracts were analysed using HPLC device in which respective chromatograms are presented in this section. Peaks appeared before 20 minutes of retention time were identified as PE peaks. Longer HPLC analysis was performed until 60 minutes of retention time, however, no peaks were observed after 20 minutes. Therefore, HPLC run time for PE detection was set to 20 minutes in order to minimise the consumable cost of chemical usage for HPLC mobile phase during analysis. Peaks detected in methanol extract were considered as pure PE while no significant fatty acids peaks appeared, as compared to chromatograms of hexane extract.

Figure 5.10 shows the chromatogram of a JM sample in methanol extract before and after 1 hour of ozonolysis. Fresh JM sample was extracted in order to analyse the PE content in original sample, before detoxification by ozonolysis was performed.

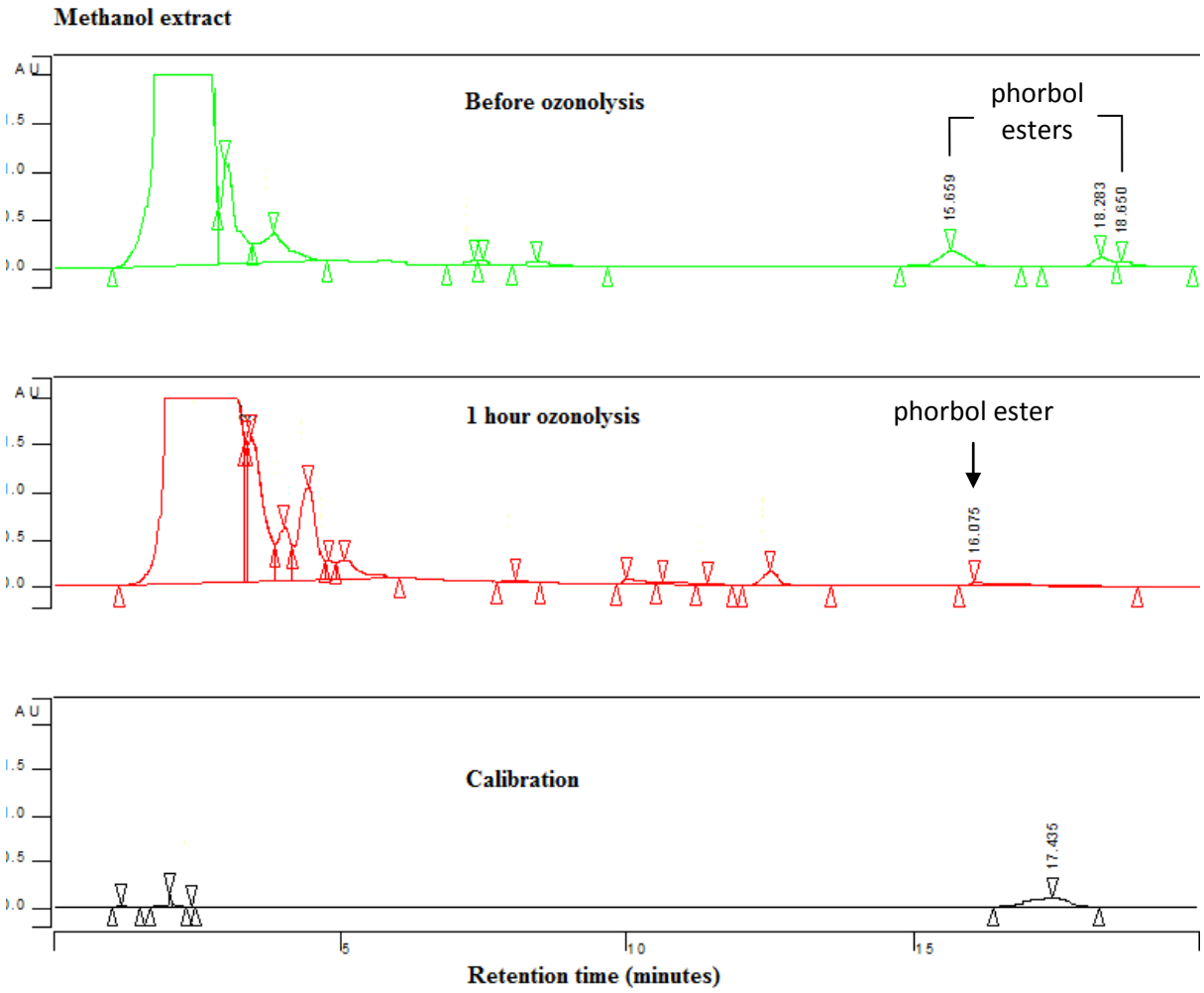

Figure 5.10 Chromatograms of methanol extract before and after 1 hour of ozonolysis

Figure 5.10 shows chromatograms before and after ozonolysis of a JM sample in methanol extract. In chromatograms of methanol extract, it was observed that the fatty acids peaks significantly were reduced compared to chromatograms of hexane extract (Figure 5.5 – Figure 5.7). This indicates that the fatty acids in JM samples have been mainly extracted by hexane

solvation (Gaur, 2009). Gogoi *et al* (2014) also studied the PE concentration during oil extraction from jatropha seeds. They found that 70-75% of PE contents were extracted with oil while the remaining 25-30% of PE was strongly bonded to JM fractions. Therefore, it was assumed that there were only pure compounds of PE remaining in the methanol extract which were not bonded to a lipid matrix. In the chromatograms before ozonolysis, there were three peaks of PE appearing in the methanol extract while one peak of PE appeared in the hexane extract (Figure 5.5). In total, there were four peaks of PE detected in chromatograms before ozonolysis. This fact is similar as reported by Haas *et al* (2002) whom confirmed that there are six types of Jatropha factors, but only four Jatropha Factors are detectable by chromatographic analysis.

Moreover, in the chromatogram of 1 hour of ozonolysis, there was a single PE peak detected at 16 minutes of retention time. In comparison to the chromatogram of hexane extract at the same ozonolysis duration (Figure 5.5), more than four peaks of PE were detected. This suggests that ozone and its derivative compounds reacted to PE which affected the chromatographic analysis. Following the hexane extraction, treated JM samples after 2 and 3 hours of ozonolysis were individually extracted using methanol as the solvent. HPLC analysis was carried out and the chromatogram is presented in Figure 5.11.

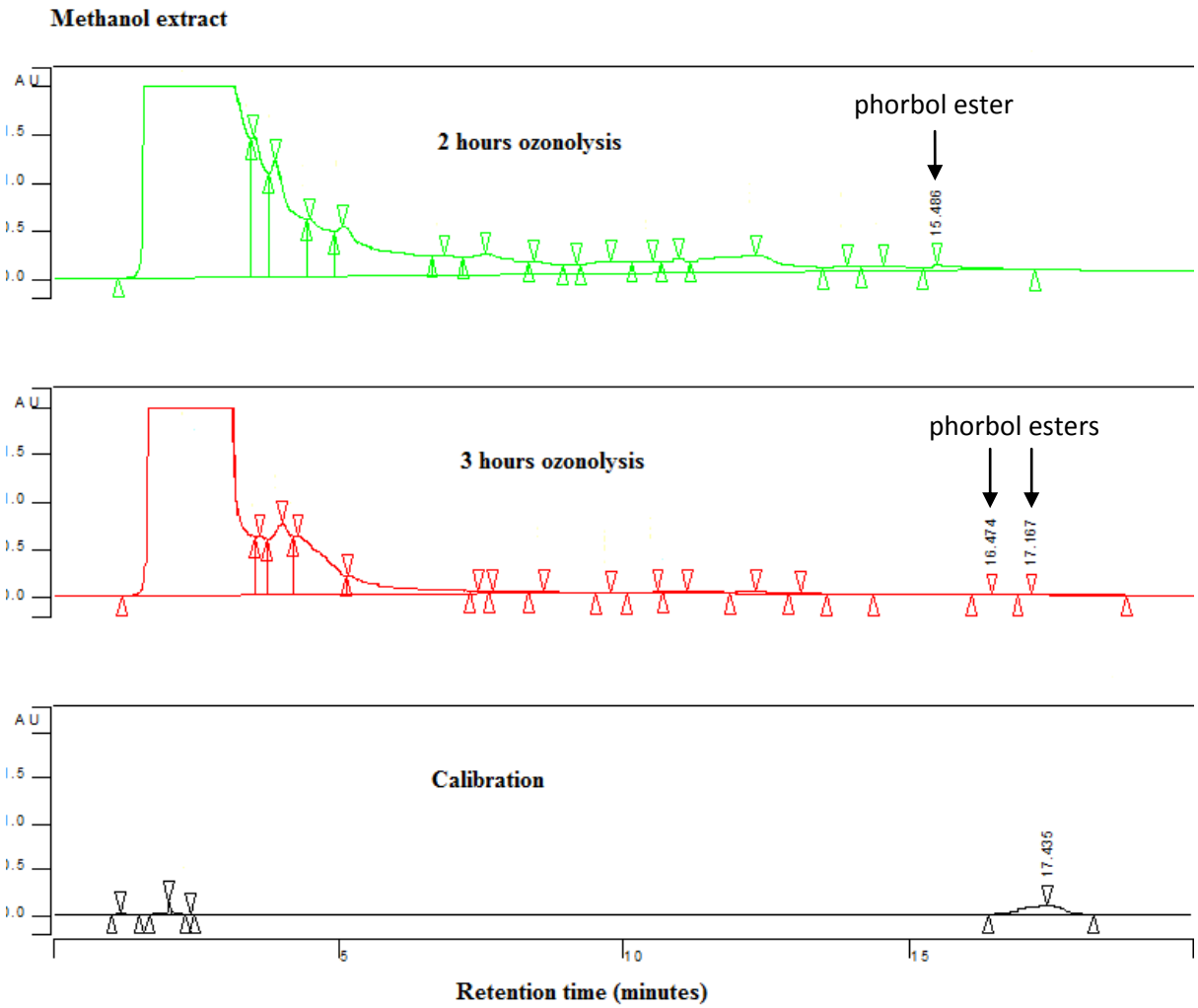

Figure 5.11 Chromatograms of methanol extract at 2 and 3 hours of ozonolysis

Figure 5.11 illustrates the chromatogram of a JM sample in a methanol extract after 2 and 3 hours of ozonolysis. Peaks appearing before 15 minutes of HPLC retention time were assumed as other forms of complex compounds resulting from ozonolysis and extraction. Further identification was not performed because the focus of interest in the methanol extract is the PE compounds. After 2 hours of ozonolysis, there was one peak of phorbol ester detected at 15 minutes of retention time. Considering the PE peaks in hexane extract at the same ozonolysis period (Figure 5.6), there were a total of six PE peaks observed.

Furthermore, two peaks of PE in methanol extract were detected after 3 hours of ozonolysis. The increasing number of PE peaks compared to PE peak at 2 hours of ozonolysis, indicated PE compound was attacked by ozone and its derivatives hence showing PE breakdown into smaller fragments. On the other hand, the height of PE peaks in the chromatogram after 3 hours of ozonolysis was lower that at 2 hours, which affects the quantitative result. The PE concentrations were calculated and presented in next part of this section. In addition, there were four PE peaks in total at 3 hours of ozonolysis, detected in hexane and methanol extract. Four PE peaks detected in chromatogram is in agreement as a number of PE peaks found by Haas *et al* (2002). Further HPLC analysis was performed in order to study the effect of ozonolysis on PE compounds after 4 hours and 5 hours of detoxification, as presented in Figure 5.12.

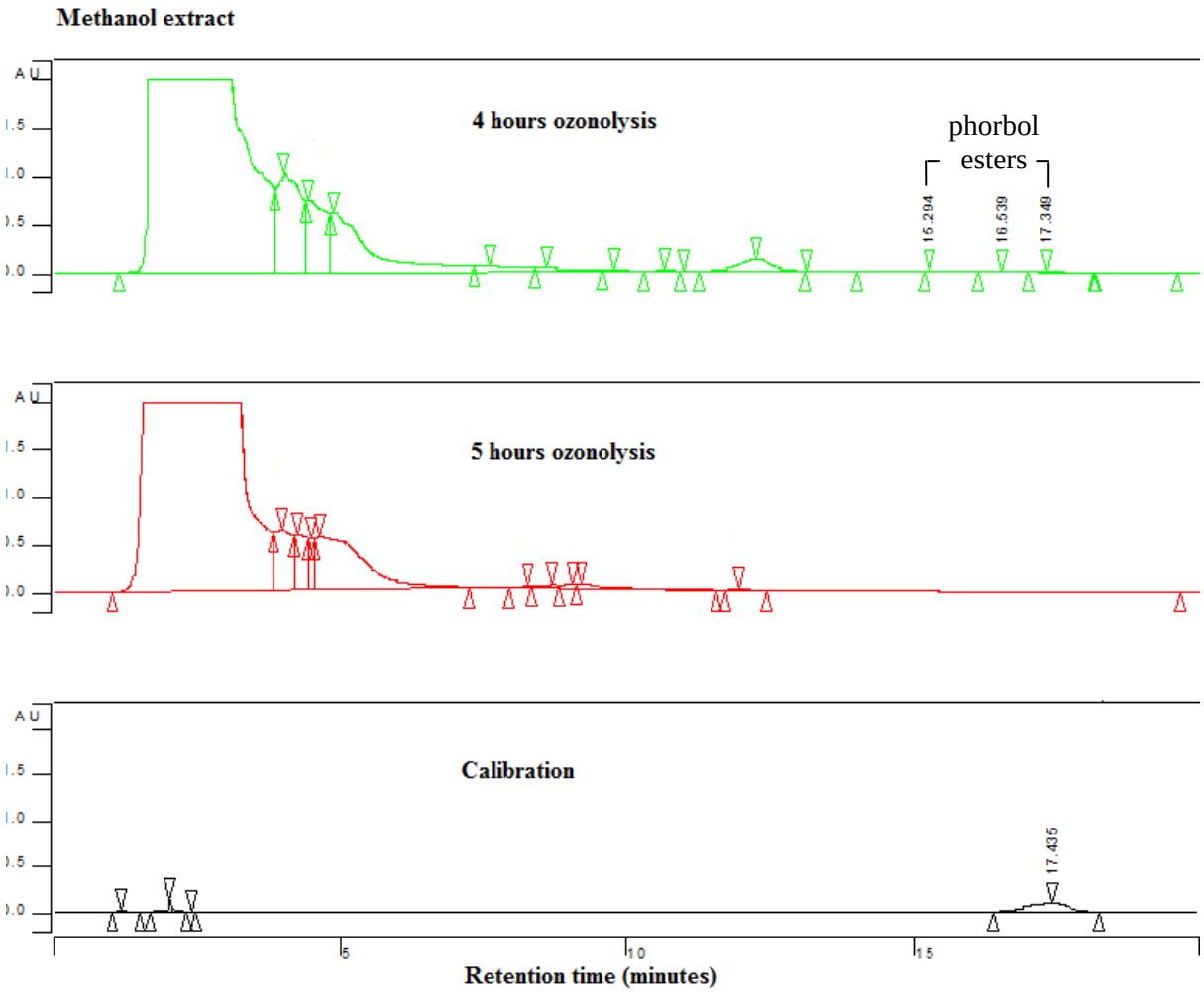

Figure 5.12 Chromatograms of methanol extract at 4 and 5 hours of ozonolysis

Figure 5.12 shows the chromatogram of JM samples in a methanol extract after 4 hours and 5 hours of ozonolysis. After 4 hours of ozonolysis, there were three peaks of PE detected at 15, 16 and 17 minutes of retention time. Compared to the chromatogram at 3 hours of ozonolysis (Figure 5.6), the number of peaks increased while the heights decreased. This phenomenon occurred due to reaction of ozone molecules and its derivatives with PE compounds. The reaction might lead to breakdown of PE compounds by which its concentration reduced. Furthermore, there was no PE peak detected in the chromatogram after 5 hours of ozonolysis. The absence of PE peaks in this case was also expected due to the HPLC detection limit.

According to numerical calculation, presented in the following section, PE concentration after 5 hours of ozonolysis was very low.

Different number of PE peaks appearing in chromatograms might be influenced by molecular cleavage and complex interference of fatty acids and other chemicals in jatropha (Devappa et al., 2013). Besides, an increasing number of PE peaks in each ozonolysis time indicated ozone reaction with PE compounds. This is caused by chemical breakdown by modification reactions. However, the rising number of PE peaks is independent of PE concentration. Numerical data of PE concentration during ozonolysis is shown in Figure 5.13, as below.

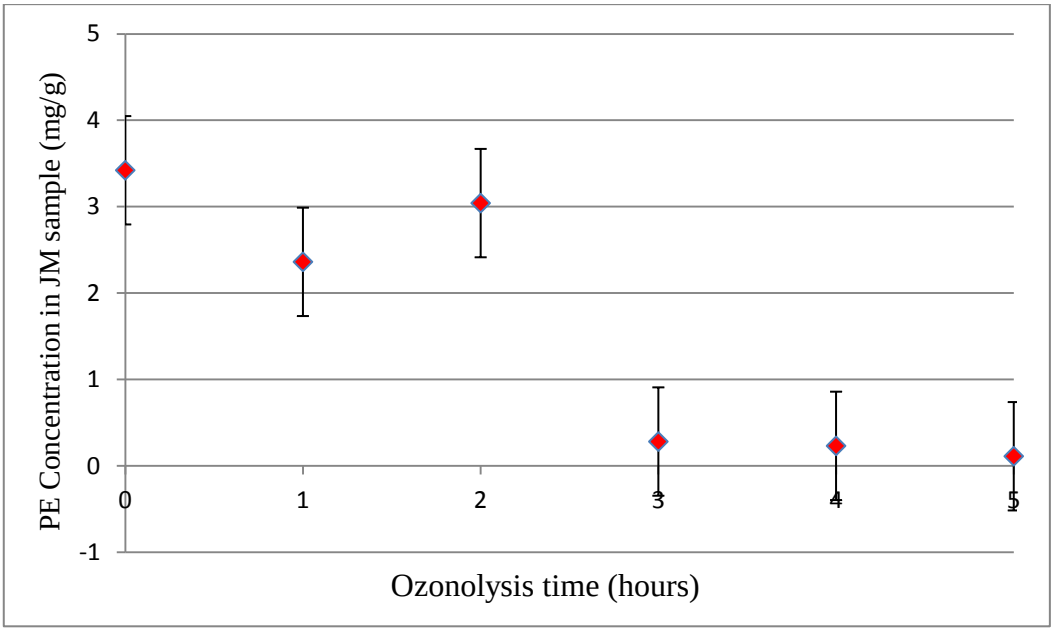

Figure 5.13 Ozonolysis effect of phorbol ester concentration in methanol extract

Figure 5.13 shows the PE concentration in a methanol extract of JM sample before and after ozonolysis. The concentration of PE compound in the untreated sample was 3.42 mg/g of JM. After 1 hour of ozonolysis, a 31% reduction of PE concentration was observed, however, its concentration increased after 2 hours of ozonolysis. The rise of PE concentration might be caused by the bulk of PE content that is abandoned in the JM shell. The longer duration of

ozonolysis induces more exposure of ozone (O_3) and its derivates into deeper layers so that molecular cell damage is more pervasive. Therefore, greater amount of PE content was released and detected during chromatographic analysis. Moreover, a substantial reduction of PE concentration was achieved after 3 hours of ozonolysis. A 92% of reduction was observed compared to the initial PE concentration in untreated JM samples. It was assumed that the ozone molecules and its derivates reacted with carbon double bonds in the PE molecular structure. Based on the Criegee mechanism, chemical reactions of ozone and carbon double bonds modify the molecular structure (Criegee, 1975). Consequently, the resulting PE concentration after 3 hours of ozonolysis decreased. Furthermore, the PE content in a JM sample is slightly reduced with the final PE concentration after 5 hours of ozonolysis as 0.11 mg/g of JM. In total, the PE content was reduced by 97% after 5 hours of detoxification. A negligible amount of PE reduction from 3 hours to 5 hours of ozonolysis occurred, presumably because ozone has damaged the deepest layer of JM molecular cell. As a result, a relatively similar amount of PE content was attacked by ozone molecules. Moreover, it is suggested that the range of PE content in toxic varieties of jatropha is 1.2-3.85 mg/g while the non toxic Mexican jatropha variety contains PE with concentration of 0.11 mg/g (Francis et al., 2013, Diwani et al., 2011, Gaur, 2009).

In accord with the reaction mechanism of ozonolysis, the direct reaction of O_3 molecules predominantly occurs under conditions with pH < 9 (Hoigné and Bader, 1978). Therefore, chemical reaction specifically leads to direct contact between carbon double bonds and O_3 molecules (Fábián, 2006). However, in ozonolysis, O_3 molecules decompose into some species due to plasma charge induction (Kogelschatz et al., 1988). During ozonolysis, the kinetic reaction of OH radicals (•OH) is defined as an initial step of ozone decomposition (Eriksson, 2005). In phorbol ester degradation by plasma application, OH radicals were

subjected in an oxidative process by electrophilic reaction (Kongmany et al., 2013). The reactions involved are stated as below.

$$O_2 + e^* \rightarrow 2O\bullet + H_2O \rightarrow 2 \bullet OH + e \quad (5.3)$$

$$O_2 + O\bullet \rightarrow O_3 \quad (5.4)$$

$$O_3 \rightarrow O_2 + O\bullet \quad (5.5)$$

$$O\bullet + H^+ + e \rightarrow \bullet OH \quad (5.6)$$

This illuminates that the reaction of PE content in jatropha samples during plasma application occurs because of high energy electrons (e^*), Equation 5.3, and •OH. Ozone molecules were further produced because of oxygen presence within plasma discharge (Eq. 5.4). In Equation 5.5, un-reacted ozone molecules were dissociated back into oxygen molecules due to the unstable nature of ozone. It was further mentioned that some free radicals were involved in plasma reaction (Eq. 5.6). Particularly, •OH reacted with PE compound in the solution through gas-liquid interface. This reaction simultaneously occurred in which •OH quickly decomposed. OH radicals (•OH) have a well known oxidative effect but it have a short life time (Barlow, 1994, Beltrán, 2004).

The safety issue was the main drawback in the PE degradation study using plasma application by Kongmany *et al* (2013). Direct plasma exposure into the samples and utilisation of helium gas in plasma generation were involved. Therefore, in this current research, a modified plasma microreactor was used to perform ozonolysis while air was used as the gas supply. A closed reactor system with no direct plasma contact offers safe operation during detoxification. In addition, the use of air provides some advantages such as cheap and easy in handling and storage.

Reaction of ozone and •OH carbon double bonds in PE compounds may modify the molecular structure of PE resulting other chemicals. Consequently, its concentration decreased hence the toxicity level in JM samples changed. Furthermore, as shown by Gopalakrishna and Anderson (1987), Protein Kinase C (PKC) is susceptible to •OH. As described in Section 2.2 of Chapter 2, stimulated PKC is involved in neurotransmission in which acts as tumour promoter. Phorbol ester plays essential role in stimulating PKC (Gaur, 2009, Caratsch, 1988, Goel et al., 2007). Therefore, PKC stimulation might also be affected by the modification of PE molecular structure after ozonolysis is performed.

5.3 Summary

A phorbol ester detoxification study by an ozonolysis technology with microbubble mediation was conducted using synthetic and natural phorbol esters. Both samples were individually investigated using the same chemical reactor with identical operating conditions. Experiments were performed at a pressure of 1 atm and a temperature of 24 °C. A flow rate of 2 L/min was set and steady flow condition was maintained during experiments. A High Performance Liquid Chromatograph (HPLC) was used to analyse PE concentration in samples before and after treatment. Chromatograms for all sets of experiments were provided in order to study peaks appeared during chromatographic analysis.

First of all, ozonolysis was performed for treatment of Phorbol-12-myristate-13-acetate (TPA) as the synthetic PE samples. This experiment aimed to study the effect of ozonolysis on artificial PE before further study using natural PEs was performed. TPA concentration was studied in two different conditions which were aeration (without ozone activation) and ozonolysis (with ozone activation). Chromatograms of TPA aeration by air microbubble showed that there was no significant difference of the peaks heights of TPA after 30 minutes

of aeration. Numerical calculation was confirmed showing that TPA concentration remained constant after 5 minutes of ozonolysis with only 40% of TPA reduction after 30 minutes of aeration. It was observed that oxygen offered insufficient energy during oxidation of synthetic PE. Oxygen molecules were unable to breakdown carbon double bonds in the TPA molecular structure. Therefore, there was no signification reduction of TPA concentration observed. Furthermore, experiments using TPA samples were continued with application of ozonolysis. Chromatograms after TPA ozonolysis showed the TPA peak was detected after 5 minutes of ozonolysis while no peak was appeared after 10 minutes until treatment completed, 30 minutes. It was observed that 64% of TPA concentration was reduced after 5 minutes of ozonolysis. In addition, the absence of TPA peaks in 10-30 minutes of ozonolysis was assumed as a result of HPLC detection limit. The current set up in this research suggests that less than 4 ppm of TPA concentration as the PE minimum level which is detectable by chromatography analysis.

Ozonolysis of natural PE was further performed by using Indonesian jatropha meal (JM) samples. Double stage extractions were conducted in order to obtain PE extracts from JM samples. Resulting extracts from both stages were individually analysed using HPLC method. Hexane solvent was used prior to the extraction and final stage of extraction was done using methanol solvent. Hexane extraction aimed to effectively extract lipid content of JM samples. Hexane is mainly used in lipid extraction. Besides, it was reported that the majority of PE contents in JM are contained in a lipid matrix. Therefore, non polar solvent such as hexane was required to extract PE from JM samples. HPLC chromatograms showed that some major fatty acid contents were found in the hexane extract of Indonesian JM samples which are linolenic acid, linoleic acid, oleic acid, palmitic acid and stearic acid. Stearic acids are reported to be stable to ozone molecules while oleic, linoleic and linolenic acids react with

ozone. In total, 65% reduction of oil content was observed in the hexane extract of JM samples after 5 hours of ozonolysis.

Moreover, a group of PE peaks were also detected in the chromatograms of hexane extract. After 1 hour of ozonolysis, 7 fold higher PE concentration was observed compared to PE content in an untreated JM sample. This might be caused by damaging the cell wall of the JM molecular structure. Afterwards, at 2 hours of ozonolysis, 47% of PE reduction was found and a stable PE concentration was achieved after 5 hours of ozonolysis. It was expected that ozone and its derivatives diffused through JM shell and acted as an auto catalyst. Further, they reacted with carbon double bonds in fatty acids compound in JM samples. Therefore, more lipid-bonded PE were released during ozonolysis in which represented by high peaks appeared in the chromatograms. In addition, microbubbles facilitated cell lysis by enhancing mass transfer across the gas-liquid interface. Ozone molecules which were introduced into the liquid in the form of microbubbles provided higher mass transfer and affected its chemical reactions.

Following the hexane extraction of JM samples, methanol solvent was used in the second stage of extraction. JM samples before and after ozonolysis were further extracted in order to obtain PE content in methanol extract. The PE content in methanol extract was considered as a pure PE because majority of fatty acids compounds have been extracted by the hexane solvent. Chromatograms showed that no significant fatty acids peaks appeared while the remaining PE peaks were detected. During ozonolysis, PE peaks were detected as groups of peaks which varied in number but the complete absence of PE peaks was found in the chromatogram after 5 hours of ozonolysis. Significant reduction of PE content was observed after 3 hours of ozonolysis in which 92% of PE was detoxified. From 3 hours to 5 hours of

ozonolysis, no substantial reduction of PE content was reported. 97% of PE content reduced by the end of ozonolysis, 5 hours of ozonolysis, which resulted 0.11 mg/g of PE in the JM sample. This value is also a PE concentration in the jatropha plant of the non-toxic Mexican variety.

The detoxification reaction of ozone and PE molecules is based on the Criegee mechanism (Criegee, 1975) which provides a chemical pathway for ozone reaction with carbon double bonds in the PE structure. During ozonolysis, ozone molecules decompose to some free radicals such as hydroxyl radicals (•OH) which is well known as a strong oxidant. •OH plays an essential role in detoxification reaction which was expected to attack carbon double bonds and modified PE structures were formed. Besides, •OH also influences Protein Kinase C (PKC) which stimulates neurotransmissions of PE, as a carcinogenic compound. Modified PE structure after ozonolysis was assumed to affect the toxicity level of PE. Therefore, the treated JM samples after ozonolysis can be utilised for further purposes which have economic value. Application of the technology used in this research also offers some benefits, especially alleviating some safety concerns, which are no direct plasma exposure during detoxification and usage of air as the gas supply for ozone generation. These advantages are promising for ozonolysis to be applied in industrial scale.

CHAPTER 6

OZONOLYSIS EFFECTSONLIGNOCELLULOSIC MATERIALS

This chapter presents the results of the investigation of microbubble ozonolysis treatment on lignocellulosic materials using an experimental reactor. The focus is on the effect of ozonolysis treatment on Jatropha biomass and lignin samples. A limited number of integrated investigations focused on detoxification and proteomic profiling of jatropha biomass. Ozonolysis enhanced by microbubble technology was used for this purpose. The study of jatropha biomass is centred on protein content after ozone treatment. An extensive profiling of jatropha biomass post-detoxification via ozonolysis for protein content is undertaken. Total protein in untreated and treated samples was assessed. It was expected that ozonolysis affected the total protein content in detoxified jatropha meal samples. Furthermore, proteomic profiling was conducted to provide information on the specific Indonesian jatropha meal proteins targeted by ozonolysis. The proteomics investigation covered several areas: (i)the study of protein molecular weight distribution after ozonolysis, (ii) protein profile identification and (iii) the morphology of jatropha meal post-ozonolysis treatment. In addition, the ozonolysis study in lignocellulosic materials is broadened beyond jatropha meal by investigating ozone impact in lignin molecular structure. It aims to study fundamental effect of ozone on lignin content generally. It is expected that the experimental results will contribute to prospective investigations related to cell lysis. Discussion on this is presented in the second part of this chapter.

Ozonolysis experiments of lignocellulosic materials were conducted using Indonesian Jatropha Biomass and lignin samples. Detailed results of the subsequent detoxification of Jatropha Meal have been discussed in Chapter 5. Total protein content of ozone treated JM

was investigated. The protein profile was identified by high performance liquid chromatography online to tandem mass spectrometry with data processing using the MASCOT search engine and Basic Local Alignment Search Tool (BLAST) program. The morphology characterisation of JM after ozonolysis was observed by Scanning Electron Microscope (SEM). Furthermore, synthetic lignin was used to explore the ozonolysis effect on lignin. The experimentation was done in collaboration with Mr Jong Min Shin at The University of Sheffield. Details of materials and methods employed in these experimentations were described in Chapter 3, Section 3.4.1 for the ozonolysis effect on Jatropha Biomass and Section 3.4.2 for the ozonolysis effect on synthetic lignin.

6.1 Ozonolysis of Jatropha Biomass

The Indonesian variety of JM was treated by ozonolysis processing for 5 hours. Samples were taken every 30 minutes to conduct proteomic profiling. For this purpose, ozonolysis duration and operation conditions were set as in detoxification experimentations. The aim is to investigate there liability of the proposed detoxification approach to total protein content of treated samples. However, sampling was done more frequently, compared to the detoxification experiments, in order to obtain temporal resolution of the protein profile. Prior to protein quantification, JM samples after ozonolysis were dried and further processed for analysis. Protein concentrations were analysed before and then after 5 hours of ozonolysis had been performed. Replicates were carried out during experimentation. Direct and indirect methods were applied to elucidate protein concentrations in samples. It aimed to corroborate total protein content through direct method to crude protein which was represented as nitrogen content by indirect method. Protein quantification by a Bradford Assay was conducted as a direct method, and Carbon-Hydrogen-Nitrogen-Sulphur (CHNS) Particle Analyser was used to quantify protein indirectly. These determine the actual value of total protein content from

the direct method, and protein equivalent nitrogen composition from the indirect method. The comparisons of results from both methods are presented in this section. Furthermore, qualitative analysis of data from jatropha biomass after ozonolysis was presented by post processing mass spectrometry (MS) results and SEM images. Figure 6.1 shows the protein concentrations of treated JM samples throughout ozonolysis.

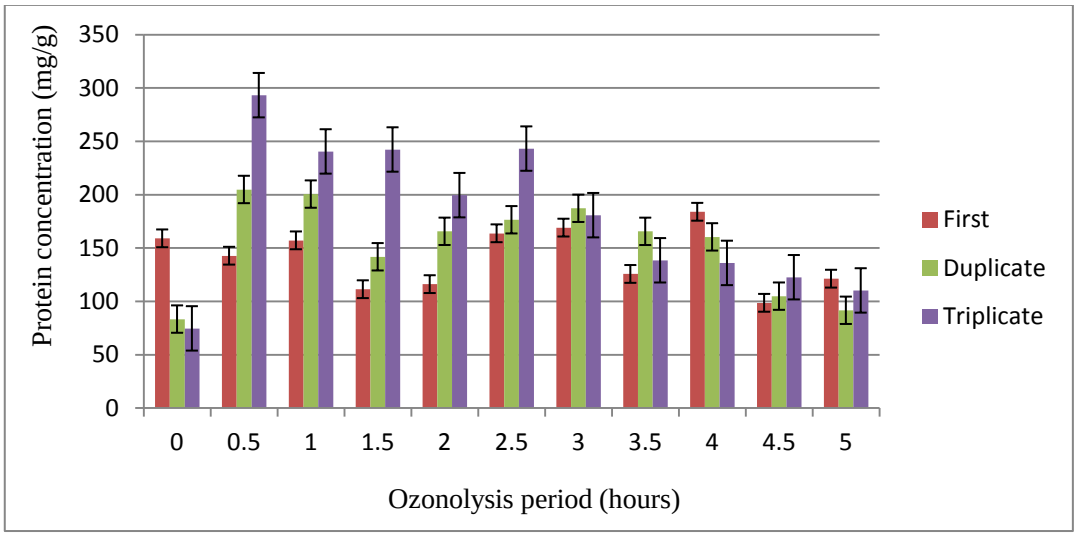

Figure 6.1 Replicate experimental result of ozonolysis effect in protein content before and after Jatropha Meal detoxification (quantified by direct method; Bradford Assay)

Figure 6.1 presents the protein concentration analysis during ozonolysis of Indonesian Jatropha Meal. It shows that after 0.5 hours of ozonolysis, protein content in the JM sample was nearly double compared to the untreated JM sample (before ozonolysis). As a result of the ozone during treatment, protein content in the meal and structure of cell wall are modified (Uzun et al., 2012, Nouwezem et al., 1993). Reaction of ozone molecules and its derivates during the ozonolysis of JM samples results in cell wall breakdown. Therefore, more protein is released subsequent to this process, reflected by the higher protein content observed after 0.5 hours of ozonolysis. Afterwards, protein content was relatively stable from 1 hour of ozonolysis until completion of treatment, 5 hours. This protein results shows dependent profile into phorbol ester content in hexane extract, as presented in Chapter 5, Figure 5.8. As discussed, phorbol esters in hexane extract are mainly bounded in fatty acids matrix (Gaur,

2009). The carbon double bonds in phorbol ester molecular structure as well as fatty acid matrix, are susceptible to ozone reaction (Baber et al., 2005, Cvetkovic et al., 2008, Neumeister et al., 1978). In proportion to shell wall breakdown of jatropha meal by ozone, more phorbol ester and protein are released after 0.5 hours of ozonolysis.

It has been reported that protein is a potential target of oxidation during ozonolysis. Some amino acids (cysteine, tryptophan and histidine) found in the protein are sensitive to reaction with ozone while other partial components of protein (glutamic acid, proline and valine) are unaffected by ozone (Mudd et al., 1969, Uzun et al., 2012).However, the study of the effect of ozonolysis on individual amino acids is beyond the scope of this research.

Ozone concentration and pH conditions have been well documented as playing key roles in reactions involving ozone based processes (Uppu and Pryor, 1994, Hoigné and Bader, 1976, Eriksson, 2005, Pryor and Uppu, 1993). Complex reactions occur during ozonolysis, resulting in the production of some derivative components such as hydroxyl ions and hydroxyl radicals. These components, under controlled conditions, react simultaneously with bonds in protein molecular structure. Furthermore, different pH conditions leads to different predominant components during ozonolysis. The presence of hydroxyl radicals is more favourable as to oxidation due to its higher standard redox potential. Ozone stability is reported to be decreased when alkalinity of solution is increased (Eriksson, 2005). On the other hand, some investigations have been done in order to study the effect of additional techniques through ozonolysis. Studies of process efficiency in relation to hydroxyl radical generation from ozone microbubbles under acidic condition have been reported (Takahashi et al., 2007, Li et al., 2009).

In this research, acidic conditions emerged during ozonolysis of JM with an approximate pH 5.3. Moreover, low concentration of gas phase and dissolved ozone were achieved which are 1.4 ppm and 1.2 ppm, respectively. Beltrán (2004) observed below pH 12, ozone reacts in a slow kinetic regime which may cause no ozone decomposition. Consequently, no ozone reaction in the experimental samples occurs. However, he argues that this condition is neglected if dissolved ozone is detected during experimentation. As explained, 1.2 ppm of dissolved ozone was detected during ozonolysis of JM which influences reaction with the JM cell wall. Microbubble utilisation in this research has enhanced the ozone delivery mechanism into the bulk of the liquid. The fast mass transfer offered by microbubbles facilitates spontaneous breakdown. This contribution is expected to play a substantial role in maintaining protein content in jatropha meal during phorbol ester detoxification. In addition, protein content remains stable due to the rapidness ozonolysis. As reported in Chapter 4, microbubble residence time in the plasma chip was less than a second, which further affects ozone contact time while treating samples. This short contact time influences in maintaining the protein content. Furthermore, a relatively low temperature, 35 °C, was detected in plasma reactor, which is considered to be an additional benefit of the approach. This condition prevents protein denaturation due to temperature sensitivity. This is consistent with the total protein content remaining stable after 5 hours of ozonolysis.

Further analysis of total protein content was performed in order to obtain secondary data to compare to the Bradford Assay. The particle analyser CHNS approach was used as indirect quantification method for this purpose. Determination of protein content via the particle analyser CHNS approach allows the inference of nitrogen content with multiplication factor of 6.25 for protein value in wheat or soybean (Tkachuk, 1969). This factor has been conventionally used for with an assumption that most nitrogen in the diet is present within

amino acids in protein, while the dietary fats and carbohydrates have no nitrogen content (FAO, 2003).Detailed protein values generated by CHNS Analyser is presented in Table 6.1.

Table 6.1 Total protein in total samples (% wt), quantified by indirect method

Ozonolysis period (hours)	Protein concentration (%)
0	21.44
0.5	16.27
1	27.68
1.5	24.48
2	22.09
2.5	29.83
3	25.86
3.5	18.1
4	25.88
4.5	32.17
5	27.85

Table 6.1 shows protein concentration of Jatropha meal after ozonolysis analysed by the CHNS Analyser approach. It demonstrates that total protein of Indonesian JM after detoxification using ozonolysis ranges from 18-32%. This range is consistent with previous studies which assert protein content in defatted seed cake is approximately 23-26% (Makkar et al., 2008, Lestari et al., 2010). Defatted is defined as treated jatropha cake after the oil extraction stage. This condition is similar to the samples of Indonesian JM studied here. In addition, this range is categorised as within the limits for good nutritional value, according to Abou-Arab and Abu-Salem (2010). Furthermore, total protein obtained in this research is higher than total protein of detoxified JM by the conventional method. Saetae and Suntornsuk (2011) reported 23% of JM crude protein was achieved after ethanol extraction was applied as the detoxification method. Besides, chemical application for detoxification has limited detoxified product with regards to edibility. In contrast to the technology adopted in this research, ozone utilisation is also a feasible method for wider benefits. Utilisation of water as a solvent during detoxification and no residual trace of ozone after processing has positively preserved protein content.

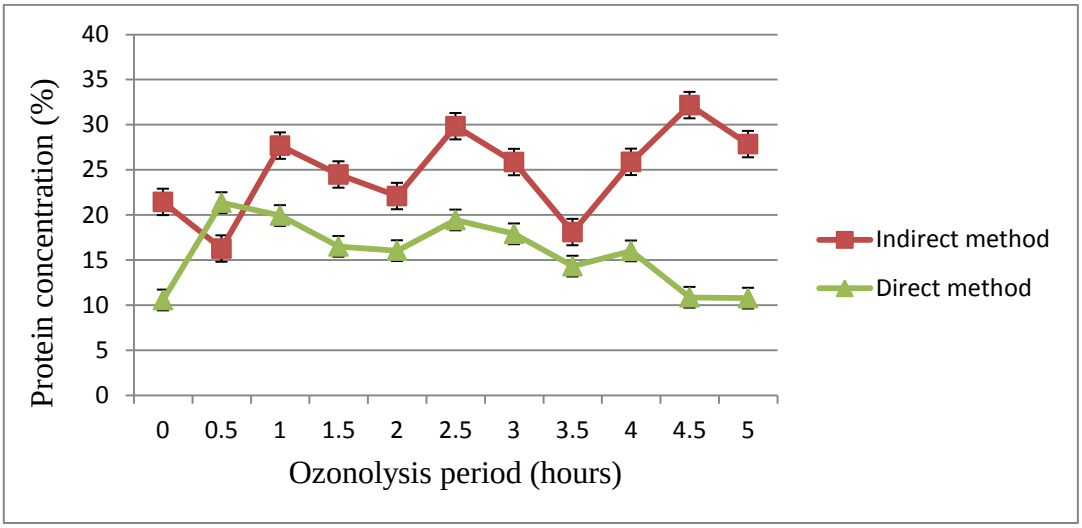

Figure 6.2 Profile of protein content during ozonolysis, calculated by indirect method (using CHNS Analyser) and direct method (using Bradford Assay)

Figure 6.2 illustrates the correlation between the analysed protein content by direct and indirect quantification. The direct method used is the Bradford Assay, while the indirect method provides CHNS results. A relatively similar trend of protein content from both methods was observed during experiments. However, protein content decreased after 0.5 hours of ozonolysis, as reported by the indirect method. This phenomenon could have occurred due to the effect of ozone in specific amino acids such as cystine, tyrosine and tryptophan. Those compounds are known by their high susceptibility to ozone (Uzun et al., 2012, Uppu and Pryor, 1994, Mudd et al., 1969). Nevertheless, further analysis is required for justification of this assumption. This future work is recommended in Chapter 7, as the final part of this thesis.

In order to further study the effect of ozonolysis on JM protein, a qualitative method was performed by using the Sodium Dodecyl Sulphate Polyacrylamide Gel Electrophoresis (SDS-PAGE) approach. The data acquired allows the estimation of the distribution of protein molecular weight in Indonesian JM after detoxification. Protein extract was treated by the standard methodology as explained in Chapter 3. The image is shown in Figure 6.3.

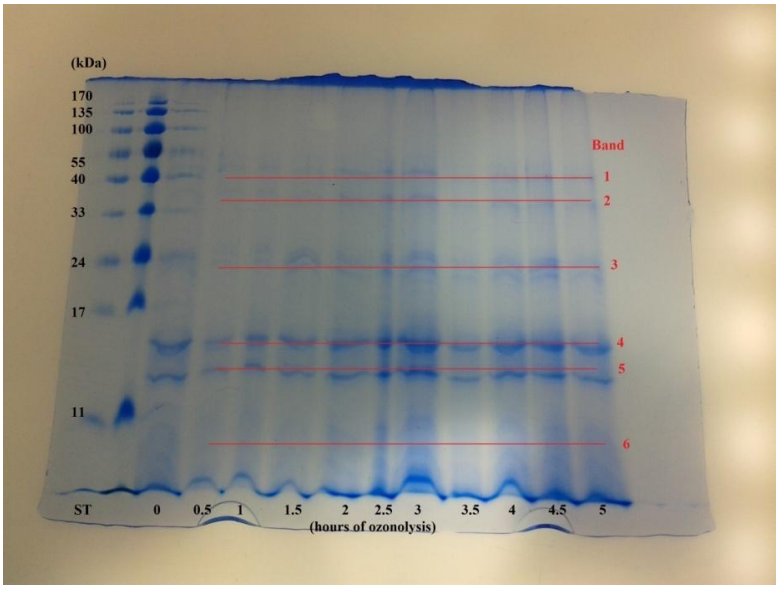

Figure 6.3 SDS-PAGE gel analysis of the Jatropha Meal sample after ozonolysis; ST is a standard marker for protein ladder

Figure 6.3 shows the SDS-PAGE patterns of the treated Indonesian JM sample. The figure illustrates that normalised protein molecular weight is distributed from 5-60 kDa. This distribution is categorised as low molecular weight of protein. Data normalisation, in which the same amount of protein was loaded in each well, supports the accuracy of the estimation of the protein molecular weight distribution. Moreover, little information on *Jatropha curcas* investigation for its protein molecular weight has been reported. Marrufo-Estrada et al (2013) have studied the profile of *Jatropha curcas* protein hydrolysates obtained from enzymatic hydrolysis of defatted flour which is from 7.97-60.63 kDA. They concluded that hydrolysis was extensively performed hence small peptides with low molecular weight were produced. In addition, Lestari *et al* (2010) showed that the protein molecular weight of the extract from jatropha seed kernels after solvent extraction is distributed from 3 to 98 kDA. Those authors suggested that the change of alkalinity due to the solvent variety results in contrasting protein intensity in particular bands. Furthermore, this indicates the possibility of certain amino acids in protein converted into different compounds such as a cysteic acid as a product of oxidised cystine (Mudd et al., 1969). In this research, the protein structure might be modified due to

ozone reaction during detoxification of jatropha meal sample. This could also affect the total protein content after ozonolysis in which stable protein concentration was achieved.

The gel used for electrophoresis, as presented in Figure 6.3, was further treated by mass spectrometry. Bands from two lanes of the gel were studied in order to generate the estimated protein identification data. Lane 6 and lane 10 were analysed, reflecting 3 and 5 hours of ozonolysis duration, respectively. These two gel bands were chosen because more than 90% of phorbol ester reduction during detoxification was achieved. It was important to explore qualitatively the protein profile in relation to the effect of ozonolysis. The complex protein profile has been characterised by six bands between 10 and 40 kDa. These series of the highest protein intensities were shown at band 1 (40 kDa), 2 (33 kDa), 3 (24 kDa), 4 (14 kDa), 5 (13 kDa) and 6 (10 kDa). Post processing of MS results was done by online protein identification software, MASCOT-BLAST. Data are summarised in Table 6.2 and Table 6.3.

Table 6.2 Protein characterisation of treated JM after ozonolysis

Ozonolysis period (hours)	Lane, Band	Number of proteins family	Nominal Mass (Mr)	Number of peptides matches		
				Non duplicate	Duplicate	Total
3	6.1	14	59272	27	6	33
	6.2	12	53994	25	0	25
	6.3	6	53994	5	3	8
	6.4	9	53994	42	28	70
	6.5	7	51301	9	2	11
	6.6	5	57530	9	2	11
		TOTAL PEPTIDES LANE 6				158
5	10.1	14	59272	17	2	19
	10.2	13	55122	15	1	16
	10.3	10	53994	19	10	29
	10.4	7	53994	25	4	29
	10.5	9	55122	33	26	59
	10.6	19	57530	22	10	32
		TOTAL PEPTIDESLANE 10				184

The protein characterisation presented in Table 6.2 was generated by using MASCOT software. Details of the data processing parameters used are given in Chapter 3. Each band

was identified individually and the premier hit of generated protein family was considered. In general, the numbers of a protein family are slightly divergent between two lanes. A greater number of protein family (a group of protein that has similar origin, such as related functions, sequences or structures) is observed in band 6 of lane 10 compare to lane 6 (10.6 to 6.6).

Additionally, nominal mass (Mr) is reported which approximately ranges from 51-59 kDa. In comparison to protein intensity presented in the SDS-PAGE pattern, protein molecular weight is distributed from 10-40 kDa. The database algorithm plays an important role in resolving this differentiation. However, nominal mass is infrequently used within peptide and protein identification because of errors accumulating during atomic weight estimation. Furthermore, the number of matched peptides is provided in a group of non duplicate and duplicate peptides. In general, total peptide data indicates that 26 of more peptides are identified in lane 10 compared to lane 6.

Data generated from MASCOT software were further used for sequence similarity against BLAST software. The premier hit (the first hit in the protein sequence list that appeared after software run) of protein sequence was taken into account for this purpose. A summary of estimated protein and sequence ID from BLAST software is presented in Table 6.3.

Table 6.3 Identification of predicted protein type on treated JM sample

Lane, Band	Premier protein*	Predicted protein**	Identification (%)	Sequence ID
6.1	A0A067JF64	nucleolar protein nop56, putative (*Ricinus communis*)	55	gi|255567546|XP_002524752.1
6.2	A0A067JUM5	11S globulin seed storage protein 2-like (*Eucalyptus grandis*)	52	gi|702283651|XP_010046000.1
6.3	A0A067JUM5	11S globulin seed storage protein 2-like (*Eucalyptus grandis*)	52	gi|702283651|XP_010046000.1
6.4	A0A067JUM5	11S globulin seed storage protein 2-like (*Eucalyptus grandis*)	52	gi|702283651|XP_010046000.1
6.5	A0A067L8B3	seed storage protein 1 (*Jatropha curcas*)	99	gi|641200029|AIA57960.1
6.6	A0A067KW23	seed storage protein 2 (*Jatropha curcas*)	100	gi|641200053|AIA57961.1
10.1	A0A067JF64	nucleolar protein nop56, putative (*Ricinus communis*)	55	gi|255567546|XP_002524752.1
10.2	A0A067K2P3	legumin B precursor, putative (*Ricinus communis*)	69	gi|255566425|XP_002524198.1
10.3	A0A067JUM5	11S globulin seed storage protein 2-like (*Eucalyptus grandis*)	52	gi|702283651|XP_010046000.1
10.4	A0A067JUM5	11S globulin seed storage protein 2-like (*Eucalyptus grandis*)	52	gi|702283651|XP_010046000.1
10.5	A0A067K2P3	legumin B precursor, putative (*Ricinus communis*)	69	gi|255566425|XP_002524198.1
10.6	A0A067KW23	seed storage protein 2 (*Jatropha curcas*)	100	gi|641200053|AIA57961.1

* protein identification generated by MASCOT
** protein identification generated by BLAST

Table 6.3 summarises protein profile identification subsequent to MS analysis. The premier hit under protein family list generated by MASCOT program was considered and checked for protein similarity against the BLAST program. The protein with a high percentage of identification index was then chosen and summarised in the results provided. This shows that two other plant species are predicted as having similar protein sequence as in the MS results of this research. Proteins in *Ricinus communis* and *Eucalyptus grandis* species are identified along with the *Jatropha curcas* identification.

Ricinus communis is a castor oil plant which belongs to Euphorbiaceae family. It has been widely used as a raw material in for biofuel production as well as *Jatropha curcas* (Sujatha et al., 2008). In consequent to same group of family as *Jatropha curcas*, this species is predicted has partially similar protein profile. Furthermore, *Eucalyptus grandis* is not grouped in Euphorbiaceae family, however, it is also recognised as a potential bioenergy crop species amongst scientists (Gordon et al., 2011).

According to the protein identification results in this research, Table 6.3, the identified proteins are dominantly consistent in both lanes with the same bands. Only proteins at 6.2 and 6.5 gave different protein identification compared to 10.2 and 10.5, respectively. The protein at 6.2 is identified as profiled in *Eucalyptus grandis* species, while the protein at 10.2 is identified as in *Ricinus communis*. Moreover, the sequence at 6.5 is identified distinctively as protein at *Jatropha curcas* compare to 10.5 which is protein of *Ricinus communis*. The majority profile of predicted proteins in *Eucalyptus grandis* and *Jatropha curcas* are equivalent as seed storage proteins. Besides, the identified protein of *Ricinus communis* is recognised as a putative protein which shares a similar sequence to the characterised protein.

Further study focuses in morphology of jatropha meal (JM) was conducted in order to investigate the ozonolysis effect on the molecular structure of JM. It aimed to provide information on cell lysis of JM structure due to the presence of ozone molecules and its derivatives. Visual observation using microscopic approach was conducted which is the results are presented in following Figure 6.4.

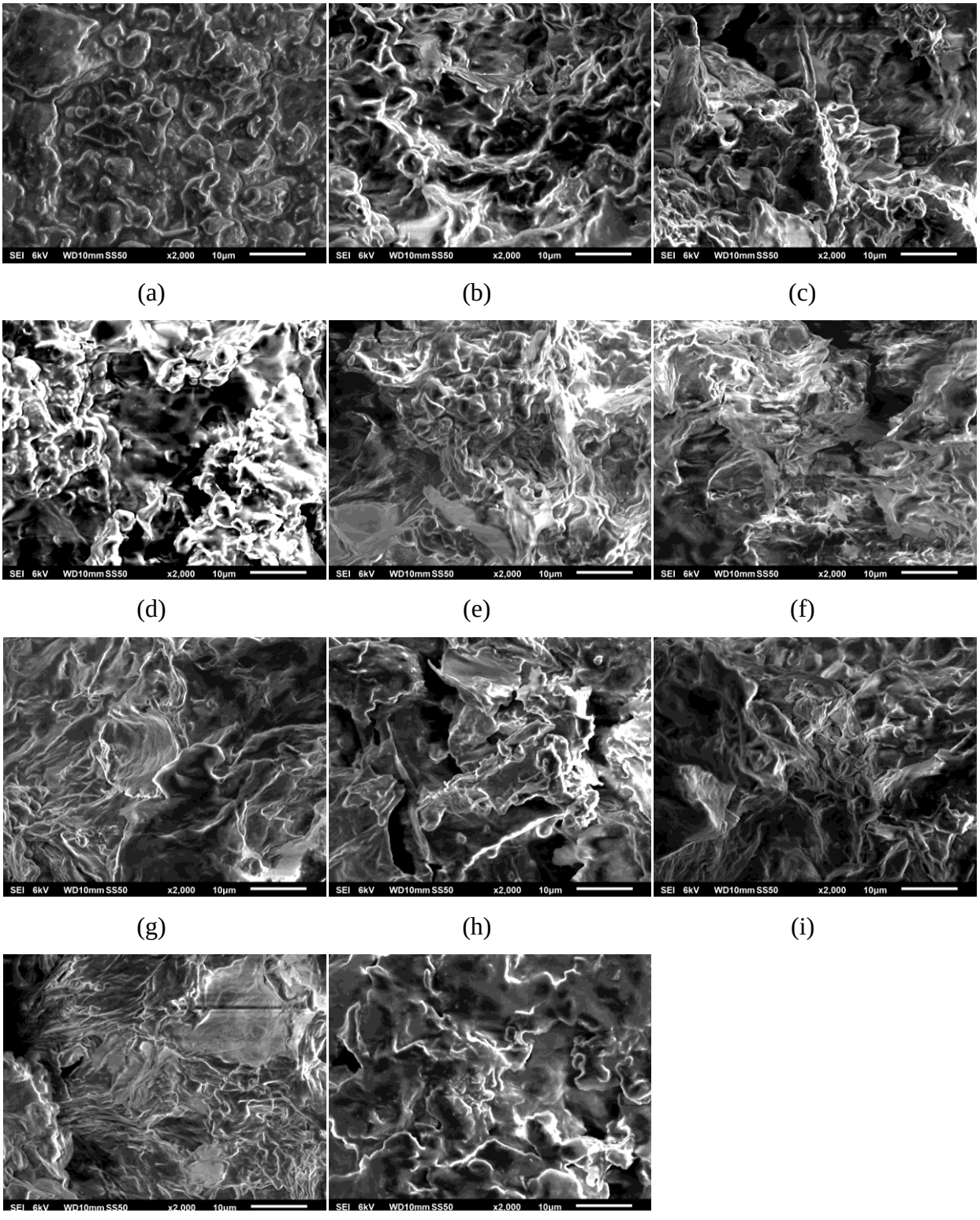

(a) (b) (c)

(d) (e) (f)

(g) (h) (i)

(j) (k)

Figure 6.4 SEM Micrograph of Indonesian JM after ozonolysis; (a) fresh sample; before ozonolysis; (b) 0.5 hour; (c) 1 hour; (d) 1.5 hours; (e) 2 hours; (f) 2.5 hours; (g) 3 hours; (h) 3.5 hours; (i) 4 hours; (j) 4.5 hours; (k) 5 hours

Figure 6.4 presents the Scanning Electron Microscope (SEM) image of Indonesian JM, before and after ozonolysis. A morphology study of JM was conducted by observing treated samples every 30 minutes of ozonolysis for 5 hours. Visual observation of SEM images shows that the morphology of JM is modified during experimentation. Ozone molecules are expected to break down the cell wall of the JM structure, hence a distinct surface is observed. The image of the raw JM sample before ozonolysis (a) shows an intact structure of JM with oily reflection. A significant change of JM structure is shown in image (b) after 30 minutes treatment by ozonolysis. A fibrous structure is observed which is expected as a result of the ozone molecular attack on JM cells. As a strong oxidation agent, ozone has the ability to break down cell walls within the JM structure. This causes more protein release which is reflected by double improvement of protein content in JM samples, as reported in the beginning of this section.

Moreover, consistent structures with smoother appearances of the JM surface were further observed (c-j). Ultimately, an even surface of JM structure was attained after 5 hours of ozonolysis (k). The fibrous structure has disappeared which is assumed as a feature of continuous long term ozonolysis exposure. This is consistent with studies done in the investigation of the influence of ozonolysis to smoothness and fibrous structure of lignocellulosic materials (Nouwezem et al., 1993, Shi et al., 2015). Ozone is found to be effective in destroying the fibrous ligament and further shortening it. Therefore, during long-term ozone exposure to the materials, less fibrous structure is achieved. The impact of this powerful ozone ability is as observed in the morphology study of the Indonesian JM sample by SEM.

6.2 Ozonolysis of synthetic lignin

The investigation of the effect of ozonolysis on synthetic lignin samples was conducted in order to study the general cell lysis phenomenon by ozone. Alkali lignin was employed as the substrate in this investigation. Samples were treated for 3 hours of ozonolysis with parameters as explained in Chapter 3, Section 3.4.2. An absorbency technique was carried out for lignin concentration analysis. A calibration was done prior to the analysis process. Triplicate experiments were performed during investigations. Moreover, pH conditions of samples were observed during ozonolysis. Data obtained in this experiment provides a fundamental study of the ozone-lignin reaction mechanism.

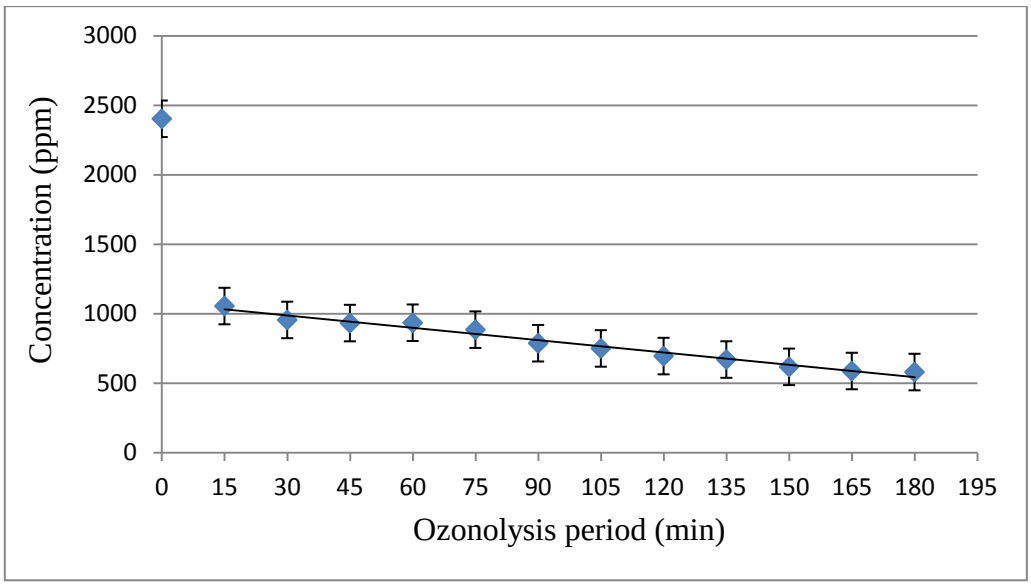

Figure 6.5 Ozonolysis effect on lignin content after 180 minutes duration

Figure 6.5 presents experimental data on the lignin concentration profile during ozonolysis. It is shown that lignin concentration is significantly decreased until 15 minutes of ozonolysis. Approximately, 56% reduction of lignin concentration is achieved during this period. Furthermore, lignin content gradually decreased until ozonolysis has completed. By the completion of ozonolysis, 76% of lignin degradation is observed. In addition, the curve shows there are two separate kinetics mechanisms occurring during the process. A fast decay, taking place from the beginning until 15 minutes of ozonolysis, followed by a slower time scale

decay, until the end of ozonolysis. As mentioned in Fogler (2006), multiple reactions typically occur in a chemical process. The fast decay mechanism occurs during ozonolysis is expected as a result of lignin cell wall breakage due to ozone molecules and its derivatives. Moreover, less lignin cell wall material was presented after 15 minutes of ozonolysis and hence slower decay and slower cell lysis rates follow thereafter. Formula of kinetics mechanism for an ozonolysis duration of 15-180 minutes is presented in Equation 6.1. C_{lignin} is defined as a concentration of lignin (ppm) while t is defined as an ozonolysis period (minutes) further the R^2 value is 0.98.

$$C_{lignin} = -2.95t + 1075.50 \quad , t > 15 \text{ min} \qquad (6.1)$$

This finding is indicative that ozone has a devastating effect on cell lysis of lignocellulosic materials for the initial period where all labile components are reacted followed by a slow relatively inert process (Eq. 6.1). Lignin naturally is susceptible to ozone-related reactions (Vidal and Molinier, 1988, Nouwezem et al., 1993). The kinetics data suggests that the reaction follows zero order of kinetic. A zero order of kinetics refers to a reaction when its rate is independent to the concentration of reactants involved in process (Fogler, 2006). In this experiment, the reaction rate depends on existence of excess reactants, lignin and ozone, neither of their concentrations. Moreover, ozonolysis duration of 15 minutes is considered as the maximum treatment period for process efficiency.

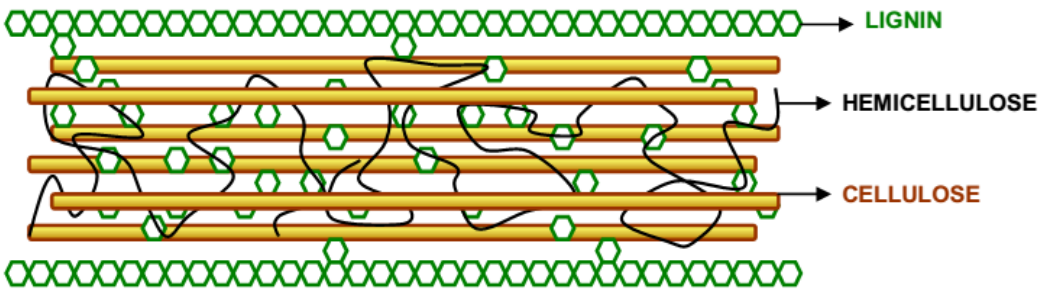

Figure 6.6 Cross sectional view of lignocellulosic structure (Mussatto and Teixeira, 2010)

Furthermore, Figure 6.6 illustrates biological structure of lignocellulosic materials. Lignin is recognised as an outer layer of the cell structure which is polymerised to hemicelluloses and cellulose. Principally, lignocellulosic materials are abundant in nature not only as raw materials but also as waste materials. Agricultural waste, food residues and organic industrial effluent mainly contain lignocellulosic materials (Chuck et al., 2013, Palmqvist and Hahn-Hägerdal, 2000). Further treatments of these materials are possible to provide alternative bio-resources for downstream industries. Hemicelluloses are cellulose that can be utilised for many industrial products such as enzymes, biofuel, organic acids and food additives. These compounds are known for their sugar based chemical composition, and therefore, can be used as economic valuable sources (Mussatto and Teixeira, 2010, Chuck et al., 2013). Lignin degradation processes are particularly desirable in order to biologically access hemicelluloses and cellulose layers. The existence of ether bonds in lignin structure limits this process. It results in lignin insusceptibility during conventional biodegradation approaches such as enzymatic and chemical treatment (Mussatto and Teixeira, 2010, Michniewicz et al., 2012, Palmqvist and Hahn-Hägerdal, 2000, Wu et al., 2013b).

Studies of ozonolysis utilisation in lignin compound treatment have been conducted over decades (Wu et al., 2013a, Nouwezem et al., 1993, Vidal and Molinier, 1988). It has become preferable due to the regular requirement of operating condition; room temperature and atmospheric pressure (Sweeney, 1981). Treated lignin was further utilised for many extended application subsequent to investigations. Nevertheless, some drawbacks have limited its industrial scale up application. Vidal and Molinier (1988) have studied ozonolysis of lignin in order to enhance sawdust digestion. They found that enzyme accessibility to experimental substrate was improved during ozonolysis. Unfortunately, high voltage input, 15-33 kV was required during ozone generation. This high power supply requirement has an associated high

processing cost. Furthermore, laboratory scale experimentation was done in 350 ml of gas washing glass by Wu *et al* (2013a) with a modern ozone generator. Ozone was used in hydrogen production pre-treatment stage by using barley straw as raw materials. Ozonolysis was conducted for 150 minutes duration which approximately 25% of lignin was reduced within 15 minutes of ozonolysis.

The adopted bespoke experimental set up in this research offers low power consumption which allows ozonolysis performance at lower voltage, 4 kV. Besides, the 2 litres volume of the aluminium reactor provides flexibility for a wide range of samples and degree of scale up that is close to industrial application. In addition, over 50% of lignin reduction is confirmed after 15 minutes of ozonolysis as significant result in preliminary study. Jablonský *et al* (2004) mentioned that ozone has been considered as strong oxidant to majority of organic materials including lignocellulosic reaction process inclusively to lignin compound. Reactions occurring during ozonolysis facilitate lignin degradation hence access through the lignocellulosic structure is easier (Nouwezem et al., 1993). Application of microbubble technology during ozonolysis in this research plays an essential role in enhancing the lignin degradation rate. Ozone is introduced to the bulk of liquid, lignin rich mixture, in form of microbubbles. A smaller size of bubbles intensifies the reaction between lignin and ozone as wider contact area is applied. In addition, longer contact time of ozone and lignin is achieved due to the low rising velocity of microbubbles. Therefore, ozone and its derivatives reacted effectively into the molecular structure of lignin compound.

Moreover, pH condition, as a principle factor in any biological process, is also considered during study of lignin degradation by ozonolysis. pH observation during experiments in this research is expressed by Figure 6.7 as provided.

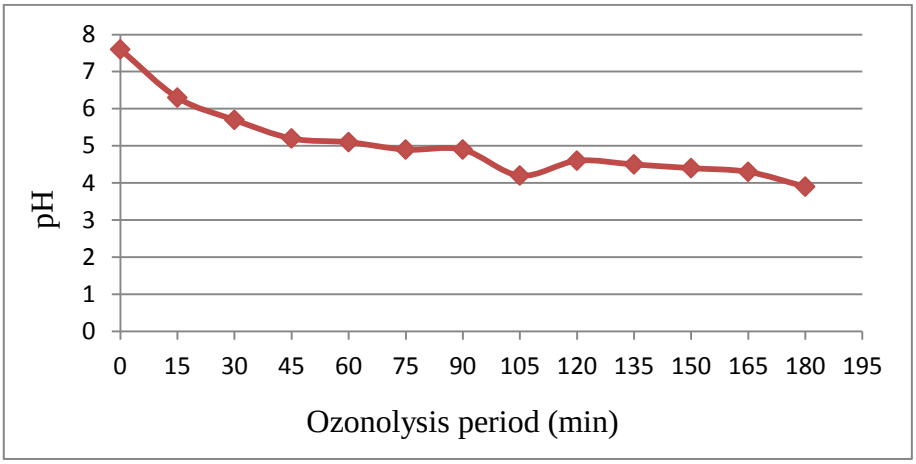

Figure 6.7 pH observation during ozonolysis of lignin alkali sample after 180 minutes

Figure 6.7 shows the pH condition of alkali lignin samples during ozonolysis. Lignin alkali sample before treatment had pH of nearly 8; however, pH was gradually decreased during ozonolysis. Approximately pH 4 was reported by the end of experiment, 180 minutes of ozone exposure. This phenomenon is consistent to Travaini *et al* (2013) which explained that reaction of ozone and its derivates to chemical bonds in lignin lead to pH reduction. However, ozone reaction in the lignin degradation process has optimally conducted in basic condition due to possibility of hydroxyl radical existence (Amat et al., 2005, Glaze et al., 1987). Hydroxyl radicals (•OH) have higher oxidation potential compared to ozone , 2.8 V for •OH and 2.07 V O_3 (Li et al., 2009, Beltrán, 2004). Hydroxyl radicals are sensitive to reaction with almost all organic materials (Hoigné and Bader, 1976). Furthermore, their existence is mainly detected under basic conditions while hydroxyl radicals are rarely found under acid conditions, pH 1.3-4.5 (Mamleeva et al., 2009).

6.3 Summary

Quantitative analytical results show stable protein content is achieved during 5 hours ozonolysis. Exclusively, total protein is doubled after 0.5 hours of ozonolysis which might have resulted from structural change of JM cell wall due to the presence of ozone. The

breakdown of cell wall allows more protein to be released hence its concentration increased. There is no significant protein reduction observed until ozonolysis was completed which 5 hours continuous treatment duration. Total protein content observed in this research is in a range of 18-32% which is equal to 75-290 mg/g in jatropha meal, where this value is grouped within good nutritional bounds. Microbubble application during ozonolysis contributes in efficiency of ozone delivery mechanism to the samples of interest. Fast mass transfer as a unique characteristic of microbubbles is assumed to have played an important role. In addition, the low temperature of the plasma reactor prevents protein denaturation. Therefore, protein content in JM samples after ozonolysis remains stable.

Furthermore, qualitative study of the effect of ozonolysis in Jatropha biomass has been done by the MS with further protein identification by the MASCOT and BLAST search engines. According to the SDS-PAGE pattern, it shows that protein molecular weight of JM is distributed at 5-60 kDa. This range is considered as low protein molecular weight which corresponds to previous studies. Six bands of two gel lanes were further investigated to identify protein sequence characterised in JM samples of this research. It is found that the protein sequence in Indonesian JM is matched to two other species which are *Ricinus communi*and *Eucalyptus grandis*. The predicted protein found in species *Eucalyptus grandis* and *Jatropha curcas* are categorised as seed storage protein whilst putative protein is identified to the protein sequence of *Ricinus communis*.

A morphology study by SEM images observation suggests that ozone has influenced the molecular structure of JM samples after ozonolysis. Fibrous structure of JM samples are observed during ozonolysis which is expected as the result of ozone attack on JM cell wall. Oily reflection is shown in raw JM sample before ozonolysis which indicates an intact structure of JM. By the end of experimentation, 5 hours of ozonolysis, relatively smooth

surfaces with no fibrous structure are captured by the SEM image. This result is confirmed by previous studies which investigated the effect of ozonolysis on surface characteristics of lignocellulosic materials.

A study is elaborated for the effect of ozonolysis on cell lysis by using synthetic lignin in order to provide fundamental knowledge of ozone-lignin reactions. Experimentation parameters for both ozonolysis studies of Jatropha biomass and synthetic lignin were maintained the same. Experimental results are expected to be used for further prospective investigations. It is reported that 56% of lignin was significantly reduced after 15 minutes of ozonolysis. Besides, 76% of lignin reduction is observed by the end of ozonolysis, 3 hours duration. This substantial amount of lignin degradation has resulted because of the devastating effect of ozone to lignocellulosic materials. Acidic pH conditions are detected during ozonolysis of lignin samples as a result of lignin degradation.

In conclusion, ozonolysis treatment of lignocellulosic materials offers various advantages in maintaining protein content and also facilitating a cell lysis mechanism. The bespoke experimental reactor with combination of ozonolysis and microbubble technology that is introduced in this research has provided some benefits. Low temperature of plasma reactor prevents protein denaturation whereas water solvent based process keep treated product to be free of chemical contaminations. In addition, the reactor requirement of low power consumption in this research is key factor for economical operation.

CHAPTER 7

CONCLUSIONS AND RECOMMENDATIONS

In this chapter, general conclusions of the study findings and future research work are presented. The main findings are chapter specific, therefore, are found in the respective chapters. They are presented as a summary section in each related chapters. Moreover, this chapter aims to synthesise these findings in order to answer the proposed research questions. Further, future works are recommended to address research continuity in related subjects. These recommendations are presented in the final section of this chapter.

7.1 Conclusions

This research aimed to develop technology which can detoxify a carcinogenic compound in jatropha biomass while maintaining its protein content. A combination of ozonolysis and microbubble technology was applied for this purpose. A compact reactor equipped with a ceramic diffuser and plasma microreactor was designed and further tested for its performance. The Indonesian variety of jatropha meal, a byproduct from biofuel industry, was treated in order to increase its economical value as a potential source of foodstuff or fertiliser. Also, jatropha meal is considered as a beneficial possible food supply which does not compete with oil crops. Aqueous solution and air are used during ozone production and investigated its effect on detoxification. Both water and air are abundant in nature and they do not have any hazardous concern in storage and handling. Therefore, these benefits are seen as promising factors for further industrial application of the technology adopted in this research.

Chapter 2 presented a comprehensive critical assessment of related literature. Detailed information on jatropha plant, as the experimental substrate, was provided and further

narrowed to phorbol ester characterisation as the toxic compound. It is mentioned that phorbol ester is hydrophobic and oil soluble in their presence in jatropha oil as well as jatropha meal. Further, previous studies of phorbol ester detoxification and its proteomic analysis were discussed. Reviews showed that heat treatment for detoxification is not applicable because phorbol ester is heat stable which withstand up to 180 °C. In addition, a process with a high heat requirement is problematic for treatment of biological materials as it can denature the nutritious contents. Other researchers conducted chemical treatment to reduce phorbol ester content in jatropha meal. However, this approach requires addition downstream process for solvent regeneration in which influences the production cost. Moreover, biological treatment was also performed by some researchers to decrease phorbol ester content. Nonetheless, detoxification demanded long duration due to slow metabolic response of bacteria involved. Therefore, a combination of ozonolysis and microbubble technology was proposed in this research to address these problems. An introduction of ozone generation through plasma technology was further explained. Various configurations of plasma reactor along with its respective advantages and disadvantages were provided. A fundamental study of the microbubble technique in relation to ozone delivery mechanism was discussed. In the summary section, an integrated work of ozonolysis effect in phorbol ester content and protein content were introduced. In addition, ozone reaction in lignocellulosic materials was also investigated. It aimed to study the effect of ozonolysis effect on general lignocellulosic materials which were represented by a synthetic lignin.

The experimental materials and procedures were presented in methodology, **Chapter 3**. The chapter was structured into four key sections. Detailed description of the designed reactor to perform experiments was provided in the first section. Experimental set up and reactor assembly were clearly described. Further, another three sections described experimental

procedures of ozonolysis. Reactor characterisation was performed prior to ozonolysis in which study of bubble size distribution, ozone concentration and temperature monitoring of DBD caps were investigated. For this purpose, a ceramic diffuser and plasma microreactor were characterised. Various ranges of air flow rates were applied and the experimental results were reported in the related chapter. Recommended operating conditions were further used in the subsequent experiments which study the effect of ozonolysis on phorbol ester detoxification and ozonolysis effect in lignocellulosic materials. Also, sample identifications, experimental protocols and analysis methods were described independently for both studies.

Reactor characterisation is the first of the results and discussion component of this thesis which was presented in **Chapter 4**. A ceramic diffuser was characterised in order to study the bubble size distribution. Experiments were performed by applying various ranges of air flow rates from 0.5 to 3.0 L/min. The effect of bubble generation was studied in both steady flow (without a fluidic oscillator application) and oscillatory flow (a fluidic oscillator was applied). Average bubble size produced and its distribution were investigated by high speed photography. Images of bubble generation through the ceramic diffuser were presented along with statistical data on bubble average diameter. An air flow rate of 2 L/min was chosen as the margin point because the uniformity and density of bubble generated at this flow rate is favourable for ozonolysis processing. An air flow rate of 2 L/min was further used in the following experiments. Moreover, the plasma microreactor was characterised by measuring ozone concentration and monitoring the temperature of DBD caps. The ozone concentration was measured at a flow rate of 2 L/min in both phases: gas and liquid phase. Ozone concentration in the liquid phase is taken to be dissolved ozone. It is reported that 1.4 ppm of ozone in gas phase while 1.2 ppm of dissolved ozone was observed. The power of plasma reactor during 5 hours of ozonolysis was calculated as 95 W while the energy consumption

was $4.75x10^{-1}$ kWh. In addition, temperature of DBD caps was measured during 60 minutes of ozonolysis in order to provide temperature distribution information. Only a small temperature rise occurred during this experiment. After 60 minutes of ozonolysis, the maximum temperature of 35 °C was detected in the DBD caps. This point is a beneficial for biological processes because many biology substances are susceptible to heat treatment.

Chapter 5 is the second part of results and discussion in this thesis. How ozonolysis affects phorbol ester detoxification was discussed in detail. Ozonolysis was performed at a pressure of 1 atm and a temperature of 24 °C with an air flow rate of 2 L/min in the steady flow condition (without the application of a fluidic oscillator). A high performance liquid chromatograph (HPLC) was used for phorbol ester analysis. Synthetic and natural phorbol esters were used as the experimental samples. In the ozonolysis of synthetic phorbol ester, two different conditions were applied: aeration (without ozone activation) and ozonolysis (with ozone activation). It was observed that only 40% reduction was achieved after 30 minutes of aeration while 64% of degradation was detected after 5 minutes of ozonolysis. In addition, 4 ppm of phorbol ester concentration was set as the minimum level of HPLC detection limit with current set up used in this research. Furthermore, the effect of ozonolysis on detoxification of natural phorbol ester was conducted using the Indonesian variety of jatropha meal. A two stage extraction was performed in order to obtain phorbol ester extract in samples, before and after ozonolysis. Hexane solvent was used during extraction followed by methanol solvent. Both extracts were further individually analysed with HPLC. Hexane extraction aimed to extract phorbol ester content bonded in lipid while methanol was used to extract the remaining phorbol ester which is not bonded in lipid fraction. Phorbol ester obtained from methanol extraction is considered as a pure phorbol ester.

It was shown in HPLC chromatograms that some major fatty acids were found in hexane extract of jatropha meal -- linolenic acid, linoleic acid, oleic acid, palmitic acid and stearic acid. There was a total of 65% oil reduction was observed in the hexane extract after 5 hours of ozonolysis. This reduction is expected as a result of selective reaction between ozone and fatty acids. Furthermore, phorbol ester concentration in hexane extract after 1 hour of ozonolysis was 7 fold higher than in the untreated sample. This phenomenon may occur due to damage of the jatropha cell wall by ozone and its derivatives. This affects ozone diffusivity into the jatropha meal molecular structure, therefore, more phorbol ester released. However, after 2 hours of ozonolysis, phorbol ester content decreased by 47% and it remained stable until 5 hours of ozonolysis. During ozonolysis, ozone molecules decomposed into free radicals for which the main product is hydroxyl radicals (•OH). These molecules act as an auto-catalyst which further reacted with carbon double bonds in phorbol ester molecular structure. Reaction of ozone with carbon double bonds is known as the Criegee Mechanism. Utilisation of microbubble in this research intensifies those reactions because microbubbles remained longer in the bulk of liquid hence mass transfer occurs effectively. Slow rising velocity of microbubbles allowed longer contact of ozone and jatropha sample which affects detoxification process during ozonolysis. In addition, microbubbles also facilitate the cell lysis of the jatropha molecular structure in which ozone and its derivatives could attack carbon double bonds in deeper layers of jatropha meals.

Furthermore, phorbol ester concentration in the methanol extract was significantly decreased after 3 hours of ozonolysis with 92% reduction observed. Besides, four phorbol ester peaks were detected in the HPLC chromatograms which correspond to the theory that only four out of six types of jatropha factors are detectable by chromatography analysis. Moreover, 97% of phorbol ester reduced after 5 hours of ozonolysis which resulted final phorbol ester

concentration of 0.11 mg/g in jatropha meal sample. This value is also phorbol ester concentration found in non-toxic Mexican variety which has become the limit of jatropha edibility level. Hydroxyl radicals (•OH) are reported to play a substantial role in phorbol ester detoxification with ozonolysis technology. These free radicals worked simultaneously with ozone molecules as strong oxidants during chemical reaction with carbon double bonds in phorbol ester structures. It was also reported that Protein Kinase C (PKC), in which stimulated neurotransmission of phorbol ester, is susceptible with •OH. Therefore, ozonolysis with generation of ozone and hydroxyl radicals was expected to modify phorbol ester structure which further affects the reaction of PKC as a tumour promoter.

How ozonolysis affects lignocellulosic materials was explored in **Chapter 6**, as the last part of the results and discussion chapters. The studies of the effect of ozonolysis on protein content after detoxification and on synthetic lignin compound were discussed. The proteomic investigation using jatropha meal substrate before and after ozonolysis aims to provide an integrated study in phorbol ester detoxification. For this purpose, qualitative and quantitative analyses were conducted. Total protein was quantified and showed that the protein content was doubled after 0.5 hours of ozonolysis. This phenomenon is a result of cell wall degradation in the jatropha molecular structure due to the presence of ozone. The damage of jatropha meal shell wall was also indicated by fibrous appearance in SEM images. The fibrous structure represents intact cells of jatropha meal which have not been reacted with ozone. Afterwards, a smooth surface of jatropha meal samples was captured in the SEM images. Moreover, there was no significant reduction of protein content in jatropha meal samples, observed until 5 hours of ozonolysis. It was reported that total protein concentration ranged from 18-32% which meets the requirement of nutritional limits. Furthermore, qualitative analysis showed that the protein molecular weight of jatropha meal was distributed from 5 to

60 kDa. In addition, it was observed that the protein sequence of Indonesian jatropha meal used in this research was matched to two other species which are *Ricinus communi*and *Eucalyptus grandis*. The study of the effect of ozonolysis on synthetic lignin samples showed that 56% of lignin reduction was reported after 15 minutes of ozonolysis. Also, 76% of lignin reduced after 3 hours duration. pH was reported as an important factor in this process in which pH reduction was observed during experiments of lignin degradation.

Finally, according to the experimental data in this research, it is observed that phorbol ester content in jatropha samples has been detoxified and the protein content remained stable. Low energy consumption of the designed reactor as well as its ability to operate at atmospheric pressure and room temperature promises significant advantage through the adopted technology. The combination of ozonolysis and microbubble technology enhances detoxification of phorbol ester. In addition, there are two time scales and two mechanisms influencing the kinetics of ozonolysis in JM -- (i) cell lysis from cell wall breakdown which releases proteins, and (ii) degradation of proteins by ozonolysis. The fact that a stable, long time protein composition develops suggests that the remaining protein content is not particularly labile to ozonolysis. Everything that was labile is oxidised, and thereafter, more ozonolysis just "burns" the labile pieces of the cell wall. A parallel can be drawn from this research is both ozonolysis of Jatropha meal and lignocellulosic material, occur in an initial fast decay mechanism, followed by a slower decay mechanism in ozonolysis of the lignocellulosic sample. Moreover, low operating temperature (maximum of 35 °C) during ozonolysis also prevents protein denaturation therefore protein content after detoxification remained stable. These advantages lead to technical feasibility for industrial application. The key findings of this research are presented in Table 7.1 which lists the hypotheses in descending order of importance with the list of evidence to support the hypotheses.

Table 7.1 List of research key findings

Hypothesis	Evidence
Ozone molecules and its derivatives can attack carbon double bonds of phorbol esters in Jatropha meal molecular structure.	Section 5.2, Figure 5.8 (page 110) and Figure 5.13 (page 119), discussion of phenomenon following to Criegee mechanism (page 120-122), Equation 5.3-5.6 (page 121).
Ozonolysis enhanced by microbubble technology can maintain protein contents of Jatropha meal after detoxification.	Section 6.1, Figure 6.1 (page 128) which also support phenomenon claims on Figure 5.8 (page 110). It shows that the increasing and further reduction of protein give similar trend to the phorbol ester content after hexane extraction.
Ozonolysis resulted in reduction of Jatropha oil content and breakdown of Jatropha shell wall.	First order of kinetic is indicated in the result of ozonolysis effect on oil content (Figure 5.9 and Equation 5.1, page 112). SEM micrographs (Figure 6.4, page 138).
Multiple reactions occur during reduction of lignocellulosic material by ozonolysis.	Section 6.2, Figure 6.5, discussion page 140-141.
A bespoke reactor can facilitate detoxification of phorbol ester while maintaining protein content of Jatropha meal by providing microbubble and plasma technology with low power consumption.	Discussion on Chapter 4 (page 81-82), Table 4.1 (page 83), Equation 4.1-4.3 (page 94-95)

7.2 Recommendations

Following to the findings from this research, some recommendations for future works are proposed in relation to research continuity in related fields. First, the introduction of fluidic oscillation is recommended in ozonolysis of jatropha meal for phorbol ester detoxification. As studied in reactor characterisation chapter in this thesis, it has been reported that fluidic oscillator influences the bubble size distribution. This finding leads to the possibility of intensification of the effect of ozonolysis for phorbol ester detoxification. Also, investigation using various type of c diffuser during ozonolysis is recommended in order to obtain the optimum diffuser material for ozone-rich microbubble generation. Different size of bubbles

generated affects mass transfer in the gas-liquid-solid interface. Besides, detoxification period and phorbol ester detoxification level may vary. Further, since ozonolysis is performed in various ranges of pH, a systematic study about its effect on phorbol ester content and protein in treated samples would be useful.

Experimental data showed that the final concentration of phorbol ester after ozonolysis is equal to the threshold of phorbol ester content in non-toxic Mexican jatropha. However, further analysis to investigate the toxicity level of jatropha meal after ozonolysis is needed. The chemical structure of phorbol ester had been modified due to ozone reaction and may form other chemical substances. This formation may also affect the toxicity of jatropha meal which could influence its edibility. Moreover, it is important to explore nutrient analysis to justify the nutritional content of treated jatropha meal for its further utilisation such as for foodstuff and fertiliser. Advanced analysis to study the effect of ozonolysis on specific amino acids in the protein of detoxified jatropha meal, is also recommended as a valuable future research in order to provide comprehensive understanding for jatropha meal utilisation as an additional food supply.

Ultimately, the main aim in an engineering research is to provide large scale processes for commercial production. By considering this aim and experimental results obtained, subsequent studies need to be performed at pilot scale following up on this laboratory bench investigation. The grand aim is to develop such a detoxification technique to meet the requirements for industrial implementation.

REFERENCES

Abou-Arab, A. A. & Abu-Salem, F. M. 2010. Nutritional quality of Jatropha curcas seeds and effect of some physical and chemical treatments on their anti-nutritional factors. *African Journal of Food Science,* 4**,** 93-103.

Aderibigbe, A. O., Johnson, C. O. L. E., Makkar, H. P. S., Becker, K. & Foidl, N. 1997. Chemical composition and effect of heat on organic matter- and nitrogen-degradability and some antinutritional components of Jatropha meal. *Animal Feed Science and Technology,* 67**,** 223-243.

Agarwal, A., Jern Ng, W. & Liu, Y. 2011. Principle and applications of microbubble and nanobubble technology for water treatment. *Chemosphere,* 84**,** 1175-1180.

Agency, U. E. P. 1999. Wastewater Technology Fact Sheet Ozone Disinfection. *In:* WATER, O. O. (ed.). Washington, D.C: EPA 832-F-99-063.

Al-Mashhadani, M. K. H. 2013. *Application of Microbubbles Generated by Fluidic Oscillation in the Anaerobic Digestion Process.* PhD, University of Sheffield.

Alemskaya, O. P., Lelevkin, V.M., Tokarev, A.V., and Yudanov, V.A 2003. Synthetics of Ozone in a Surface Barrier Discharge with a Plasma Electrode. *High Energy Chemistry,* 39**,** 263-267.

Amat, A. M., Arques, A., Miranda, M. A. & López, F. 2005. Use of ozone and/or UV in the treatment of effluents from board paper industry. *Chemosphere,* 60**,** 1111-1117.

Annongu, A. A., Joseph, J. K., Apata, D. F., Adeyina, A. O., Yousuf, M. B. & Ogunjimi, K. B. 2010. Detoxification of Jatropha curcas seeds for Use in nutrition of monogastric livestock as alternative feedstuff. *Pakistan Journal of Nutrition,* 9**,** 902-904.

Aregheore, E. M., Becker, K. & Makkar, H. P. S. 2003. Detoxification of a toxic variety of Jatropha curcas using heat and chemical treatments, and preliminary nutritional evaluation with rats. *The South Pacific Journal of Natural and Applied Sciences,* 21**,** 51-56.

Avery, L., Jarvis, P. & Macadam, J. 2013. Review of literature to determine the uses for ozone in the treatment of water and wastewater. Aberdeen: The James Hutton Institute.

Baber, T. M., Graiver, D., Lira, C. T. & Narayan, R. 2005. Application of catalytic ozone chemistry for improving biodiesel product performance. *Biomacromolecules,* 6**,** 1334-1344.

Babikov, D., Kendrick, B.K., Walker, R. B., and Pack, R.T 2003. Formation of ozone: Metastable states and anomalous isotope effect. *Journal of Chemical Physics,* 119.

Bader, H. & Hoigné, J. 1981. Determination of ozone in water by the indigo method. *Water Research,* 15**,** 449-456.

Banerjee, S. & Wong, S. S. 2002. Rational sidewall functionalization and purification of single-walled carbon nanotubes by solution-phase ozonolysis. *Journal of Physical Chemistry B,* 106**,** 12144-12151.

Bari, S. D. & Robinson, A. J. 2012. Experimental study of gas injected bubble growth from submerged orifices. *Experimental Thermal and Fluid Science,* Article In Press.

Barlow, P., J 1994. An Introduction to Ozone Generation. *Technical Director.* Watertec Engineering Pty Ltd.

Beltrán, F. 2004. *Ozone Reaction Kinetics for Water and Wastewater Systems,* Boca Raton, FL, Lewis Publisher.

Biń, A. K. 2004. Ozone dissolution in aqueous systems treatment of the experimental data. *Experimental Thermal and Fluid Science,* 28**,** 395-405.

Bitra, V. S. P., Womac, A. R., Chevanan, N. & Sokhansanj, S. 2008. Comminution Properties of Biomass in Hammer Mill and its Particle Size Characterization. *In:* ENGINEERS, A. S. O. A. A. B. (ed.) *ASABE Annual International Meeting.* Rhode Island.

Brittle, S., Desai, P., Ng, W. C., Dunbar, A., Howell, R., Tesař, V. & Zimmerman, W. B. 2015. Minimising microbubble size through oscillation frequency control. *Chemical Engineering Research and Design,* 104**,** 357-366.

Burgassi, S., Zanardi, I., Travagli, V., Montomoli, E. & Bocci, V. 2009. How much ozone bactericidal activity is compromised by plasma components? *Journal of Applied Microbiology*.

Burns, S. E., Yiacoumi, S. & Tsouris, C. 1997. Microbubble Generation for Environmental and Industrial Separations. *Separation Purification Technology,* 11**,** 221-232.

Caratsch, C. G., Schumacher, S., Grassi, F., and Eusebi, F. 1988. Influence of protein Kinase C-Stimulation by a phorbol ester on neurotransmitter release at frog end-plates. *Naunyn-Schmiedeberg's Arch Pharmacol,* 337**,** 9-12.

Chalmers, I. D., Baird, R C and Kelly, T 1998. Control of an Ozone Generator-theory and practice. *Meas. Sci. Technol,* 9**,** 983-988.

Cheng, H.-H., Chen, S.-S., Wu, Y.-C. & Ho, D.-L. 2007. Non-thermal Plasma Technology for Degradation of Organic Compounds in Wastewater Control: A Critical Review. *Environ. Eng. Management,* 17**,** 427-433.

Chuck, C. J., Parker, H. J., Jenkins, R. W. & Donnelly, J. 2013. Renewable biofuel additives from the ozonolysis of lignin. *Bioresource Technology,* 143**,** 549–554.

Clift, R., Grace, J. R. & Weber, M. E. 1978. *Bubbles, Drops and Particles,* London, Academic Press, Inc.

Colt, J., Kroeger, E. & Rust, M. 2010. Characteristics of oxygen flow through fine bubble diffusers used in the aquaculture hauling applications. *Aquacultural Engineering,* 43**,** 62-70.

Corke, T., Post, M. & Orlov, D. 2009. Single dielectric barrier discharge plasma enhanced aerodynamics: physics, modeling and applications. *Experiments in Fluids,* 46**,** 1-26.

Criegee, R. 1975. Mechanism of Ozonolysis. *Angew. Chem. Internat. Edit.,* 14**,** 745-752.

Cvetkovic, I., Milic, J., Ionescu, M. & Petrovic, Z. S. 2008. PREPARATION OF 9-HYDROXYNONANOIC ACID METHYL ESTER BY OZONOLYSIS OF VEGETABLE OILS AND ITS POLYCONDENSATION. *Hemijska Industrija,* 62**,** 319-328.

De Barros, C. R. M., Ferreira, L. M. M., Nunes, F. M., Bezerra, R. M. F., Dias, A. A., Guedes, C. V., Cone, J. W., Marques, G. S. M. & Rodrigues, M. A. M. 2011. The potential of white-rot fungi to degrade phorbol esters of Jatropha curcas L. seed cake. *Engineering in Life Sciences,* 11**,** 107-110.

Deachathai, S., Suteerapataranon, S. & Sitichai, W. 2010. Determination of phorbol esters in Jatropha curcas using HPLC technique. *36th Congress on Science and Technology of Thailand.* 26-28 October, Thailand.

Devappa, R. K., Bingham, J.-P. & Khanal, S. K. 2013. High performance liquid chromatography method for rapid quantification of phorbol esters in Jatropha curcas seed. *Industrial Crops and Products,* 49**,** 211-219.

Devappa, R. K., Makkar, H. P. S. & Becker, K. 2010a. Biodegradation of Jatropha curcas phorbol esters in soil. *Journal of the Science of Food and Agriculture,* 90**,** 2090-2097.

Devappa, R. K., Makkar, H. P. S. & Becker, K. 2010b. Nutritional, Biochemical, and Pharmaceutical Potential of Proteins and Peptides from Jatropha: Review. *Journal of Agricultural and Food Chemistry,* 58**,** 6543-6555.

Devappa, R. K., Makkar, H. P. S. & Becker, K. 2011. Jatropha Diterpenes: a Review. *Journal of the American Oil Chemists Society,* 88**,** 301-322.

Dietrich, N., Mayoufi, N., Poncin, S., Midoux, N. & Li, H., Z. 2013. Bubble formation at an orifice: A multiscale investigation. *Chemical Engineering Science,* 92**,** 118-125.

Dimitrijevic, S. M., Humer, U., Shehadeh, M., Ryves, W. J., Hassan, N. M. & Evans, F. J. 1996. Analysis and purification of phorbol esters using normal phase HPLC and photodiode-array detection. *Journal of Pharmaceutical and Biomedical Analysis,* 15**,** 393-401.

Diwani, G. I. E., Rafei, S. A. E. & Hawash, S. I. 2011. Ozone for Phorbol Esters Removal from Egyptian Jatropha Oil Seed Cake. *Advances in Applied Science Research,* 2**,** 221-232.

Engelsen, C. W., Isarin, J. C., Gooijer, H., M.M.C.G, W. & Groot Wassink, J. 2002. Bubble Size Distribution of Foam. *AUTEX Research Journal,* 2.

Epa 1999. Alternative Disinfectants and Oxidants. *In:* MANUAL, E. G. (ed.) *Ozone Chemistry.*

Eriksson, M. 2005. *Ozone Chemistry in Aqueous Solution, Ozone Decomposition and Stabilisation.* Licentiate Thesis, Royal Institute of Technology.

Fábián, I. 2006. Reactive Intermediates in Aqueous Ozone Decomposition: A mechanistic Approach. *Pure Appl. Chem,* 78**,** 1559-1570.

Fao 2003. FAO Food and Nutrition Paper. *In:* NATIONS, F. A. A. O. O. T. U. (ed.) *Food energy - methods of analysis and conversion factors.* Rome.

Feshitan, J. A., Chen, C. C., Kwan, J. J. & Borden, M. A. 2009. Microbubble size isolation by differential centrifugation. *Journal of Colloid and Interface Science,* 329**,** 316-324.

Fogler, H. S. 2006. *Elements of Chemical Reaction Engineering,* New Jersey, Pearson International Education.

Forson, F. K., Oduro, E. K. & Hammond-Donkoh, E. 2004. Performance of jatropha oil blends in a diesel engine. *Renewable Energy,* 29**,** 1135-1145.

Francis, G., Oliver, J. & Sujatha, M. 2013. Non-toxic jatropha plants as a potential multipurpose multi-use oilseed crop. *Industrial Crops and Products,* 42**,** 397-401.

Franken, L. 2005. The Application of Ozone Technology for Public Health and Industry. Food Safety and Security at Kansas State University.

Fridman, A. 2008. Plasma Chemistry. Cambridge University Press.

Garbin, V. 2006. *Optical Tweezers for The Study of Microbubble Dynamics in Ultrasound.* Doctorate, Universita Degli Studi Di Trieste.

Gaur, S. 2009. *Development and evaluation of an effective process for the recovery of oil and detoxification of meal from jatropha curcas.* Master of Science in chemical engineering, Missouri University of Science and Technology.

Glaze, W. H., Kang, J. W. & Chapin, D. H. 1987. The chemistry of water treatment processes involving ozone, hydrogen peroxide and UV radiation. *Ozone Sci. Eng,* 9**,** 335–352.

Goel, G., Makkar, H. P. S., Francis, G. & Becker, K. 2007. Phorbol esters: Structure, biological activity, and toxicity in animals. *International Journal of Toxicology,* 26**,** 279-288.

Gogoi, R., Niyogi, U. K. & Tyagi, A. K. 2014. Reduction of phorbol ester content in jatropha cake using high energy gamma radiation. *Journal of Radiation Research and Applied Sciences,* 7**,** 305-309.

Gopalakrishna, R. & Anderson, W. B. 1987. Susceptibility of protein kinase C to oxidative inactivation: Loss of both phosphotransferase activity and phorbol diester binding. *FEBS Letters,* 225**,** 233-237.

Gordon, D. R., Tancig, K. J., Onderdonk, D. A. & Gantz, C. A. 2011. Assessing the invasive potential of biofuel species proposed for Florida and the United States using the Australian Weed Risk Assessment. *Biomass and bioenergy,* 35**,** 74-79.

Grau, R. A. 2006. *An Investigation of The Effect of PHysical and Chemical Variables on Bubble Generation and Coalescence in Laboratory Scale Flotation Cells.* Doctoral, Helsinki University of Technology.

Gübitz, G. M., Mittelbach, M. & Trabi, M. 1999. Exploitation of the tropical oil seed plant Jatropha curcas L. *Bioresource Technology,* 67**,** 73-82.

Haas, W. & Mittelbach, M. 2000. Detoxification experiments with the seed oil from Jatropha curcas L. *Industrial Crops and Products,* 12**,** 111-118.

Haas, W., Sterk, H. & Mittelbach, M. 2002. Novel 12-Deoxy-16-hydroxyphorbol Diesters Isolated from the Seed Oil of Jatropha curcas. *Journal of Natural Products,* 65**,** 1434-1440.

Hancocks, R. D. 2011. *Controlled Emulsification using Microporous Membranes.* PhD, University of Birmingham.

Hanotu, J. 2013. *Development of A Fluidic Oscillator-Driven Flotation System.* PhD, University of Sheffield.

Hanotu, J., Bandulasena, H., H. C, Chiu, T. Y. & Zimmerman, W. B. 2013. Oil Emulsion Separation with Fluidic Oscillator Generated Microbubbles. *International Journal of Multiphase Flow,* 56**,** 119-125.

He, W. 2011. *Biochemical and genetic analysis of Jatropha curcas L seed composition.* PhD, University of York.

Hecker, E. 1977. New Toxic. Irritant and Cocarcinogenic Diterpene esters from Euphorbiaceae and from Thymelaeaceae. *Pure and Appl Chem,* 49**,** 1423-1431.

Heller, J. 1996. Physic nut. Jatropha curcas L. Promoting the conservation and use of underutilized and neglected crops. *Institute of Plant Genetics and Crop Plant Research, Gatersleben/ International Plant Genetic Resources Institute, Rome.*

Hirota, M., Suttajit, M., Suguri, H. 1988. A New Tumor Promoter from the Seed Oil of Jatropha curcas L., an Intramolecular Diester of 12-Deoxy-16-hydroxyphorbol. *Cancer Research,* 48**,** 5800 - 5804

Hoigné, J. & Bader, H. 1976. The role of hydroxyl radical reactions in ozonation processes in aqueous solutions. *Water Research,* 10**,** 377-386.

Hoigné, J. & Bader, H. 1978. Ozonation of Water: Kinetics of Oxidation of Ammonia by Ozone and Hydroxyl Radicals. *American Chemical Society,* 12**,** 79-84.

Irfan, M., Glasnov, T. N. & Kappe, C. O. 2011. Continuous Flow Ozonolysis in a Laboratory Scale Reactor. *Organic Letters,* 13**,** 984-987.

Jablonský, M., Vrška, M. & Katuščák, S. 2004. Cellulose protectors for improving ozone bleaching: Review. *Wood Research,* 49.

Ján A. Miernyk & Hajduch, M. 2011. Seed proteomics - Review. *Journal of Proteomics,* 74**,** 389 – 400.

Jian Xie, Xun Zhu, Qiang Liao, Hong Wang & Ding, Y.-D. 2012. Dynamics of bubble formation and detachment from an immersed micro-orifice on a plate. *International Journal of Heat and Mass Transfer,* 55**,** 3205–3213.

Jongschaap, R. E. E., Corre, W. J., Bindraban, P. S. & Bradenburg, W. A. 2007. Claims and Facts on Jatropha curcas L. *Global Jatropha curcas evaluation, breeding and propagation programme.* Wageningen: Plant Research International B.V.

Joshi, C., Mathur, P. & Khare, S. K. 2011. Degradation of phorbol esters by Pseudomonas aeruginosa PseA during solid-state fermentation of deoiled Jatropha curcas seed cake. *Bioresource Technology,* 102**,** 4815-4819.

Kandpal, J. B. & Madan, M. 1995. Jatropha curcas: a renewable source of energy for meeting future energy needs. *Renewable Energy,* 6**,** 159-160.

Kaushik, N. & Bhardwaj, D. 2013. Screening of Jatropha curcas germplasm for oil content and fatty acid composition. *Biomass and bioenergy,* 58**,** 210-218.

Kawahara, A., Sadatomi, M., Matsuyama, F., Matsuura, H., Tominaga, M. & Noguchi, M. 2009. Prediction of micro-bubble dissolution characteristics in water and seawater. *Experimental Thermal and Fluid Science,* 33**,** 883-894.

Khirani, S., Kunwapanitchakul, P., Augier, F., Guigui, C., Guiraud, P. & Hébrard, G. 2011. Microbubble Generation through Porous Membrane under Aqueous or Organic Liquid Shear Flow. *Industrial & Engineering Chemistry Research,* 51**,** 1997-2009.

King, A. J., He, W., Cuevas, J.A., Freudenberger, M., Ramiaramanana, D., and Graham, I. A 2009. Potential of Jatropha curcas as a source of renewable oil and animal feed. *Journal of Experimental Botany,* 60**,** 2897-2905.

Kogelschatz, U., Eliasson, B. & Hirth, M. 1988. Ozone Generation From Oxygen and Air: Discharge Physics and Reaction Mechanisms. *Ozone Science and Engineering,* 10**,** 367-378.

Kogelschatz, U., Eliasson, B and Egli, W 1997. Dielectric Barrier Discharge. Principles and Applications. *J Phys IV France,* 7.

Kongmany, S., Matsuura, H., Furuta, M., Okuda, S., Imamura. K. & Maeda, Y. 2013. Plasma Application for Detoxification of Jatropha Phorbol ester. *Journal of Physics: Conference Series 11th APCPST and 25th SPSM,* 441.

Küçük, A. 2009. *Development of Porous Ceramics for Air Diffuser Applications.* Master of Science, İzmir Institute of Technology.

Kumar, A. & Sharma, S. 2008. An evaluation of multipurpose oil seed crop for industrial uses (Jatropha curcas L.): A review. *Industrial Crops and Products,* 28**,** 1-10.

Kumar, V., Makkar, H. P. S. & Becker, K. 2011. Detoxified Jatropha curcas kernel meal as a dietary protein source: growth performance, nutrient utilization and digestive enzymes in common carp (Cyprinus carpio L.) fingerlings. *Aquaculture Nutrition,* 17**,** 313-326.

Kuntia, S., Majumder, S. K. & Ghosh, P. 2013. Removal of Ammonia from Water by Ozone Microbubbles. *Industrial and Engineering Chemistry Research,* 52**,** 318-326.

Kuvshinov, D., Siswanto, A., Lozano-Parada, J. & Zimmerman, W. B. 2014a. Efficient Compact Micro DBD Plasma Reactor for Ozone Generation for Industrial Application in Liquid and Gas Phase Systems. *International Journal of Chemical, Materials Science and Engineering,* 8**,** 82-85.

Kuvshinov, D., Siswanto, A. & Zimmerman, W. B. 2014b. Microbubbles Enhanced Synthetic Phorbol Ester Degradation by Ozonolysis. *International Journal of Chemical, Materials Science and Engineering,* 8**,** 78-81.

Lago, R. C. A. 2009. Castor and jatropha oils: Production strategies - A review. *OCL - Oleagineux Corps Gras Lipides,* 16**,** 241-247.

Langmuir, I. Year. Oscillations in Ionized Gases. *In:* National Academy of Science of the United States of America, 1928. 627-637.

Laskowski, J. & Kitchener, J. A. 1969. The hydrophilic—hydrophobic transition on silica. *Journal of Colloid and Interface Science,* 29**,** 670-679.

Lestari, D., Mulder, W. & Sanders, J. 2010. Improving Jatropha curcas seed protein recovery by using counter current multistage extraction. *Biochemical Engineering Journal,* 50.

Li, P. 2006a. *Development of Advanced Water Treatment Technology Using Microbubbles* Keio University, Japan.

Li, P., and Tsuge, H 2006b. Ozone transfer in a new gas-induced contractor with microbubbles. *Journal of Chemical Engineering of Japan,* 39**,** 1213-1220.

Li, P., Takahashi, M. & Chiba, K. 2009. Enhanced free-radical generation by shrinking microbubbles using a copper catalyst. *Chemosphere,* 77**,** 1157-1160.

Liu, H., Wang, C., Komatsu, S., He, M., Liu, G. & Shen, S. 2013. Proteomic analysis of the seed development in Jatropha curcas: From carbon flux to the lipid accumulation. *Journal of Proteomics,* 91.

Lozano-Parada, J. H. & Zimmerman, W. B. 2010. The role of kinetics in the design of plasma microreactors. *Chemical Engineering Science,* 65**,** 4925-4930.

Lozano-Parada, J. H., Zimmerman, W.B 2010. The role of kinetics in the design of plasma microreactors. *Chemical Engineering Science,* 65**,** 4925-4930.

Makkar, H., Maes, J., De Greyt, W. & Becker, K. 2009. Removal and Degradation of Phorbol Esters during Pre-treatment and Transesterification of Jatropha curcas Oil. *Journal of the American Oil Chemists' Society,* 86**,** 173-181.

Makkar, H. P. S., Aderibigbe, A. O. & Becker, K. 1998. Comparative evaluation of non-toxic and toxic varieties of Jatropha curcas for chemical composition, digestibility, protein degradability and toxic factors. *Food Chemistry,* 62**,** 207-215.

Makkar, H. P. S. & Becker, K. 1999. Plant toxins and detoxification methods to improve feed quality of tropical seeds - Review. *Asian-Australasian Journal of Animal Sciences,* 12**,** 467-480.

Makkar, H. P. S. & Becker, K. 2009. Jatropha curcas, a promising crop for the generation of biodiesel and value-added coproducts. *European Journal of Lipid Science and Technology,* 111**,** 773-787.

Makkar, H. P. S., Becker, K., Sporer, F. & Wink, M. 1997. Studies on Nutritive Potential and Toxic Constituents of Different Provenances of Jatropha curcas. *Journal of Agricultural and Food Chemistry,* 45**,** 3152-3157.

Makkar, H. P. S., Francis, G. & Becker, K. 2008. Protein concentrate from Jatropha curcas screw-pressed seed cake and toxic and antinutritional factors in protein concentrate. *Journal of the Science of Food and Agriculture,* 88**,** 1542-1548.

Mamleeva, N. A., Autlov, S. A., Bazarnova, N. G. & Lunin, V. V. 2009. Delignification of softwood by ozonation. *Pure Appl. Chem,* 81**,** 2081-2091.

Marrufo-Estrada, D. M., Segura-Campos, M. R., Chel-Guerrero, L. A. & Betancur-Ancona, D. A. 2013. Defatted Jatropha curcas flour and protein isolate as materials for protein hydrolysates with biological activity. *Food Chemistry,* 138**,** 77–83.

Martínez-Herrera, J., Siddhuraju, P., Francis, G., Dávila-Ortíz, G. & Becker, K. 2006. Chemical composition, toxic/antimetabolic constituents, and effects of different treatments on their levels, in four provenances of Jatropha curcas L. from Mexico. *Food Chemistry,* 96**,** 80-89.

Michniewicz, M., Stufka-Olczyk, J. & Milczarek, A. 2012. Ozone Degradation of Lignin; its Impact Upon the Subsequent Biodegradation. *FIBRES & TEXTILES in Eastern Europe,* 20**,** 191-196.

Mittelbach, M. & Poklukar, N. 1990. Ozonolysis of Olefins. 4. Ozonolysis of Polyunsaturated Fatty Esters in HCl Methanol. *Chemistry and Physics of Lipids,* 55**,** 67-72.

Mudd, J. B., Leavitt, R., Ongun, A. & Mcmanus, T. T. 1969. Reaction of ozone with amino acids and proteins. *Atmospheric Environment (1967),* 3**,** 669-681.

Mukherjee, P., Varshney, A., Johnson, T. & Jha, T. 2011. Jatropha curcas: a review on biotechnological status and challenges. *Plant Biotechnology Reports,* 5**,** 197-215.

Muroyama, K., Imai, K., Oka, Y. & Hayashi, J. 2013. Mass transfer properties in a bubble column associated with micro-bubble dispersions. *Chemical Engineering Science,* 100**,** 464-473.

Mussatto, S. I. & Teixeira, J. A. 2010. Lignocellulose as raw material in fermentation processes. *in A. Mendez-Vilas (Ed.), Current Research, Technology and Education, Topics in Applied Microbiology and Microbial Biotechnology*. Badajoz: Formatex Research Center.

Nehra, V., Kumar, A. & Dwivedi, H. K. 2008. Atmospheric non-thermal plasma source. *International Journal of Engineering,* 2.

Neumeister, J., Keul, H., Saxena, M. P. & Griesbaum, K. 1978. OZONE CLEAVAGE OF OLEFINS WITH FORMATION OF ESTER FRAGMENTS. *Angewandte Chemie-International Edition in English,* 17**,** 939-940.

Nokkaew, R. 2008. *Elimination of Phorbol esters in seed oil and press cake of Jatropha curcas L.* Master of Science, Kasetsart University.

Nouwezem, R., Borredon, M. E., Parisi, J. P. & Gaset, A. 1993. Improvement of thermosetting properties of lignocellulosic waste by treatment with ozone. *Bioresource Technology,* 45**,** 43-46.

Opalinska, T. 2002. Cold Plasma Reactor with Dielectric Barrier Discharge. *International Symposium on High Pressure, Low Temperature Plasma Chemistry. Proceedings,* 1**,** 254.

Pabst, W., Mikač, J., Gregorova, E. & Havrda, J. 2002. An Estimate of Orientation Effects on The Results of SIize Distribution Measurements for Oblate Particles. *Ceramics − Silikaty* 46**,** 41-48.

Palmqvist, E. & Hahn-Hägerdal, B. 2000. Fermentation of lignocellulosic hydrolysates. II: inhibitors and mechanisms of inhibition: Review Paper. *Bioresource Technology,* 74**,** 25-33.

Parmar, R. & Majumder, S. K. 2013. Microbubble generation and microbubble-aided transport process intensification—A state-of-the-art report. *Chemical Engineering and Processing: Process Intensification,* 64**,** 79-97.

Pekárek, S. 2003. Non-Thermal Plasma Ozone Generation. *Acta Polytechnica,* 43**,** 47-51.

Phasukarratchai, N., Tontayakom, V. & Tongcumpou, C. 2012. Reduction of phorbol esters in Jatropha curcas L. pressed meal by surfactant solutions extraction. *Biomass and bioenergy,* 45**,** 48-56.

Phengnuam, T. & Suntornsuk, W. 2013. Detoxification and anti-nutrients reduction of Jatropha curcas seed cake by Bacillus fermentation. *Journal of Bioscience and Bioengineering,* 115**,** 168-172.

Pryor, W. A., Das, B. & Church, D. F. 1991. The Ozonation of Unsaturated Fatty Acids: Aldehydes and Hydrogen Peroxide as Products and Possible Mediators of Ozone Toxicity. *Chem. Res. Toxicol.,* 4**,** 341-348.

Pryor, W. A. & Uppu, R. M. 1993. A Kinetic Model for the Competitive Reactions of Ozone with Amino Acid Residues in Proteins in Reverse Micelles. *The Journal of Bological Chemistry,* 268**,** 3120-3126.

Rehman, F., Medley, G. J. D., Bandulasena, H. & Zimmerman, W. B. J. 2015. Fluidic oscillator-mediated microbubble generation to provide cost effective mass transfer and mixing efficiency to the wastewater treatment plants. *Environmental Research,* 137**,** 32-39.

Reif, M. & Dittmeyer, R. 2003. Porous, catalytically active ceramic membranes for gas–liquid reactions: a comparison between catalytic diffuser and forced through flow concept. *Catalysis Today,* 82**,** 3-14.

Rodríguez, R. P., Perez, L. G., Alfonso, M., Duarte, M., Caro, R., Galle, J., Sierens, R. & Verhelst, S. 2011. Characterization of Jatropha curcas oils and their derived fatty acid ethyl esters obtained from two different plantations in Cuba. *Biomass and bioenergy,* 35**,** 4092-4098.

Rosso, D., Libra, J. A., Wiehe, W. & Stenstrom, M. K. 2008. Membrane properties change in fine-pore aeration diffusers: Full-scale variations of transfer efficiency and headloss. *Water Research,* 42**,** 2640– 2648.

Saetae, D. & Suntornsuk, W. 2010. Antifungal Activities of Ethanolic Extract from Jatropha curcas Seed Cake. *J. Microbiol. Biotechnol,* 20**,** 319–324.

Saetae, D. & Suntornsuk, W. 2011. Toxic compound, anti-nutritional factors and functional properties of protein isolated from detoxified Jatropha curcas seed cake. *International Journal of Molecular Sciences,* 12**,** 66-77.

Schiaffo, C. E. & Dussault, P. H. 2008. Ozonolysis in Solvent/Water Mixtures: Direct Conversion of Alkenes to Aldehydes and Ketones. *The Journal of Organic Chemistry,* 73**,** 4688-4690.

Schmidt, R. & Hecker, E. 1975. Autoxidation of Phorbol esters under normal storage condition. *Cancer Res.,* 35**,** 1375-1377.

Selje-Assmann, N., Makkar, H. P. S., Hoffmann, E. M., Francis, G. & Becker, K. 2007. Quantitative and qualitative analyses of seed storage proteins from toxic and non-toxic varieties of Jatropha curcas L. *In:* ORTIGUESMARTY, I. (ed.) *Energy and Protein Metabolism and Nutrition.*

Sheikhi, A., Sotudeh-Gharebagh, R., Zarghami, R., Mostoufi, N. & Alfi, M. 2013. Understanding bubble hydrodynamics in bubble columns. *Experimental Thermal and Fluid Science,* 45**,** 63-74.

Shi, F., Xiang, H. & Li, Y. 2015. Combined pretreatment using ozonolysis and ball milling to improve enzymatic saccharification of corn straw. *Bioresource Technology,* 179**,** 444–451.

Singh, K., Pal and Roy, Subrata 2007. Impedance matching for an asymmetric dielectric barrier discharge plasma actuator. *Applied Physics Letters,* 91.

Siswanto, A., Kuvshinov, D. & Zimmerman, W. Year. Investigation of Bubble Size Distributions in Oscillatory Flow at Various Flow Rates. *In:* PROCEEDING, U. C., ed. The University of Sheffield Engineering Symposium, 2014 The Octagon Centre, University of Sheffield, United Kingdom.: White Rose.

Sujatha, M., Reddy, T. P. & Mahasi, M. J. 2008. Role of biotechnological interventions in the improvement of castor (Ricinus communis L.) and Jatropha curcas L. *Biotechnology Advances,* 26**,** 424-435.

Sweeney, M. 1981. Comparative studies in the ozonolysis of lignin and coal. *Thermochimica Acta,* 48**,** 263-275.

Takahashi, M., Chiba, K. & Li, P. 2007. Free-Radical Generation from Collapsing Microbubbles in the Absence of a Dynamic Stimulus. *The Journal of Physical Chemistry B,* 111**,** 1343-1347.

Tesar, V. 2014. Shape oscillation of microbubbles. *Chemical Engineering Journal,* 235**,** 368-378.

Tesař, V. Year. Microbubble Generation by Fluidics. Part I: Development of The Oscillator. *In:* Colloquium FLUID DYNAMICS, October 24 - 26, 2012 2012 Institute of Thermomechanics AS CR, Prague.

Tkachuk, R. 1969. Nitrogen-to-Protein Conversion Factors for Cereals and Oilseed Meals. *51st Annual Meeting.* New York: Grain Research Laboratory, Manitoba.

Travaini, R., Otero, M. D. M., Coca, M., Da-Silva, R. & Bolado, S. 2013. Sugarcane bagasse ozonolysis pretreatment: Effect on enzymatic digestibility and inhibitory compound formation. *Bioresource Technology,* 133**,** 332-339.

Uppu, R. M. & Pryor, W. A. 1994. The Reactions of Ozone with Proteins and Unsaturated Fatty Acids in Reverse Micelles. *Chem. Res. Toxicol.,* 7**,** 47-55.

Uzun, H., Ibanoglu, E., Catal, H. & Ibanoglu, S. 2012. Effects of ozone on functional properties of proteins. *Food Chemistry,* 134**,** 647-654.

Vagle, S. A. F., David M 1998. A Comparison of Four Methods for Bubble Size and Void Fraction Measurements. *IEEE JOURNAL OF OCEANIC ENGINEERING,* 23**,** 211 - 222.

Vaknin, Y., Ghanim, M., Samra, S., Dvash, L., Hendelsman, E., Eisikowitch, D. & Samocha, Y. 2011. Predicting Jatropha curcas seed-oil content, oil composition and protein content using near-infrared spectroscopy—A quick and non-destructive method. *Industrial Crops and Products,* 34**,** 1029-1034.

Vidal, P. F. & Molinier, J. 1988. Ozonolysis of Lignin-Improvement of in vitro Digestibility of Poplar Sawdust *Biomass,* 16**,** 1-17.

Wagner, H.-E., Brandenburg, R., Kozlov, K. V., Sonnenfeld, A., Michel, P., and Behnke, J.F 2003. The Barrier Discharge: Basic Properties and Applications to Surface Treatment. *Vacuum,* 71**,** 417-436.

Wakandigara, A., Nhamo, L.R.M., and Kugara, J 2013. Chemistry of Phorbol ester Toxicity in Jatropha curcas seed-a Review. *International Journal of Biochemistry Research & Review,* 3**,** 146-161.

Waled Abdo Ahmed & Salimon., J. 2009. Phorbol Ester as Toxic Constituents of Tropical Jatropha Curcas Seed Oil. *European Journal of Scientific Research,* 31**,** 429-436.

Warsito, A., Syakur, A., Syafruddin & Susilowati, G. 2011. An Ozone Reactor Design with Various Electrode Configurations. *International Journal of Electrical and Computer Engineering,* 1**,** 93-101.

Weiner, B. B. 2011. What is a Continuous Particle Size Distribution? *In:* PAPER, B. I. C. W. (ed.). New York: Brookhaven Instruments.

Wilkes, J. O. 1999. *Fluid Mechanics for Chemical Engineer,* New Jersey, Prentice Hall, Inc.

Wink, M., Koschmieder, C., Sauerwein, M. & Sporer, F. 1997. Phorbol Esters of J. curcas - Biological Activities and Potential Applications. *In:* GUBITZ, MITTLEBACH & TRABI, M. (eds.) *Biofuels and Industrial Products from J.Curcas.*

Wu, J., Ein-Mozaffari, F. & Upreti, S. 2013a. Effect of ozone pretreatment on hydrogen production from barley straw. *Bioresource Technology,* 144**,** 344-349.

Wu, J., Upreti, S. & Ein-Mozaffari, F. 2013b. Ozone pretreatment of wheat straw for enhanced biohydrogen production. *International Journal of Hydrogen Energy,* 38**,** 10270-10276.

Wu, Z., Zhang, Pengyan., Tao, Lin., Zhao, Duo., Wu, Ailing. And Gao, Xingang 2012. An Atmospheric Press Dielectric Barrier Discharge and its Application for Detection of Environmentl Pollutants. *Asia Pacific Conference on Environmental Science and Technology. Adavance in Biomedical Engineering.*

Xiao, J., Zhang, H., Niu, L., Wang, X. & Lu, X. 2011. Evaluation of Detoxification Methods on Toxic and Antinutritional Composition and Nutritional Quality of Proteins in Jatropha curcas Meal. *Journal of Agricultural and Food Chemistry,* 59**,** 4040-4044.

Zhang, J. I., Tao, W. A. & Cooks, R. G. 2011. Facile Determination of Double Bond Position in Unsaturated Fatty Acids and Esters by Low Temperature Plasma Ionization Mass Spectrometry. *Analytical Chemistry,* 83**,** 4738-4744.

Zimmerman, W., Lozano-Parada, J. & Bandulasena, H. H. 2010. Ozone regenerated: low power consumption and high dispersal rates with microbubbles. *J Sewerage Water*.

Zimmerman, W. B., Hewakandamby, B. N., Tesař, V., Bandulasena, H. C. H. & Omotowa, O. A. 2009. On the design and simulation of an airlift loop bioreactor with microbubble generation by fluidic oscillation. *Food and Bioproducts Processing,* 87**,** 215-227.

Zimmerman, W. B. & Tesar, V. 2008. *Bubble Generation for Aeration and Other Purposes*. WO 2008/053174 A1.

Zimmerman, W. B., Tesar, V., Butler, S., Bandulusen, H.C.H 2008. Microbubble generation. *Recents Patents on Engineering,* 2**,** 1-8.

Zucker, M. B., Troll, W., and Belma, S. 1974. The tumor promoter phorbol ester (12-0-tetradecanoyl-phorbol-13-acetate), a potent aggregating agents for blood platelets. *The Journal of Cell Biology,* 60**,** 325-336.

Cheng, H.-H., Chen, S.-S., Wu, Y.-C. & Ho, D.-L. 2007. Non-thermal Plasma Technology for Degradation of Organic Compounds in Wastewater Control: A Critical Review. *J. Environ. Eng. Manage,* 17**,** 427-433.

APPENDIX

Qualitative analysis of protein profile in Indonesian jatropha samples

Gel band 6.1

Determination of protein characteristic (by MASCOT program)

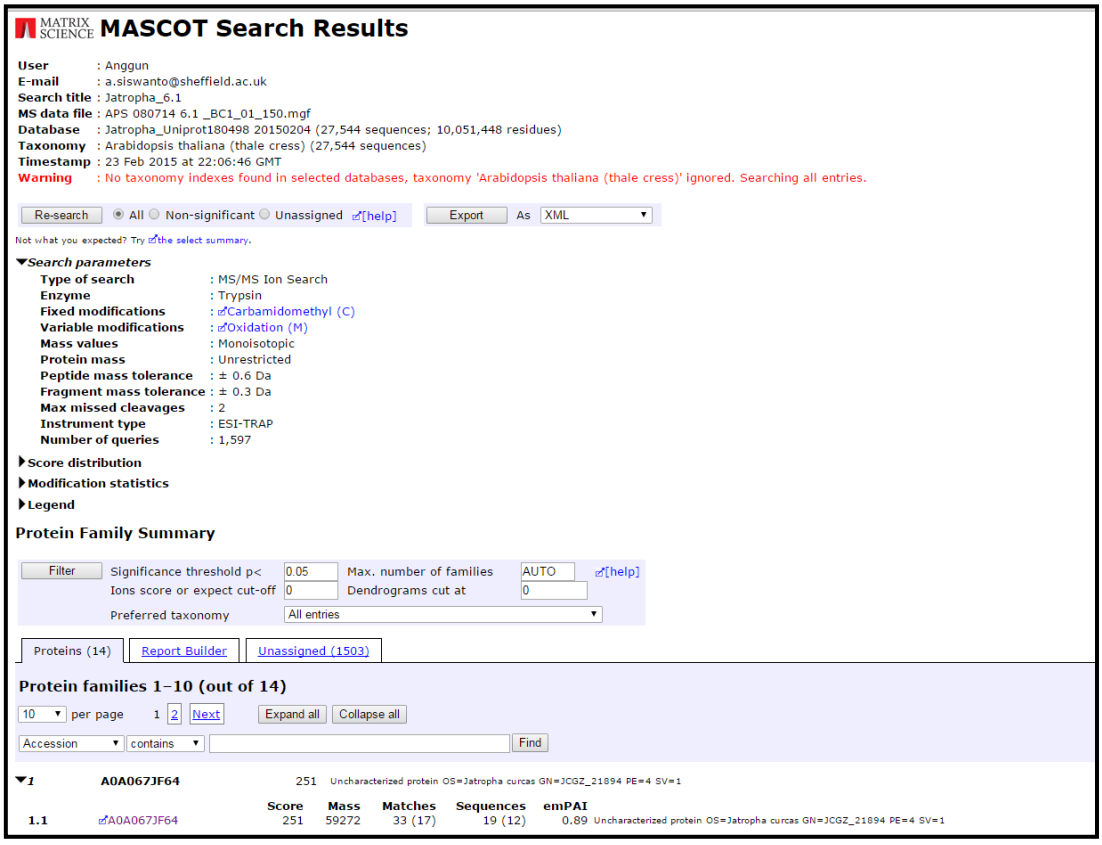

MATRIX SCIENCE **MASCOT Search Results**

User : Anggun
E-mail : a.siswanto@sheffield.ac.uk
Search title : Jatropha_6.1
MS data file : APS 080714 6.1 _BC1_01_150.mgf
Database : Jatropha_Uniprot180498 20150204 (27,544 sequences; 10,051,448 residues)
Taxonomy : Arabidopsis thaliana (thale cress) (27,544 sequences)
Timestamp : 23 Feb 2015 at 22:06:46 GMT
Warning : No taxonomy indexes found in selected databases, taxonomy 'Arabidopsis thaliana (thale cress)' ignored. Searching all entries.

Re-search | All | Non-significant | Unassigned [help] | Export As XML

Not what you expected? Try the select summary.

Search parameters

Type of search	: MS/MS Ion Search
Enzyme	: Trypsin
Fixed modifications	: Carbamidomethyl (C)
Variable modifications	: Oxidation (M)
Mass values	: Monoisotopic
Protein mass	: Unrestricted
Peptide mass tolerance	: ± 0.6 Da
Fragment mass tolerance	: ± 0.3 Da
Max missed cleavages	: 2
Instrument type	: ESI-TRAP
Number of queries	: 1,597

Score distribution
Modification statistics
Legend

Protein Family Summary

Filter | Significance threshold p< 0.05 | Max. number of families AUTO [help]
Ions score or expect cut-off 0 | Dendrograms cut at 0
Preferred taxonomy All entries

Proteins (14) | Report Builder | Unassigned (1503)

Protein families 1–10 (out of 14)

10 per page | 1 2 Next | Expand all | Collapse all

Accession contains | Find

1 **A0A067JF64** 251 Uncharacterized protein OS=Jatropha curcas GN=JCGZ_21894 PE=4 SV=1

		Score	Mass	Matches	Sequences	emPAI	
1.1	A0A067JF64	251	59272	33 (17)	19 (12)	0.89	Uncharacterized protein OS=Jatropha curcas GN=JCGZ_21894 PE=4 SV=1

Identification of predicted protein (by BLAST search engine)

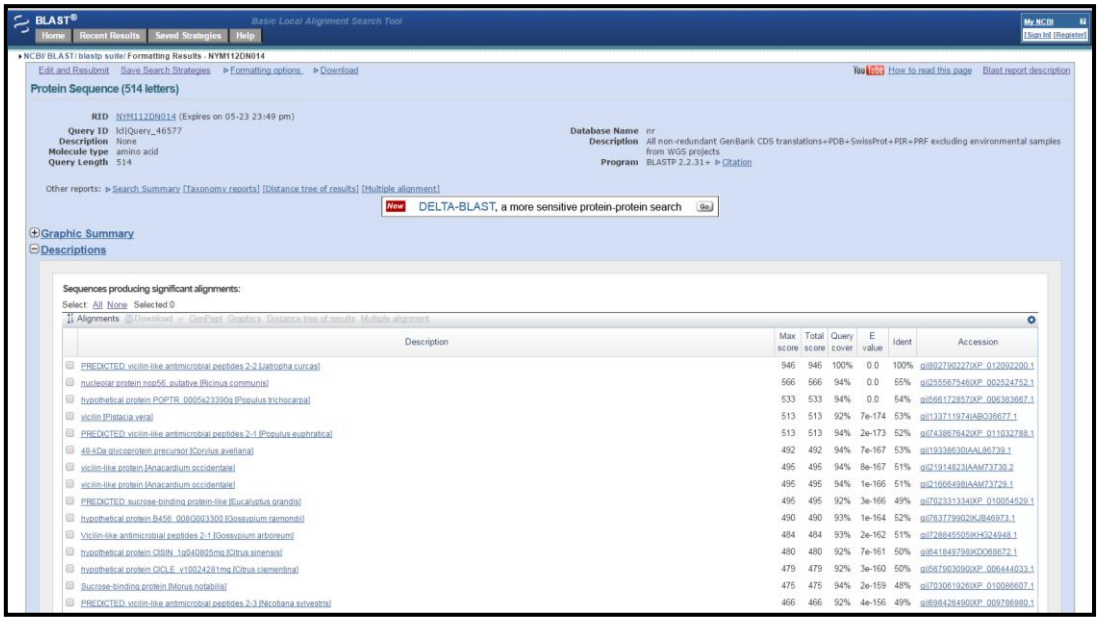

BLAST® Basic Local Alignment Search Tool

Home | Recent Results | Saved Strategies | Help

NCBI/BLAST/blastp suite/Formatting Results - NYM112DN014

Edit and Resubmit | Save Search Strategies | Formatting options | Download | How to read this page | Blast report description

Protein Sequence (514 letters)

RID NYM112DN014 (Expires on 05-23 23:49 pm)
Query ID lcl|Query_46577
Description None
Molecule type amino acid
Query Length 514

Database Name nr
Description All non-redundant GenBank CDS translations+PDB+SwissProt+PIR+PRF excluding environmental samples from WGS projects
Program BLASTP 2.2.31+ Citation

Other reports: Search Summary [Taxonomy reports] [Distance tree of results] [Multiple alignment]

New DELTA-BLAST, a more sensitive protein-protein search

Graphic Summary
Descriptions

Sequences producing significant alignments:

Select: All None Selected:0

Alignments | Download | GenPept | Graphics | Distance tree of results | Multiple alignment

Description	Max score	Total score	Query cover	E value	Ident	Accession
PREDICTED: vicilin-like antimicrobial peptides 2-2 [Jatropha curcas]	946	946	100%	0.0	100%	gi|802790227|XP_012092200.1
nucleolar protein nop56, putative [Ricinus communis]	566	566	94%	0.0	55%	gi|255567546|XP_002524752.1
hypothetical protein POPTR_0005s23390g [Populus trichocarpa]	533	533	94%	0.0	54%	gi|566172857|XP_006383667.1
vicilin [Pistacia vera]	513	513	92%	7e-174	53%	gi|133711974|ABO36677.1
PREDICTED: vicilin-like antimicrobial peptides 2-1 [Populus euphratica]	513	513	94%	2e-173	52%	gi|743867642|XP_011032788.1
48-kDa glycoprotein precursor [Corylus avellana]	492	492	94%	7e-167	53%	gi|19338630|AAL86739.1
vicilin-like protein [Anacardium occidentale]	495	495	94%	8e-167	51%	gi|21914823|AAM73730.2
vicilin-like protein [Anacardium occidentale]	495	495	94%	1e-166	51%	gi|21666498|AAM73729.1
PREDICTED: sucrose-binding protein-like [Eucalyptus grandis]	496	496	92%	3e-166	49%	gi|702331334|XP_010054529.1
hypothetical protein B456_008G003300 [Gossypium raimondii]	490	490	93%	1e-164	52%	gi|763779902|KJB46973.1
Vicilin-like antimicrobial peptides 2-1 [Gossypium arboreum]	484	484	93%	2e-162	51%	gi|728845505|KHG24948.1
hypothetical protein CISIN_1g040805mg [Citrus sinensis]	480	480	92%	7e-161	50%	gi|641849798|KDO68672.1
hypothetical protein CICLE_v10024281mg [Citrus clementina]	479	479	92%	3e-160	50%	gi|567903090|XP_006444033.1
Sucrose-binding protein [Morus notabilis]	475	475	94%	2e-159	48%	gi|703061926|XP_010096607.1
PREDICTED: vicilin-like antimicrobial peptides 2-3 [Nicotiana sylvestris]	466	466	92%	4e-156	49%	gi|698426490|XP_009786980.1

Gel band 6.2

Determination of protein characteristic (by MASCOT program)

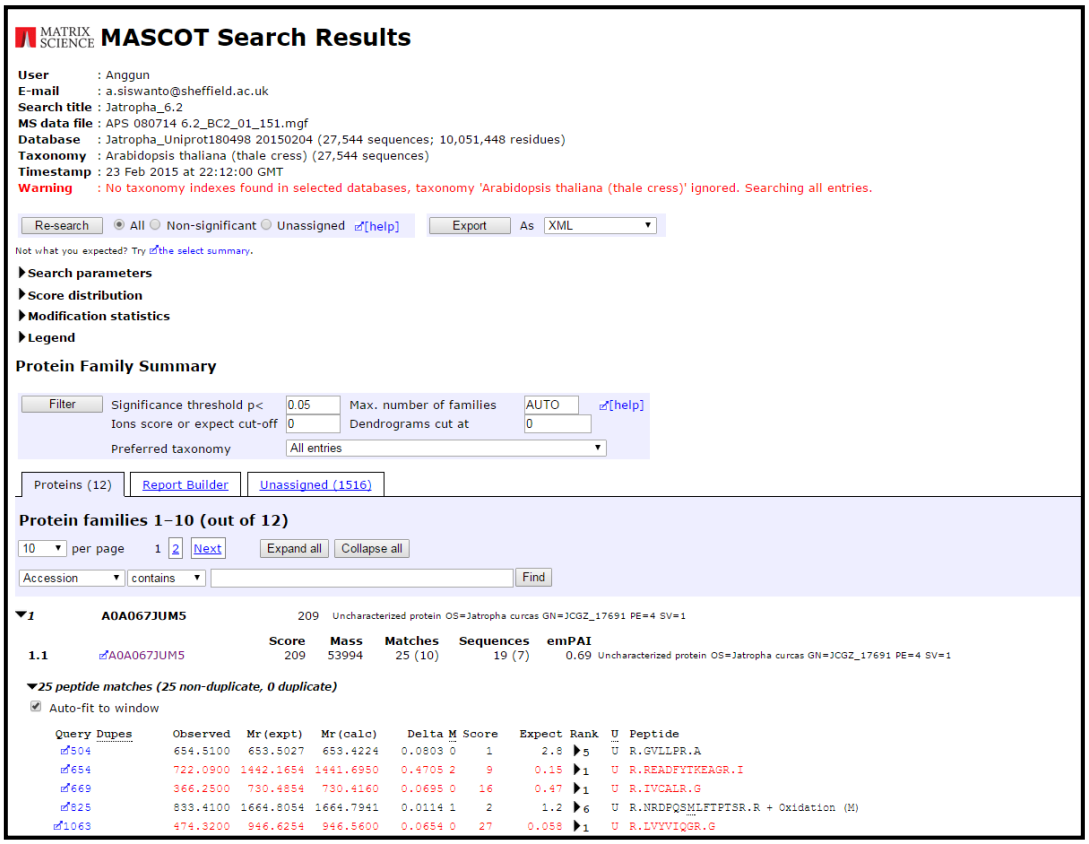

MATRIX SCIENCE **MASCOT Search Results**

User : Anggun
E-mail : a.siswanto@sheffield.ac.uk
Search title : Jatropha_6.2
MS data file : APS 080714 6.2_BC2_01_151.mgf
Database : Jatropha_Uniprot180498 20150204 (27,544 sequences; 10,051,448 residues)
Taxonomy : Arabidopsis thaliana (thale cress) (27,544 sequences)
Timestamp : 23 Feb 2015 at 22:12:00 GMT
Warning : No taxonomy indexes found in selected databases, taxonomy 'Arabidopsis thaliana (thale cress)' ignored. Searching all entries.

Re-search | All | Non-significant | Unassigned [help] | Export As XML

Not what you expected? Try the select summary.

▸ Search parameters
▸ Score distribution
▸ Modification statistics
▸ Legend

Protein Family Summary

Filter | Significance threshold p< 0.05 | Max. number of families AUTO [help]
Ions score or expect cut-off 0 | Dendrograms cut at 0
Preferred taxonomy All entries

Proteins (12) | Report Builder | Unassigned (1516)

Protein families 1–10 (out of 12)

10 per page 1 2 Next | Expand all | Collapse all

Accession contains | Find

1	A0A067JUM5	209	Uncharacterized protein OS=Jatropha curcas GN=JCGZ_17691 PE=4 SV=1			
		Score	**Mass**	**Matches**	**Sequences**	**emPAI**
1.1	A0A067JUM5	209	53994	25 (10)	19 (7)	0.69 Uncharacterized protein OS=Jatropha curcas GN=JCGZ_17691 PE=4 SV=1

25 peptide matches (25 non-duplicate, 0 duplicate)

Auto-fit to window

Query	Dupes	Observed	Mr(expt)	Mr(calc)	Delta	M	Score	Expect	Rank	U	Peptide
504		654.5100	653.5027	653.4224	0.0803	0	1	2.8	5	U	R.GVLLFR.A
654		722.0900	1442.1654	1441.6950	0.4705	2	9	0.15	1	U	R.READFYTKEAGR.I
669		366.2500	730.4854	730.4160	0.0695	0	16	0.47	1	U	R.IVCALR.G
825		833.4100	1664.8054	1664.7941	0.0114	1	2	1.2	6	U	R.NRDFQSMLFTPTSR.R + Oxidation (M)
1063		474.3200	946.6254	946.5600	0.0654	0	27	0.058	1	U	R.LVYVIQGR.G

Identification of predicted protein (by BLAST search engine)

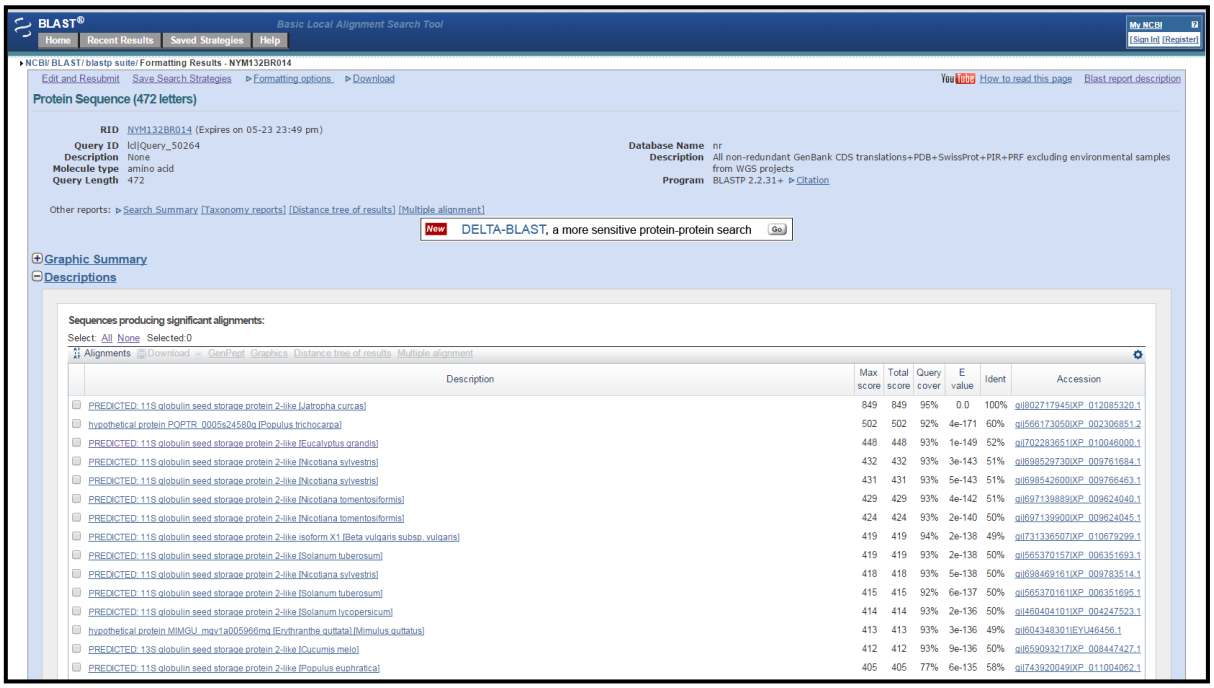

BLAST® Basic Local Alignment Search Tool

Home | Recent Results | Saved Strategies | Help

NCBI/BLAST/blastp suite/Formatting Results - NYM132BR014

Edit and Resubmit | Save Search Strategies | Formatting options | Download | How to read this page | Blast report description

Protein Sequence (472 letters)

RID NYM132BR014 (Expires on 05-23 23:49 pm)
Query ID lcl|Query_50264
Description None
Molecule type amino acid
Query Length 472

Database Name nr
Description All non-redundant GenBank CDS translations+PDB+SwissProt+PIR+PRF excluding environmental samples from WGS projects
Program BLASTP 2.2.31+ Citation

Other reports: Search Summary [Taxonomy reports] [Distance tree of results] [Multiple alignment]

New DELTA-BLAST, a more sensitive protein-protein search Go

Graphic Summary
Descriptions

Sequences producing significant alignments:

Select: All None Selected:0

Alignments | Download | GenPept | Graphics | Distance tree of results | Multiple alignment

Description	Max score	Total score	Query cover	E value	Ident	Accession
PREDICTED: 11S globulin seed storage protein 2-like [Jatropha curcas]	849	849	95%	0.0	100%	gi|802717945|XP_012085320.1
hypothetical protein POPTR_0005s24580g [Populus trichocarpa]	502	502	92%	4e-171	60%	gi|566173050|XP_002306851.2
PREDICTED: 11S globulin seed storage protein 2-like [Eucalyptus grandis]	448	448	93%	1e-149	52%	gi|702283651|XP_010046000.1
PREDICTED: 11S globulin seed storage protein 2-like [Nicotiana sylvestris]	432	432	93%	3e-143	51%	gi|698529730|XP_009761684.1
PREDICTED: 11S globulin seed storage protein 2-like [Nicotiana sylvestris]	431	431	93%	5e-143	51%	gi|698542600|XP_009766463.1
PREDICTED: 11S globulin seed storage protein 2-like [Nicotiana tomentosiformis]	429	429	93%	4e-142	51%	gi|697139889|XP_009624040.1
PREDICTED: 11S globulin seed storage protein 2-like [Nicotiana tomentosiformis]	424	424	93%	2e-140	50%	gi|697139900|XP_009624045.1
PREDICTED: 11S globulin seed storage protein 2-like isoform X1 [Beta vulgaris subsp. vulgaris]	419	419	94%	2e-138	49%	gi|731336507|XP_010679299.1
PREDICTED: 11S globulin seed storage protein 2-like [Solanum tuberosum]	419	419	93%	2e-138	50%	gi|565370157|XP_006351693.1
PREDICTED: 11S globulin seed storage protein 2-like [Nicotiana sylvestris]	418	418	93%	5e-138	50%	gi|698469161|XP_009783514.1
PREDICTED: 11S globulin seed storage protein 2-like [Solanum tuberosum]	415	415	92%	6e-137	50%	gi|565370161|XP_006351695.1
PREDICTED: 11S globulin seed storage protein 2-like [Solanum lycopersicum]	414	414	93%	2e-136	50%	gi|460404101|XP_004247523.1
hypothetical protein MIMGU_mgv1a005966mg [Erythranthe guttata] [Mimulus guttatus]	413	413	93%	3e-136	49%	gi|604348301|EYU46456.1
PREDICTED: 13S globulin seed storage protein 2-like [Cucumis melo]	412	412	93%	9e-136	50%	gi|659093217|XP_008447427.1
PREDICTED: 11S globulin seed storage protein 2-like [Populus euphratica]	405	405	77%	6e-135	58%	gi|743920049|XP_011004062.1

Gel band 6.3

Determination of protein characteristic (by MASCOT program)

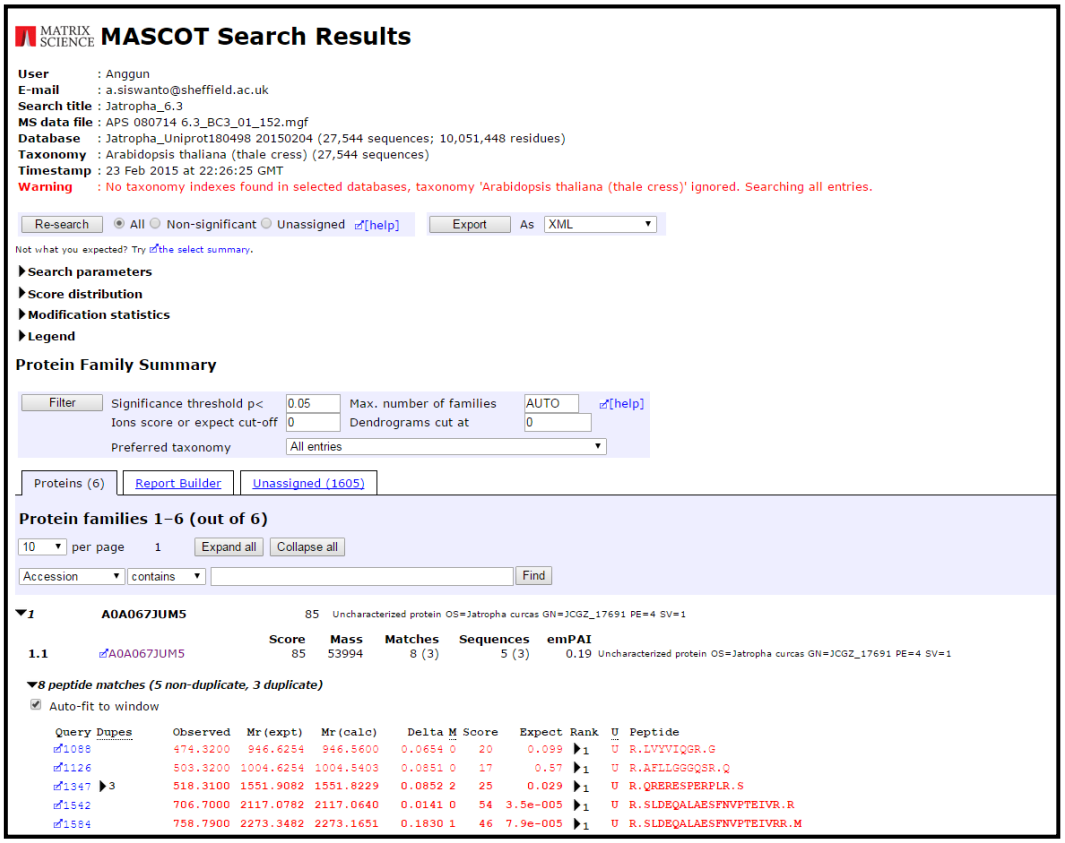

MATRIX SCIENCE **MASCOT Search Results**

User : Anggun
E-mail : a.siswanto@sheffield.ac.uk
Search title : Jatropha_6.3
MS data file : APS 080714 6.3_BC3_01_152.mgf
Database : Jatropha_Uniprot180498 20150204 (27,544 sequences; 10,051,448 residues)
Taxonomy : Arabidopsis thaliana (thale cress) (27,544 sequences)
Timestamp : 23 Feb 2015 at 22:26:25 GMT
Warning : No taxonomy indexes found in selected databases, taxonomy 'Arabidopsis thaliana (thale cress)' ignored. Searching all entries.

Re-search | All | Non-significant | Unassigned [help] | Export As XML

Not what you expected? Try the select summary.

Search parameters
Score distribution
Modification statistics
Legend

Protein Family Summary

Filter | Significance threshold p< 0.05 | Max. number of families AUTO [help]
Ions score or expect cut-off 0 | Dendrograms cut at 0
Preferred taxonomy All entries

Proteins (6) | Report Builder | Unassigned (1605)

Protein families 1–6 (out of 6)

10 per page 1 | Expand all | Collapse all

Accession contains | Find

1	A0A067JUM5	85	Uncharacterized protein OS=Jatropha curcas GN=JCGZ_17691 PE=4 SV=1				
		Score	**Mass**	**Matches**	**Sequences**	**emPAI**	
1.1	A0A067JUM5	85	53994	8 (3)	5 (3)	0.19	Uncharacterized protein OS=Jatropha curcas GN=JCGZ_17691 PE=4 SV=1

8 peptide matches (5 non-duplicate, 3 duplicate)

Auto-fit to window

Query	Dupes	Observed	Mr(expt)	Mr(calc)	Delta	M	Score	Expect	Rank	U	Peptide
1088		474.3200	946.6254	946.5600	0.0654	0	20	0.099	1	U	R.LVYVIQGR.G
1126		503.3200	1004.6254	1004.5403	0.0851	0	17	0.57	1	U	R.AFLLGGGQSR.Q
1347	3	518.3100	1551.9082	1551.8229	0.0852	2	25	0.029	1	U	R.QRERESPERPLR.S
1542		706.7000	2117.0782	2117.0640	0.0141	0	54	3.5e-005	1	U	R.SLDEQALAESFNVPTEIVR.R
1584		758.7900	2273.3482	2273.1651	0.1830	1	46	7.9e-005	1	U	R.SLDEQALAESFNVPTEIVRR.M

Identification of predicted protein (by BLAST search engine)

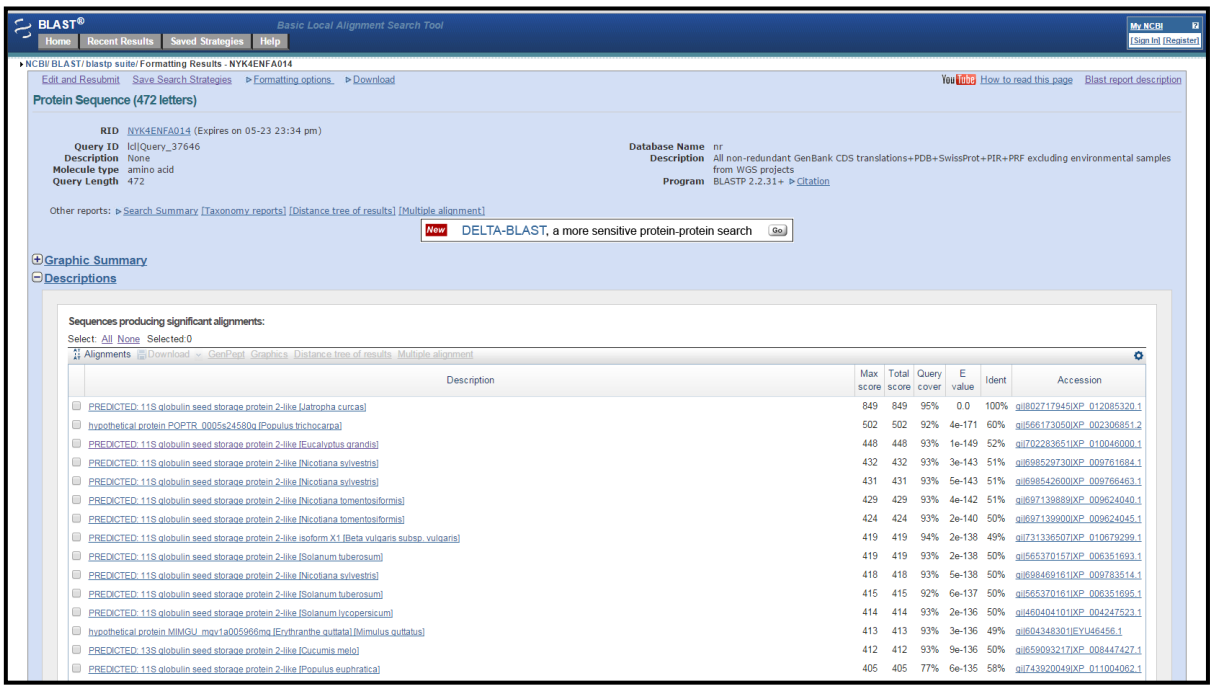

BLAST® Basic Local Alignment Search Tool

Home | Recent Results | Saved Strategies | Help

NCBI/ BLAST/ blastp suite/ Formatting Results - NYK4ENFA014

Edit and Resubmit | Save Search Strategies | Formatting options | Download | How to read this page | Blast report description

Protein Sequence (472 letters)

RID NYK4ENFA014 (Expires on 05-23 23:34 pm)
Query ID lcl|Query_37646
Description None
Molecule type amino acid
Query Length 472

Database Name nr
Description All non-redundant GenBank CDS translations+PDB+SwissProt+PIR+PRF excluding environmental samples from WGS projects
Program BLASTP 2.2.31+ Citation

Other reports: Search Summary [Taxonomy reports] [Distance tree of results] [Multiple alignment]

New DELTA-BLAST, a more sensitive protein-protein search Go

Graphic Summary
Descriptions

Sequences producing significant alignments:

Select: All None Selected:0

Alignments Download GenPept Graphics Distance tree of results Multiple alignment

Description	Max score	Total score	Query cover	E value	Ident	Accession
PREDICTED: 11S globulin seed storage protein 2-like [Jatropha curcas]	849	849	95%	0.0	100%	gi|802717945|XP_012085320.1
hypothetical protein POPTR_0005s24580g [Populus trichocarpa]	502	502	92%	4e-171	60%	gi|566173050|XP_002306851.2
PREDICTED: 11S globulin seed storage protein 2-like [Eucalyptus grandis]	448	448	93%	1e-149	52%	gi|702283651|XP_010046000.1
PREDICTED: 11S globulin seed storage protein 2-like [Nicotiana sylvestris]	432	432	93%	3e-143	51%	gi|698529730|XP_009761684.1
PREDICTED: 11S globulin seed storage protein 2-like [Nicotiana sylvestris]	431	431	93%	5e-143	51%	gi|698542600|XP_009766463.1
PREDICTED: 11S globulin seed storage protein 2-like [Nicotiana tomentosiformis]	429	429	93%	4e-142	51%	gi|697139889|XP_009624040.1
PREDICTED: 11S globulin seed storage protein 2-like [Nicotiana tomentosiformis]	424	424	93%	2e-140	50%	gi|697139900|XP_009624045.1
PREDICTED: 11S globulin seed storage protein 2-like isoform X1 [Beta vulgaris subsp. vulgaris]	419	419	94%	2e-138	49%	gi|731336507|XP_010679299.1
PREDICTED: 11S globulin seed storage protein 2-like [Solanum tuberosum]	419	419	93%	2e-138	50%	gi|565370157|XP_006351693.1
PREDICTED: 11S globulin seed storage protein 2-like [Nicotiana sylvestris]	418	418	93%	5e-138	50%	gi|698469161|XP_009783514.1
PREDICTED: 11S globulin seed storage protein 2-like [Solanum tuberosum]	415	415	92%	6e-137	50%	gi|565370161|XP_006351695.1
PREDICTED: 11S globulin seed storage protein 2-like [Solanum lycopersicum]	414	414	93%	2e-136	50%	gi|460404101|XP_004247523.1
hypothetical protein MIMGU_mgv1a005966mg [Erythranthe guttata] [Mimulus guttatus]	413	413	93%	3e-136	49%	gi|604348301|EYU46456.1
PREDICTED: 13S globulin seed storage protein 2-like [Cucumis melo]	412	412	93%	9e-136	50%	gi|659093217|XP_008447427.1
PREDICTED: 11S globulin seed storage protein 2-like [Populus euphratica]	405	405	77%	6e-135	58%	gi|743920049|XP_011004062.1

Gel band 6.4

Determination of protein characteristic (by MASCOT program)

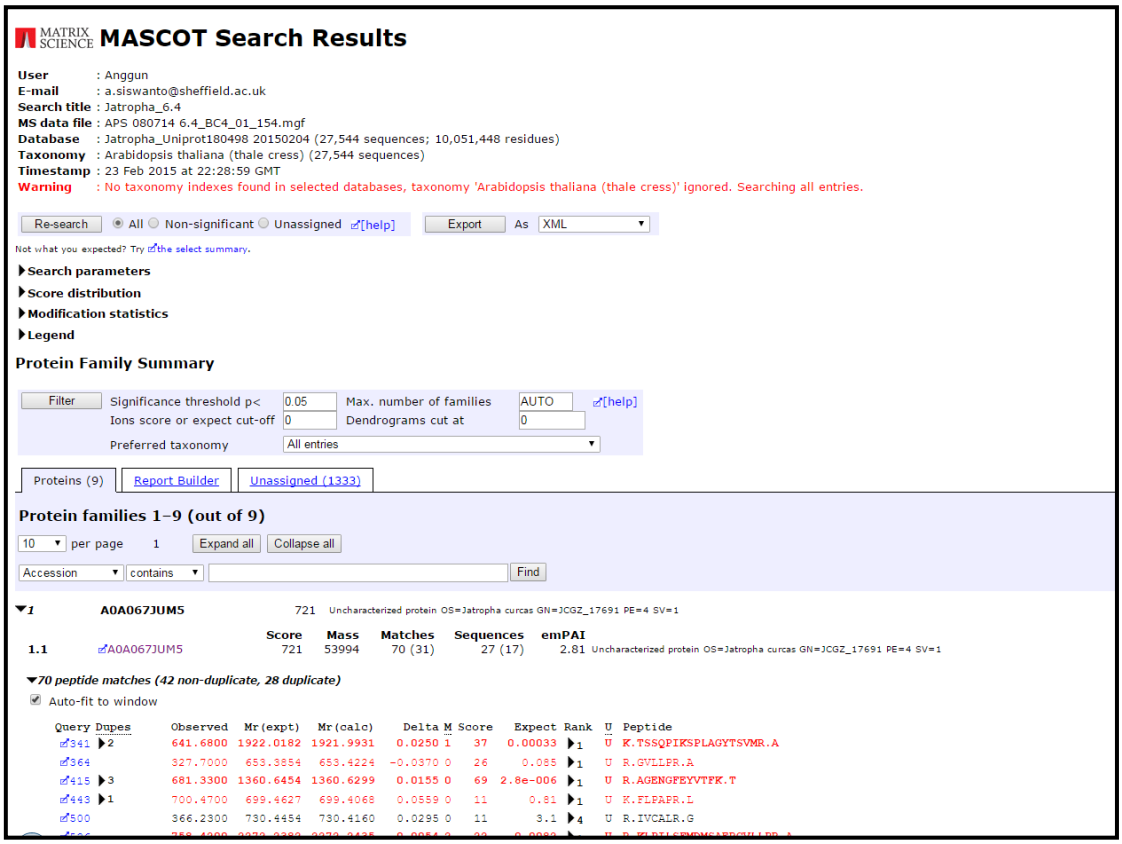

MATRIX SCIENCE **MASCOT Search Results**

User : Anggun
E-mail : a.siswanto@sheffield.ac.uk
Search title : Jatropha_6.4
MS data file : APS 080714 6.4_BC4_01_154.mgf
Database : Jatropha_Uniprot180498 20150204 (27,544 sequences; 10,051,448 residues)
Taxonomy : Arabidopsis thaliana (thale cress) (27,544 sequences)
Timestamp : 23 Feb 2015 at 22:28:59 GMT
Warning : No taxonomy indexes found in selected databases, taxonomy 'Arabidopsis thaliana (thale cress)' ignored. Searching all entries.

Re-search | All | Non-significant | Unassigned [help] | Export As XML

Not what you expected? Try the select summary.

Search parameters
Score distribution
Modification statistics
Legend

Protein Family Summary

Filter | Significance threshold p< 0.05 | Max. number of families AUTO [help]
Ions score or expect cut-off 0 | Dendrograms cut at 0
Preferred taxonomy All entries

Proteins (9) | Report Builder | Unassigned (1333)

Protein families 1–9 (out of 9)

10 per page 1 | Expand all | Collapse all

Accession contains | Find

1	A0A067JUM5	721	Uncharacterized protein OS=Jatropha curcas GN=JCGZ_17691 PE=4 SV=1				
		Score	**Mass**	**Matches**	**Sequences**	**emPAI**	
1.1	A0A067JUM5	721	53994	70 (31)	27 (17)	2.81	Uncharacterized protein OS=Jatropha curcas GN=JCGZ_17691 PE=4 SV=1

70 peptide matches (42 non-duplicate, 28 duplicate)

Auto-fit to window

Query	Dupes	Observed	Mr(expt)	Mr(calc)	Delta	M	Score	Expect	Rank	U	Peptide
341	2	641.6800	1922.0182	1921.9931	0.0250	1	37	0.00033	1	U	K.TSSQPIKSPLAGYTSVMR.A
364		327.7000	653.3854	653.4224	-0.0370	0	26	0.085	1	U	R.GVLLPR.A
415	3	681.3300	1360.6454	1360.6299	0.0155	0	69	2.8e-006	1	U	R.AGENGFEYVTFK.T
443	1	700.4700	699.4627	699.4068	0.0559	0	11	0.81	1	U	K.FLPAPR.L
500		366.2300	730.4454	730.4160	0.0295	0	11	3.1	4	U	R.IVCALR.G

Identification of predicted protein (by BLAST search engine)

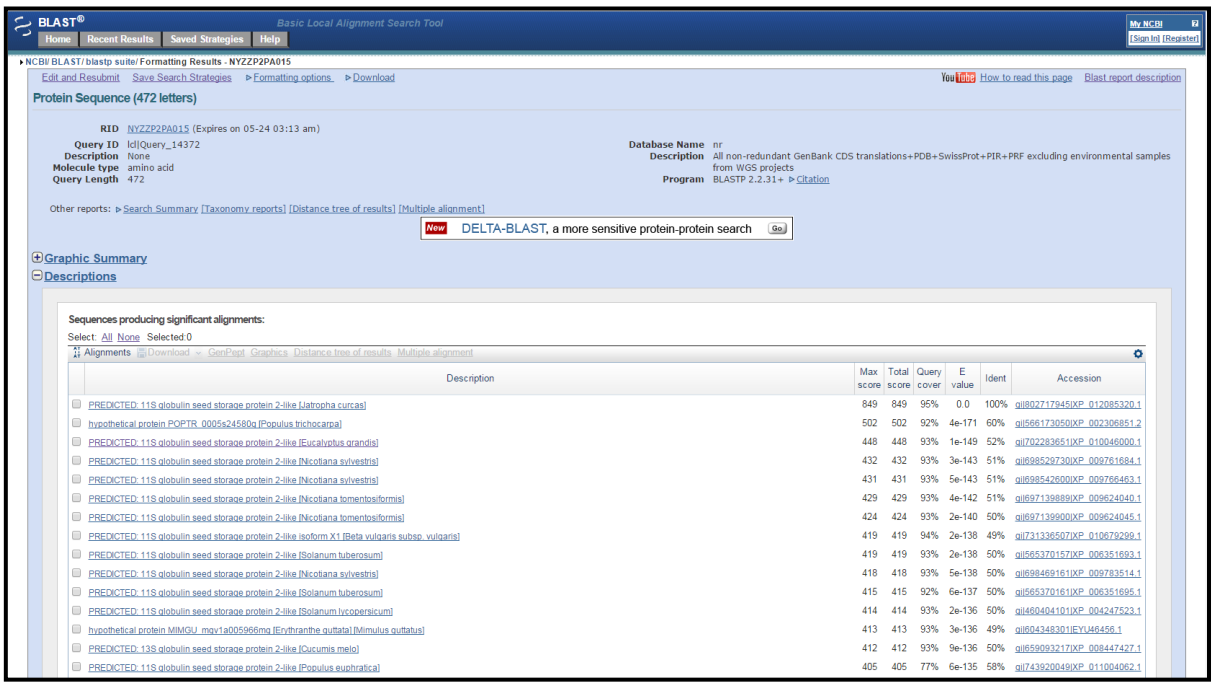

BLAST® Basic Local Alignment Search Tool

Home | Recent Results | Saved Strategies | Help

My NCBI [Sign In] [Register]

NCBI/ BLAST/ blastp suite/ Formatting Results - NYZZP2PA015

Edit and Resubmit | Save Search Strategies | Formatting options | Download | How to read this page | Blast report description

Protein Sequence (472 letters)

RID NYZZP2PA015 (Expires on 05-24 03:13 am)
Query ID lcl|Query_14372
Description None
Molecule type amino acid
Query Length 472

Database Name nr
Description All non-redundant GenBank CDS translations+PDB+SwissProt+PIR+PRF excluding environmental samples from WGS projects
Program BLASTP 2.2.31+ | Citation

Other reports: Search Summary [Taxonomy reports] [Distance tree of results] [Multiple alignment]

New DELTA-BLAST, a more sensitive protein-protein search Go

Graphic Summary
Descriptions

Sequences producing significant alignments:

Select: All None Selected:0

Alignments | Download | GenPept | Graphics | Distance tree of results | Multiple alignment

Description	Max score	Total score	Query cover	E value	Ident	Accession
PREDICTED: 11S globulin seed storage protein 2-like [Jatropha curcas]	849	849	95%	0.0	100%	gi|802717945|XP_012085320.1
hypothetical protein POPTR_0005s24580g [Populus trichocarpa]	502	502	92%	4e-171	60%	gi|566173050|XP_002306851.2
PREDICTED: 11S globulin seed storage protein 2-like [Eucalyptus grandis]	448	448	93%	1e-149	52%	gi|702283651|XP_010046000.1
PREDICTED: 11S globulin seed storage protein 2-like [Nicotiana sylvestris]	432	432	93%	3e-143	51%	gi|698529730|XP_009761684.1
PREDICTED: 11S globulin seed storage protein 2-like [Nicotiana sylvestris]	431	431	93%	5e-143	51%	gi|698542600|XP_009766463.1
PREDICTED: 11S globulin seed storage protein 2-like [Nicotiana tomentosiformis]	429	429	93%	4e-142	51%	gi|697139889|XP_009624040.1
PREDICTED: 11S globulin seed storage protein 2-like [Nicotiana tomentosiformis]	424	424	93%	2e-140	50%	gi|697139900|XP_009624045.1
PREDICTED: 11S globulin seed storage protein 2-like isoform X1 [Beta vulgaris subsp. vulgaris]	419	419	94%	2e-138	49%	gi|731336507|XP_010679299.1
PREDICTED: 11S globulin seed storage protein 2-like [Solanum tuberosum]	419	419	93%	2e-138	50%	gi|565370157|XP_006351693.1
PREDICTED: 11S globulin seed storage protein 2-like [Nicotiana sylvestris]	418	418	93%	5e-138	50%	gi|698469161|XP_009783514.1
PREDICTED: 11S globulin seed storage protein 2-like [Solanum tuberosum]	415	415	92%	6e-137	50%	gi|565370161|XP_006351695.1
PREDICTED: 11S globulin seed storage protein 2-like [Solanum lycopersicum]	414	414	93%	2e-136	50%	gi|460404101|XP_004247523.1
hypothetical protein MIMGU_mgv1a005966mg [Erythranthe guttata] [Mimulus guttatus]	413	413	93%	3e-136	49%	gi|604348301|EYU46456.1
PREDICTED: 13S globulin seed storage protein 2-like [Cucumis melo]	412	412	93%	9e-136	50%	gi|659093217|XP_008447427.1
PREDICTED: 11S globulin seed storage protein 2-like [Populus euphratica]	405	405	77%	6e-135	58%	gi|743920049|XP_011004062.1

Gel band 6.5

Determination of protein characteristic (by MASCOT program)

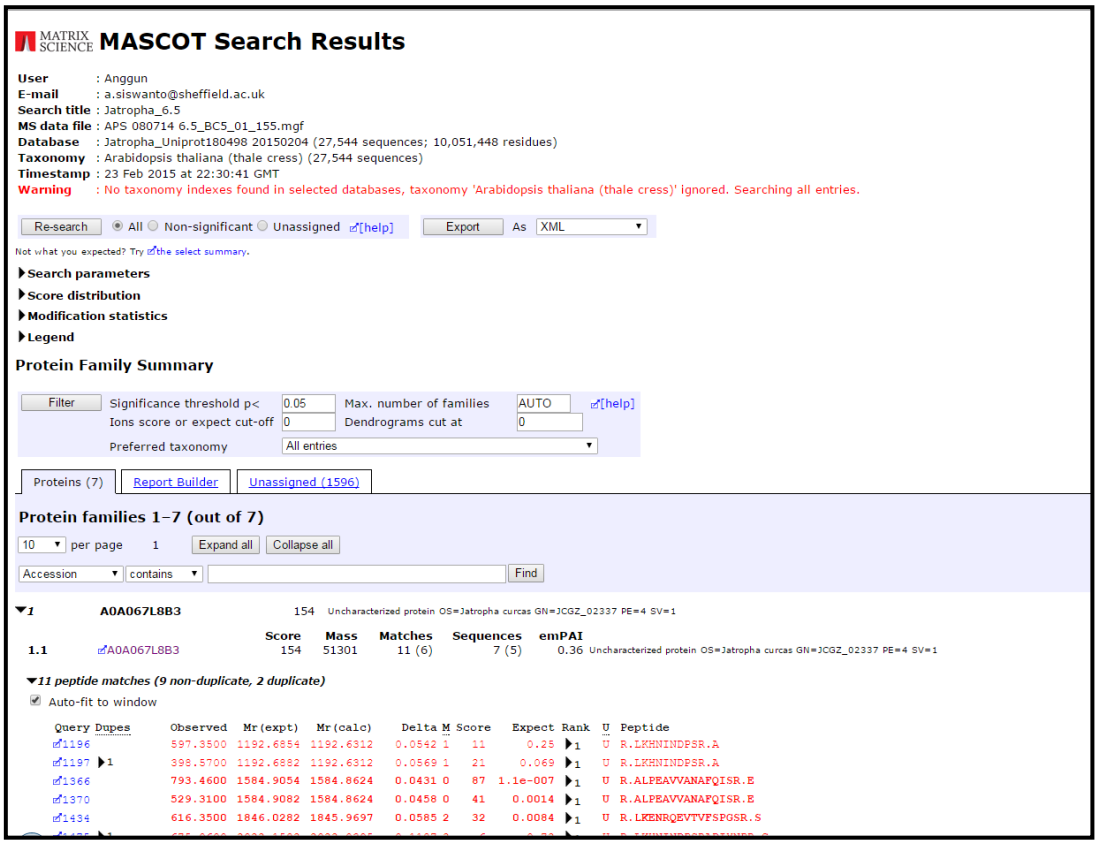

MATRIX SCIENCE **MASCOT Search Results**

User : Anggun
E-mail : a.siswanto@sheffield.ac.uk
Search title : Jatropha_6.5
MS data file : APS 080714 6.5_BC5_01_155.mgf
Database : Jatropha_Uniprot180498 20150204 (27,544 sequences; 10,051,448 residues)
Taxonomy : Arabidopsis thaliana (thale cress) (27,544 sequences)
Timestamp : 23 Feb 2015 at 22:30:41 GMT
Warning : No taxonomy indexes found in selected databases, taxonomy 'Arabidopsis thaliana (thale cress)' ignored. Searching all entries.

Re-search | All | Non-significant | Unassigned [help] | Export As XML

Not what you expected? Try the select summary.

▸ Search parameters
▸ Score distribution
▸ Modification statistics
▸ Legend

Protein Family Summary

Filter | Significance threshold p< 0.05 | Max. number of families AUTO [help]
Ions score or expect cut-off 0 | Dendrograms cut at 0
Preferred taxonomy All entries

Proteins (7) | Report Builder | Unassigned (1596)

Protein families 1–7 (out of 7)

10 per page 1 | Expand all | Collapse all

Accession contains | Find

▾1	A0A067L8B3	154	Uncharacterized protein OS=Jatropha curcas GN=JCGZ_02337 PE=4 SV=1				
		Score	**Mass**	**Matches**	**Sequences**	**emPAI**	
1.1	A0A067L8B3	154	51301	11 (6)	7 (5)	0.36	Uncharacterized protein OS=Jatropha curcas GN=JCGZ_02337 PE=4 SV=1

▾*11 peptide matches (9 non-duplicate, 2 duplicate)*

Auto-fit to window

Query	Dupes	Observed	Mr(expt)	Mr(calc)	Delta	M	Score	Expect	Rank	U	Peptide
1196		597.3500	1192.6854	1192.6312	0.0542	1	11	0.25	1	U	R.LKHNINDPSR.A
1197	1	398.5700	1192.6882	1192.6312	0.0569	1	21	0.069	1	U	R.LKHNINDPSR.A
1366		793.4600	1584.9054	1584.8624	0.0431	0	87	1.1e-007	1	U	R.ALPEAVVANAFQISR.E
1370		529.3100	1584.9082	1584.8624	0.0458	0	41	0.0014	1	U	R.ALPEAVVANAFQISR.E
1434		616.3500	1846.0282	1845.9697	0.0585	2	32	0.0084	1	U	R.LKENRQEVTVFSPGSR.S

Identification of predicted protein (by BLAST search engine)

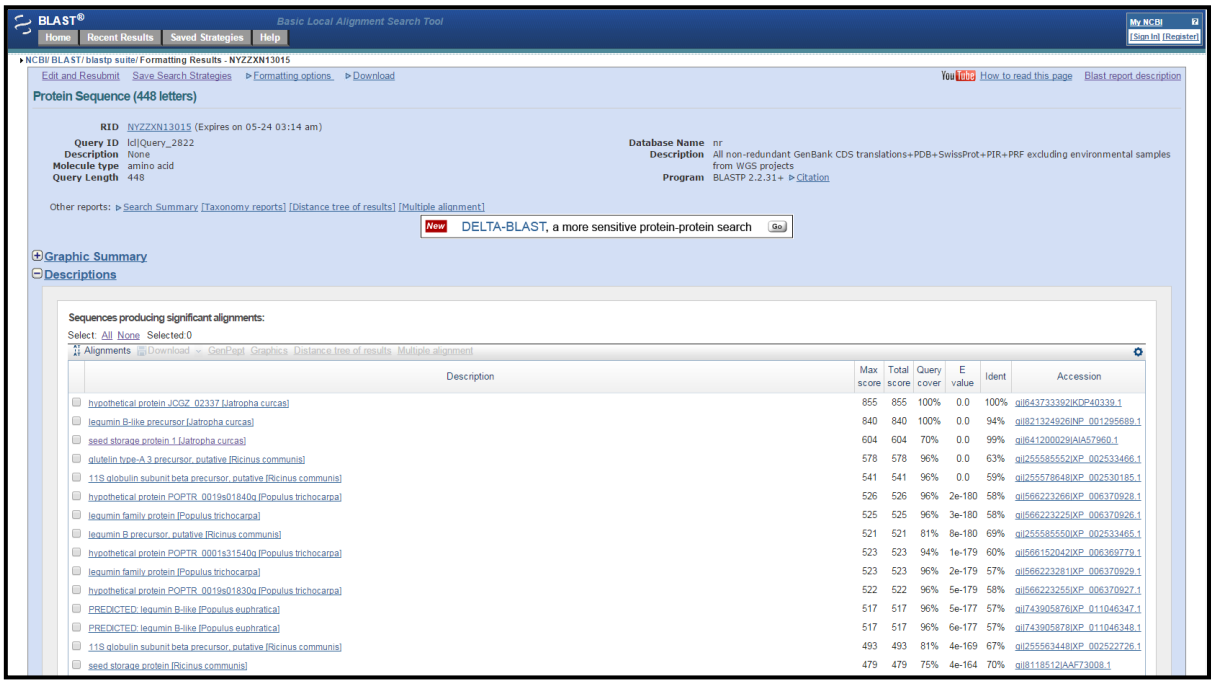

BLAST® Basic Local Alignment Search Tool

Home | Recent Results | Saved Strategies | Help

NCBI/BLAST/blastp suite/Formatting Results - NYZZXN13015

Edit and Resubmit | Save Search Strategies | Formatting options | Download | How to read this page | Blast report description

Protein Sequence (448 letters)

RID NYZZXN13015 (Expires on 05-24 03:14 am)
Query ID lcl|Query_2822
Description None
Molecule type amino acid
Query Length 448

Database Name nr
Description All non-redundant GenBank CDS translations+PDB+SwissProt+PIR+PRF excluding environmental samples from WGS projects
Program BLASTP 2.2.31+ Citation

Other reports: Search Summary [Taxonomy reports] [Distance tree of results] [Multiple alignment]

New DELTA-BLAST, a more sensitive protein-protein search Go

Graphic Summary
Descriptions

Sequences producing significant alignments:

Select: All None Selected:0

Alignments Download GenPept Graphics Distance tree of results Multiple alignment

Description	Max score	Total score	Query cover	E value	Ident	Accession
hypothetical protein JCGZ_02337 [Jatropha curcas]	855	855	100%	0.0	100%	gi|643733392|KDP40339.1
legumin B-like precursor [Jatropha curcas]	840	840	100%	0.0	94%	gi|821324926|NP_001295689.1
seed storage protein 1 [Jatropha curcas]	604	604	70%	0.0	99%	gi|641200029|AIA57960.1
glutelin type-A 3 precursor, putative [Ricinus communis]	578	578	96%	0.0	63%	gi|255585552|XP_002533466.1
11S globulin subunit beta precursor, putative [Ricinus communis]	541	541	96%	0.0	59%	gi|255578648|XP_002530185.1
hypothetical protein POPTR_0019s01840g [Populus trichocarpa]	526	526	96%	2e-180	58%	gi|566223266|XP_006370928.1
legumin family protein [Populus trichocarpa]	525	525	96%	3e-180	58%	gi|566223225|XP_006370926.1
legumin B precursor, putative [Ricinus communis]	521	521	81%	8e-180	69%	gi|255585550|XP_002533465.1
hypothetical protein POPTR_0001s31540g [Populus trichocarpa]	523	523	94%	1e-179	60%	gi|566152042|XP_006369779.1
legumin family protein [Populus trichocarpa]	523	523	96%	2e-179	57%	gi|566223281|XP_006370929.1
hypothetical protein POPTR_0019s01830g [Populus trichocarpa]	522	522	96%	5e-179	58%	gi|566223255|XP_006370927.1
PREDICTED: legumin B-like [Populus euphratica]	517	517	96%	5e-177	57%	gi|743905876|XP_011046347.1
PREDICTED: legumin B-like [Populus euphratica]	517	517	96%	6e-177	57%	gi|743905878|XP_011046348.1
11S globulin subunit beta precursor, putative [Ricinus communis]	493	493	81%	4e-169	67%	gi|255563448|XP_002522726.1
seed storage protein [Ricinus communis]	479	479	75%	4e-164	70%	gi|8118512|AAF73008.1

Gel band 6.6

Determination of protein characteristic (by MASCOT program)

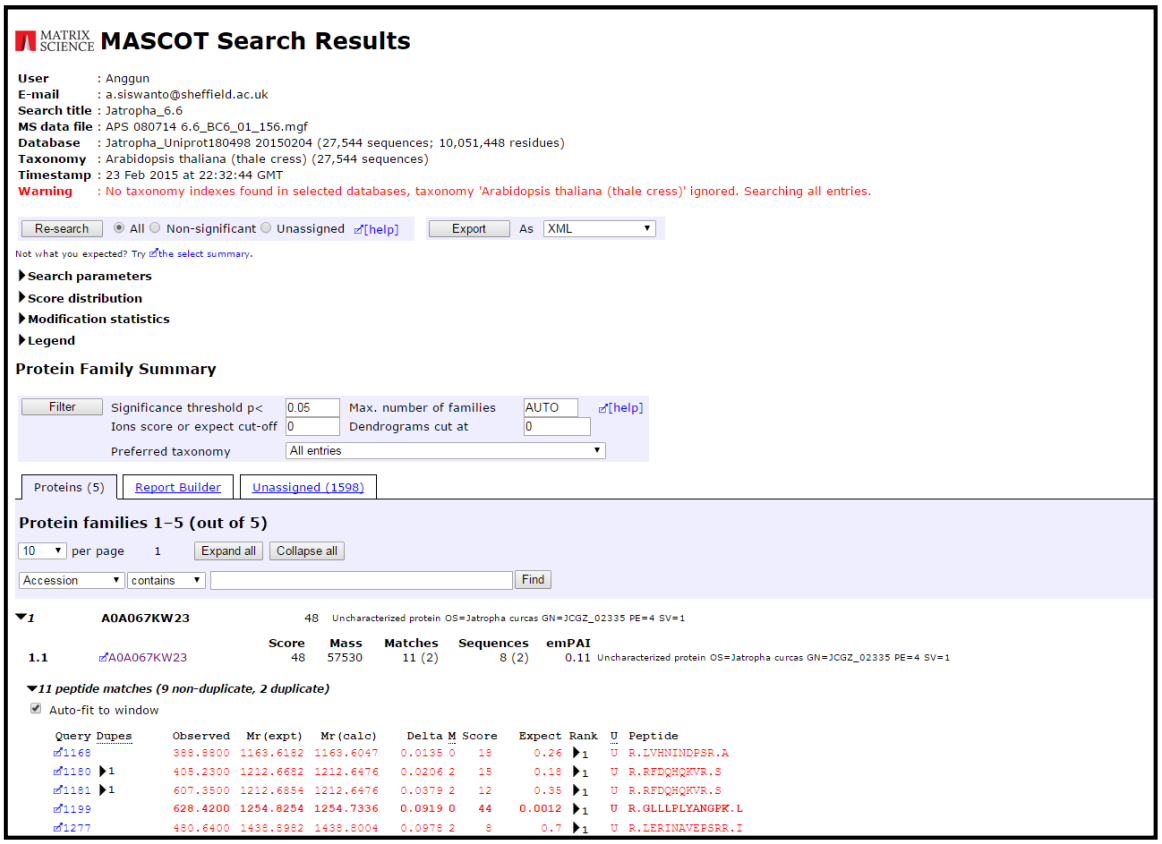

MATRIX SCIENCE **MASCOT Search Results**

User : Anggun
E-mail : a.siswanto@sheffield.ac.uk
Search title : Jatropha_6.6
MS data file : APS 080714 6.6_BC6_01_156.mgf
Database : Jatropha_Uniprot180498 20150204 (27,544 sequences; 10,051,448 residues)
Taxonomy : Arabidopsis thaliana (thale cress) (27,544 sequences)
Timestamp : 23 Feb 2015 at 22:32:44 GMT
Warning : No taxonomy indexes found in selected databases, taxonomy 'Arabidopsis thaliana (thale cress)' ignored. Searching all entries.

Re-search | All | Non-significant | Unassigned [help] | Export As XML

Not what you expected? Try the select summary.

Search parameters
Score distribution
Modification statistics
Legend

Protein Family Summary

Filter | Significance threshold p< 0.05 | Max. number of families AUTO [help]
Ions score or expect cut-off 0 | Dendrograms cut at 0
Preferred taxonomy All entries

Proteins (5) | Report Builder | Unassigned (1598)

Protein families 1–5 (out of 5)

10 per page 1 | Expand all | Collapse all

Accession contains | Find

1	A0A067KW23				48	Uncharacterized protein OS=Jatropha curcas GN=JCGZ_02335 PE=4 SV=1			
		Score	Mass	Matches	Sequences	emPAI			
1.1	A0A067KW23	48	57530	11 (2)	8 (2)	0.11	Uncharacterized protein OS=Jatropha curcas GN=JCGZ_02335 PE=4 SV=1		

11 peptide matches (9 non-duplicate, 2 duplicate)

Auto-fit to window

Query	Dupes	Observed	Mr(expt)	Mr(calc)	Delta	M	Score	Expect	Rank	U	Peptide
1168		388.8800	1163.6182	1163.6047	0.0135	0	18	0.26	1	U	R.LVHNINDPSR.A
1180	1	405.2300	1212.6682	1212.6476	0.0206	2	15	0.18	1	U	R.RFDQHQKVR.S
1181	1	607.3500	1212.6854	1212.6476	0.0379	2	12	0.35	1	U	R.RFDQHQKVR.S
1199		628.4200	1254.8254	1254.7336	0.0919	0	44	0.0012	1	U	R.GLLLPLYANGPK.L
1277		480.6400	1438.8982	1438.8004	0.0978	2	8	0.7	1	U	R.LERINAVEPSRR.I

Identification of predicted protein (by BLAST search engine)

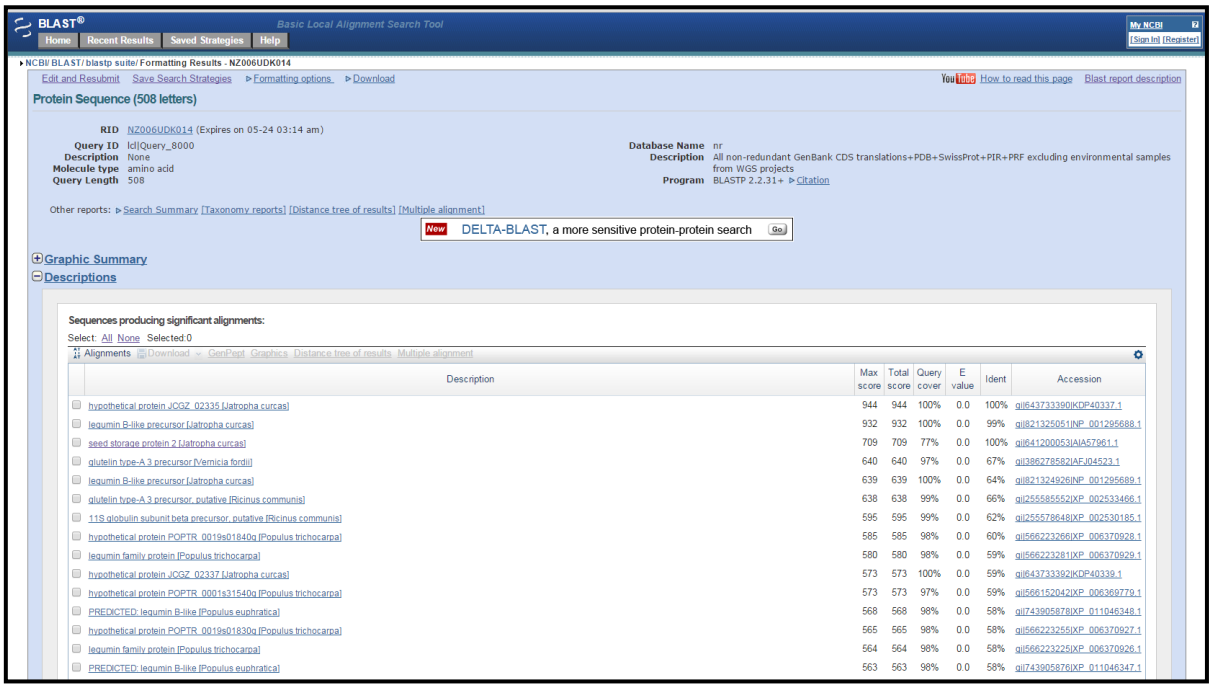

BLAST® Basic Local Alignment Search Tool
Home | Recent Results | Saved Strategies | Help
My NCBI [Sign In] [Register]

NCBI/ BLAST/ blastp suite/ Formatting Results . NZ006UDK014

Edit and Resubmit | Save Search Strategies | Formatting options | Download | How to read this page | Blast report description

Protein Sequence (508 letters)

RID NZ006UDK014 (Expires on 05-24 03:14 am)
Query ID lcl|Query_8000
Description None
Molecule type amino acid
Query Length 508

Database Name nr
Description All non-redundant GenBank CDS translations+PDB+SwissProt+PIR+PRF excluding environmental samples from WGS projects
Program BLASTP 2.2.31+ | Citation

Other reports: Search Summary [Taxonomy reports] [Distance tree of results] [Multiple alignment]

New DELTA-BLAST, a more sensitive protein-protein search Go

Graphic Summary
Descriptions

Sequences producing significant alignments:

Select: All None Selected:0

Alignments | Download | GenPept | Graphics | Distance tree of results | Multiple alignment

Description	Max score	Total score	Query cover	E value	Ident	Accession
hypothetical protein JCGZ_02335 [Jatropha curcas]	944	944	100%	0.0	100%	gi|643733390|KDP40337.1
legumin B-like precursor [Jatropha curcas]	932	932	100%	0.0	99%	gi|821325051|NP_001295688.1
seed storage protein 2 [Jatropha curcas]	709	709	77%	0.0	100%	gi|641200053|AIA57961.1
glutelin type-A 3 precursor [Vernicia fordii]	640	640	97%	0.0	67%	gi|386278582|AFJ04523.1
legumin B-like precursor [Jatropha curcas]	639	639	100%	0.0	64%	gi|821324926|NP_001295689.1
glutelin type-A 3 precursor, putative [Ricinus communis]	638	638	99%	0.0	66%	gi|255585552|XP_002533466.1
11S globulin subunit beta precursor, putative [Ricinus communis]	595	595	99%	0.0	62%	gi|255578648|XP_002530185.1
hypothetical protein POPTR_0019s01840g [Populus trichocarpa]	585	585	98%	0.0	60%	gi|566223266|XP_006370928.1
legumin family protein [Populus trichocarpa]	580	580	98%	0.0	59%	gi|566223281|XP_006370929.1
hypothetical protein JCGZ_02337 [Jatropha curcas]	573	573	100%	0.0	59%	gi|643733392|KDP40339.1
hypothetical protein POPTR_0001s31540g [Populus trichocarpa]	573	573	97%	0.0	59%	gi|566152042|XP_006369779.1
PREDICTED: legumin B-like [Populus euphratica]	568	568	98%	0.0	58%	gi|743905878|XP_011046348.1
hypothetical protein POPTR_0019s01830g [Populus trichocarpa]	565	565	98%	0.0	58%	gi|566223255|XP_006370927.1
legumin family protein [Populus trichocarpa]	564	564	98%	0.0	58%	gi|566223225|XP_006370926.1
PREDICTED: legumin B-like [Populus euphratica]	563	563	98%	0.0	58%	gi|743905876|XP_011046347.1

Gel band 10.1

Determination of protein characteristic (by MASCOT program)

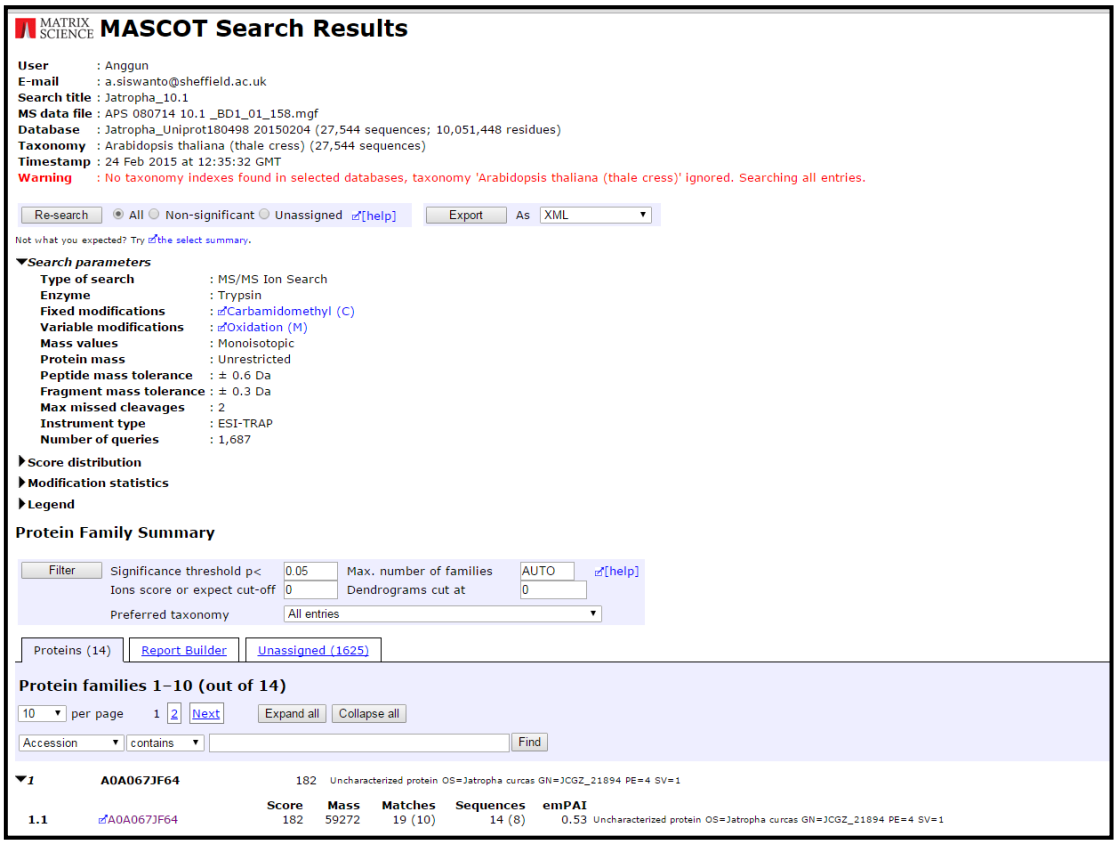

MATRIX SCIENCE **MASCOT Search Results**

User : Anggun
E-mail : a.siswanto@sheffield.ac.uk
Search title : Jatropha_10.1
MS data file : APS 080714 10.1 _BD1_01_158.mgf
Database : Jatropha_Uniprot180498 20150204 (27,544 sequences; 10,051,448 residues)
Taxonomy : Arabidopsis thaliana (thale cress) (27,544 sequences)
Timestamp : 24 Feb 2015 at 12:35:32 GMT
Warning : No taxonomy indexes found in selected databases, taxonomy 'Arabidopsis thaliana (thale cress)' ignored. Searching all entries.

Re-search | All | Non-significant | Unassigned [help] | Export As XML

Not what you expected? Try the select summary.

Search parameters

Type of search	: MS/MS Ion Search
Enzyme	: Trypsin
Fixed modifications	: Carbamidomethyl (C)
Variable modifications	: Oxidation (M)
Mass values	: Monoisotopic
Protein mass	: Unrestricted
Peptide mass tolerance	: ± 0.6 Da
Fragment mass tolerance	: ± 0.3 Da
Max missed cleavages	: 2
Instrument type	: ESI-TRAP
Number of queries	: 1,687

Score distribution
Modification statistics
Legend

Protein Family Summary

Filter | Significance threshold p< 0.05 | Max. number of families AUTO [help]
Ions score or expect cut-off 0 | Dendrograms cut at 0
Preferred taxonomy All entries

Proteins (14) | Report Builder | Unassigned (1625)

Protein families 1–10 (out of 14)

10 per page 1 2 Next | Expand all | Collapse all

Accession contains | Find

1	A0A067JF64		182				Uncharacterized protein OS=Jatropha curcas GN=JCGZ_21894 PE=4 SV=1
		Score	**Mass**	**Matches**	**Sequences**	**emPAI**	
1.1	A0A067JF64	182	59272	19 (10)	14 (8)	0.53	Uncharacterized protein OS=Jatropha curcas GN=JCGZ_21894 PE=4 SV=1

Identification of predicted protein (by BLAST search engine)

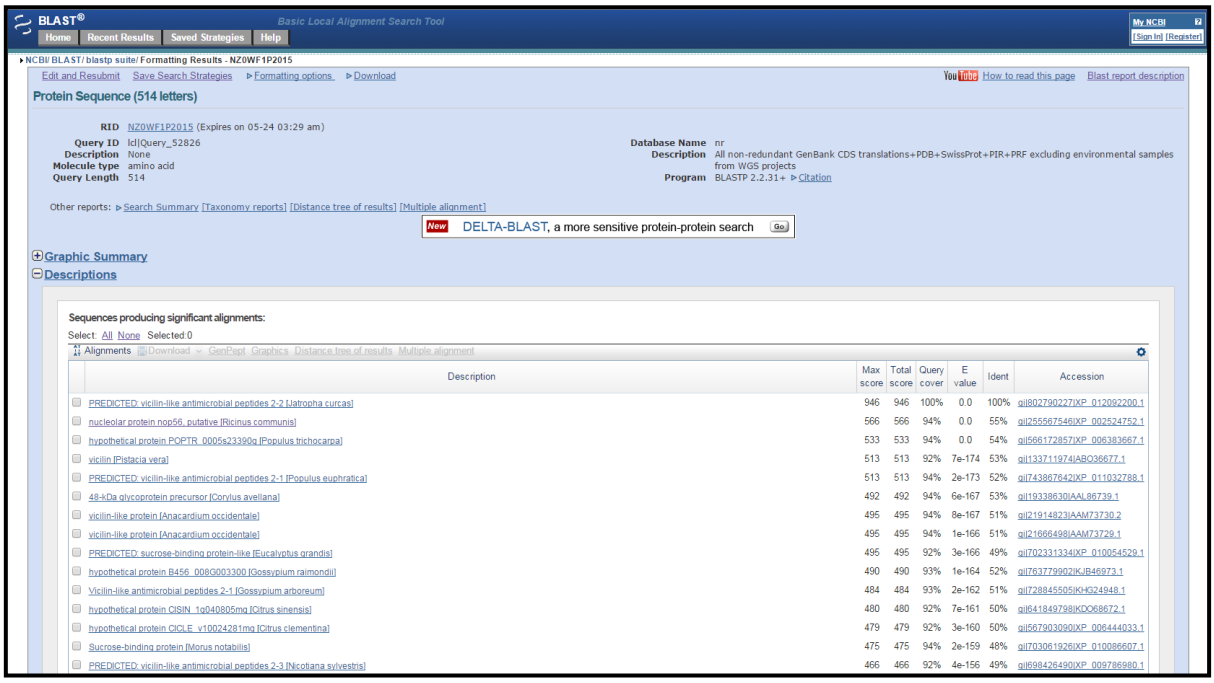

BLAST® Basic Local Alignment Search Tool

Home | Recent Results | Saved Strategies | Help

NCBI/ BLAST/ blastp suite/ Formatting Results - NZ0WF1P2015

Edit and Resubmit | Save Search Strategies | Formatting options | Download | How to read this page | Blast report description

Protein Sequence (514 letters)

RID NZ0WF1P2015 (Expires on 05-24 03:29 am)
Query ID lcl|Query_52826
Description None
Molecule type amino acid
Query Length 514

Database Name nr
Description All non-redundant GenBank CDS translations+PDB+SwissProt+PIR+PRF excluding environmental samples from WGS projects
Program BLASTP 2.2.31+ Citation

Other reports: Search Summary [Taxonomy reports] [Distance tree of results] [Multiple alignment]

New DELTA-BLAST, a more sensitive protein-protein search Go

Graphic Summary
Descriptions

Sequences producing significant alignments:

Select: All None Selected:0

Alignments | Download | GenPept | Graphics | Distance tree of results | Multiple alignment

Description	Max score	Total score	Query cover	E value	Ident	Accession
PREDICTED: vicilin-like antimicrobial peptides 2-2 [Jatropha curcas]	946	946	100%	0.0	100%	gi|802790227|XP_012092200.1
nucleolar protein nop56, putative [Ricinus communis]	566	566	94%	0.0	55%	gi|255567546|XP_002524752.1
hypothetical protein POPTR_0005s23390g [Populus trichocarpa]	533	533	94%	0.0	54%	gi|566172857|XP_006383667.1
vicilin [Pistacia vera]	513	513	92%	7e-174	53%	gi|133711974|ABO36677.1
PREDICTED: vicilin-like antimicrobial peptides 2-1 [Populus euphratica]	513	513	94%	2e-173	52%	gi|743867642|XP_011032788.1
48-kDa glycoprotein precursor [Corylus avellana]	492	492	94%	6e-167	53%	gi|19338630|AAL86739.1
vicilin-like protein [Anacardium occidentale]	495	495	94%	8e-167	51%	gi|21914823|AAM73730.2
vicilin-like protein [Anacardium occidentale]	495	495	94%	1e-166	51%	gi|21666498|AAM73729.1
PREDICTED: sucrose-binding protein-like [Eucalyptus grandis]	495	495	92%	3e-166	49%	gi|702331334|XP_010054529.1
hypothetical protein B456_008G003300 [Gossypium raimondii]	490	490	93%	1e-164	52%	gi|763779902|KJB46973.1
Vicilin-like antimicrobial peptides 2-1 [Gossypium arboreum]	484	484	93%	2e-162	51%	gi|728845505|KHG24948.1
hypothetical protein CISIN_1g040805mg [Citrus sinensis]	480	480	92%	7e-161	50%	gi|641849798|KDO68672.1
hypothetical protein CICLE_v10024281mg [Citrus clementina]	479	479	92%	3e-160	50%	gi|567903090|XP_006444033.1
Sucrose-binding protein [Morus notabilis]	475	475	94%	2e-159	48%	gi|703061926|XP_010086607.1
PREDICTED: vicilin-like antimicrobial peptides 2-3 [Nicotiana sylvestris]	466	466	92%	4e-156	49%	gi|698426490|XP_009786980.1

Gel band 10.2

Determination of protein characteristic (by MASCOT program)

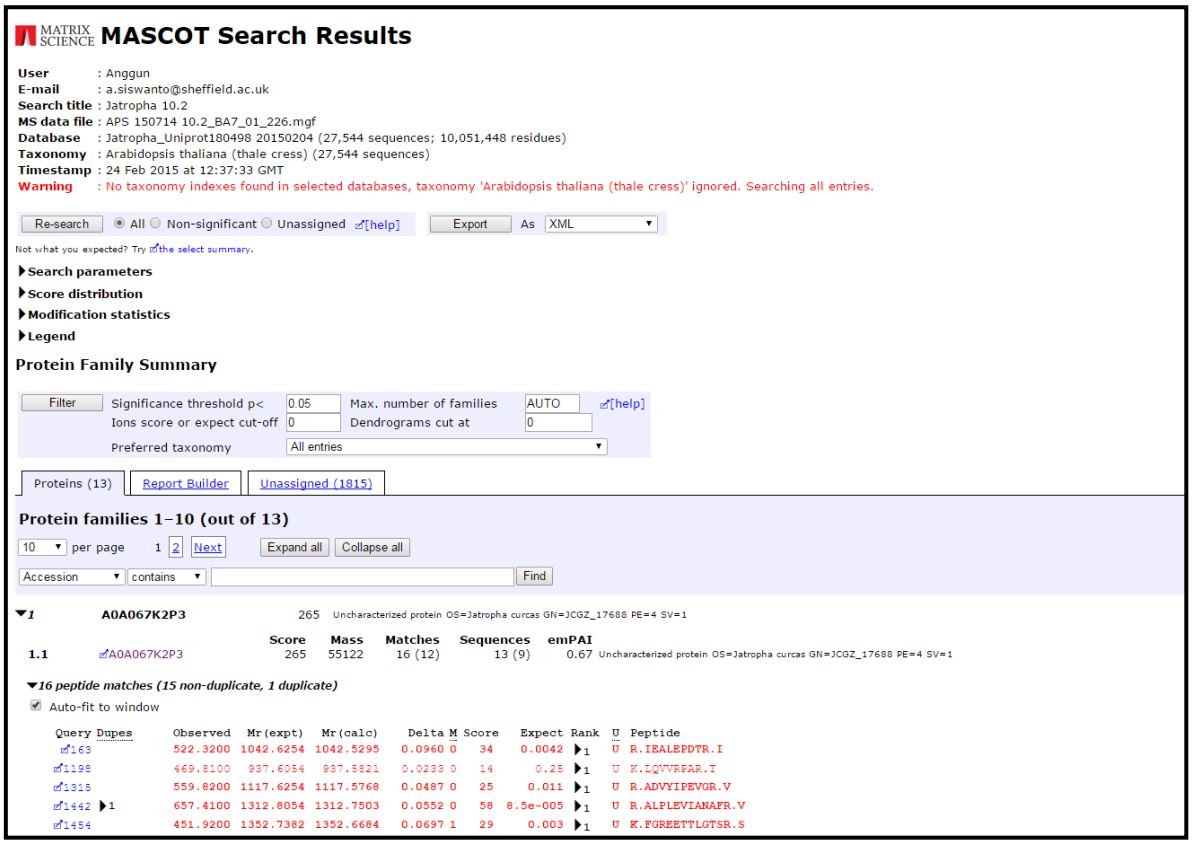

MATRIX SCIENCE **MASCOT Search Results**

User : Anggun
E-mail : a.siswanto@sheffield.ac.uk
Search title : Jatropha 10.2
MS data file : APS 150714 10.2_BA7_01_226.mgf
Database : Jatropha_Uniprot180498 20150204 (27,544 sequences; 10,051,448 residues)
Taxonomy : Arabidopsis thaliana (thale cress) (27,544 sequences)
Timestamp : 24 Feb 2015 at 12:37:33 GMT
Warning : No taxonomy indexes found in selected databases, taxonomy 'Arabidopsis thaliana (thale cress)' ignored. Searching all entries.

Re-search | All | Non-significant | Unassigned [help] | Export As XML

Not what you expected? Try the select summary.

▸ Search parameters
▸ Score distribution
▸ Modification statistics
▸ Legend

Protein Family Summary

Filter | Significance threshold p< 0.05 | Max. number of families AUTO [help]
Ions score or expect cut-off 0 | Dendrograms cut at 0
Preferred taxonomy All entries

Proteins (13) | Report Builder | Unassigned (1815)

Protein families 1–10 (out of 13)

10 per page 1 2 Next | Expand all | Collapse all

Accession contains | Find

1 A0A067K2P3 265 Uncharacterized protein OS=Jatropha curcas GN=JCGZ_17688 PE=4 SV=1

		Score	Mass	Matches	Sequences	emPAI	
1.1	A0A067K2P3	265	55122	16 (12)	13 (9)	0.67	Uncharacterized protein OS=Jatropha curcas GN=JCGZ_17688 PE=4 SV=1

16 peptide matches (15 non-duplicate, 1 duplicate)

Auto-fit to window

Query	Dupes	Observed	Mr(expt)	Mr(calc)	Delta	M	Score	Expect	Rank	U	Peptide
163		522.3200	1042.6254	1042.5295	0.0960	0	34	0.0042	1	U	R.IEALEPDTR.I
1198		469.8100	937.6054	937.5821	0.0233	0	14	0.25	1	U	K.LQVVRPAR.I
1315		559.8200	1117.6254	1117.5768	0.0487	0	25	0.011	1	U	R.ADVYIPEVGR.V
1442	1	657.4100	1312.8054	1312.7503	0.0552	0	58	8.5e-005	1	U	R.ALPLEVIANAFR.V
1454		451.9200	1352.7382	1352.6684	0.0697	1	29	0.003	1	U	K.FGREETTLGTSR.S

Identification of predicted protein (by BLAST search engine)

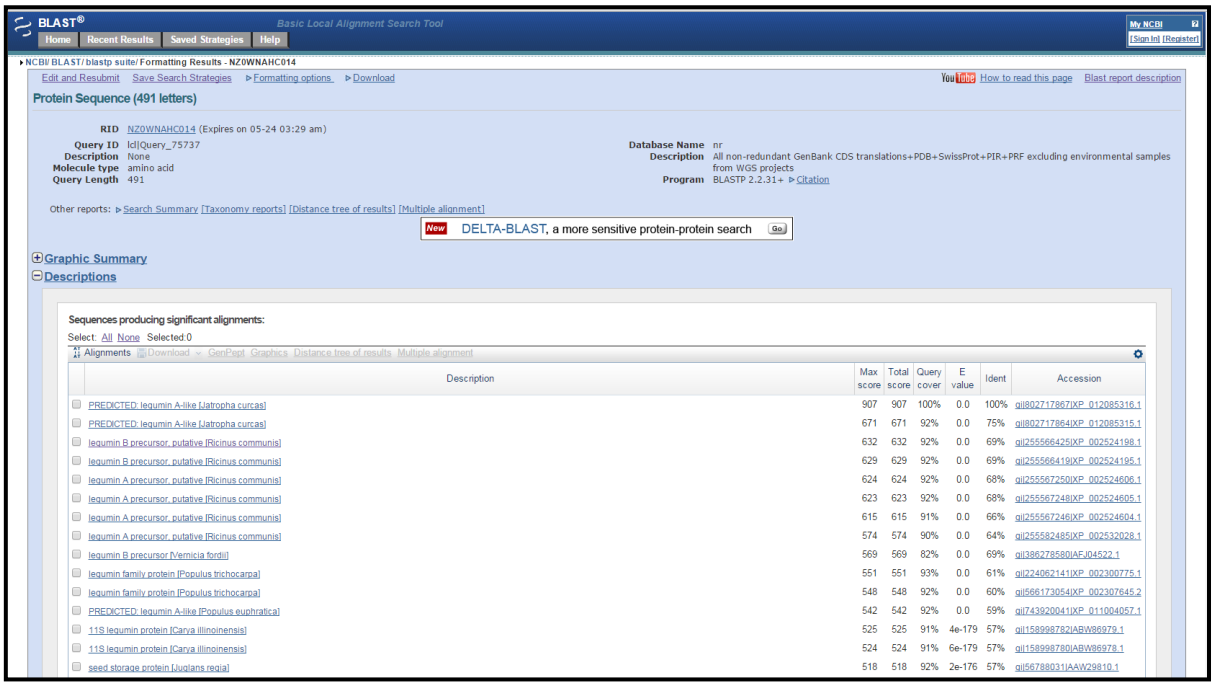

BLAST® Basic Local Alignment Search Tool
Home | Recent Results | Saved Strategies | Help
My NCBI [Sign In] [Register]

NCBI/ BLAST/ blastp suite/ Formatting Results - NZ0WNAHC014

Edit and Resubmit | Save Search Strategies | Formatting options | Download | How to read this page | Blast report description

Protein Sequence (491 letters)

RID NZ0WNAHC014 (Expires on 05-24 03:29 am)
Query ID lcl|Query_75737
Description None
Molecule type amino acid
Query Length 491

Database Name nr
Description All non-redundant GenBank CDS translations+PDB+SwissProt+PIR+PRF excluding environmental samples from WGS projects
Program BLASTP 2.2.31+ Citation

Other reports: Search Summary [Taxonomy reports] [Distance tree of results] [Multiple alignment]

New DELTA-BLAST, a more sensitive protein-protein search Go

Graphic Summary
Descriptions

Sequences producing significant alignments:

Select: All None Selected:0

Alignments | Download | GenPept | Graphics | Distance tree of results | Multiple alignment

Description	Max score	Total score	Query cover	E value	Ident	Accession
PREDICTED: legumin A-like [Jatropha curcas]	907	907	100%	0.0	100%	gi|802717867|XP_012085316.1
PREDICTED: legumin A-like [Jatropha curcas]	671	671	92%	0.0	75%	gi|802717864|XP_012085315.1
legumin B precursor, putative [Ricinus communis]	632	632	92%	0.0	69%	gi|255566425|XP_002524198.1
legumin B precursor, putative [Ricinus communis]	629	629	92%	0.0	69%	gi|255566419|XP_002524195.1
legumin A precursor, putative [Ricinus communis]	624	624	92%	0.0	68%	gi|255567250|XP_002524606.1
legumin A precursor, putative [Ricinus communis]	623	623	92%	0.0	68%	gi|255567248|XP_002524605.1
legumin A precursor, putative [Ricinus communis]	615	615	91%	0.0	66%	gi|255567246|XP_002524604.1
legumin A precursor, putative [Ricinus communis]	574	574	90%	0.0	64%	gi|255582485|XP_002532028.1
legumin B precursor [Vernicia fordii]	569	569	82%	0.0	69%	gi|386278580|AFJ04522.1
legumin family protein [Populus trichocarpa]	551	551	93%	0.0	61%	gi|224062141|XP_002300775.1
legumin family protein [Populus trichocarpa]	548	548	92%	0.0	60%	gi|566173054|XP_002307645.2
PREDICTED: legumin A-like [Populus euphratica]	542	542	92%	0.0	59%	gi|743920041|XP_011004057.1
11S legumin protein [Carya illinoinensis]	525	525	91%	4e-179	57%	gi|158998782|ABW86979.1
11S legumin protein [Carya illinoinensis]	524	524	91%	6e-179	57%	gi|158998780|ABW86978.1
seed storage protein [Juglans regia]	518	518	92%	2e-176	57%	gi|56788031|AAW29810.1

Gel band 10.3

Determination of protein characteristic (by MASCOT program)

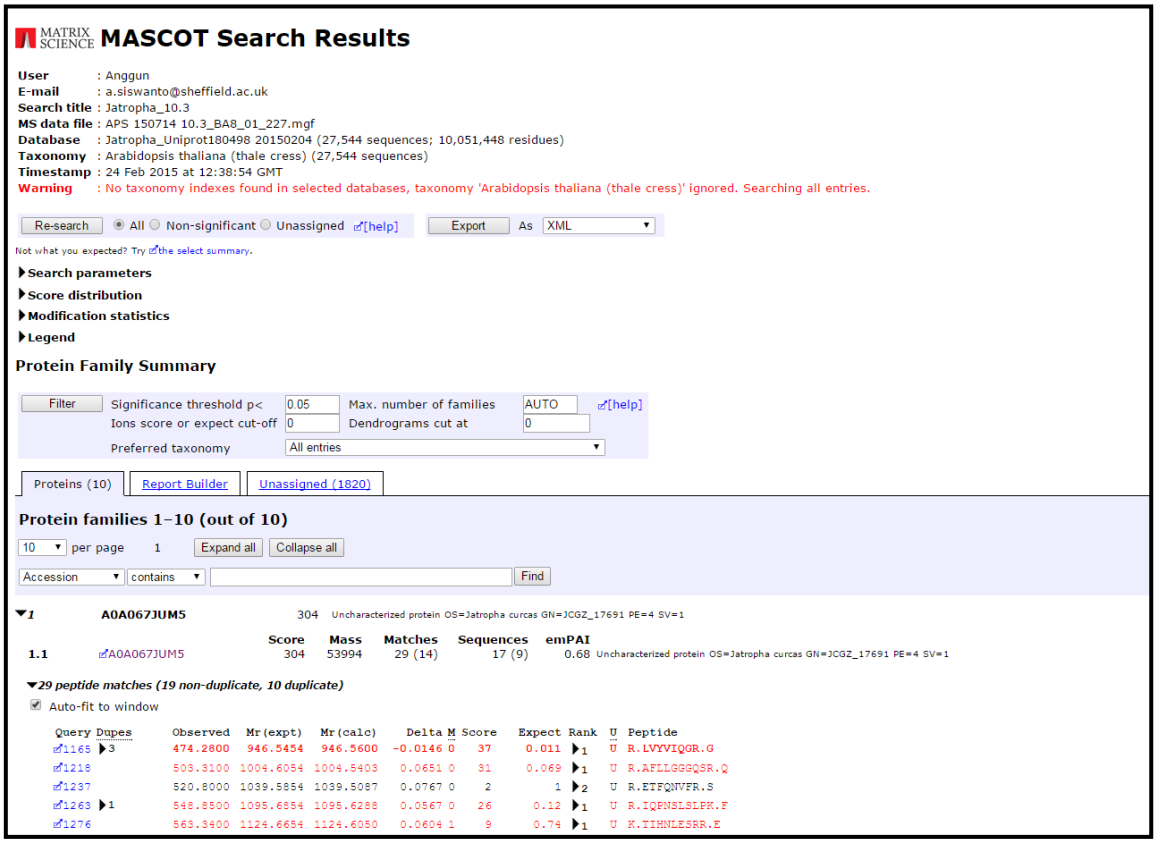

MATRIX SCIENCE **MASCOT Search Results**

User : Anggun
E-mail : a.siswanto@sheffield.ac.uk
Search title : Jatropha_10.3
MS data file : APS 150714 10.3_BA8_01_227.mgf
Database : Jatropha_Uniprot180498 20150204 (27,544 sequences; 10,051,448 residues)
Taxonomy : Arabidopsis thaliana (thale cress) (27,544 sequences)
Timestamp : 24 Feb 2015 at 12:38:54 GMT
Warning : No taxonomy indexes found in selected databases, taxonomy 'Arabidopsis thaliana (thale cress)' ignored. Searching all entries.

Re-search | All | Non-significant | Unassigned [help] | Export As XML

Not what you expected? Try the select summary.

▸ Search parameters
▸ Score distribution
▸ Modification statistics
▸ Legend

Protein Family Summary

Filter | Significance threshold p< 0.05 | Max. number of families AUTO [help]
Ions score or expect cut-off 0 | Dendrograms cut at 0
Preferred taxonomy All entries

Proteins (10) | Report Builder | Unassigned (1820)

Protein families 1–10 (out of 10)

10 per page 1 | Expand all | Collapse all

Accession contains | Find

1	A0A067JUM5	304	Uncharacterized protein OS=Jatropha curcas GN=JCGZ_17691 PE=4 SV=1			
		Score	Mass	Matches	Sequences	emPAI
1.1	A0A067JUM5	304	53994	29 (14)	17 (9)	0.68 Uncharacterized protein OS=Jatropha curcas GN=JCGZ_17691 PE=4 SV=1

29 peptide matches (19 non-duplicate, 10 duplicate)

Auto-fit to window

Query	Dupes	Observed	Mr(expt)	Mr(calc)	Delta	M	Score	Expect	Rank	U	Peptide
1165	3	474.2800	946.5454	946.5600	-0.0146	0	37	0.011	1	U	R.LVYVIQGR.G
1218		503.3100	1004.6054	1004.5403	0.0651	0	31	0.069	1	U	R.AFLLGGGQSR.Q
1237		520.8000	1039.5854	1039.5087	0.0767	0	2	1	2	U	R.ETFQNVFR.S
1263	1	548.8500	1095.6854	1095.6288	0.0567	0	26	0.12	1	U	R.IQPNSLSLPK.F
1276		563.3400	1124.6654	1124.6050	0.0604	1	9	0.74	1	U	K.TIHNLESRR.E

Identification of predicted protein (by BLAST search engine)

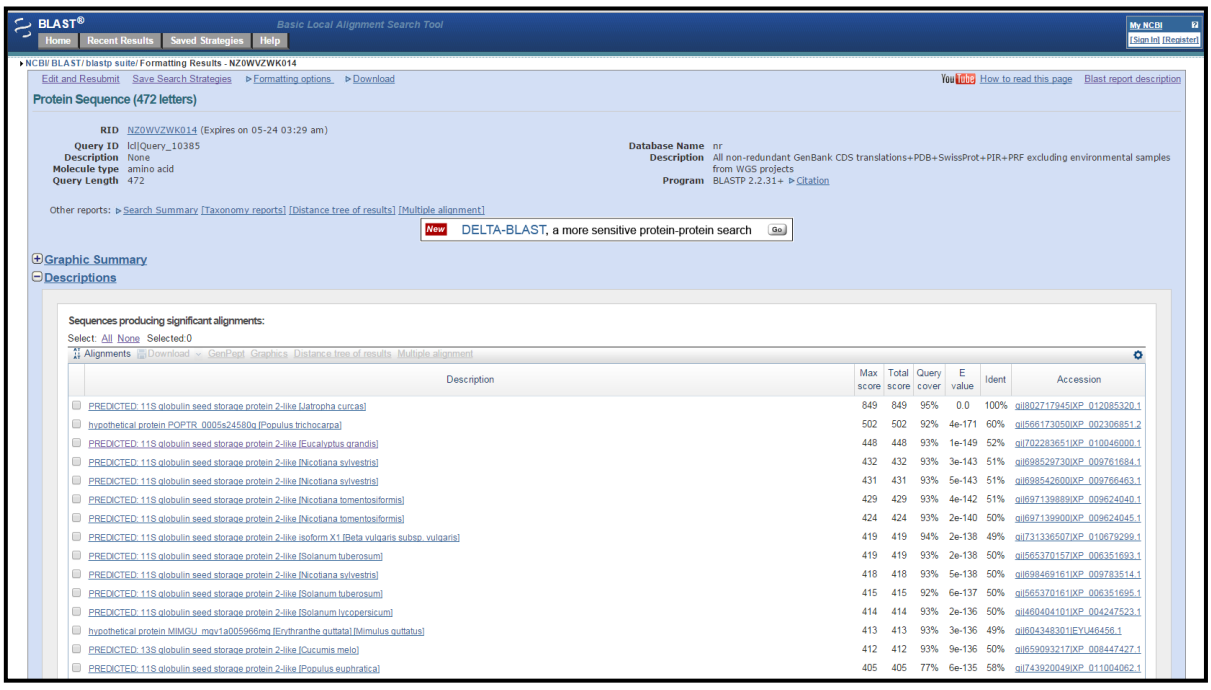

BLAST® Basic Local Alignment Search Tool

Home | Recent Results | Saved Strategies | Help

NCBI/BLAST/blastp suite/Formatting Results - NZ0WVZWK014

Edit and Resubmit | Save Search Strategies | Formatting options | Download | How to read this page | Blast report description

Protein Sequence (472 letters)

RID NZ0WVZWK014 (Expires on 05-24 03:29 am)
Query ID lcl|Query_10385
Description None
Molecule type amino acid
Query Length 472

Database Name nr
Description All non-redundant GenBank CDS translations+PDB+SwissProt+PIR+PRF excluding environmental samples from WGS projects
Program BLASTP 2.2.31+ Citation

Other reports: Search Summary [Taxonomy reports] [Distance tree of results] [Multiple alignment]

New DELTA-BLAST, a more sensitive protein-protein search Go

Graphic Summary
Descriptions

Sequences producing significant alignments:

Select: All None Selected:0

Alignments | Download | GenPept | Graphics | Distance tree of results | Multiple alignment

Description	Max score	Total score	Query cover	E value	Ident	Accession
PREDICTED: 11S globulin seed storage protein 2-like [Jatropha curcas]	849	849	95%	0.0	100%	gi|802717945|XP_012085320.1
hypothetical protein POPTR_0005s24580g [Populus trichocarpa]	502	502	92%	4e-171	60%	gi|566173050|XP_002306851.2
PREDICTED: 11S globulin seed storage protein 2-like [Eucalyptus grandis]	448	448	93%	1e-149	52%	gi|702283651|XP_010046000.1
PREDICTED: 11S globulin seed storage protein 2-like [Nicotiana sylvestris]	432	432	93%	3e-143	51%	gi|698529730|XP_009761684.1
PREDICTED: 11S globulin seed storage protein 2-like [Nicotiana sylvestris]	431	431	93%	5e-143	51%	gi|698542600|XP_009766463.1
PREDICTED: 11S globulin seed storage protein 2-like [Nicotiana tomentosiformis]	429	429	93%	4e-142	51%	gi|697139889|XP_009624040.1
PREDICTED: 11S globulin seed storage protein 2-like [Nicotiana tomentosiformis]	424	424	93%	2e-140	50%	gi|697139900|XP_009624045.1
PREDICTED: 11S globulin seed storage protein 2-like isoform X1 [Beta vulgaris subsp. vulgaris]	419	419	94%	2e-138	49%	gi|731336507|XP_010679299.1
PREDICTED: 11S globulin seed storage protein 2-like [Solanum tuberosum]	419	419	93%	2e-138	50%	gi|565370157|XP_006351693.1
PREDICTED: 11S globulin seed storage protein 2-like [Nicotiana sylvestris]	418	418	93%	5e-138	50%	gi|698469161|XP_009783514.1
PREDICTED: 11S globulin seed storage protein 2-like [Solanum tuberosum]	415	415	92%	6e-137	50%	gi|565370161|XP_006351695.1
PREDICTED: 11S globulin seed storage protein 2-like [Solanum lycopersicum]	414	414	93%	2e-136	50%	gi|460404101|XP_004247523.1
hypothetical protein MIMGU_mgv1a005966mg [Erythranthe guttata] [Mimulus guttatus]	413	413	93%	3e-136	49%	gi|604348301|EYU46456.1
PREDICTED: 13S globulin seed storage protein 2-like [Cucumis melo]	412	412	93%	9e-136	50%	gi|659093217|XP_008447427.1
PREDICTED: 11S globulin seed storage protein 2-like [Populus euphratica]	405	405	77%	6e-135	58%	gi|743920049|XP_011004062.1

Gel band 10.4

Determination of protein characteristic (by MASCOT program)

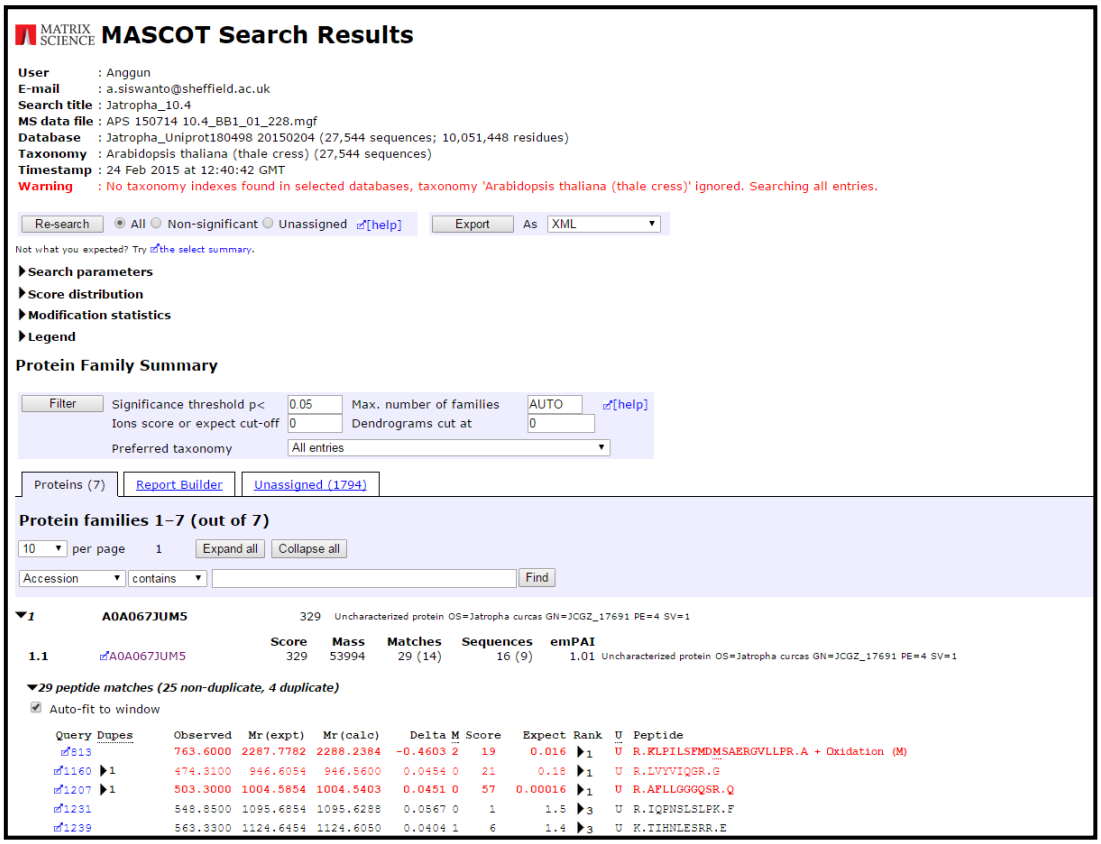

MATRIX SCIENCE **MASCOT Search Results**

User : Anggun
E-mail : a.siswanto@sheffield.ac.uk
Search title : Jatropha_10.4
MS data file : APS 150714 10.4_BB1_01_228.mgf
Database : Jatropha_Uniprot180498 20150204 (27,544 sequences; 10,051,448 residues)
Taxonomy : Arabidopsis thaliana (thale cress) (27,544 sequences)
Timestamp : 24 Feb 2015 at 12:40:42 GMT
Warning : No taxonomy indexes found in selected databases, taxonomy 'Arabidopsis thaliana (thale cress)' ignored. Searching all entries.

Re-search | All | Non-significant | Unassigned [help] | Export As XML

Not what you expected? Try the select summary.

Search parameters
Score distribution
Modification statistics
Legend

Protein Family Summary

Filter | Significance threshold p< 0.05 | Max. number of families AUTO [help]
Ions score or expect cut-off 0 | Dendrograms cut at 0
Preferred taxonomy All entries

Proteins (7) | Report Builder | Unassigned (1794)

Protein families 1–7 (out of 7)

10 per page 1 | Expand all | Collapse all

Accession contains | Find

1	A0A067JUM5	329	Uncharacterized protein OS=Jatropha curcas GN=JCGZ_17691 PE=4 SV=1			
		Score	**Mass**	**Matches**	**Sequences**	**emPAI**
1.1	A0A067JUM5	329	53994	29 (14)	16 (9)	1.01

29 peptide matches (25 non-duplicate, 4 duplicate)

Auto-fit to window

Query	Dupes	Observed	Mr(expt)	Mr(calc)	Delta	M	Score	Expect	Rank	U	Peptide
813		763.6000	2287.7782	2288.2384	-0.4603	2	19	0.016	1	U	R.KLPILSFMDMSAERGVLLPR.A + Oxidation (M)
1160	1	474.3100	946.6054	946.5600	0.0454	0	21	0.18	1	U	R.LVYVIQGR.G
1207	1	503.3000	1004.5854	1004.5403	0.0451	0	57	0.00016	1	U	R.AFLLGGGQSR.Q
1231		548.8500	1095.6854	1095.6288	0.0567	0	1	1.5	3	U	R.IQPNSLSLPK.F
1239		563.3300	1124.6454	1124.6050	0.0404	1	6	1.4	3	U	K.TIHNLESRR.E

Identification of predicted protein (by BLAST search engine)

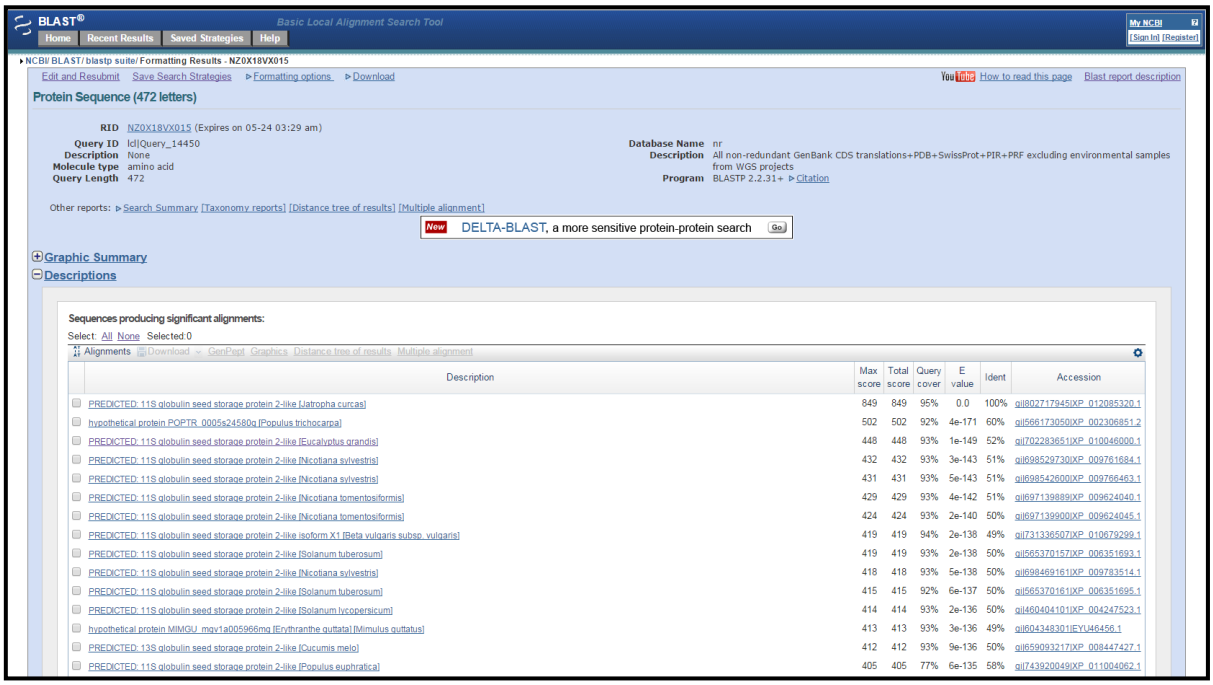

BLAST® Basic Local Alignment Search Tool

Home | Recent Results | Saved Strategies | Help

NCBI/BLAST/blastp suite/Formatting Results - NZ0X18VX015

Edit and Resubmit | Save Search Strategies | Formatting options | Download | How to read this page | Blast report description

Protein Sequence (472 letters)

RID NZ0X18VX015 (Expires on 05-24 03:29 am)
Query ID lcl|Query_14450
Description None
Molecule type amino acid
Query Length 472

Database Name nr
Description All non-redundant GenBank CDS translations+PDB+SwissProt+PIR+PRF excluding environmental samples from WGS projects
Program BLASTP 2.2.31+ Citation

Other reports: Search Summary [Taxonomy reports] [Distance tree of results] [Multiple alignment]

New DELTA-BLAST, a more sensitive protein-protein search Go

Graphic Summary
Descriptions

Sequences producing significant alignments:

Select: All None Selected:0

Alignments Download GenPept Graphics Distance tree of results Multiple alignment

Description	Max score	Total score	Query cover	E value	Ident	Accession
PREDICTED: 11S globulin seed storage protein 2-like [Jatropha curcas]	849	849	95%	0.0	100%	gi|802717945|XP_012085320.1
hypothetical protein POPTR_0005s24580g [Populus trichocarpa]	502	502	92%	4e-171	60%	gi|566173050|XP_002306851.2
PREDICTED: 11S globulin seed storage protein 2-like [Eucalyptus grandis]	448	448	93%	1e-149	52%	gi|702283651|XP_010046000.1
PREDICTED: 11S globulin seed storage protein 2-like [Nicotiana sylvestris]	432	432	93%	3e-143	51%	gi|698529730|XP_009761684.1
PREDICTED: 11S globulin seed storage protein 2-like [Nicotiana sylvestris]	431	431	93%	5e-143	51%	gi|698542600|XP_009766463.1
PREDICTED: 11S globulin seed storage protein 2-like [Nicotiana tomentosiformis]	429	429	93%	4e-142	51%	gi|697139889|XP_009624040.1
PREDICTED: 11S globulin seed storage protein 2-like [Nicotiana tomentosiformis]	424	424	93%	2e-140	50%	gi|697139900|XP_009624045.1
PREDICTED: 11S globulin seed storage protein 2-like isoform X1 [Beta vulgaris subsp. vulgaris]	419	419	94%	2e-138	49%	gi|731336507|XP_010679299.1
PREDICTED: 11S globulin seed storage protein 2-like [Solanum tuberosum]	419	419	93%	2e-138	50%	gi|565370157|XP_006351693.1
PREDICTED: 11S globulin seed storage protein 2-like [Nicotiana sylvestris]	418	418	93%	5e-138	50%	gi|698469161|XP_009783514.1
PREDICTED: 11S globulin seed storage protein 2-like [Solanum tuberosum]	415	415	92%	6e-137	50%	gi|565370161|XP_006351695.1
PREDICTED: 11S globulin seed storage protein 2-like [Solanum lycopersicum]	414	414	93%	2e-136	50%	gi|460404101|XP_004247523.1
hypothetical protein MIMGU_mgv1a005966mg [Erythranthe guttata] [Mimulus guttatus]	413	413	93%	3e-136	49%	gi|604348301|EYU46456.1
PREDICTED: 13S globulin seed storage protein 2-like [Cucumis melo]	412	412	93%	9e-136	50%	gi|659093217|XP_008447427.1
PREDICTED: 11S globulin seed storage protein 2-like [Populus euphratica]	405	405	77%	6e-135	58%	gi|743920049|XP_011004062.1

Gel band 10.5

Determination of protein characteristic (by MASCOT program)

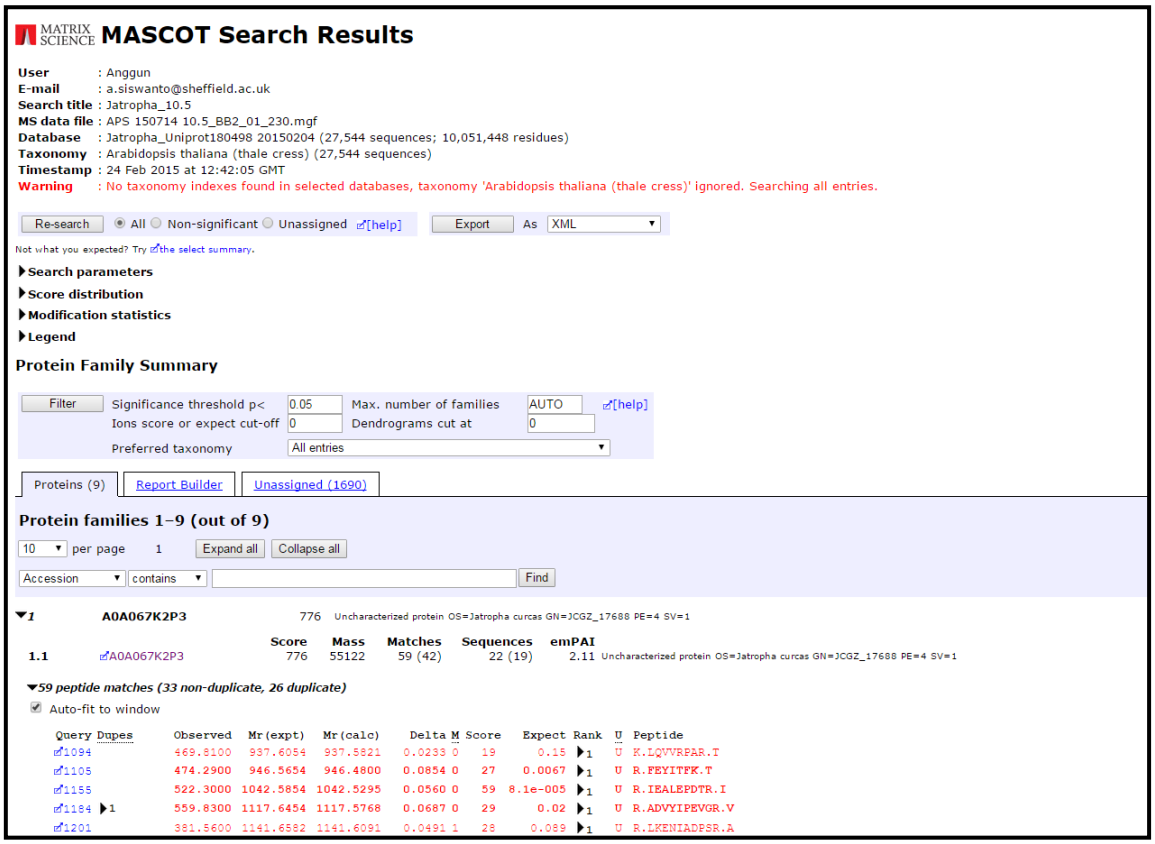

MASCOT Search Results

User : Anggun
E-mail : a.siswanto@sheffield.ac.uk
Search title : Jatropha_10.5
MS data file : APS 150714 10.5_BB2_01_230.mgf
Database : Jatropha_Uniprot180498 20150204 (27,544 sequences; 10,051,448 residues)
Taxonomy : Arabidopsis thaliana (thale cress) (27,544 sequences)
Timestamp : 24 Feb 2015 at 12:42:05 GMT
Warning : No taxonomy indexes found in selected databases, taxonomy 'Arabidopsis thaliana (thale cress)' ignored. Searching all entries.

Re-search | All | Non-significant | Unassigned [help] | Export As XML

Not what you expected? Try the select summary.

Search parameters
Score distribution
Modification statistics
Legend

Protein Family Summary

Filter | Significance threshold p< 0.05 | Max. number of families AUTO [help]
Ions score or expect cut-off 0 | Dendrograms cut at 0
Preferred taxonomy All entries

Proteins (9) | Report Builder | Unassigned (1690)

Protein families 1–9 (out of 9)

10 per page 1 | Expand all | Collapse all

Accession contains | Find

1 A0A067K2P3 776 Uncharacterized protein OS=Jatropha curcas GN=JCGZ_17688 PE=4 SV=1

		Score	Mass	Matches	Sequences	emPAI	
1.1	A0A067K2P3	776	55122	59 (42)	22 (19)	2.11	Uncharacterized protein OS=Jatropha curcas GN=JCGZ_17688 PE=4 SV=1

59 peptide matches (33 non-duplicate, 26 duplicate)

Auto-fit to window

Query	Dupes	Observed	Mr(expt)	Mr(calc)	Delta	M	Score	Expect	Rank	U	Peptide
1094		469.8100	937.6054	937.5821	0.0233	0	19	0.15	1	U	K.LQVVRPAR.T
1105		474.2900	946.5654	946.4800	0.0854	0	27	0.0067	1	U	R.FEYITFK.T
1155		522.3000	1042.5854	1042.5295	0.0560	0	59	8.1e-005	1	U	R.IEALEPDTR.I
1184	1	559.8300	1117.6454	1117.5768	0.0687	0	29	0.02	1	U	R.ADVYIPEVGR.V
1201		381.5600	1141.6582	1141.6091	0.0491	1	28	0.089	1	U	R.LKENIADPSR.A

Identification of predicted protein (by BLAST search engine)

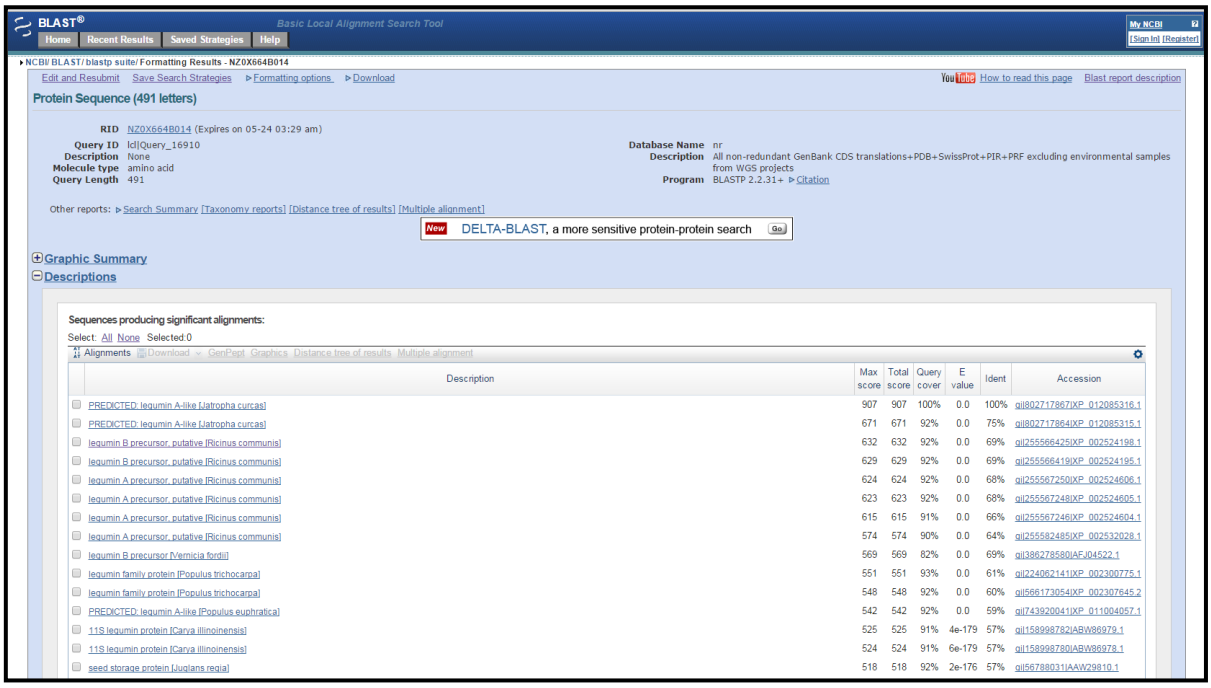

BLAST® Basic Local Alignment Search Tool

Home | Recent Results | Saved Strategies | Help

NCBI/BLAST/blastp suite/Formatting Results - NZ0X664B014

Edit and Resubmit | Save Search Strategies | Formatting options | Download | How to read this page | Blast report description

Protein Sequence (491 letters)

RID NZ0X664B014 (Expires on 05-24 03:29 am)
Query ID lcl|Query_16910
Description None
Molecule type amino acid
Query Length 491

Database Name nr
Description All non-redundant GenBank CDS translations+PDB+SwissProt+PIR+PRF excluding environmental samples from WGS projects
Program BLASTP 2.2.31+ Citation

Other reports: Search Summary [Taxonomy reports] [Distance tree of results] [Multiple alignment]

New DELTA-BLAST, a more sensitive protein-protein search Go

Graphic Summary
Descriptions

Sequences producing significant alignments:

Select: All None Selected:0

Alignments Download GenPept Graphics Distance tree of results Multiple alignment

Description	Max score	Total score	Query cover	E value	Ident	Accession
PREDICTED: legumin A-like [Jatropha curcas]	907	907	100%	0.0	100%	gi|802717867|XP_012085316.1
PREDICTED: legumin A-like [Jatropha curcas]	671	671	92%	0.0	75%	gi|802717864|XP_012085315.1
legumin B precursor, putative [Ricinus communis]	632	632	92%	0.0	69%	gi|255566425|XP_002524198.1
legumin B precursor, putative [Ricinus communis]	629	629	92%	0.0	69%	gi|255566419|XP_002524195.1
legumin A precursor, putative [Ricinus communis]	624	624	92%	0.0	68%	gi|255567250|XP_002524606.1
legumin A precursor, putative [Ricinus communis]	623	623	92%	0.0	68%	gi|255567248|XP_002524605.1
legumin A precursor, putative [Ricinus communis]	615	615	91%	0.0	66%	gi|255567246|XP_002524604.1
legumin A precursor, putative [Ricinus communis]	574	574	90%	0.0	64%	gi|255582485|XP_002532028.1
legumin B precursor [Vernicia fordii]	569	569	82%	0.0	69%	gi|386278580|AFJ04522.1
legumin family protein [Populus trichocarpa]	551	551	93%	0.0	61%	gi|224062141|XP_002300775.1
legumin family protein [Populus trichocarpa]	548	548	92%	0.0	60%	gi|566173054|XP_002307645.2
PREDICTED: legumin A-like [Populus euphratica]	542	542	92%	0.0	59%	gi|743920041|XP_011004057.1
11S legumin protein [Carya illinoinensis]	525	525	91%	4e-179	57%	gi|158998782|ABW86979.1
11S legumin protein [Carya illinoinensis]	524	524	91%	6e-179	57%	gi|158998780|ABW86978.1
seed storage protein [Juglans regia]	518	518	92%	2e-176	57%	gi|56788031|AAW29810.1

Gel band 10.6

Determination of protein characteristic (by MASCOT program)

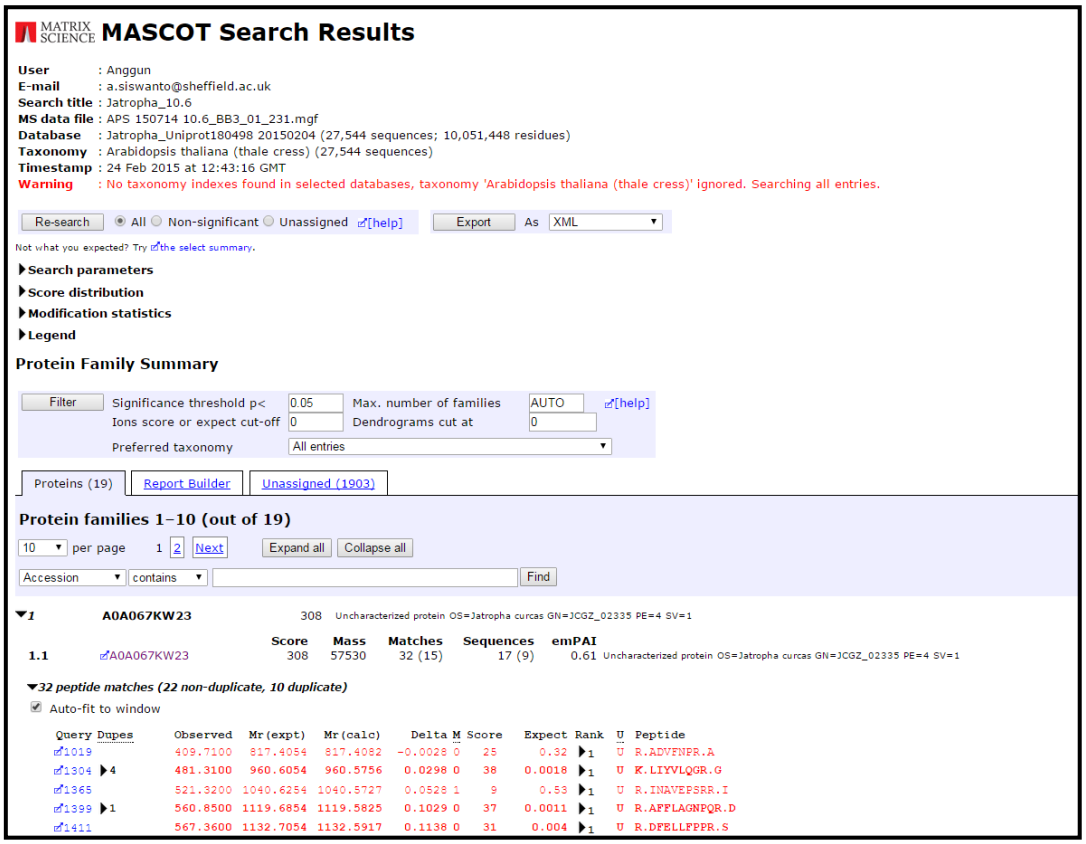

MATRIX SCIENCE **MASCOT Search Results**

User : Anggun
E-mail : a.siswanto@sheffield.ac.uk
Search title : Jatropha_10.6
MS data file : APS 150714 10.6_BB3_01_231.mgf
Database : Jatropha_Uniprot180498 20150204 (27,544 sequences; 10,051,448 residues)
Taxonomy : Arabidopsis thaliana (thale cress) (27,544 sequences)
Timestamp : 24 Feb 2015 at 12:43:16 GMT
Warning : No taxonomy indexes found in selected databases, taxonomy 'Arabidopsis thaliana (thale cress)' ignored. Searching all entries.

Re-search | All | Non-significant | Unassigned [help] | Export As XML

Not what you expected? Try the select summary.

Search parameters
Score distribution
Modification statistics
Legend

Protein Family Summary

Filter | Significance threshold p< 0.05 | Max. number of families AUTO [help]
Ions score or expect cut-off 0 | Dendrograms cut at 0
Preferred taxonomy All entries

Proteins (19) | Report Builder | Unassigned (1903)

Protein families 1–10 (out of 19)

10 per page 1 2 Next | Expand all | Collapse all

Accession contains Find

1	A0A067KW23	308	Uncharacterized protein OS=Jatropha curcas GN=JCGZ_02335 PE=4 SV=1			
		Score	**Mass**	**Matches**	**Sequences**	**emPAI**
1.1	A0A067KW23	308	57530	32 (15)	17 (9)	0.61

32 peptide matches (22 non-duplicate, 10 duplicate)

Auto-fit to window

Query	Dupes	Observed	Mr(expt)	Mr(calc)	Delta	M	Score	Expect	Rank	U	Peptide
1019		409.7100	817.4054	817.4082	-0.0028	0	25	0.32	1	U	R.ADVFNPR.A
1304	4	481.3100	960.6054	960.5756	0.0298	0	38	0.0018	1	U	K.LIYVLQGR.G
1365		521.3200	1040.6254	1040.5727	0.0528	1	9	0.53	1	U	R.INAVEPSRR.I
1399	1	560.8500	1119.6854	1119.5825	0.1029	0	37	0.0011	1	U	R.AFFLAGNPQR.D
1411		567.3600	1132.7054	1132.5917	0.1138	0	31	0.004	1	U	R.DFELLFPPR.S

Identification of predicted protein (by BLAST search engine)

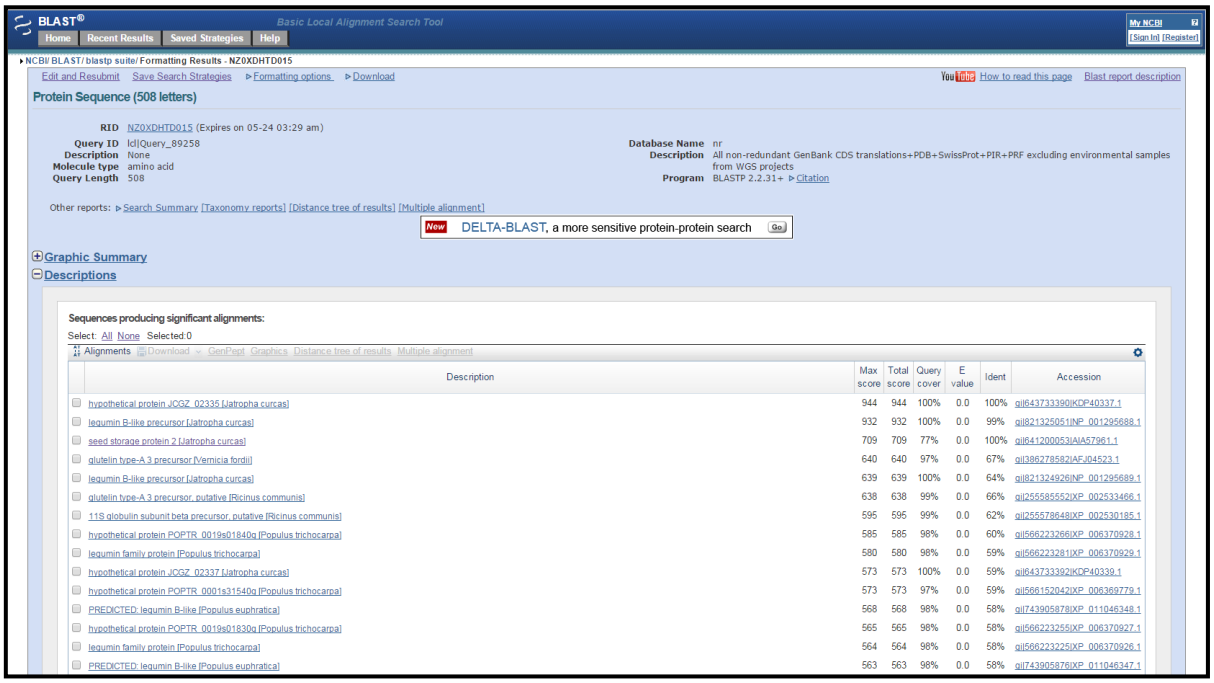

BLAST® Basic Local Alignment Search Tool

Home | Recent Results | Saved Strategies | Help

NCBI/BLAST/blastp suite/Formatting Results - NZ0XDHTD015

Edit and Resubmit | Save Search Strategies | Formatting options | Download | How to read this page | Blast report description

Protein Sequence (508 letters)

RID NZ0XDHTD015 (Expires on 05-24 03:29 am)
Query ID lcl|Query_89258
Description None
Molecule type amino acid
Query Length 508

Database Name nr
Description All non-redundant GenBank CDS translations+PDB+SwissProt+PIR+PRF excluding environmental samples from WGS projects
Program BLASTP 2.2.31+ Citation

Other reports: Search Summary [Taxonomy reports] [Distance tree of results] [Multiple alignment]

New DELTA-BLAST, a more sensitive protein-protein search Go

Graphic Summary
Descriptions

Sequences producing significant alignments:

Select: All None Selected:0

Alignments | Download | GenPept | Graphics | Distance tree of results | Multiple alignment

Description	Max score	Total score	Query cover	E value	Ident	Accession
hypothetical protein JCGZ_02335 [Jatropha curcas]	944	944	100%	0.0	100%	gi|643733390|KDP40337.1
legumin B-like precursor [Jatropha curcas]	932	932	100%	0.0	99%	gi|821325051|NP_001295688.1
seed storage protein 2 [Jatropha curcas]	709	709	77%	0.0	100%	gi|641200053|AIA57961.1
glutelin type-A 3 precursor [Vernicia fordii]	640	640	97%	0.0	67%	gi|386278582|AFJ04523.1
legumin B-like precursor [Jatropha curcas]	639	639	100%	0.0	64%	gi|821324926|NP_001295689.1
glutelin type-A 3 precursor, putative [Ricinus communis]	638	638	99%	0.0	66%	gi|255585552|XP_002533466.1
11S globulin subunit beta precursor, putative [Ricinus communis]	595	595	99%	0.0	62%	gi|255578648|XP_002530185.1
hypothetical protein POPTR_0019s01840g [Populus trichocarpa]	585	585	98%	0.0	60%	gi|566223266|XP_006370928.1
legumin family protein [Populus trichocarpa]	580	580	98%	0.0	59%	gi|566223281|XP_006370929.1
hypothetical protein JCGZ_02337 [Jatropha curcas]	573	573	100%	0.0	59%	gi|643733392|KDP40339.1
hypothetical protein POPTR_0001s31540g [Populus trichocarpa]	573	573	97%	0.0	59%	gi|566152042|XP_006369779.1
PREDICTED: legumin B-like [Populus euphratica]	568	568	98%	0.0	58%	gi|743905878|XP_011046348.1
hypothetical protein POPTR_0019s01830g [Populus trichocarpa]	565	565	98%	0.0	58%	gi|566223255|XP_006370927.1
legumin family protein [Populus trichocarpa]	564	564	98%	0.0	58%	gi|566223225|XP_006370926.1
PREDICTED: legumin B-like [Populus euphratica]	563	563	98%	0.0	58%	gi|743905876|XP_011046347.1